Effect of mechanical stress on the integrity, signalling mechanisms and function of bovine mammary epithelial cells

A thesis submitted in partial fulfilment of the requirements for the degree of

Doctor of Philosophy

in

Animal Science

at

Massey University, Manawatū

Palmerston North, New Zealand

Juliane Biet

2014

Abstract

Mammary gland engorgement due to milk accumulation in late lactation leads to changes in cell morphology and has been recognised as a potential key initiator of involution and remodelling of the mammary gland. The physical distension of mammary epithelial cells (MEC), due to udder filling, is likely to result in mechanical tension on cell-cell and cell-matrix interactions. Cell-cell and cell-matrix junctions provide tissue integrity, promote cell polarity, guarantee sufficient communication between cells to ensure synchronised milk secretion and support cell survival. Their disruption may be one of the early initiators of the mammary gland remodelling process. As a consequence, the primary goal of this study was to determine the potential effects of MEC stretch on changes in cell sensing within the mechanical micro-environment in the initiation of bovine MEC involution. During this investigation, particular emphasis was put on three potential mechanosensors: tight junctions (TJ), focal adhesions (FA) and primary cilia (PC), and their regulation in the early stages of involution using *in vivo* and *in vitro* experimental approaches. Static, biaxial *in vitro* cell stretch and acute physical distension *in vivo* resulted in changes in TJ protein expression levels implying a potential disruption of cell-cell communication as well as communication with the cell's cytoskeleton. Furthermore, down-regulation of Akt and pAkt following different periods of mechanical strain applied *in vitro* and decreased levels of pAkt following acute physical distension *in vivo* indicated a disruption of β1-integrin-FAK survival signalling through the PI3K-Akt pathway downstream of FA interactions. Increased numbers of ciliated MEC following extended periods of non-milking indicated a dedifferentiation of MEC.

Furthermore, increased levels of STAT6 transcription (part of PC signalling following mechanical stimulation) factor indicates the initiation of macrophage accumulation and promotion of tissue remodelling of the bovine mammary gland. In conclusion, this study supports the hypothesis that local factors play an important role during bovine mammary gland involution and that mechanical stimulation may play a part in the initiation of this process.

Acknowledgements

This project would not have been completed without the help and support of various people throughout and I would like to take this opportunity to express my appreciation to everybody involved.

Firstly, I would like to thank my AgResearch supervisor, Dr Kuljeet Singh, and my Massey University supervisor, Dr Jean Margerison, for the constant advice and guidance throughout the project. Your enthusiasm and positive attitudes were always inspiring. Furthermore, you always encouraged me to follow my own ideas, but you also kept me focused when I needed it. Many thanks for making this Ph.D. project a very memorable experience.

Special thanks to my supervisors Dr Kerst Stelwagen, SciLactis Ltd., and Assoc. Prof. Tony Poole, Department of Medicine, University of Otago, for the support, dedication and knowledge provided throughout the project. While planning/setting up my experiments, your expertise was much needed and very helpful.

Moreover, I would like to especially thank all of my supervisors for their feedback and guidance during the course of writing this thesis.

Many thanks to AgResearch Ltd. for funding my PhD stipend, all experimental laboratory and field research, and for providing me with the use of their facilities and resources (MSI programme [C10X0702] entitled “Future Proofing of the NZ Dairy Cow”). Generous financial support from the Kathleen Spragg Agricultural

Resarch Trust and the Johannes August Anderson PhD scholarship have been greatly appreciated.

I would also like to thank the entire ‘Dairy Science’- and ‘Animal Physiology’-Building staff who generously gave their time to demonstrate new techniques, devices, and/or to provide me with technical advice and assistance. Many special thanks to Chris McMahon, Chris Couldrey, Jo Dobson, Regan Murney, Kim Oden, Shona Pryor, Harold Henderson, Ali Cullum, Adrian Molenaar, Craig Smith, Marita Broadhurst, Brian Atkins, etc.

The list of people from AgResearch I would like to thank is long and they all made this journey less overwhelming. Thank you for keeping me sane and making this experience more entertaining.

Furthermore, I would like to thank Melanie Millier for her help with the primary cilia staining/analysis. Also many thanks go to Jacqui Ross and Hilary Holloway, Department of Anatomy with Radiology, University of Auckland, for the help and support with confocal microscopy.

Finally, I would like to express many thanks to my parents, sister, extended family, and friends who have been very supportive and encouraging during this project. Thanks for your love and patience. Personal thanks to Pita and his family for the emotional support and reminding me that there is more to life than bovine mammary glands.

Contents

List of Figures

List of Tables

List of Abbreviations

1X	Once daily milking
2X	Twice daily milking
3X	Thrice daily milking
BM	Basement membrane
CTK18	Cytokeratin 18
DIM	Days in milk
ECM	Extracellular matrix
EGF	Epidermal growth factor
FA	Focal adhesion
FAC	Focal adhesion complex
GAPDH	Glyceraldehyde 3-phosphate dehydrogenase
IFT	Intraflagellar transport
JAM	Junctional adhesion molecule
MEC	Mammary epithelial cell
NFMP	Non-fat milk powder
PC	Primary cilium
PC-1	Polycystin-1
PC-2	Polycystin-2
PRL	Prolactin
PRLR	Prolactin receptor
qRT-PCR	Quantitative real time-polymerase chain reaction
RIN	RNA integrity number
RT	Room temperature
SCC	Somatic cell count
SMA	Smooth muscle actin
TJ	Tight junction
TRP	Transient receptor potential
ZO-1/2/3	Zonula occludens 1/2/3

Chapter 1:

Introduction

Chapter 1 General Introduction

1.1 Dairy industry

New Zealand is the world's largest exporter of dairy commodities accounting for one-third of cross-border trade in dairy products. Approximately 95 % of the milk produced in New Zealand is exported into over 150 countries worldwide. Thus, the dairy industry accounts for one-quarter of all merchandise exports and represents New Zealand's largest export earner (Source: MPI, 2012; Statistics New Zealand, 2012; Fonterra Co-operative Group Ltd.; DairyNZ).

In 2011/12, New Zealand had 4.6 million dairy cattle in 11798 herds with an average size of 392 cows and an average milk solid production per cow of 364 kg per year. In contrast to the dairy industry in Europe or North America, the temperate climate and the small seasonal variation in pasture growth rates allow for pasture-based management systems and seasonal calving, resulting in a lower-cost dairy production model. In the 2011/2012 season the dairy companies processed 19.1 billion litres of milk containing 1.69 billion kilograms of milk solids, with a total export value of 14 billion NZD, a Figure which has continuously increased over past decades (Source: MPI, 2012; Statistics New Zealand, 2012; Fonterra Co-operative Group Ltd.; DairyNZ; LIC).

Furthermore, the dairy industry employs 37000 people with Fonterra Co-operative Group Ltd. being the largest milk processing company representing 89 % of the

country's milk production. A number of smaller dairy companies include Tatua Co-operative Dairy Company, Westland Milk Products, Synlait and Open Country Dairy Limited (Source: MPI, 2012; Statistics New Zealand, 2012; Fonterra Co-operative Group Ltd.; DairyNZ).

Thus, the New Zealand economy is reliant on the success and profitability of the dairy sector. Therefore, the continued research in this area could help to improve and/or development novel strategies to enhance lifetime lactation performance of dairy cattle to ultimately enhance competitiveness of the New Zealand dairy industry.

1.2 Mammary gland

The mammary gland represents a modified apocrine dermal gland that produces milk to nourish the offspring (Kass *et al.*, 2007). Although, the strategy to secrete a nutritious product to feed the young is not limited to mammals, it is only in mammals that milk is secreted by a specific organ, the mammary gland (Mepham, 1987; Hennighausen & Robinson, 2001; Akers, 2002).

Furthermore, postnatal terminal differentiation is a unique feature of the mammary gland (Anderson *et al.*, 2007). At birth, the mammary gland is rather rudimentary containing no more than the fat pad with a few primary and secondary sprouts (Mepham, 1987; Akers, 2002; Anderson *et al.*, 2007). It is only after parturition that the mammary gland is fully developed and able to synthesise and secrete milk in order to nurse the offspring (Anderson *et al.*, 2007).

1.2.1 Structure of the mammary gland

Even though there is much variation in the number of mammary glands, location of mammary glands, and composition of secretions among different species, the histological structures of the glands are very similar (Mepham, 1987; Akers, 2002).

Despite the species of origin, each gland is composed of the epithelium (or parenchyma), which includes ducts and milk-producing cells, and the stroma, or connective tissue, which includes the fat pad (Hennighausen & Robinson, 2005).

In general, the mammary gland is comprised of a branching network of ducts and secretory alveoli clustered together creating a tubulo-alvealor structure (McManaman & Neville, 2003). The alveolus, a basic secretory unit, is lined by a single layer of luminal, functionally differentiated secretory epithelial cells which form a hollow lumen (Fig. 1.1). Each individual alveolus in turn is surrounded by a basket-like mesh of contractile basal, myoepithelial cells (Hennighausen & Robinson, 2005; Watson *et al.*, 2011). The myoepithelium contracts in response to oxytocin, a hormone secreted by the pituitary gland, to aid ejection of the synthesised milk from the lumen into the duct system (Davis *et al.*, 1999; Bruckmaier, 2005). To enable the luminal secretory cells to directly contact the underlying stroma, the myoepithelium forms a discontinuous layer. Direct contact to the basement membrane (BM) surrounding the connective tissue, or stroma, ensures sufficient supply of nutrients, oxygen, and hormonal signals which are transferred via embedded blood vessels and nerves. Several alveoli clustered together with their ductules drain into one larger duct and form grape-like structures encapsulated by a thin sheet of connective tissue, the so-called lobules (Mepham, 1987; Akers, 2002).

Milk components are produced within the alveoli by the luminal epithelial cells and secreted into the lumen (Fig. 1.1). From the lumen the milk is drained via a duct system. The duct system is a series of narrow ducts that drain into progressively larger collecting ducts. The location of storage of secreted milk until milk removal differs among species (Larson, 1985a; Mepham, 1987; Akers, 2002). In ruminants (e.g. cows), large ducts empty into a system of large cisterns (Mepham, 1987; Frandson, 1992). Eventually the milk is removed from the gland

to transfer milk to the suckling young. In, for example, cows, rats, sheep, and mice milk removal takes place through a single teat orifice at the end of the teat (Mepham, 1987; Akers, 2002).

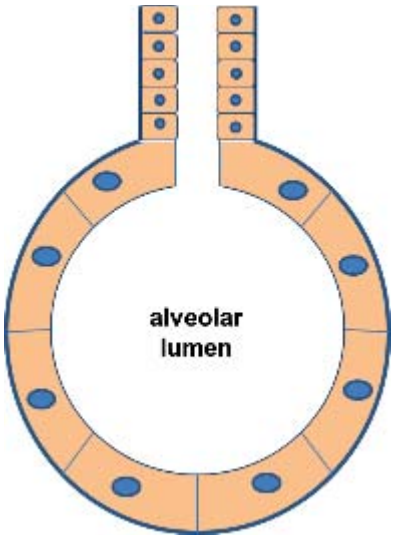

Figure 1.1 Schematic of an alveolus. The alveolus is a basic functional unit of production in which a single layer of milk secretory cells are grouped in a sphere with a hollow centre. Milk components are produced within the alveoli by the luminal epithelial cells and secreted into the alveolar lumen. In ruminants, e.g. cows, milk is drained via a duct system into a system of large storage cisterns until milk removal

1.2.2 Secretory cells of the lactating mammary gland

During lactation, secretory mammary epithelial cells (MECs) are highly metabolically active and contain a spherical nucleus, a well-developed Golgi-apparatus, extensive endoplasmic reticulum network, several mitochondria, numerous free ribosomes, lysozymes, and products of synthesis, such as fat globules and protein granules. The MECs are columnar in shape and show a polarized structure. On the apical cell surface microvilli are present oriented into the lumen. They also have a folded basal membrane which probably accounts for

high efficiency in removing precursors from the blood (Linzell & Peaker, 1971; Larson, 1985b; McManaman & Neville, 2003).

Individual MECs are connected via a series of junctional complexes, including tight junctions (TJs), desmosomes, and adherent junctions (Fig. 1.2). Cell-cell junctions provide tissue integrity and promote cell polarity. Furthermore, they guarantee sufficient communication between cells to ensure synchronised milk secretion and support cell survival (Mepham, 1987; Maeda *et al.*, 2005).

1.2.2.1 Junctional complexes

The TJs are located near the apical portion of each MEC forming a tight barrier dividing the plasma membrane into the apical and basolateral domains (Fig. 1.2) (Schneeberger & Lynch, 1992; Stelwagen & Singh, 2013). Thus, the TJs inhibit direct paracellular exchange of substances between vascular and milk compartments and promote polarised function of the secretory cells by preventing apical factors from being exposed to the basolateral side (Linzell & Peaker, 1971; Larson, 1985b; McManaman & Neville, 2003).

Encircling the MEC more basal than the TJs are the adherent junctions which play a pivotal role in regulating the entire junctional complex (Fig. 1.2). Through the transmembrane molecules, the cadherins, adherent junctions form a direct link between the cytoskeleton of neighbouring cells providing a strong mechanical attachment to each other (Maeda *et al.*, 2005).

Desmosomes are spot-like, randomly located junctional complexes linking cell-surface adhesion proteins to the intercellular keratin cytoskeleton, thereby holding two cells tightly together helping cells to resist shear stress (Larson, 1985b).

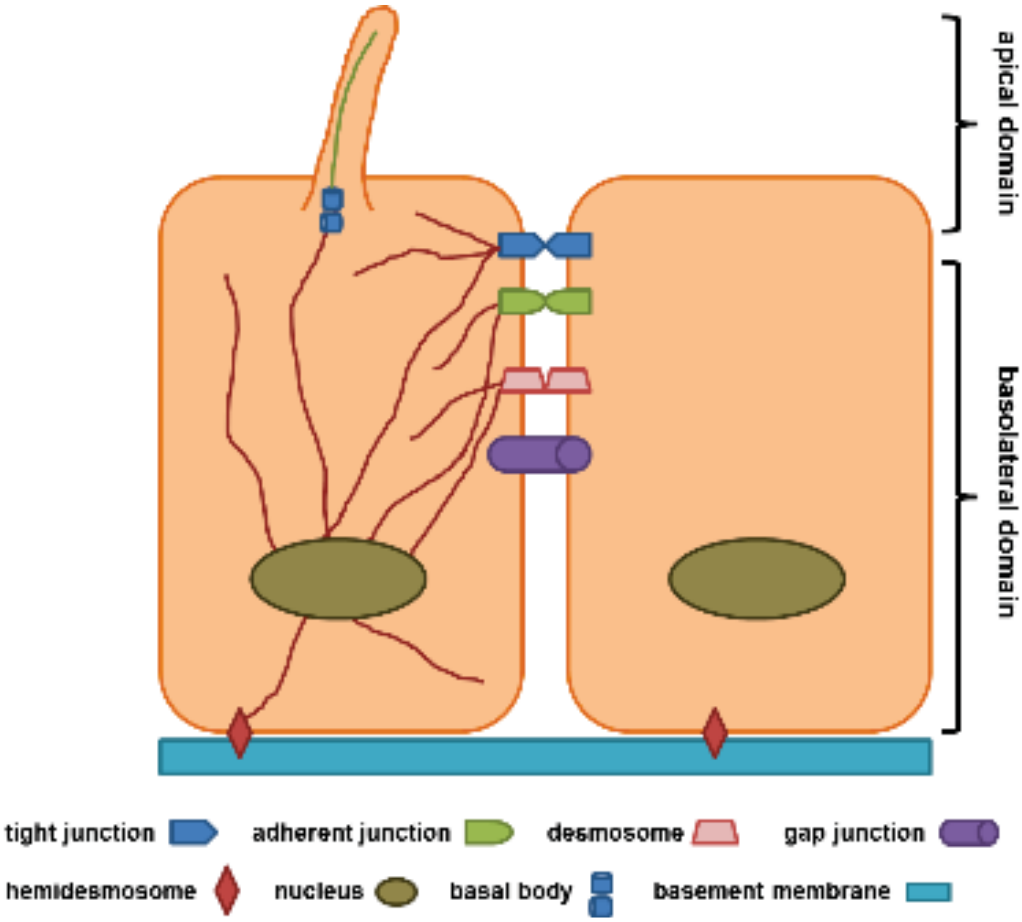

Figure 1.2 Schematic diagram of epithelial cells and the principal types of cell junctions that connect them. The tight junctions are located near the apical portion of each cell forming a tight barrier dividing the plasma membrane into the apical and basolateral domains. Encircling the cell more basal than the tight junctions are the adherent junctions which play a pivotal role in regulating the entire junctional complex. The remaining types of junctions include, desmosomes, and hemidesmosomes and are critical to cell-cell and cell-matrix adhesion. Gap junctions form channels to directly link the cytosol of two neighbouring cells in order to allow low molecular weight material or currents to pass from cell to cell

1.2.2.1.1 Tight junctions

Three transmembrane proteins enriched at TJs with the potential to mediate cell-cell adhesion have been identified; occludin, claudin, and junctional adhesion molecules (JAM) (Fig. 1.3) (Aijaz *et al.*, 2006; Niessen, 2007; Anderson & Van Itallie, 2009; Furuse, 2010).

Occludins were the first transmembrane TJ component to be discovered. They seal and regulate permeability in endothelial and epithelial cells (Furuse, 2010). Claudins, however, have emerged as critical for defining junction selectivity (including size, electrical resistance and ionic charge preference) (Van Itallie & Anderson, 2004). Mammalian claudins form the seal in the TJs of endothelial and epithelial cells and regulate paracellular permeability in an organ- and tissue-specific manner (Van Itallie & Anderson, 2004).

Finally, the third group of transmembrane receptors found in TJs are the IgG-like family of JAMs. JAMs are glycoproteins concentrated at the intercellular TJs of endothelial and epithelial cells, where they assist in regulating cell-cell adhesion, cell-ECM adhesion, endothelial cell motility and cell polarisation (Fig. 1.3).

The scaffolding function must be achieved through cytoplasmic binding partners, since no direct interaction between the transmembrane receptors has been found. An important group of scaffolding molecules are the zonula occludens proteins: ZO-1, ZO-2, and ZO-3. By interacting directly with occludin, claudin, and actin respectively or indirectly via singulin, they provide a link between the

transmembrane receptors and the cytoskeleton. Additionally, ZO-1 can also directly interact with JAMs and form homodimers or heterodimers with either ZO-2 or ZO-3 (Fig. 1.3) (McManaman & Neville, 2003; Niessen, 2007; Michaelson & Huang, 2012).

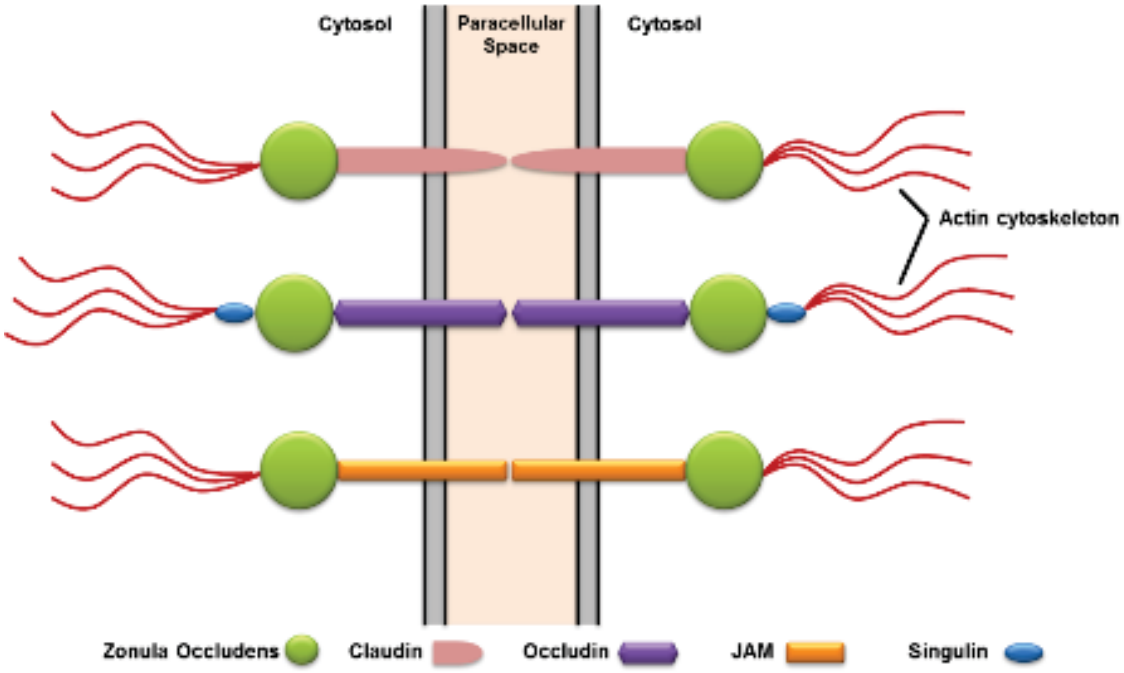

Figure 1.3 Schematic representation of the tight junction. Tight junctions consist of transmembrane proteins (occludin, claudin and junctional adhesion molecule (JAM) and the cytoplasmic proteins zonula occludens (ZO-1, ZO-2, ZO-3). The transmembrane proteins mediate cell-cell adhesion. However, no direct interaction between the transmembrane receptors and the actin cytoskeleton has been found; therefore the scaffolding function must be achieved through cytoplasmic binding partners, such as zonula occludens or singulin. By interacting directly with occludin, claudin, and actin respectively or indirectly via singulin, they provide a link between the transmembrane receptors and the cytoskeleton

1.2.2.2 Primary cilia

Another important cell organelle involved in the transduction of mechanical and extracellular signals from the extracellular space towards intracellular responses is the primary cilium (PC) (Fig. 1.4). Nearly every MEC contains a PC, a hair-like shaft projecting perpendicular from the apical surface of a polarised and

differentiated, or quiescent, cell into the internal lumen of tissues. The PCs vary in length from 1 to 5 μm with a diameter of 0.2 μm (Poole *et al.*, 1985; Poole *et al.*, 2001; Satir & Christensen, 2007; Abou Alaiwi *et al.*, 2009; Satir *et al.*, 2010; Hoey *et al.*, 2012; Jones & Nauli, 2012).

In spite of the diversity of cilia and their specialised function as cellular organelles, all cilia types share basic structural units, the ciliary and sub-ciliary compartments. The ciliary compartment consists of a cylindrical array of nine doublet microtubule-based axoneme extending out from the cell surface. The axoneme is ensheathed by a bilayer lipid membrane that is continuous with the plasma membrane of the cell body, but contains a distinct subset of receptors and other proteins involved in signalling (Abou Alaiwi *et al.*, 2009; Veland *et al.*, 2009; Satir *et al.*, 2010; Hoey *et al.*, 2012). The doublets consist of two tubules with a complete microtubule containing 13 protofilaments and an incomplete tubule containing 10 protofilaments (Hoey *et al.*, 2012).

The sub-ciliary compartment consists of the basal body and associated anchoring elements within the interior of the cell body. The PCs arise from a basal body, derived from the mother centriole which provides a template for the formation of the 9-fold symmetry of the ciliary axoneme as well as an origin for the cell's microtubular meshwork (Veland *et al.*, 2009). The alar sheets are transitional fibres important for the structural stability of the entire complex through attachment to the plasma membrane. Separating the ciliary and plasma membrane compartments is a region known as the ciliary necklace (Gilula & Satir, 1972). The ciliary necklace is connected via fibres to the transition zone of

the basal body, and these fibres are thought to be part of a 'ciliary pore complex' through which only selected proteins are allowed to enter the ciliary compartment (Rosenbaum & Witman, 2002). Proximal to the alar sheets is a collar of conical structures known as basal feet. These basal feet extend laterally forming attachment points for cytoskeletal microtubules. The number of basal feet differs depending on whether the PC is motile or non-motile (Poole *et al.*, 1985; Poole *et al.*, 1997; Poole *et al.*, 2001; Hoey *et al.*, 2012).

Initiation of ciliogenesis involves docking of post-Golgi vesicles to the distal end of the mother centriole, emergence of a ciliary bud within the lumen of the vesicle and extension of the axoneme. Responsible for building and maintaining the structure and function of PC by transporting structural components up and down the microtubular structure is the process of intraflagellar transport (IFT) (Rosenbaum & Witman, 2002; Singla & Reiter, 2006). The IFT particles and their associated cargo proteins are transported along axonemal microtubules by kinesin 2 motor proteins in the anterograde (base-to-tip) direction, after which cargo is delivered to the growing tip. The cytoplasmic dynein 2 mediates transport in the retrograde (tip-to-base) direction (Satir & Christensen, 2007; Satir *et al.*, 2010).

The PCs play critical and distinct roles in sensing and transducing extracellular signals, for example fluid shear stress, into intracellular biochemical responses, such as calcium signalling and nitric oxide synthesis. Hence, changes in the structural mechanics of the PC greatly affect the molecular mechanism of mechanosensing (Veland *et al.*, 2009; Satir *et al.*, 2010; Hoey *et al.*, 2012).

Signalling in the cilium coordinates key processes during development and in tissue homeostasis, including cell migration, differentiation and/or re-entry into the cell cycle, specification of the plane of cell division and apoptosis. Sensory modalities to which the PC responds, includes mechanical stimulation (bending of the cilium) and chemosensation (detection of a specific ligand, growth factor, hormone or morphogen). In some specialised cases, PCs can also respond to light, temperature, osmolality or gravity (Veland *et al.*, 2009; Satir *et al.*, 2010). Hence, the primary ciliary membrane is enriched for a number of receptors and ion channels, including polycystins-1 (PC-1) and -2 (PC-2), receptor tyrosine kinases, G-protein- coupled receptors, receptors for extracellular matrix, transient receptor potential ion channels, as well as various transporter proteins (Veland *et al.*, 2009; Christensen *et al.*, 2012).

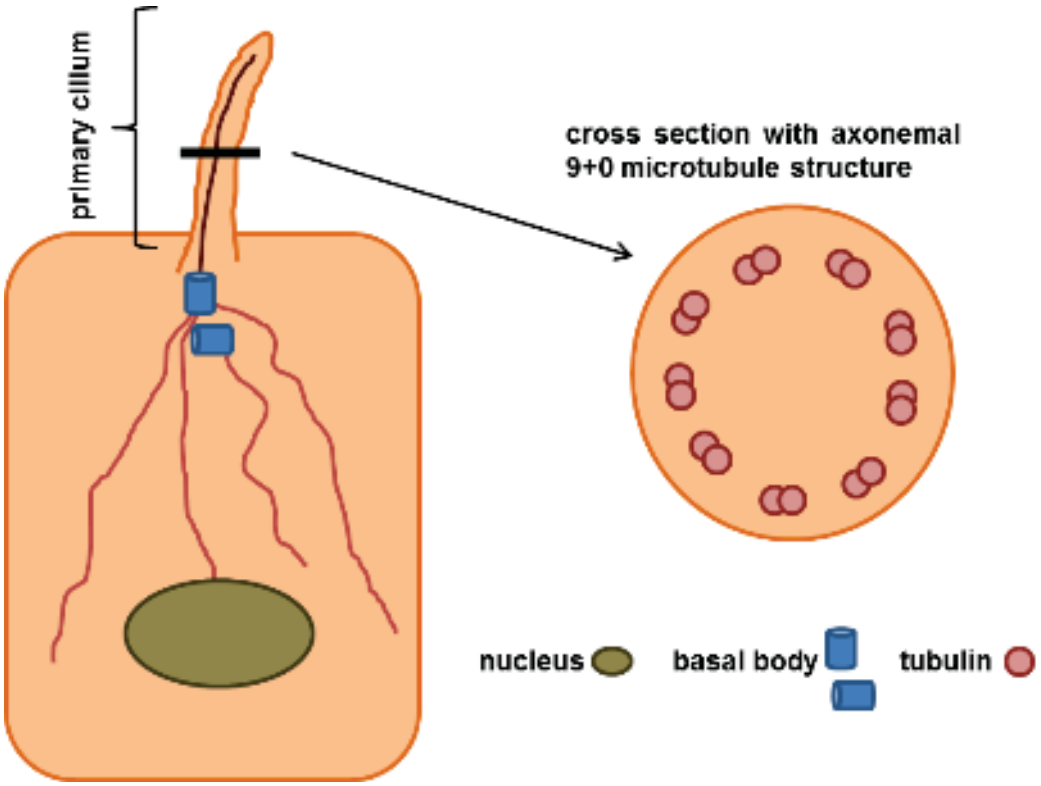

Figure 1.4 Schematic of structure of a primary cilium. The primary cilium emerges from the centrosomal mother centriole (basal body) into the lumen which provides a template for the formation of the 9-fold symmetry of the ciliary axoneme as well as an origin for the cell's microtubular meshwork

1.2.3 Extracellular matrix

Tissues, however, are not exclusively made up of cells. Additionally, they are embedded by a condensed network of scaffolding proteins, such as collagen type I, to mediate structural and/or biological properties, called the extracellular matrix (ECM). The ECM consists of a complex mixture of macromolecules, proteins and polysaccharides, which are arranged in unique three-dimensional patterns suited to the tissue in which they are found (Aumailley & Gayraud, 1998; Alberts *et al.*, 2002; Nelson & Bissell, 2006; Badylak *et al.*, 2009). Therefore, the ECM promotes the appropriate tissue construction by determining the pattern of gene expression resulting in a differentiated phenotype. The molecules forming the ECM are secreted by the resident cells of each tissue and organ, for example laminin I is secreted by myoepithelial cells (Alberts *et al.*, 2002; Nelson & Bissell, 2006). Consequently, much variation in composition and distribution of the ECM can be found (Badylak *et al.*, 2009).

The ECM consists of the connective tissue and the BM (Fig. 1.5). The BM represents a thin layer of specialized ECM separating the epithelial cells from the underlying connective tissue and will be discussed in more detail in section 1.2.3.2 Basement Membrane.

The connective tissue underlying the BM contains not only ECM molecules, but also cells. The predominant cell types within the connective tissue are the fibroblasts which secrete a large proportion of the ECM proteins. Other cell types, such as adipocytes and macrophages, can also be found within the ECM. The macromolecules found in the ECM are produced locally and the cells influence

the organisation of the matrix molecules via the actin cytoskeleton from inside the cell (Alberts *et al.*, 2002).

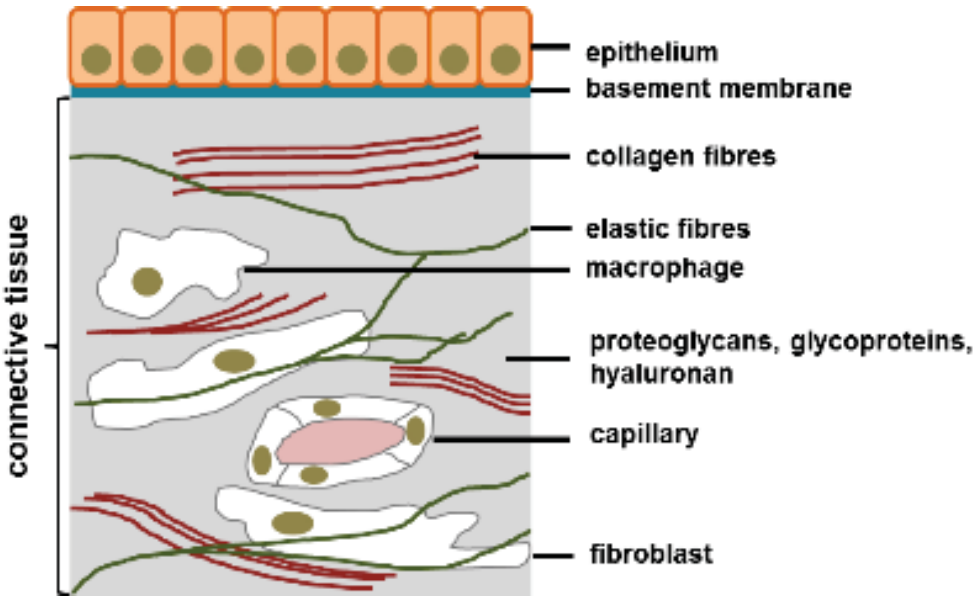

Figure 1.5 Schematic of the connective tissue underlying an epithelium. The connective tissue contains a variety of cells and extracellular matrix (ECM) components. In turn, the ECM consists of the connective tissue and the basement membrane. As in all epithelia, the BM, a thin sheet of specialised, condensed macromolecules, separates all monolayers of epithelial cells from the underlying connective tissue in the body. The predominant cell type within the connective tissue is the fibroblast. The macromolecules found in the ECM are produced locally, and the cells influence the organisation of the matrix molecules via the actin cytoskeleton from inside the cell

1.2.3.1 Major macromolecules of the connective tissue

Two main classes of macromolecules can be found in the connective tissue, these being polysaccharides and fibrous proteins. The former are polysaccharide chains called anionic glycosaminoglycan which are usually covalently linked to a protein in the form of a proteoglycan and the latter are proteins such as collagen, elastin, fibronectin, and laminin (Alberts *et al.*, 2002).

Proteoglycan molecules form a gel-like substance in which fibrous proteins are embedded. The gel-like structure resists compressive forces on the matrix while permitting rapid diffusion of nutrients, metabolites, and hormones between blood and tissue cells, whereas the collagen fibres strengthen (i.e. aid to resist stretching forces) and organise the matrix. Furthermore, elastin fibres provide resilience (Alberts *et al.*, 2002). Proteoglycans not only provide hydrated space, they also form gels varying in pore size and charge density to serve as a selective sieve by size, charge, or both. They also bind various secreted signal molecules, thus they play a role in the chemical signalling between cells. Moreover, they can act as co-receptors (e.g. syndecans) when either inserted across the lipid bilayer, or attached to the bilayer. In general, they aid in binding cells to the ECM and/or initiate response to ECM signal (Alberts *et al.*, 2002).

Collagens, secreted by connective tissue and other cell types respectively, are the most abundant proteins in mammals, constituting 25 % of the total protein mass. After secretion into the extracellular space, fibrillar collagens self-assemble into higher-order polymers, called collagen fibrils, which then form even larger cable-like-bundles several micrometres in diameter, the collagen fibres. Connective tissue cells determine size and arrangement of collagen fibres by guiding collagen fibril formation in close association with the plasma-membrane (Alberts *et al.*, 2002).

Elastin gives tissue the resilience needed against stretch, because elastic fibres are five times more extensible than rubber bands. Inelastic, interwoven collagen fibres limit the extent of stretch to give support and prevent tissue from tearing (Alberts *et al.*, 2002).

Finally, fibronectin, a large, non-collagen, glycoprotein with multiple domains, each with specific binding sites for other matrix macromolecules and receptors on the cell surface, helps matrix organisation, cell attachment to the ECM and cell migration. The main type of domain, called type III fibronectin repeat, contains a binding site for integrins. The type III repeat is the most common among all protein repeats. It is approxiamtely 90 amino sequences long and occurs at least 15 times in each subunit. A specific tripeptide sequence (Arginine-Glycine-Aspartic acid, or RGD) found in one of the type III repeats is a central binding site recognised by several members of the integrin family. Unlike the self-assembling collagen molecules, fibronectin molecules assemble into fibrils only on the surface of certain cells. Additional proteins are required, such as the fibronectin binding integrins. Intercellular actin stress fibres promote assembly of secreted fibronectin molecules into fibrils and influence fibril orientation (Alberts *et al.*, 2002; Villard *et al.*, 2006).

1.2.3.2 Basement membrane

The BM is a 50 to 100 μm thin sheet of specialised, condensed macromolecules, similar to, but not the same, to those found elsewhere in the ECM. It separates all monolayers of epithelial cells from the underlying connective tissue in the body (Grant *et al.*, 1981; Stanley *et al.*, 1982; LeBleu *et al.*, 2007). The BMs molecular composition and biochemical complexity is unique and depends on its biological function. It provides structural support, organises compartmentalisation, and possesses binding sites for cell adhesion molecules, guides cell proliferation, differentiation, and migration, and influences and modifies cellular behaviour via outside-in signalling. The basal surfaces of the MECs rest upon the BM.

Therefore, the composition of the BM directly influences BM-mediated cell signalling events to regulate intercellular signalling pathways that influence behaviour in a tissue-specific manner (Yurchenco & Schittny, 1990; LeBleu *et al.*, 2007).

In general, the BM's principal components are collagenous proteins, primarily collagen type IV, and glycoproteins, including laminin, entactin/nidogen, fibronectin, and heparan sulphate proteoglycan (perlecan). Numerous other minor components, such as agrin and fibulin, contribute to tissue specificity and heterogeneity (LeBleu *et al.*, 2007). Varying amounts of each component and subtypes within each BM result in extremely diverse, tissue-specific and dynamic compositions. As a consequence, transcription of a particular protein chain might be up- or down-regulated according to the physiological and/or pathophysiological state. In addition, posttranslational modifications modulate functions and binding affinities to other components, thus affecting their composition. Collagen type IV and laminin heterogeneity is the major molecular basis for tissue-specific BM composition (Grant *et al.*, 1981; LeBleu *et al.*, 2007).

Collagen type IV and laminin can self-assemble into a sheet-like network. The ability of nidogen/entactin and perlecan to bind to both collagen type IV and laminin is thought to connect the two networks to form a multi-layered network of macromolecules. Moreover, collagens type IV and laminins prefer to polymerise while bound to the cell-surface receptors of the cells producing the protein. The majority of the cell-surface receptors for type IV collagen and laminin are members of the integrin family. Therefore, integrins aid the organisation of the assembly of the BM (Alberts *et al.*, 2002).

1.3 Lactation cycle

The term lactation refers to a process during which milk components are produced by the epithelial cells, secreted into the lumen, and, subsequently, the milk is removed from the mammary gland (McManaman & Neville, 2003). As mentioned above, the mammary gland is composed of different tissues and cell types and can repeatedly undergo the different phases of the lactation cycle: growth, functional differentiation, lactation and regression (Akers, 2002). The whole process is coordinated by hormones secreted by the pituitary, ovaries, adrenal glands and the mammary gland itself, which are essential for optimal development of the ducts and the lobular-alveolar structure (Knight & Peaker, 1982; Plath *et al.*, 1997).

A detailed account of the entire lactation cycle is beyond the scope of this review and for further information the reader is referred to comprehensive literature by Linzell and Peaker (1971), Knight & Peaker (1982), Anderson (1985), Mepham (1987), Akers (2002), or McManaman and Neville (2003). However, a short summary of important key stages of the lactation cycle will be given below to emphasise the unique development and function of the mammary gland.

1.3.1 Lactogenesis

In late pregnancy (2 to 3 weeks prior to parturition), bovine MECs convert from a non-secretory state into a secretory state. This initiates the onset of copious milk production referred to as lactogenesis (McManaman & Neville, 2003). During this time, epithelial cells show a high metabolic activity secreting 1 to 2 ml of milk per

g of tissue per day (Linzell & Peaker, 1971; Neville & Daniel, 1987). Milk yield and composition are affected by numerous factors, including genotype, nutrient supply, the stage in lactation, hormone and growth factor levels, age, pregnancy, environmental temperature, disease and mastitis, milking practices and the frequency and/or completeness of milk removal (Linzell & Peaker, 1971; McManaman & Neville, 2003).

The main milk components include lactose, fat, and protein. However, a wide species variation of milk composition can be found. For example, the milk of horses and humans contains 6 to 7 % lactose, cow's milk contains 4 to 5 % lactose, while the milk of rabbits is only made up of 1 to 2 % lactose. Fat content in the milk ranges from almost 0 % in rhinoceroses, 4 % in cows, to up to 50 % in whales and seals. Equally, protein concentration can range from 1 % in horses and humans, 3 to 4 % in cows, up to 10 to 14 % in rats, rabbits and dogs (Linzell & Peaker, 1971; Wattiaux, 2013).

Initially, immediately prior to birth, the mammary gland produces a fluid different to mature milk that contains large amounts of immunoglobulins and other immune defence proteins, but very little, if any, lactose, called colostrum (Linzell & Peaker, 1971; Larson, 1985b; McManaman & Neville, 2003). After parturition, however, the mammary gland begins producing large volumes of mature milk to support growth of the newborn (Anderson *et al.*, 2007).

The main hormones involved in lactogenesis are progesterone, prolactin (PRL), estrogens, and glucocorticoids, such as cortisol. While the former plays a major

role in inhibiting lactogenesis, the latter three are important in initiating lactogenesis. Cortisol induces differentiation of the rough endoplasmic reticulum and the Golgi apparatus which are vital for a number of synthesising pathways within the MEC. Differentiation of the MEC also allows PRL to directly induce milk protein synthesis via the prolactin receptor (PRLR). Estrogens increase the number of PRLRs on the cells surface and furthermore stimulate secretion of PRL from the pituitary gland (Anderson *et al.*, 2007).

1.3.2 Galactopoeisis

Galactopoeisis is the time of maintenance and/or enhancement of established milk production until involution. It is partly controlled by systemic galactopoeitic hormones, such as PRL, growth hormone, thyroid hormones, and glucocorticoids, which are released by the suckling and/or milking stimulus, which on the other hand triggers regulation by local factors (McManaman & Neville, 2003; Hickson *et al.*, 2006). Conversely, despite adequate hormone status and frequent milk removal, lactation will not persist indefinitely.

1.3.2.1 Persistency

Persistency of lactation is the measure of the rate at which milk production declines after peak yield (i.e., the cows' ability to maintain milk production after peak yield). Milk production at any stage is determined by the number and activity of secretory cells present which can differ depending on the species. Until peak lactation, the udder continues to grow due to an increase in number of secretory cells. Once peak yield is reached, a shift occurs and the rate of apoptosis

increases in contrast to rate of proliferation. Moreover, in late lactation, secretory cells are less active. The combination of the decrease in cell numbers and activity leads to a continuous decline in milk yield up to the point where the cow is usually dried off (Kumar *et al.*, 2000; Capuco *et al.*, 2003; Boutinaud *et al.*, 2004; Hickson *et al.*, 2006).

In contrast to the dairy industry in Europe or North America, cows in New Zealand are predominantly fed more fresh pasture, therefore persistency of lactation of grazing cows is dependent on the availability of pasture during lactation. In accordance with the variability in pasture growth rates, seasonal peak productions are inevitable leading to large quantities of milk supply during summer and low quantities of milk supply during winter (Hickson *et al.*, 2006).

1.3.2.2 Milk storage and milk removal

The bovine udder is composed of four functionally separate glands, each with its own secretory tissue and cisternal cavities that are drained via a separate teat. Secreted milk is stored in the udder in two fractions, the alveolar fraction and the cisternal fraction. The smaller cisternal fraction, approximately 20 %, is stored in the teat cistern, gland cistern and in the larger ducts, and is removed 'passively' once the teat sphincter barrier is overcome. However, the bulk of the milk is stored in the alveoli and needs to be removed actively to overcome the capillary forces by the milk ejection reflex or milk let down (Bruckmaier, 2005). This active ejection is achieved by the release of oxytocin from the pituitary gland. Oxytocin stimulates the myoepithelial cells surrounding the alveoli to contract, thereby increasing the intra-mammary pressure. The milk is then forcefully shifted via

draining ducts into the cisternal space where it can be removed by suckling/machine milking. But even after active milk ejection, residual milk (5 to 15 %) is left in the udder that cannot be removed (Mepham, 1987; Bruckmaier & Blum, 1998).

1.3.2.2.2 Completeness of milk removal

The process of milk secretion is regulated by frequency and completeness of milk removal (Wilde *et al.*, 1995). Therefore, the amount of residual milk left in the udder after each milking is important for persistency. During a normal lactation the volume of residual milk remains fairly constant, around 5 to 15 %. However, cows with short lactation periods show a gradual increase in the amount of residual milk and an overall lower milk yield during a lactation cycle (Costa, 2003).

Efficient milk removal is important for maintenance of milk production, e.g. less frequent milking results in reduced milk production and shorter lactation periods. However, efficiency of milk removal can be supported by injection of oxytocin to aid the ejection process (Carruthers *et al.*, 1993; Costa, 2003).

1.3.2.2.2.1 Milking frequency

Considering that milking frequency affects total yield, peak yield, day of peak yield, and persistency for all milk components, it is obvious that more-frequent milking would result in higher yield (Stelwagen, 2001). However, twice-daily milking is the most common practice in New Zealand and many other countries in

Europe. In goats and cows, increased milking frequency enhances MEC proliferation and milk production due to a rapid increase in activity of MEC, often followed by proliferation of secretory tissue (Capuco *et al.*, 2003; Boutinaud *et al.*, 2004).

Around calving time 83 % of the mammary gland is epithelial, at day 90 of lactation only 79 % are epithelial and during late lactation the number of secretory epithelial cells in the gland decreases to 73 %. Studies with three times daily milking over a period of 37 weeks show an increase in milk yield of 47 % and an increase in parenchyma mass of 34 % (Capuco *et al.*, 2003).

1.3.3 Involution

When milk accumulates within the mammary gland, it becomes engorged which leads to an increased intra-mammary pressure which in turn results in a decrease in blood flow to the mammary gland. Consequently, local concentrations of hormones and nutrients supplied by the blood stream are decreased. Furthermore, possible inhibitory factors within the milk may become more concentrated.

As a result, the mammary gland loses its ability to produce milk due to morphological changes (Mielke, 1986) and, in rodents, an extensive lobular-alveolar remodelling process occurs (Marti *et al.*, 1994). Changes in pattern of gene expression lead to a switch from MEC survival to death signalling and, thus, the mammary gland returns to a mature virgin-like state by replacing parenchyma

tissue with connective and adipose tissue (Mepham, 1987; Marti *et al.*, 1994; Marti *et al.*, 1999; Kumar *et al.*, 2000; Marti *et al.*, 2001; Strange *et al.*, 2007).

Involution can occur gradually after peak lactation which leads to a progressive regression in the lactating mammary gland. Senile involution leads to regression in milk production over several lactation cycles due to aging. However, the form of involution most investigated is initiated by the sudden cessation of milking, usually after peak lactation (Mepham, 1987; Hurley, 1989; Marti *et al.*, 1994; Marti *et al.*, 1999; Marti *et al.*, 2001; Strange *et al.*, 2007).

The majority of studies investigating the involution process used rodent models and the following paragraphs will outline the process of involution as described in the literature according to observations in rodents. The process of involution occurs in two stages. First stage is reversible and characterised by a down-regulation of milk protein expression and extensive apoptosis of MECs without major changes in the mammary gland architecture. Usually essential for tissue homeostasis, an up-regulation of apoptosis occurs during involution due to a decrease in survival factors and an increase in pro-apoptotic factors which triggers up to 80 % of epithelial cells to undergo apoptosis (Marti *et al.*, 1994; Rosfjord & Dickson, 1999; Marti *et al.*, 2001). However, overall during the first stage of involution the integrity of the alveolar wall remains intact and lactation can be re-initiated by re-milking and/or return of the young (Baxter *et al.*, 2007). Expression of milk protein genes, such as α_{S1}-casein and β-casein, is down-regulated, while proteins such as sulphated glycoprotein-2, tissue inhibitor of metalloproteinases-1, interleukin-1β converting enzyme, cell cycle control

proteins (e.g. c-jun, junb, jund, c-fos, c-myc) and death inducers (e.g. bax and bak) are up-regulated (Li *et al.*, 1997).

The second stage of involution is irreversible, requires systemic factors and is associated with degradation of the BM, collapse of the alveoli, infiltration of macrophages, re-differentiation of adipocytes, and reconstruction of the gland to a mature pre-pregnancy state (Talhouk *et al.*, 1992; Lund *et al.*, 1996; Li *et al.*, 1997; Baxter *et al.*, 2007). The expression of matrix metalloproteinases, including gelatinase A and stromelysin-1, and serine protease urokinase-type plasminogen activativator is up-regulated (Lund *et al.*, 1996; Mott & Werb, 2004).

In contrast to most other mammalian species, cows are usually pregnant during the dry period. Therefore, elevated reproductive mammogenic hormone levels delay the involution process. Consequently, during the entire phase of involution the alveolar structure remains intact. No major rejection of epithelial cells into the lumen or loss of contact to the BM occurs (Capuco & Akers, 1999). However, Capuco (2003) suggested that a dry period of at least 40 to 60 days is necessary to replace senescent cells and renew the population of mammary cell progenitors to ensure sufficient milk yield in the subsequent lactation period. Even though, comparing cows with and without a dry period at the onset of the subsequent lactation period, both have the same amount of MEC. At mid-lactation, however, fewer cells are present in the gland without a dry period. Consequently, subsequent milk production may be reduced by as much as 20 % without a dry period (Capuco & Akers, 1999).

Nonetheless, during the first 24 h of milk accumulation a number of physiological changes occur within the bovine mammary gland similar to the initial phase in rodents, albeit at a much slower rate. At around 16 to 18 h post-milking the rate of milk secretion declines, mammary blood flow decreases, TJ become more permeable, lactose efflux occurs, intra-mammary pressure increases and an inflammatory response is initiated (Davis *et al.*, 1999). Furthermore, if mammary engorgement is not relived, these physiological changes are intensified and eventually will lead to progressive induction of regenerative involution replacing senescent cells with mammary cell progenitors (Capuco *et al.*, 2003). Furthermore, within 24 h post-milking changes in gene expression related to the involution process will occur which will lead to further reduction in milk secretion (Singh *et al.*, 2005; Singh *et al.*, 2008).

1.4 Mechanobiology

Although little is known about the role of mechanobiology in the bovine mammary gland, previous research suggests that mechanotransduction may play a role in the initiation of mammary involution (Davis *et al.*, 1999). Furthermore, in other cell types it has been shown that cells experience a variety of mechanical forces. These are either exogenous, e.g. gravity as an ubiquitous force, or endogenous, e.g. tensile muscular forces that act on bones through tendons, compressive loads on cartilage, shear stress on vessels due to blood flow, cyclic stretch and mechanical forces from blood flow, and surface tension on lung tissue (Orr *et al.*, 2006; Wang & Thampatty, 2006; Reichelt, 2007; Schwartz & DeSimone, 2008; Jaalouk & Lammerding, 2009).

Moreover, it is generally accepted that tissues grow and remodel in response to changes in mechanical forces. These mechanical forces play a fundamental role in regulation of cell function, including gene induction, protein synthesis, cell growth and death, cell morphology and differentiation, which are essential for tissue homeostasis. Conversely, abnormal mechanical loading conditions alter cellular functions and change the structure and composition of the ECM. Therefore, depending on their respective needs, tissues constantly adapt to the environmental mechanical stress by modulating sensitivity to exogenous stimuli (Huang & Ingber, 1999; Chen *et al.*, 2004; Wang & Thampatty, 2006; Reichelt, 2007; Jaalouk & Lammerding, 2009; Gjorevski & Nelson, 2011). For example, as reviewed by Nelson & Bissell (2006), MECs respond to the stiffness of their matrix environment by altering their differentiation and/or developmental state (Nelson & Bissell, 2006).

Consequently, it is important for cells to sense and to transform a mechanical stimulus into a cascade of cellular and molecular events, a mechanism termed mechanobiology or mechanotransduction. Moreover, adhesive mammalian cell types, like MECs, require adhesion and spreading on a solid substratum (i.e., anchorage-dependence) for cell communication to receive signals from neighbouring cells or the ECM. Loss of ECM contact triggers anoikis (i.e., cell death due to loss of cell adhesion) and tissue regression in anchorage dependent tissues like the mammary gland will occur (Wernig *et al.*, 2003; Orr *et al.*, 2006; Reichelt, 2007).

The transduction of physical forces appears to occur through changes in protein conformation. The effects of internal or external forces are generally similar, indicating that the force per se across specific structures is sensed origin-independent (Schwartz, 2010). These force-induced effects on conformation change represent a general mechanism which may regulate enzymatic activity, enable new molecular interactions, or liberate soluble bond factors which in turn may activate signalling pathways in an autocrine and paracrine fashion. This ability to react to environmental triggers appears to distinguish a fundamental mechanism whereby cells sense, integrate and coordinate responses to combined physical and chemical signals (Huang & Ingber, 1999; Orr *et al.*, 2006; Wang & Thampatty, 2006; Reichelt, 2007; Schwartz & DeSimone, 2008; Jones & Nauli, 2012). For example, lengthening of the ECM protein fibronectin due to tension exposes cryptic binding sites and mechanical stretching of immobilised fibronectin induces matrix assembly by exposing self-assembly sites (Smith *et al.*, 2007).

In order to explain how a cell senses and responds to an adhesion-based mechanical stress a model for architectural building systems was applied to cells and further developed by Ingber (1993, 1997). This was termed the 'tensegrity' model (tensional integrity) (Ingber, 1993; Ingber, 1997). According to this model the cytoskeleton provides the cell with a pre-tension that is necessary to respond to mechanical stimuli. Tensegrity relies not only on the cytoskeleton, but also on the cell's adhesion structures that link cytoskeleton to the ECM and probably additional proteins that provide a link to the nucleus (Reichelt, 2007; Jones & Nauli, 2012). Initial interaction and mechanosensing events occur within seconds. However, early cellular responses take up to minutes and involve cytoskeletal redistribution, reinforcement of linkages and changes in cell motifs (Vogel & Sheetz, 2006). For example, studies have shown that changes in cell shape (i.e. shape-dependence) due to mechanical stress correlates with several changes in gene expression, especially for proteins of cytoskeleton, proliferation, transcription, translation, ECM-production, and inter- and intracellular signalling complexes (Huang & Ingber, 2000).

However, it is worth noting that not all forms of mechanotransduction take place at cell adhesions. Non-adhesion-based mechanotransduction occurs at mechanosensitive protein channels with a huge structural diversity driven by the physiological necessity to detect mechanical stimuli from thermal energy to high pressure as changes in conductivity (Vogel & Sheetz, 2006). These protein channels are able to transform a physical signal (e.g. shear stress applied onto the plasma membrane) into an ion flux, such as Ca^{2+} influx, due to channel

opening by a force-dependent conformational change (Chen *et al.*, 2004; Vogel & Sheetz, 2006; Reichelt, 2007; Jones & Nauli, 2012).

1.4.1 The role of integrins, tight junctions, and primary cilia as mechanosensors

Major cellular components involved in mechanotransduction are integrins, the cytoskeleton, G proteins, receptor tyrosine kinases, mitogen-activated protein kinases, TJs, PC and stretch-sensitive channels. The focus for this work will be on integrins, PC and TJs. Although the three potential mechanosensors are all connected through the cytoskeleton, it is the interaction between them and the number of adhesions to the substrate that diffuses the magnitude of the stress throughout the cell. In general, the conformational change in response to an applied force initiates a cascade of biochemical events inside the cell (Nelson & Gleghorn, 2011).

1.4.1.1 Integrins

Integrins appear to be the main mechanoreceptors that link the ECM with the cytoskeleton. They are localised within the focal adhesion complexes (FACs). Integrins contain a large ECM domain responsible for binding to multiple components of the matrix including fibronectin and collagen, a single transmembrane domain containing alpha and beta subunits, and a cytoplasmic domain which binds to the cytoskeleton (Fig. 1.6). Hence, integrins serve as adhesive receptors and mechanotransducers by transmitting and amplifying signals across the membrane after binding their ECM ligands. This ability allows

for an uninterrupted passage of extracellular mechanical signals to the cytoskeleton and contributing to gene expression (Maniotis *et al.*, 1997; Zamir & Geiger, 2001; Orr *et al.*, 2006; Wang & Thampatty, 2006; Schwarz & Gardel, 2012; Glukhova & Streuli, 2013).

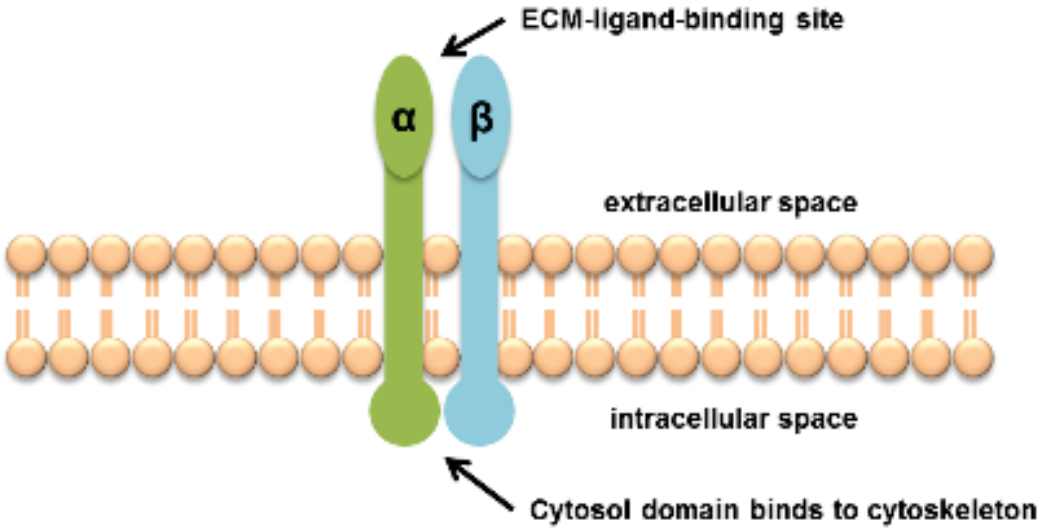

Figure 1.6 Schematic representation of the basic structure of the integrin, a cell surface receptor. Integrins contain a large extracellular matrix (ECM) domain responsible for binding to multiple components of the matrix including fibronectin and collagen, a single transmembrane domain containing alpha and beta subunits, and a cytoplasmic domain which binds to the cytoskeleton

Furthermore, integrins are able to recruit kinases to activate different intracellular pathways and to cluster a set of cells' 'unoccupied' integrins which induces their binding to the ECM proteins (Fig. 1.7). The integrin clustering mechanism probably adjusts adhesion strength, since rupture of a single-band does not result in failure of attachment (Schwartz & DeSimone, 2008; Schwarz & Gardel, 2012).

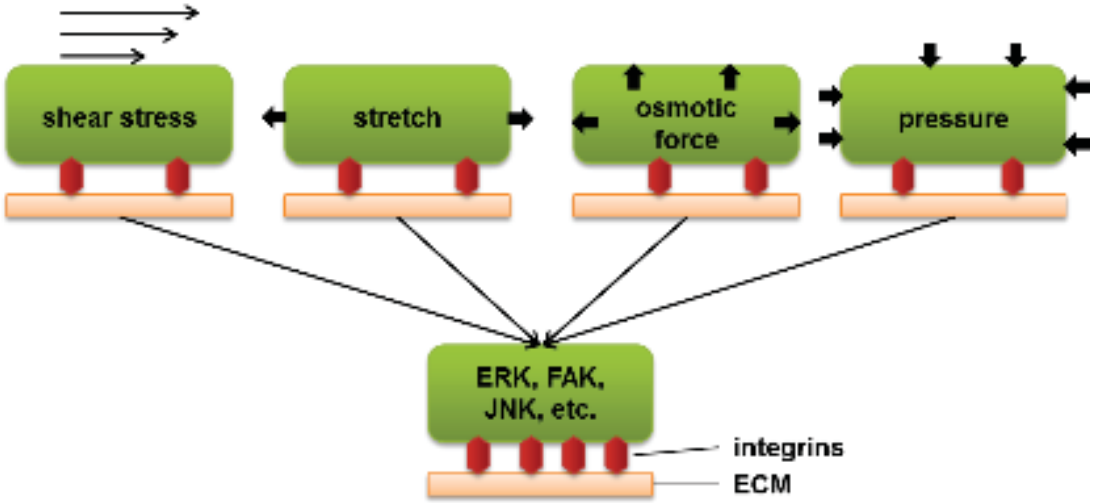

Figure 1.7 Schematic of common mechanical forces acting on cells in vivo. Numerous types of mechanical stimuli may trigger integrins to recruit 'unoccupied' integrins into clusters which induces their binding to the ECM to strengthen adhesion and to ensure attachment during applied forces. Despite different origins of mechanical stimuli, subsequently similar signalling pathways are activated which share common responses, such as FAK, JNK and ERK activation. Abbreviations: ECM: extracellular matrix; FAK: focal adhesion kinase, ERK: extracellular-signal-regulated kinases, JNK: c-Jun N-terminal kinases

1.4.1.2 Tight junctions

With the formation of TJs, a focal point for mechanical stress is generated which enables adjacent cells to communicate cytoskeletal changes caused by mechanical stimuli (Jones & Nauli, 2012). Moreover, two different pathways have been identified that regulate selective movement of solutes across the epithelium that may be altered by mechanical forces. One pathway is a system of charge selective claudin-based pores that only allow paracellular transport of solutes below 2 nm in diameter. A second pathway lacking charge or size discrimination is created by larger discontinuities in the TJ barrier properties (Anderson & Van Itallie, 2009; Tarbell, 2010).

In-vitro experiments using epithelial and endothelial cells exposed to either shear stress or stretch showed increased levels of occludin phosphorylation and changes in occludin content in a time-dependent manner which in turn increases TJ permeability (Cavanaugh *et al.*, 2001; DeMaio *et al.*, 2001; Rao, 2009; Tarbell, 2010; Michaelson & Huang, 2012). Hence, even in fully polarised cells TJs are highly dynamic protein complexes able to rearrange without losing their adhesive strength or barrier properties (Niessen, 2007). This ability to change properties is important in the mammary gland at different stages of the lactation cycle. During pregnancy, mammary TJs are 'leaky', undergoing conformational changes around parturition which lead to a closure to prevent mixing of the milk constituents and the interstitial fluid (Itoh & Bissell, 2003). Furthermore, reduced milking frequency, weaning of the offspring and cessation of milking result in increased permeability of TJs (Stelwagen, Davis, Farr, Eichler*, et al.*, 1994; Stelwagen *et al.*, 1997).

Additionally, previous studies showed that milk stasis induces local serotonin synthesis in the mammary epithelium leading to further TJ opening post-milking which in turn causes involution-related morphological changes acting as a feedback inhibitor of lactation in the bovine mammary gland (Hernandez *et al.*, 2009; Hernandez *et al.*, 2011). Also, increased TJ permeability due to increased intra-mammary pressure leads to serotonin relocation from the basolateral to the apical side which in turn results in a negative, autocrine-paracrine feedback loop (Matsuda *et al.*, 2004).

1.4.1.3 Primary cilium

The PC appears to be a key signalling organelle for sensing a number of biochemical and biophysical extracellular stimuli. It has several characteristics that position it in an ideal cellular location for sensing and transducing signals. Protrusion into the extracellular space enables access to environmental signalling molecules, and its elongated geometry provides a high surface-to-volume ratio, while the regulated entry of proteins into the cilium leads to specialisation and compartmentalisation (Singla & Reiter, 2006; Hoey *et al.*, 2012). However, the ability to sense and transduce signals depends on its mechanical properties. The PC has the capability to dynamically modify its length and fine tune its sensitivity to extracellular environment which in turn may alter the responsiveness to biochemical and mechanical stimuli (Abou Alaiwi *et al.*, 2009; Christensen *et al.*, 2012; Hoey *et al.*, 2012). As a consequence, the PC has emerged as a mechanosensor in numerous tissues, such as bone, liver, kidney and lungs, sensing not only fluid flow, but also mechanical signals, such as pressure, touch and vibration. Although the exact mechanisms of mechanotransduction are still unknown, alterations in PC length, deflection of the cilium and possible other mechanical properties and features may be central mechanisms for regulating cellular mechanosensitivity (Abou Alaiwi *et al.*, 2009; Hoey *et al.*, 2012).

Mechanical forces imposed upon a cellular network tend to initiate changes in the levels of intracellular calcium (Fig. 1.8). The PC contributes to this response by amplifying mechanical cues through a two-step process: 1) immediate response, the ciliary bending and subsequent activation of the polycystin-complex leads to an increase in intracellular calcium and 2) long-term response, mediated through cellular adaption and cytoskeletal rearrangements (Abou Alaiwi *et al.*, 2009; Jones & Nauli, 2012).

Additionally, the basal body directly links the PC to the cytoskeleton providing an interaction with integrins (Poole *et al.*, 1997; McGlashan *et al.*, 2006), TJs and the ECM (Poole *et al.*, 1985; Alenghat *et al.*, 2004). Thus, the direct interaction between the PC and the cytoskeleton provides an uninterrupted connection between the ECM and intracellular remodelling responses (Jones & Nauli, 2012).

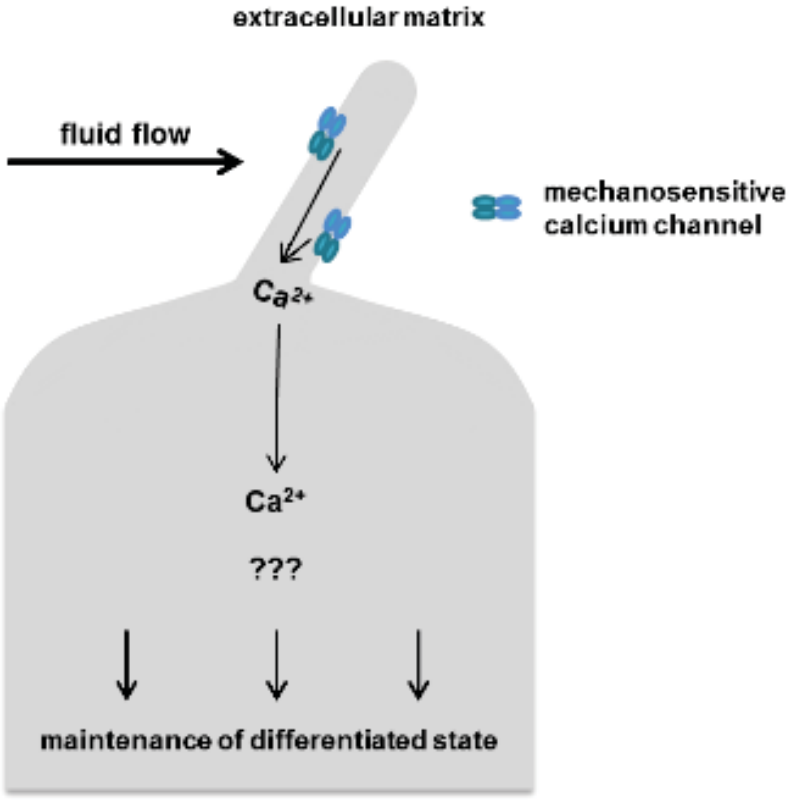

Figure 1.8 Response pathway of primary cilia to fluid-flow-induced bending. Upon mechanical stimulation, such as fluid flow, resulting in a bent primary cilium, stretch-sensitive ion channels are activated leading to a calcium-influx and a subsequent increase in intracellular calcium. Intracellular calcium in turn plays an important role in the regulation of cytoskeletal proteins, cell adhesion, morphology and motility

Previous studies showed that a mechanosensory complex preferentially located at the base of the PC is the mediator of the calcium response within the kidney (Nauli *et al.*, 2003). Fluid flow in the kidney causes a deflection of the PC which in turn activates the complex of two membrane bound proteins (PC-1 and PC-2) resulting in an extracellular calcium influx which acts as a messenger

molecule for control of cell growth and differentiation (Nauli *et al.*, 2003). This extracellular calcium influx, in turn, induces release of additional calcium from the intracellular store via a ryanodine-sensitive mechanism that further amplifies the response (Nauli *et al.*, 2003). In addition, the cilium is firmly anchored to the cell through the basal body and it would experience large movements at its base. Hence, mechanical loads from the ECM are transferred through the cilium to the underlying cytoskeleton regulating the activity of sodium channels and converting the mechanical stimuli into a rapid electrical response (Singla & Reiter, 2006; Abou Alaiwi *et al.*, 2009; Satir *et al.*, 2010; Yuan *et al.*, 2010; Hoey *et al.*, 2012; Jones & Nauli, 2012).

The PC-1 and PC-2 comprise a mechanosensitive heterodimeric calcium channel from the family of transient receptor potential (TRP) ion channels regulating calcium entry and activity. Furthermore, PC-2 is also found in numerous intracellular compartments with its highest concentration in the endoplasmic reticulum. The C-terminal domain of PC-2 contains an endoplasmic reticulum retention sequence that prevents membrane trafficking in the absence of PC-1 (Newby *et al.*, 2002). Previously, Nauli *et al.* (2003) showed that blocking the PC-1 function inhibits the PC-2 mediated intracellular calcium mobilisation. Therefore, the mechanosensing ability of the PC is important and defects in the structure, assembly or function may result in congenital diseases, termed ‘ciliopathies’, such as polycystin kidney disease or arthritis (Badano *et al.*, 2006).

1.4.2 Mechanotransduction in *in vitro* studies

Over the past decades, research in mechanotransduction has expanded from sensory cell studies, such as hair cells in the inner ear, to diverse cell types, including smooth muscle cells, MECs and several alveolar type cells, which indicates its involvement in a broad range of cellular functions (Table 1.1). Generally *in vitro* studies examine the mechanical state of a cell by changing the rigidity of the substrate to which cells adhere, the magnitude of force the cells are exposed to, or the ability of a cell to generate intracellular forces by adding agents that interact with the cytoskeletal filaments (Chen *et al.*, 2004).

It is worth noting that physical forces that act upon cells are often described by terms, such as ‘stretch’ or ‘distension’. However, the term ‘stress’ can be defined more accurately as force per unit of area, while ‘strain’ is any forced change in length in relation to the initial length. Stress itself can be subdivided into ‘shear stress’ (force is parallel to the plane), ‘compressive stress’ (stress is directed toward the part on which it acts) and ‘tensile stress’ (stress is directed away from the part on which it acts) (Garcia *et al.*, 2006). Furthermore, different types of stress can act upon the same cell, e.g. hydrostatic pressure acts on the apical surface of a MEC, while strain acts upon the basolateral side of one cell. Therefore, different types of mechanical stimuli that act on the same cell may activate different pathways to mediate different biological functions (Eyckmans *et al.*, 2011).

Exactly how a cell senses different types of mechanical stimuli and converts it into a distinct biochemical signal to control various cellular functions is not well

understood. However, most studies have focused on stretch-sensitive ion channels and ECM-integrin-cytoskeleton pathway as mechanosensors (Alenghat *et al.*, 2004; Chen *et al.*, 2004; Garcia *et al.*, 2006; Vogel & Sheetz, 2006; Reichelt, 2007).

Zhang (2003) showed that changes in the ECM, e.g. caused by injury or inflammation, would change the intestinal CaCo2 epithelial cells response to stretch(Zhang, Li, Sumpio*, et al.*, 2003). While human intestinal epithelial cells grown on type I collagen, type IV collagen and laminin coating would increase activation levels of p38 kinases and c-Jun N-terminal kinases upon applied strain, whereas cells grown on fibronectin showed no change in either activation level (Reichelt, 2007). Moreover, Fujita (2010) demonstrated that an increase in activation of p38 kinase and extracellular-signal-regulated kinases in ureteric bud cells grown on type I collagen occurred in a stretch-dependent manner (Fujita *et al.*, 2010).

Stretch experiments with different types of epithelial cells showed that not only ECM remodelling occurs and β1-integrin is up-regulated in order to adjust the cells' adhesion strength (Wernig *et al.*, 2003), but cell stretch also mediates reorganisation of the cytoskeleton to possibly improve transmission of information between the ECM and the cell (Cavanaugh *et al.*, 2001; DiPaolo *et al.*, 2010; Koshihara *et al.*, 2010). Moreover, Provenzano (2009) tested different levels of matrix stiffness and showed that high matrix stiffness promotes increased activation levels of FA kinase and cell proliferation (Provenzano *et al.*, 2009).

Overall, several stretch experiments have shown that stretching different types of epithelial cells attached to a substratum elevated levels of proliferation and apoptosis in a stretch-dependent manner. These results indicate that cell stretch may cause cell turnover in order to replace senescent cells for homeostasis. In cases where homeostasis cannot be maintained, uncontrolled cell growth may cause tumorous growths which can cause cancer (Tschumperlin *et al.*, 2000; Zhang, Li, Sanders*, et al.*, 2003; Hammerschmidt *et al.*, 2005; Ali *et al.*, 2006; Chaturvedi, Marsh, & Basson, 2007; Craig *et al.*, 2007; Hammerschmidt *et al.*, 2007; Mohan *et al.*, 2007; Amura *et al.*, 2008; Gayer, Chaturvedi, Wang, Alston*, et al.*, 2009; Gayer, Chaturvedi, Wang, Craig*, et al.*, 2009; Koshihara *et al.*, 2010).

Quaglino *et al.* (2009) demonstrated that stretching murine MECs *in vitro* leads to an initial switch from survival to apoptotic mode. Weaning-like events were reproduced which are comparable to *in vivo* actions occurring during the involution process with the use of flexible membranes with type I collagen coating. Although the cell stretch experiment itself was not able to trigger the entire apoptotic program, it initiated the process by increasing levels of apoptotic factors and decreasing levels of survival factors respectively (Quaglino *et al.*, 2009).

Praetorius and Spring (2001) showed that the PC responds to bending stimuli with an extracellular calcium influx which in turn causes calcium-induced calcium release from intracellular stores. Furthermore, these researchers showed that the increase in intracellular calcium spreads to neighbouring cells through the gap junctions in a wave-like manner mediating events within the tissue (Praetorius & Spring, 2001).

Table 1.1 Summary of cell responses to mechanical stimuli in various stretch experiments, cpm: cycles per minute (1 cycle = stretch + relaxation)

Cell Type	Type of force/load/duration	Surface coating	Cell response	Reference
Chondrocytes, wild-type, IFT88^{orpk} mutant, murine	Compression force of 15 %; 60 cpm; 1 h	5x5 mm cyclindrical agarose gels	No mechanosensitive activation of Ca^{2+} signalling, loss of ATP-mediated Ca^{2+} signalling	(Wann *et al.*, 2012b)
Gastric mucosal cell line, murine, GSM06	5 to 10 %, 5 cpm, 60 h	Type I collagen	Impaired cell migration and wound healing in strain strength-dependent manner	(Osada *et al.*, 1999)
Amnion epithelial cells, human	11 %, static conditions, 0 to 6 h	Type I collagen	NF-κB and AP-1 activation levels increased	(Mohan *et al.*, 2007)
Intestinal epithelial cells, caco2, human	10 %, 10 cpm or static conditions, 24 h	Type I collagen	FAK and SRC phosphorylation increased, cell proliferation increased	(Chaturvedi, Marsh, & Basson, 2007)
Intestinal epithelial cells, caco2, human	10 %, 10 cpm or static conditions, 1 h	Type I collagen	ERK1/2 activation increased, cell proliferation increased	(Craig *et al.*, 2007)
Intestinal epithelial cells, caco2, human	10 %, 10 cpm or static conditions, 24 h	Type I collagen	PI3K and AKT activation increased, cell proliferation increased	(Gayer, Chaturvedi, Wang, Alston, *et al.*, 2009)
Intestinal epithelial cells, caco2, human	10 %, 10 cpm, 0 to 60 %	Fibronectin	Cell migration increased	(Gayer, Chaturvedi, Wang, Craig, *et al.*, 2009)
Intestinal epithelial cells, caco2, human	10 %, 10 cpm, 0 to 30 min	Type I collagen	Tyrosine-phosphorylation increased, like peptide growth factors	(Han, Li, *et al.*, 1998)

Table 1.2 Cont. Summary of cell responses to mechanical stimuli in various stretch experiments, cpm: cycles per minute (1 cycle = stretch + relaxation)

Cell Type	**Type of force/load/duration**	**Surface coating**	**Cell response**	**Reference**
Intestinal epithelial cells, caco2, human	10 %, 10 cpm, 24 h	Type I collagen	Tyrosine kinase activity increased, PKC activation increased, phoshorylation increased in soluble fraction	(Han, Sumpio*, et al.*, 1998)
Intestinal epithelial cells, caco2, human	10 %, 10 cpm, 24 h	Type I collagen	FAK-dependent and integrins-modulated MAPK activation increased (important for strain-associated proliferation	(Li *et al.*, 2001)
Intestinal epithelial cells, caco2, human	10 %, 10 cpm, 0 to 30 min	Type I and Type IV collagen, laminin, fibronectin	Collagens and laminin: cell proliferation increased, FAK; ERK and JNK activation increased, fibronectin: no effect	(Zhang, Li, Sumpio*, et al.*, 2003)
Intestinal epithelial cells, caco2, human	10 %, 10 cpm,	Type I and Type IV collagen, laminin, fibronectin	Collagens and laminin: cell proliferation increased, FAK; ERK and JNK activation increased, fibronectin: no effect	(Zhang, Li, Sanders*, et al.*, 2003)
Kidney epithelial cells, wild-type, murine	Shear stress with flow rate at 0.75 dyn/cm^2	parallel- plate flow chamber	Increase in intracellular Ca^{2+} levels, drug-induced cytoskeleton modulation prohibited cilia-mediated mechanosensation	(Alenghat *et al.*, 2004)
Mammary epithelial cells, murine, HC11	0 to 30 % biaixial strain, static, 15 min to 3 h	Type I collagen	Reduction of survival factors, activation of apoptotic factors	(Quaglino et al., 2009)
MDCK cells, kidney, canine	Flow rate from 0 to 8 µl/sec	custom-designed flow chamber	Increase in intracellular Ca2+ levels, calcium-induced calcium release from intracellular stores	(Praetorius & Spring, 2001)

Table 1.3 Cont. Summary of cell responses to mechanical stimuli in various stretch experiments, cpm: cycles per minute (1 cycle = stretch + relaxation)

Cell Type	Type of force/load/duration	Surface coating	Cell response	Reference
Mammary epithelial cells, murine, MCF10A TF7D, MDA-MB-23, NMuMG	10 %, static, 20 min	Type I collagen	FAK activation increased, high matrix stiffness promotes cell proliferation	(Provenzano *et al.*, 2009)
Porcine ERM cells	18 %, 30 cpm, 60 min	Type I collagen	Remodelling of actin filaments, increase in cell proliferation	(Koshihara *et al.*, 2010)
Primary alveolar type II cells, rat	25 % or 37 %, 15 cpm, 1 h	Fibronectin	Perturbed occluding distribution and overall expression, ATP reduction in cultured cells	(Cavanaugh *et al.*, 2001)
Primary alveolar type II cells, rat	15 % biaxial stretch, 10 cpm, 0 to 24 h	Cell-derived matrix	Impaired wound healing and cell migration, cell proliferation reduced, apoptosis increased	(Crosby *et al.*, 2011)
Primary alveolar type II cells, rat	12, 25, or 37 %; 15 cpm or static conditions; 1, 10 or 60 min	Fibronectin	Actin cytoskeleton rearranges in a magnitude- and frequency-dependent manner	(DiPaolo *et al.*, 2010)
Primary alveolar type II cells, rat	30 %, 40 cpm, 24 h	Fibronectin	Impaired PI3K-AKT-bad pathway, reduction of BCL-2 content, apoptosis rate increased	(Hammerschmidt *et al.*, 2007)
Primary alveolar type II cells, rat	25 %; 37 %; 50 %, static conditions, 1 h	Fibronectin	Induced cell death in magnitude- and amplitude- dependent manner	(Tschumperlin *et al.*, 2000)

Table 1.4 Cont. Summary of cell responses to mechanical stimuli in various stretch experiments, cpm: cycles per minute (1 cycle = stretch + relaxation)

Cell Type	**Type of force/load/duration**	**Surface coating**	**Cell response**	**Reference**
Primary liver cyst epithelial and endothelial cell line, murine, MZ-CHA	5 %; 7.5 %; 10 %; 15 %; 20 %, every 5 h applied strain increased, 20 cpm, 25 h	Silicon-elastomer	Cell proliferation increased, IL-8 synthesis increased	(Amura *et al.*, 2008)
Primary aortic endothelial cells, bovine	shear stress at flow rate of 10 and 20 dyn/cm^2, 3 h	Glass slides	Increase in occludin phosphorylation, decrease in occludin expression over 1 to 4 h	(DeMaio *et al.*, 2001)
Pulmonary artery endothelial cells, bovine	25 %, 15 cpm (3s stretch/1s relaxation), 0 to 6 h	Silicone-elastomer	FAK and PKC activation increased, induced inflammatory response	(Ali *et al.*, 2006)
Smooth muscle cell, rat	20 %, 30 cpm, 6 to 12 h	Type I collagen	Apoptosis rate increased, endothelin B receptor mRNA increased (associated with apoptosis induction)	(Cattaruzza *et al.*, 2000)
Smooth muscle cells, rat	7 or 15 % strain, 60 cpm, 48 h	Type I collagen	Induction of ECM protein synthesis and apoptosis, β1-Integrin upregulated	(Wernig *et al.*, 2003)
Ureteric bud cells, murine	20 %, 20 cpm, 10 min to 48 h	Type I collagen	P38 and ERK activation increased (in stretch-dependent manner), cell proliferation and apoptosis increased	(Fujita *et al.*, 2010)

AKT: Protein Kinase B; **AP-1**: activator protein 1; **ERK**: extracellular-signal-regulated kinases; **ERM**: epithelial rests of Malassez; **FAK**: Focal Adhesion Kinase; **IL-8:** Interleukin-8; **JNK**: c-Jun N-terminal kinases; **MAPK**: Mitogen-activated protein kinases; **NFκB**: nuclear factor kappa-light-chain-enhancer of activated B cells; **PI3K**: Phosphatidylinositol 3-kinases; **PKC**: Protein Kinase C; **Src**: Proto-oncogene tyrosine-protein kinase

1.5 Objective of this study

The primary goal of this research is to determine the potential effects of bovine mammary epithelial cell stretch and change in cell shape due to mammary gland engorgement on lactation at the onset of involution in dairy cattle. In particular, the role of physical distension of the mammary epithelium and the mechanisms involved in cell sensing for the initiation of apoptosis and mammary gland involution will be investigated in this research. The hypotheses to be examined are 1) that mechanosensors play a fundamental role in the initiation of the involution process, and 2) that the change in MEC shape from a cuboidal to a flattened/stretched morphology leads to compromised cell-cell and cell-matrix contacts which in turn triggers the onset of mammary apoptosis and involution. The main focus of this research will be on three potential mechanosensors: TJs, FAs and PC, and their role in the regulation of local mammary function in response to mechanical stimulation.

Cell-cell and cell-matrix junctions provide tissue integrity, promote cell polarity, guarantee sufficient communication between cells to ensure synchronised milk secretion and support cell survival. Their disruption may be one of the early initiators of the mammary gland remodelling process. Therefore, this research project consists of three experimental approaches for examining the influence of cell stretch on mammary epithelial cells: *in vitro* cell stretch experiments, an *in vivo* dairy cattle infusion experiment and an *in vivo* dairy cattle re-milking experiment.

In the first study, the presence of PC following extended periods of non-milking and their potential role in the initiation of the involution process in dairy cattle will be determined *in vivo*. For that purpose, an immunofluorescent dual-staining method was applied to specifically detect PC in the mammary gland. Furthermore, to gain a better understanding of the potential role of the STAT6 transcription factor as part of the PC signalling pathway, gene and protein expression levels will be determined.

In the second study, an *in vitro* approach using a homemade cell stretching device, which clearly separates the effects of physical stretching of MECs from the actions of possible chemical inhibitors in milk, will be applied. The effect of stretching MECs *in vitro* on the expression of TJ proteins and FAs will then be determined.

Finally, in an *in vivo* study, the effect of acute physical distension of the bovine mammary gland on changes in MEC sensing and signalling, and the initiation of the involution process, will be determined. Bovine mammary glands will be artificially distended, using a sterile, isosmotic saline solution, in order to investigate changes in cellular signalling pathways associated with mammary cell survival, such as TJ integrity or β1-integrin disruption *in vivo*.

Therefore, this project aims to improve our understanding and knowledge of the role of mechanotransduction events in late lactation, in particular, in the regulation of local mammary function in the initiation of mammary involution.

Chapter 2:

Primary Cilia: Potential Mechanosensors in the Bovine Mammary Gland

Chapter 2 Introduction

Tissue function arises from the highly coordinated, yet extremely dynamic behaviour of cells and their surrounding network of scaffolding proteins in a time- and space-dependent manner (Aumailley & Gayraud, 1998; Alberts *et al.*, 2002; Nelson & Bissell, 2006; Badylak *et al.*, 2009). A perfect example of this dynamic process is the mammary gland, which is composed of different tissues and repeatedly undergoes the phases of lactation: growth, functional differentiation, lactation, and regression (Anderson, 1985; Akers, 2002; Hurley & Loor, 2011). Consequently, cells need to sense and transform the various forms of external stimuli they receive through interactions with the ECM, neighbouring cells, and soluble cues from the microenvironment into a cascade of cellular and molecular events (DuFort *et al.*, 2011). However, there are important differences between force-generated or mechanical signalling (e.g. bending of the primary cilium) and chemical signalling (e.g. soluble signals, such as growth factors) (Wells, 2013). Mechanical signals can be highly directional and thereby convey and transmit complex information directly in three dimensions. Soluble factors, on the other hand, diffuse radially, provide limited directional information and require translation into secondary messengers. Consequently, unlike soluble signals, force-mediated signals can be started and stopped quickly, allowing increased control in time (Wells, 2013). Moreover, stress-induced signal transduction is at least 40 times faster than growth factor-induced signal transduction (Na *et al.*, 2008).

The transduction of physical forces appears to occur through changes in protein conformation (Schwartz, 2010). These force-induced effects on conformational change represent a general mechanism which may regulate enzymatic activity, enable new molecular interactions, open mechanosensitive protein channels, or liberate soluble bound factors which in turn may activate signalling pathways in an autocrine and/or paracrine fashion (Hoey *et al.*, 2012; Jones & Nauli, 2012). Therefore, mechanical and chemical signals are often interdependent (Wells, 2013). Hence, mechanical forces can act directly and indirectly on chemical signals, but seem to exceed the speed of signalling through soluble factors by several orders of magnitude (DuFort *et al.*, 2011; Wells, 2013).

Nonetheless, the mechanical forces experienced by cells are generally small. Therefore, the force sensor must either be much softer than the typical protein complex, or highly elongated and projected into the environment in order to sense and/or amplify the force experienced (Janmey & McCulloch, 2007).

2.1 Primary cilium

The primary cilium appears to be a key signalling organelle for sensing a number of biochemical and biophysical extracellular stimuli. It has several characteristics that indicate it is an ideal cellular organelle for sensing and transducing signals in a number of organs and tissues, such as kidney, pancreas, liver, cartilage, and bone. Protrusion into the extracellular space enables access to environmental signal reception, its elongated geometry provides a high surface-to-volume ratio, and the regulated entry of proteins into the cilium leads to specialisation and compartmentalisation (Singla & Reiter, 2006; Hoey *et al.*, 2012). Sensory modalities like mechanical stimulation (bending of the cilium), chemosensation (detection of a specific ligand, growth factor, hormone or morphogen), or in some cases stimulation by light, temperature, osmolality, or gravity are achieved by a bilayered lipid membrane that is continuous with the plasma membrane of the cell body, but contains a distinct subset of receptors and other proteins involved in signalling (Veland *et al.*, 2009; Jones & Nauli, 2012). Hence, the primary ciliary membrane is enriched for a number of receptors and ion channels, including PC-1 and PC-2, receptor tyrosine kinases, G-protein-coupled receptors, receptors for extracellular matrix, transient receptor potential ion channels, as well as various transporter proteins (Veland *et al.*, 2009; Christensen *et al.*, 2012).

The presence of the PC is a cell cycle-dependent and dynamic process of assembly and resorption (Nguyen & Jacobs, 2013). During the interphase, assembly of the PC will occur on non-proliferating G0-G1 cells. Primary cilia arise from a basal body, derived from the mother centriole anchoring the cilium to cell's cytoskeleton as the IFT extends its length. The IFT particles and their associated

cargo proteins are transported along axonemal microtubules by kinesin-2 motor proteins in the anterograde (base-to-tip) direction, which delivers cargo to the growing tip, and by cytoplasmic dynein-2 in the retrograde (tip-to-base) direction (Satir & Christensen, 2007; Satir *et al.*, 2010). Resorption of the cilium occurs prior to mitosis and the cell's entry into the cell cycle (Nguyen & Jacobs, 2013).

The idea that the PC could play a fundamental role in sensing mechanical stimuli is not new. In fact, in 1961 it was suggested that immotile PC may retain a role in conducting and/or amplifying mechanical stimuli acting upon the elongated ciliary shaft extending from the apical cell surface in contrast to their motile relatives (Barnes, 1961). Furthermore, a close spatial interrelationship between PC, the secretory organelles, and the ECM has been revealed which indicated a potential role as a multifunctional, cellular probe (Poole *et al.*, 1985). This has been supported through several studies which demonstrated the potential role of PC in mechanotransduction in various tissues, such as kidneys and chondrocytes. The analysis of PC of various established kidney cell lines demonstrated PC bend in response to fluid flow (Roth *et al.*, 1988). This allowed the development of a mathematical model to calculate the PC bending as a cantilevered beam. This model supported the hypothesis that PC have a mechanosensory role via detection of fluid flow in kidney cells (Schwartz *et al.*, 1997). Further experimental evidence indicated that cilia were mechanically sensitive to fluid flow and served as part of a calcium signalling system (Praetorius & Spring, 2001). Additionally, a study working with chondrocytes provided more evidence that PC are essential for

mechanotransduction and the control of ECM secretion in response to physiological compressive strain. In particular, the chondrocyte primary cilium is required for ATP-induced Ca^{2+}signaling (Wann *et al.*, 2012a). In the bovine mammary gland, the presence of PC on myoepithelial cells as well as epithelial cells was first documented in 1989, suggesting a potential role as mechanosensor within the mammary gland (Nickerson, 1989).

2.1.1 Mechanotransduction at the primary cilium

Mechanical forces imposed upon a cellular network initiate changes in the levels of intracellular calcium. The primary cilium contributes to this response by amplifying mechanical cues through a two-step process: 1) immediate response, the ciliary bending and subsequent activation of the polycystin-complex lead to an increase in intracellular calcium, 2) long-term response, mediated through cellular adaption and cytoskeletal rearrangements (Poelmann *et al.*, 2008; Abou Alaiwi *et al.*, 2009; Jones & Nauli, 2012).

The polycystins are a family of membrane proteins divided into PC-1 and PC-2 topologies (Zhou, 2009). They comprise a mechanosensitive heterodimeric calcium channel from the family of TRP ion channels regulating calcium entry and activity. These TRP ion channels are divided into seven categories based on sequence homology and multimeric state (Newby *et al.*, 2002). PC-1 contains 11 putative transmembrane-spanning segments, is proposed to function as a G-protein-coupled receptor and its domain structure suggests that it acts as a cell-surface receptor in both cell-cell and cell-matrix interactions. PC-2, on the other

hand, contains six transmembrane-spanning domains and is presumed to form a cation-selective ion channel permeable to Ca^{2+}. Physical interaction between PC-1 and PC-2 is accomplished through their C-terminal cytoplasmic domains (Zhou, 2009).

Besides mediating the mechanosensitive calcium influx, in the absence of fluid flow PC-1 also undergoes post-translational processing, resulting in cleavage of the carboxy-terminal region (Berbari *et al.*, 2009). The carboxy-terminal region translocates to the nucleus where it associates with the transcription factor STAT6 and the co-activator P100 to stimulate gene expression (Low *et al.*, 2006; Berbari *et al.*, 2009).

2.1.2 STAT6/p100 pathway

A novel signalling mechanism has been revealed by which PC-1 regulates STAT6-dependent transcription in kidney cells (Low *et al.*, 2006; Olsan *et al.*, 2011). Studies showed that PC-1 undergoes proteolytic cleavage which releases the C-terminal half of the tail from the membrane. Subsequently, this fragment binds to the transcription factor STAT6 and its transcriptional co-activator p100 followed by nuclear translocation and activation of STAT6-dependent transcription (Low *et al.*, 2006; Olsan *et al.*, 2011). The STAT6 transcription factor is widely expressed in many tissues, including the mammary gland, where it has been shown to be important for alveolar differentiation and proliferation (Clarkson *et al.*, 2004; Low *et al.*, 2006; Khaled *et al.*, 2007). Furthermore, its co-activator p100 is strongly up-regulated in MECs during lactation (Broadhurst & Wheeler,

2001). Nevertheless, generally stimulated by a small group of cytokines, PC-1 appears to be a non-classical activator of STAT6 function in the mammary gland (Low *et al.*, 2006; Haricharan & Li, 2013). While mechanosensitive calcium signalling results in a fast and temporary cellular response, the STAT6-mediated signalling pathway was proposed to play a role in long-term responses to changes in fluid flow in kidney cells (Low *et al.*, 2006).

2.1.3 Objective

The aim of this study was to investigate the presence of PC and their potential role in the initiation of the involution process in dairy cattle. For that purpose, an immunofluorescent dual-staining method was applied to specifically detect PC in the mammary gland. The number and morphology of PC from each experimental group were then determined to analyse potential changes due to extended periods of non-milking. To gain a better understanding of the potential role of the STAT6 transcription factor, gene and protein expression levels were determined to detect changes in expression patterns following extended periods of non-milking.

2.2 Materials and Methods

2.2.1 Animal experiment

The tissue provided was collected by investigators at AgResearch, Ruakura, for a study of the effects of re-milking subsequent to extended non-milking periods (Singh *et al.*, 2012).

Briefly, 18 non-pregnant, primiparous Friesian cows (97±2 days in milk (DIM)) were randomly allocated to three groups (n=6/group). All cows were kept on pasture prior to the start of the experiment, and milked twice-daily. During the experiment, the different groups were subjected to non-milking (NM) intervals of 7 (7-d NM), 14 (14-d NM) and 28 (28-d NM) days followed by a period of re-milking twice a day for seven days prior to slaughter. The control group (0-d NM) was milked twice daily throughout the experiment until tissue collection. A systemic antibiotic was administered for three consecutive days prior to the non-milking intervals and to the re-milking to prevent mastitis (Singh *et al.*, 2012). All animal experimental procedures were conducted in compliance with the Ruakura Animal Ethics Committee.

2.2.2 Tissue collection

The cows were slaughtered by captive bolt and exsanguination at the Ruakura abattoir following standard slaughterhouse protocols.

Secretory alveolar tissue samples, approximately 50 mm in length and 10 mm thick, were collected post-mortem, snap frozen in liquid nitrogen, pulverised and stored at -80°C for gene and protein analysis.

Additional tissue samples were fixed in 4 % phosphate-buffered paraformaldehyde, routinely processed using the Leica TP 1050 tissue processor (Leica, Solms, Germany) and paraffin embedded using a tissue embedding machine (Thermolyne Sybron, Milwaukee, USA). Seven-µm thick serial sections of approximately 15 x 20 mm^2 cross-sectional area were cut onto polysine glass slides for histological analysis.

2.2.3 Fluorescent immunohistochemistry

For immunoflourescent staining of PC, tissue sections from the lactating (0 d NM, control), the 7 d NM and 28 d NM group were selected (n=3/group) based on the αS1-casein mRNA levels in each animal. Animals with high levels of αS1-casein mRNA were chosen for the control group (0 d NM), while animals with low levels of αS1-casein mRNA were selected for the 7 d NM and 28 d NM group. The protocol for dual labelling of PC was kindly provided by M Millier, Otago University (Millier *et al.*, 2013) and modified for this research.

Briefly, the tissue sections were dewaxed and rehydrated as per standard histology protocol followed by an overnight wash with two changes of 0.1 M glycine (Invitrogen, Carlsbad, USA) in 1x phosphate buffered saline (PBS) (Oxoid Limited, Hampshire, UK) to reduce autofluorescence. Antigen retrieval was

achieved by incubating the slides in citrate buffer (0.01 M, pH 6.0) (Merck, Darmstadt, Germany) for 25 min at 95°C, followed by a pepsin digest (0.5 % w/v, pH 2.0) (Sigma, St. Louis, USA) for 15 min at 37°C. Afterwards, sections were permeabilised using Triton X-100 (0.5 % v/v) (Sigma) for 5 min at room temperature (RT) and non-specific antigens were blocked with normal goat serum/bovine serum albumin solution [10 % NGS, v/v (Invitrogen); 1 % BSA, w/v (Gibco, Life Technologies, Carlsbad, USA)] for 1 h at RT. Centrioles were detected by applying anti-γ-tubulin antibody; clone GTU-88 (Sigma), at 1:3000 overnight at 4 °C. The axoneme was detected by applying the anti-acetylated-α-tubulin, clone C3B9 (Woods *et al.*, 1989), antibody at 1:300 for 1 h at 37 °C. Secondary antibodies AlexaFluor 488 and 546 goat anti-mouse IgGs (Molecular Probes, Invitrogen, Carlsbad, USA) were applied at 1:500 for 1 h at RT. Nuclei were stained using Hoechst 33258 (0.66 µg/ml) (Molecular Probes, Invitrogen). Finally, coverslips were mounted using Prolong Gold mounting media (Molecular Probes, Invitrogen) and left to set overnight at RT.

2.2.3.1 Confocal microscopy

Each tissue section per glass slide was divided into 10 equal-sized areas. Per area, at least one alveolus was imaged using a Zeiss LSM 510 META laser scanning confocal microscope with a 100x, N.A=1.40, oil immersion objective (Zeiss, Oberkochen, Germany) at the Biomedical Imaging Research Unit (BIRU) at the University of Auckland. A series of Z slices were used to image PC at immunofluorescent-specific laser excitation lines 488 and 543 nm. Nuclei were imaged in the mid-section Z slice using standard fluorescence excitation. ImageJ 1.45s (National Institutes of Health, Bethesda, USA) was used to process

all LSM files, create composite RGB micrographs, enhance contrast, and add scale bars.

2.2.3.1.1 Primary cilia analysis

Using suitable double-immunofluorescent labelled composite micrographs of mammary tissue sections, PC incidence and morphology was assessed. According to the number and thickness of Z-slices used for image compilation, individual micrographs ranged in depth from 1.1 to 2.1 µm, with an average depth of 1.5 µm. Primary cilia were identified by green basal body/centriole staining (will appear yellow when all layers are merged) and co-localisation with red axoneme staining in close proximity to the blue-stained nuclei of the alveoli and surrounding structures.

Only clearly-interpretable images, where the PC morphology and cells of origin could be identified, were used to eliminate potential errors due to increased background fluorescence. Defined by the angle of orientation relative to an orientation directly perpendicular to the alveolar wall, a cilium was classed as "deflected" if its axomene lay at an angle greater than 45° in either direction from the perpendicular angle. If the base of the axoneme appeared to be perpendicular, but its tip was almost parallel to the cell surface, the PC was classed as "bent". Data were gathered from luminal cells and total alveolar cells, obtaining the number of Hoechst-stained nuclei and the number of associated PC with their centriole. For each animal, multiple composite micrographs were assessed (at least 10/animal), and the average percentage of bent, deflected or non-deflected cilia were obtained. The total average of incidence assessment for

each experimental group was obtained by averaging the data from all animals of each group.

2.2.3.1.1.1 Automated nuclei counting

Hoechst-stained nuclei were counted automatically using the ImageJ 1.45s software. Before creating a composite image of all layers, the images of nuclei were converted to an 8-bit image, followed by contrast enhancement by 0.4 % and a conversion into a binary image. Outliers (smaller than 5 pixels) were removed and the detection threshold was set to 50. After the application of the watershed filter (automatically separates particles that touch), the number of particles (in this case nuclei) were counted and any particle smaller than 5 µm was disregarded.

2.2.4 RNA preparation

Total RNA was extracted from 100 mg of ground tissue, resuspended in 1 ml of TRIzol® solution (Invitrogen) and homogenised for 10 s using a mechanical homogeniser (Omni PCR Tissue Homogenising Kit, Omni International Inc., Kennesaw, USA) according to the manufacturer's instructions. After extraction, the RNA was purified and digested with DNaseI to remove potential DNA contaminations by using the RNeasy® Kit according to the manufacturer's manual (Qiagen, Venlo, Netherlands). The amount of extracted RNA and potential solvent and/or protein contamination in each sample was measured using the NanoDrop^{TM}spectrophotometer (NanoDrop Products, Wilmington, USA; results not shown). The RNA quality was measured by obtaining RNA integrity

numbers (RIN) using the Agilent 2100 bioanalyzer system in conjunction with the Agilent RNA 6000 Nano Kit in accordance with the manufacturer's instructions (Agilent Technologies, Santa Clara, USA; results not shown).

2.2.4.1 cDNA synthesis

One µg of total RNA was used to synthesise first-strand cDNA using the SuperScript^{TM}III First-Strand Synthesis System for RT-PCR according to the manufacturer's manual (Invitrogen). The RNA was primed using the oligo $(dT)_{20}$ system component. The generated cDNA was diluted 3-fold (equivalent to approximately 17 ng/µl reverse transcribed total RNA) in nuclease-free water (Ambion®, Life Technologies, Carlsbad, USA) for downstream analysis.

2.2.4.2 Quantitative Real-Time PCR

Each RNA sample (1 µl) was assayed in triplicate, by quantitative Real-Time-Polymerase Chain Reaction (qRT-PCR) with SYBR Premix Ex Taq System (Takara, Otsu, Japan) using a Corbett Thermocycler (Corbett Life Science, Qiagen, Venlo, Netherlands). Three different reference genes were used as endogenous control: glyceraldehyde 3-phosphate dehydrogenase (GAPDH); ubiquitin; and cyclophilin A. Additionally, each assay included RT-negative and 'no-template' control reactions. Real-time PCR experiments were performed under the following conditions: initially 95°C for 3 min; followed by 40 cycles of 95°C for 10 s, 60°C for 20 s, 72 or 75°C for 20 s (for individual experimental conditions see Table 2.1). After the last cycle of each RT-PCR experiment a dissociation curve was obtained starting at 72°C, followed by a continuous

temperature increase of 1 degree increments every 30 s until 95 °C was reached. Analysis of the melting temperature (Tm) of amplified products allowed for the detection of the target product as well as any non-specific products, including primer dimers which typically had a lower Tm of between 70 to 75 °C.

One PCR reaction mix (total final reaction volume = 10 µl) contained 5 µl SYBR Premix Ex Taq System (Takara), 3.8 µl of sterile, nuclease-free water (Ambion®, Life Technologies), 1 µl of cDNA and 0.1 µl of each of the forward and reverse primers. All primers were used at a final concentration of 100 nM in each 10 µl real-time reaction.

Prior to each experiment, optimal experimental conditions, such as annealing and acquisition temperatures, were determined in separate experiments to maximise the amplification of a single specific product and prevent primer dimer formation during the final PCR reactions for each gene of interest. Three milk protein genes (αS1-casein, α-lactalbumin and κ-casein) and one component of the body's immune response (lactoferrin) which is present in body fluids such as milk, and is generally up-regulated during mammary gland involution, were tested as indicators for overall milk production and progression of involution. The STAT6 transcription factor has previously been associated with mechanical stimulation of the PC in kidney cells. To investigate its potential role in the bovine mammary gland the mRNA expression levels of STAT6 were determined.

The primer sequences and other relevant details about individual experimental conditions are outlined in Table 2.1.

Table 2.1 Sequences of PCR primers (forward and reverse), primer position, PCR product sizes and individual experimental conditions of bovine nucleic acid sequences used for investigating gene expression by real-time RT-PCR

Gene	Nuclei acid sequence	Primer sequence (5'→3')	Primer position[1] [bp]	Product size [bp]	Annealing [°C]	Acquisition [°C]
Cyclophilin A	AC_000167.1	Forward: gca tac agg tcc tgg cat ct	310	279	60	72
		Reverse: tct cct ggg cta cag aag ga	589			
GAPDH	AC_000162.1	Forward: ctc cca acg tgt ctg ttg tg	141	222	60	72
		Reverse: tga gct tga caa agt ggt cg	362			
Lactoferrin	AC_000179.1	Forward: ggc ctt tgc ctt gga atg tat c	484	338	60	72
		Reverse: att tag cca cag ctc cct gga g	821			
STAT6[2]	AC_000162.1	Forward: agc ggc tct atg tcg act ttc	209	219	60	72
		Reverse: gat aaa tgg tct cca gag tgc tga	427			
α-Lactalbumin	AC_000162.1	Forward: tgg gtc tgt acc acg ttt ca	133	251	60	72
		Reverse: gct tta tgg gcc aac cag ta	383			
αS1-casein	AC_000163.1	Forward: tac cct gag ctt ttc aga ca	547	201	60	72
		Reverse: cat aac tgt gga gtc cct ca	747			
κcasein	AC_000163.1	Forward: ata ctg tgc ctg cca agt cc	371	238	60	75
		Reverse: ttg atc tca ggt ggg ctc tc	608			
Ubiquitin	AC_000176.1	Forward: ggc aag acc atc acc ctg gaa	731	200	60	72
		Reverse: gcc acc cct cag acg aag ga	931			

[1] Refers to the 5' position of the primers in the nucleic acid sequence

[2] NCBI primer blast tool was used to design sequences to detect the bovineSTAT6 gene

The PCR products were then QIAquick column-purified (Qiagen) and submitted for DNA sequencing which verified their authenticity (University of Canterbury, New Zealand, DNA Sequencing Facility, results not shown).

2.2.4.3 Agarose gel electrophoresis for DNA

Agarose gels (1.5 % (w/v)), containing 1x TAE (40 mM Tris, 0.1 % (v/v) glacial acetic acid, 1 mM EDTA pH 8.0) and 1x SYBR® Safe DNA gel stain (Life Technologies), were used to visualise DNA samples. Wells were loaded with 5 µl of PCR product mixed with DNA loading buffer (0.25 % (w/v) bromophenol blue, 0.25 % (w/v) xylene cyanol FF, 30 % (v/v) glycerol) in 12 µl total volume. The gel was run at a constant 100 V in electrophoresis buffer (1x TAE) for approximately 1 h. The DNA was then visualised under UV transillumination using a Gel Doc and Quantity One software (Bio-Rad Laboratories, Hercules, USA) to confirm the size and number of bands present.

2.2.4.4 Analysis of real-time PCR data

Following qRT-PCR experiments, average take-off values for reference genes and genes of interest were generated for each sample using the Rotor-Gene Q software (version: 2.1.0). The take-off value represents the cycle number at which the fluorescence of each reaction crossed the threshold, which was placed above background fluorescence and within the log-linear phase of exponential product amplification. Therefore, the lower the take-off value the higher the amplification of PCR products. Relative quantification of gene expression was performed using comparative quantification to analyse changes in gene expression in a given

sample relative to a reference sample, the lactating group (0 d NM). The amount of gene of interest in each sample was normalised by dividing by the amount of reference gene and the resulting values were $\log_{10}$-transformed before statistical analysis. Averages for each treatment group were back-transformed and results expressed as the fold-change relative to a control sample.

2.2.5 Protein preparation

One hundred mg of ground tissue was resuspended in 1 ml low salt buffer (10 mM 4-[2-hydroxyethyl]-1-piperazineethanesulphonic acid (HEPES), pH 7.9, 1.5 mM magnesium chloride, 10 mM potassium chloride) containing 1 % (v/v) NP-40 detergent and protease inhibitors [1 mM sodium orthovanadate (Sigma), 1 tablet protease inhibitor cocktail per 10 ml buffer (Roche, Basel, Switzerland)], homogenised using an Omni Tissue Homogeniser (Omni PCR Tissue Homogenizing Kit, Omni International Inc.) and rotated for 30 min at 4°C. A 500 µl aliquot was saved for analysis of the total homogenate fraction. Next, the remaining homogenate was centrifuged at 10,000 x g for 30 min at 4 °C and the supernatant collected as the NP-40-soluble protein fraction. To collect the NP-40-insoluble protein fraction, the remaining pellet was resuspended by sonication in 250 µl low salt buffer (containing 1 % (v/v) NP-40 detergent, 1 % (w/v) SDS, and protease inhibitors) and rotated for 30 min at 4 °C. Samples were mixed with 2x Laemmli loading buffer (62.5 mM Tris pH 6.8, 2 % (w/v) SDS, 5 % (v/v) BME, 10 % (v/v) glycerol) (Laemmli, 1970), boiled for 5 min, and stored at -20˚C until required for subsequent western analysis. Prior to mixing in loading buffer, the amount of protein present in 1 µl of each sample was determined using Qubit®

2.0 Fluorometer in conjunction with the Qubit® Protein Assay kit as per the manufacturer's instructions (Invitrogen).

2.2.5.1 Protein integrity

Bis-Tris protein (10 %) gels were used for this experiment. Protein samples of each animal from the control (0 d NM), the 7 d NM, and the 28 d NM group (n=3/group) were analysed. Each lane was loaded with 20 µg of total protein from the soluble fraction, except the marker lane which contained 5 µl of the SeeBlue® Plus2 Pre-Stained standard. After SDS-Page electrophoresis, gels were stained and fixed for 2 h, then de-stained overnight in 20 % methanol.

2.2.5.2 Western blot analysis

Protein samples (20 µg) from three animals of each group (0 d NM, 7 d NM, 28 d NM; n=3/group) were loaded onto a precast NuPAGE® Novex® Bis-Tris protein gel (LifeTechnologies). Furthermore, each gel contained a marker loaded with 5 µl of the SeeBlue® Plus2 Pre-Stained standard (LifeTechnologies). Electrophoresis was then carried out in the XCell4 SureLock™ Midi-Cell apparatus (LifeTechnologies) for approximately 1 h at 200 V in 1x NuPAGE® MES SDS running buffer (LifeTechnologies). Next, separated proteins were transferred onto Hybond-ECL nitrocellulose membranes (Amersham Biosciences, GE Healthcare, Little Chalfont, UK) using the Trans-Blot Cell (Bio-Rad Laboratories) wet blotting system. After transfer, membranes were stained with Ponceau S (0.1 % (v/v) Ponceau S; 1.0 % (v/v) acetic acid) to visualise successful transfer of proteins onto the membranes, scanned using a GS-800

densitometer (Bio-Rad Laboratories) and washed with distilled water to remove the ponceau stain. Blocking of non-specific binding was achieved by immersing the membrane in a solution of 4 % non-fat milk powder (NFMP) for 2 h at RT on a rocker. Subsequently, membranes were probed with primary antibodies (for detailed information on antibodies refer to Table 2.2) overnight at 4 °C on a rocker, followed by incubation with horseradish-conjugated secondary antibodies (goat-anti rabbit at a 1:10,000 dilution) for 1 h at RT. Membranes were washed in multiple changes of wash buffer (1x TBS/0.1 % Tween 20/0.1 % BSA) following each antibody incubation. Immunoreactive protein bands were detected using a chemioluminescence system (Amersham ECL Western Blotting Detection Reagents; GE Healthcare Life Sciences, Little Chalfont, UK), BioMax XAR film (Kodak, Rochester, USA) and the 100 Plus film processor (AllPro^{TM}Imaging, Melville, USA). The developed films were scanned using the GS-800 densitometer (Bio-Rad Laboratories) and analysed using the Quantity One software (version 4.6.6) (Bio-Rad Laboratories). Commercially available STAT6 293T transfected lysate (2 µl, Abcam, Cambridge, UK) was used to determine STAT6 protein detection.

Table 2.2 Information on antibodies used for Western Blot analysis, including species of origin, molecular weight, supplier, dilution and gel percentage for used SDS page gel electrophoresis

Antibody	Species of origin	Molecular Weight [kDa]	Supplier	Dilution	Gel %[1]
STAT6	rabbit	110	Pierce	1:1000	10
pSTAT6 (pTyr641)	rabbit	110	Pierce	1:1000	10

[1] Precast NuPAGE® Novex® Bis-Tris protein gel (LifeTechnologies) were used for all SDS-PAGE gel electrophoresis experiments in combination with the 1x NuPAGE® MES SDS running buffer (LifeTechnologies).

2.2.6 Statistical analysis

2.2.6.1 Statistical analysis of primary cilia data

Data on PC acquired from composite micrographs was analysed as a binomial distribution by GenStat (16th edition, version 16.1.0.10916 (64-bit version)) to allow cow effects to be factored in. The results are displayed as the proportion of PC incidence with the standard error of the mean (± SEM). Means were considered different at $P<0.05$ and within the range of a statistical trend at $P<0.1$. ** $P<0.01$, * $P<0.05$, $^{+}$ $P<0.1$.

2.2.6.2 Statistical analysis of qRT-PCR results

Differences in levels of mRNA expression from each group were analysed using the Student's paired t-test with a two-tailed distribution (MS Excel, 2010). Data are presented as normalised, back-transformed means for each treatment group with the standard error of the mean (SEM) between means with their corresponding P-values. Data from individual animals are expressed as back-

transformed mRNA expression levels (relative units). Means were considered different at $P<0.05$ and within the range of a statistical trend at $P<0.1$. ** $P<0.01$, * $P<0.05$, $^{+}$ $P<0.1$.

2.2.6.3 Statistical analysis of Western Blot results

Densitometry data from western blotting were $\log_{10}$-transformed and analysed by ANOVA in GenStat (16^{th} edition, version 16.1.0.10916 (64-bit version)) with blocking on replicate and adjusting for between gel variations to detect differences between control (0 d NM) and treatment samples (7 d NM and 28 d NM). Results are graphed as back-transformed mean fold changes relative to the control (0 d NM) with the SED. Means were considered different at $P<0.05$ and within the range of a statistical trend at $P<0.1$. ** $P<0.01$, * $P<0.05$, $^{+}$ $P<0.1$.

2.3 Results

2.3.1 Histological analysis

The slides and pictures of hematoxylin and eosin stained tissue sections for histological assessment were kindly provided by Dr Adrian Molenaar, AgResearch, Ruakura. Prior to fluorescent immunohistochemistry, histological morphology of representative tissue sections from each group were assessed to define the lactating appearance of the tissue within each experimental group (Fig. 2.1; A - M).

2.3.1.1 Lactating group (control group)

No significant inter-animal variations were observed within this group. Large uniform areas of moderately-sized, open alveoli surrounded by cuboidal MECs with a small visible amount of inter-alveolar stromal tissue were observed throughout the tissue. At low magnification, the alveoli appear to be of similar size, open and relaxed (Fig. 2.1; A and B). Furthermore, the alveoli were made up of a single MEC layer surrounding each lumen and a small amount of accumulated milk product can be seen within some lumina, apparent as light to darkly-stained a-cellular material (Fig. 2.1; A). Minimal variation in size of aveoli and thickness of alveolar walls can be observed across all alveoli (Fig. 2.1; A and B). At higher magnification, the alveolar walls appear to be intact without any obvious signs of disruption of the highly ordered alveolar structure (Fig. 2.1; C and D). The majority of the tissue section was dominated by open alveolar

structure in relation to the connective tissue component, although a few thick bands of stromal tissue can been seen, which encompass multiple lobules (Fig.2.1; A and B).

2.3.1.2 Seven days non-milking group

The majority of alveoli appeared to be larger and engorged with accumulated milk. At low magnification, some inter-animal variation could be found in this group. While some animals displayed more histological features associated with active lactation, others exhibited first signs of involution (Fig. 2.1; E and F). Furthermore, heterogeneity was present within animals, which could be observed at low magnification. Although most alveoli were still large with a stretched morphology, a few localised, collapsed areas were apparent. These were characterised by smaller alveoli with a "ruffled" appearance due to vesicle accumulation within the epithelial cells (Fig. 2.1; E). Nearly all alveoli contained accumulated milk product and large milk vesicles were present within some lumina (Fig. 2.1; E - H). At higher magnification, large vacuoles containing fat droplets and material from secretory vesicles are present within MECs and high numbers of vesicles containing coalescing fat droplets and proteins exist in the alveolar lumen (Fig. 2.1; G and H). The ratio of secretory tissue to connective tissue appeared to shift with more obvious inter-lobular connective tissue separating the lobules (Fig. 2.1; E - H).

2.3.1.3 Twenty-eight days non-milking group

While inter-animal variation can be found within this group, the majority of tissue was dominated by a non-lactating appearance (Fig. 2.1; J and K). This appearance was characterised by collapsed alveoli, abundance of large vesicles within MECs and alveolar lumens, thickened areas of stromal tissue between alveoli and broad bands of supportive connective tissue containing adipocytes (Fig. 2.1; J - M). Infiltration of the highly involuted tissue with leukocytes resulted in a highly cellular appearance and made it difficult to distinguish alveolar boundaries (Fig. 2.1; K and L). At higher magnification, the majority of alveoli were collapsed with ruffled edges, cells protruded into the lumen and discernible gaps occurred between adjacent cells (Fig. 2.1; L and M).

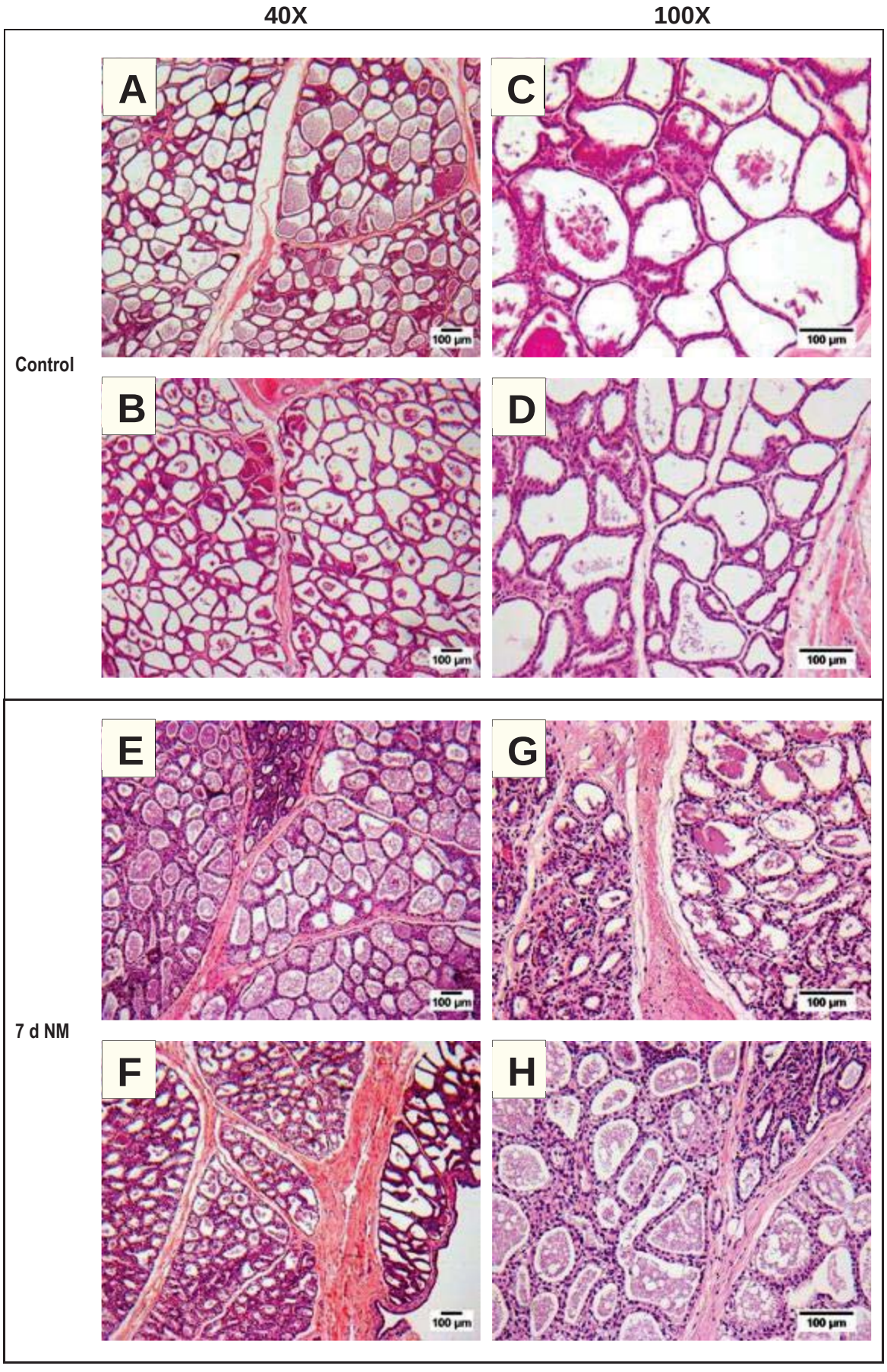
40X
100X
Control
7 d NM
A
B
C
D
E
F
G
H
100 µm

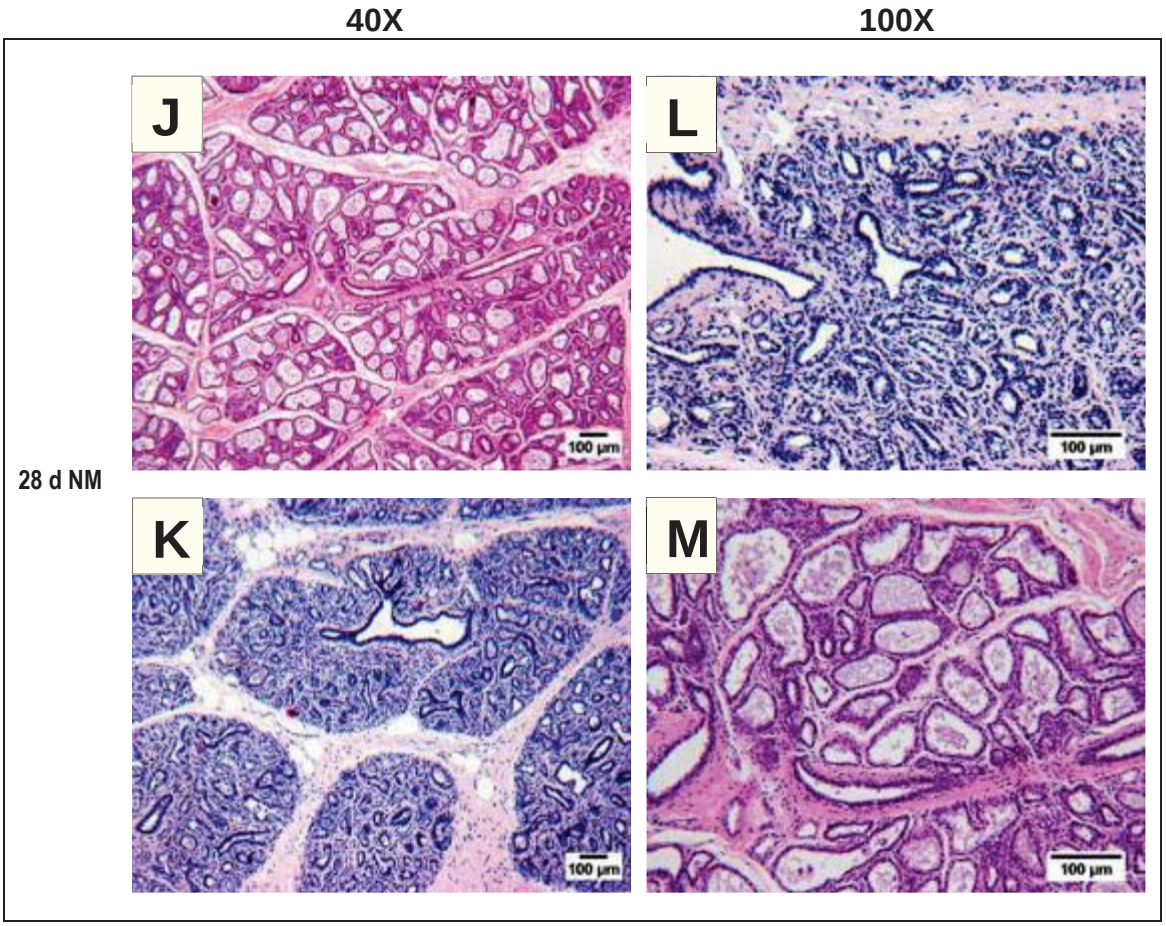

Figure 2.1 Hematoxylin and eosin-stained sections of mammary alveolar tissue from animals following extended periods of non-milking: lactating, 7 d NM (non-milking) and 28 d NM, respectively. A to D: representative micrographs from animals of the lactating group; E to H: representative micrographs from animals of the 7 d NM group; J to K: representative micrographs from animals of the 28 d NM group. Images A, B, E, F, J and K taken using 40x objective; Images C, D, G, H, L and M taken using 100x objective. Scale bars are 100 µm

2.3.2 Confocal imaging of primary cilia in mammary tissue

Alveolar tissue sections from three animals of each group (control, 7 d NM and 28 d NM) were analysed to obtain representative composite images of PC. Representative images from each group where PC could be detected are shown (Fig. 2.2 to 2.4), however, some alveoli appeared to have no (or very few) obvious PC.

2.3.2.1 Lactating group (control group)

Representative composite images of immunofluorescent labelled PC in alveolar tissue from animals during active lactation are shown in Fig. 2.2; A to F. In alveoli where PC could be detected, they projected from the apical side of the luminal MECs. Most PC appeared to be short, although, predictions about the exact cilia length could not be made due to the slicing process during tissue sectioning. Some cilia appeared to be bent (Fig. 2.2; C and D), while others were generally straight and projected into the luminal space at various orientations/angles (Fig. 2.2; A, B, E and F). Their associated centriole was commonly seen in close proximity to the nuclei; as a result, their cell of origin could generally be identified. In sections with lots of PC and/or lots of surrounding tissue, the alveolar structure and cells of PC origin were more difficult to interpret (Fig. 2.2; B). Moreover, PC had also been detected in underlying myoepithelial cells projecting into the inter-alveolar space (Fig. 2.2; D). Nonetheless, in distended alveoli (indicated by widely-spaced nuclei) the PC of MECs were often deflected or bent to lie more parallel to the alveolar wall, suggesting a potential deflection against the apical cell surface (Fig. 2.2; B,C, E and F).

2.3.2.2 Seven days non-milking group

Similar results to those from animals of the control group were found in animals that were not milked for seven days prior to tissue collection (Fig. 2.3; A to F). In accordance with the histological analysis (section 2.3.1), the majority of the alveoli appeared to be open and the PC and their cells of origin could be identified. As described for the control samples, some cilia appeared to be bent (Fig. 2.3; C, D and F), while others were generally straight and projected into the luminal space at various orientations/angles (Fig. 2.3; A, B and E). At this stage, more surrounding/connective tissue could be detected; hence, more PC were detected within the inter-alveolar space (Fig. 2.3; B and E). However, cells of origin within the inter-alveolar space could easily be detected due to the close proximity of their associated centrioles and the nuclei.

2.3.2.3 Twenty-eight days non-milking group

After a period of not milking for 28 days, more alveoli appeared to be collapsed. As a result, more connective tissue was present at this stage which resulted in an increase of background autofluorescence in comparison to the other two groups (Fig. 2.4; A to F). Of the clearly-interpretable images, PC were seen in alveolar cells and PC morphology was similar to that observed in the other two groups. However, fewer PC appeared to project into the luminal space, but appeared to be flat against the apical cell surface (Fig. 2.4; C) or projected towards the inter-alveolar space (Fig. 2.4; B and F). Moreover, the cell origin could not always be identified and thus the PC was not counted. With the increase in connective tissue, more PC could be detected within the inter-lobular stromal tissue with similar morphology to the PC projecting towards the luminal space (Fig. 2.4; C, E and F).

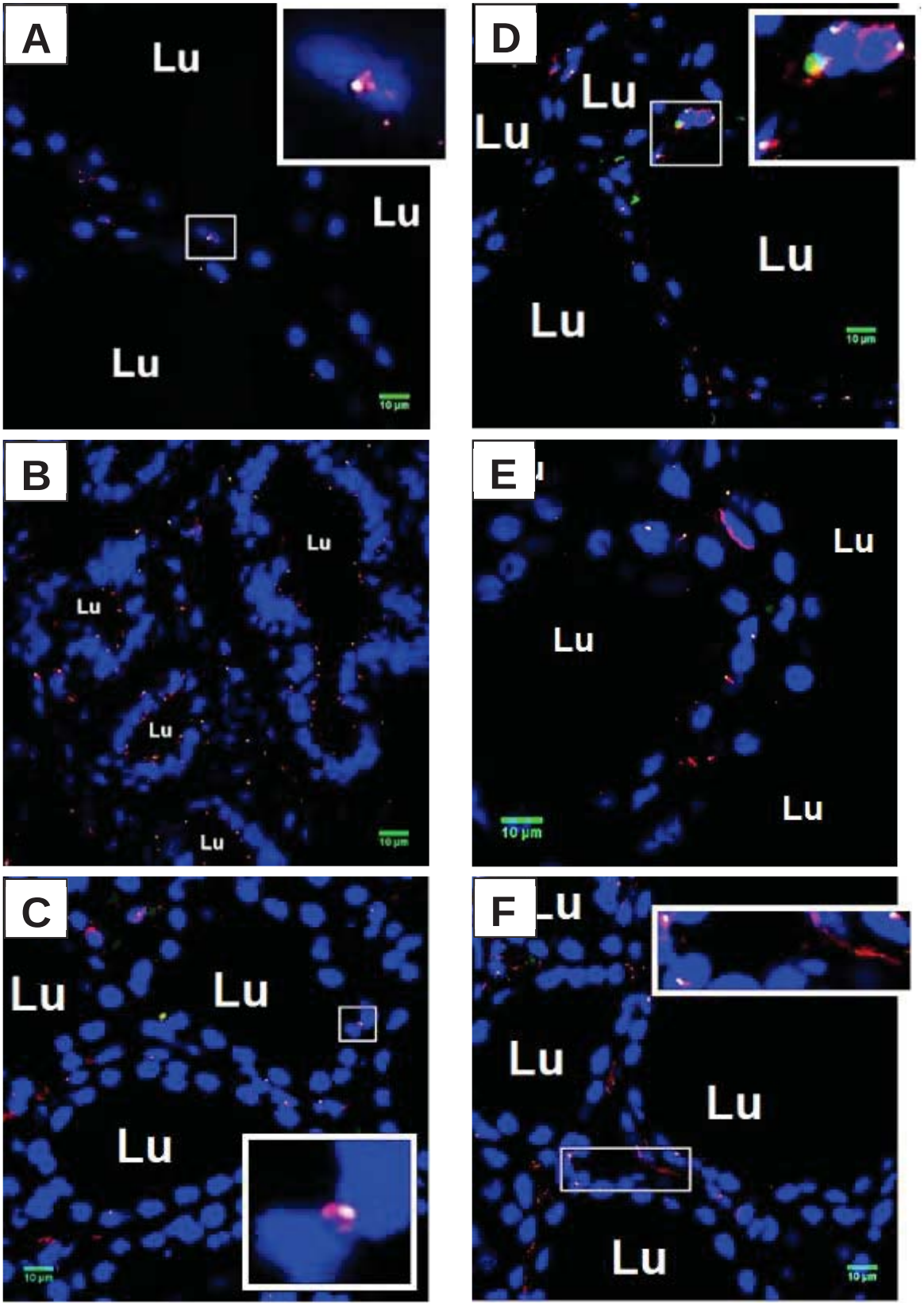

Figure 2.2 Representative composite images of primary cilia in lactating alveolar tissue sections

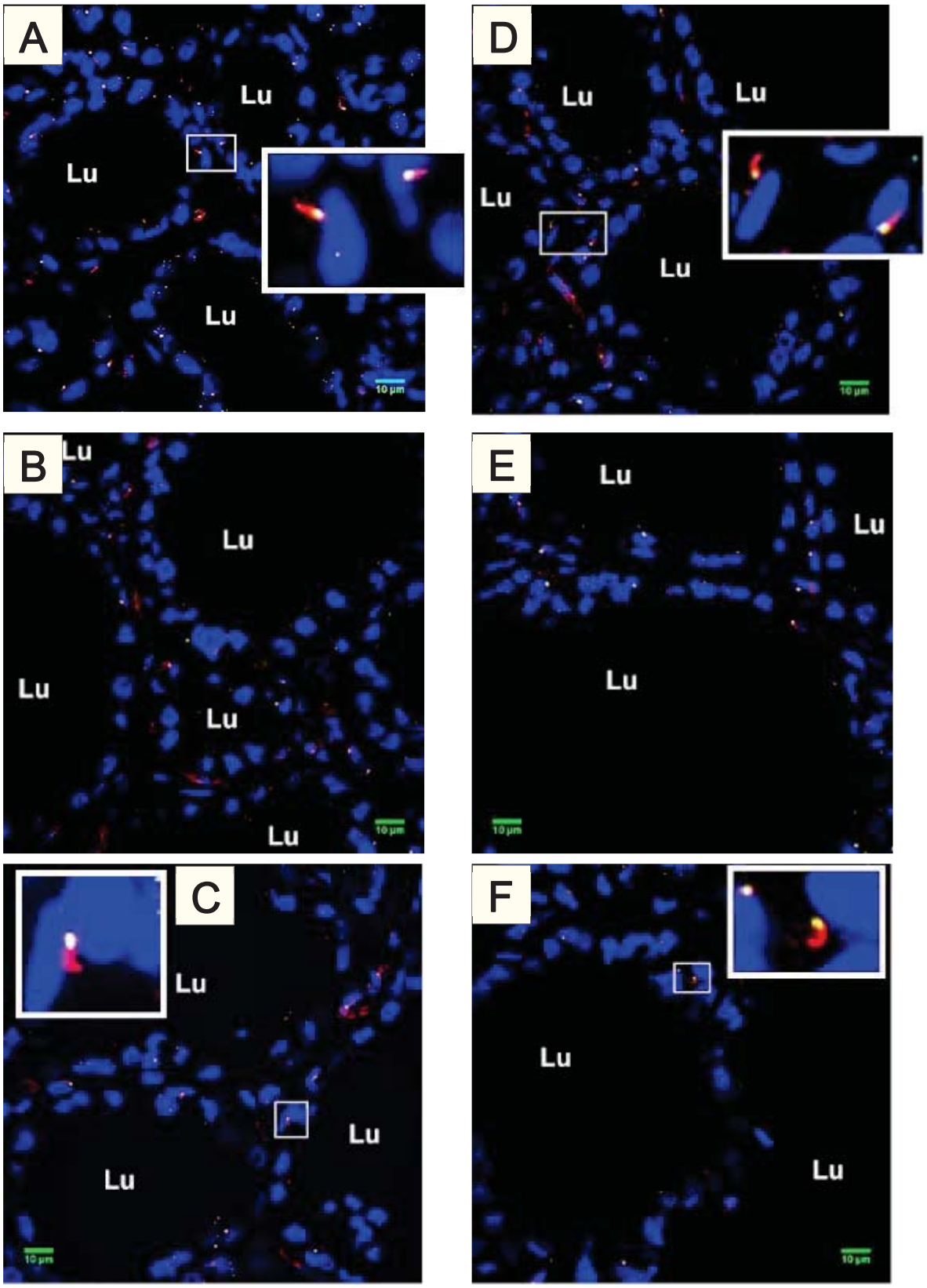

Figure 2.3 Representative composite images of primary cilia in alveolar tissue sections from the 7 d NM (non-milking) group

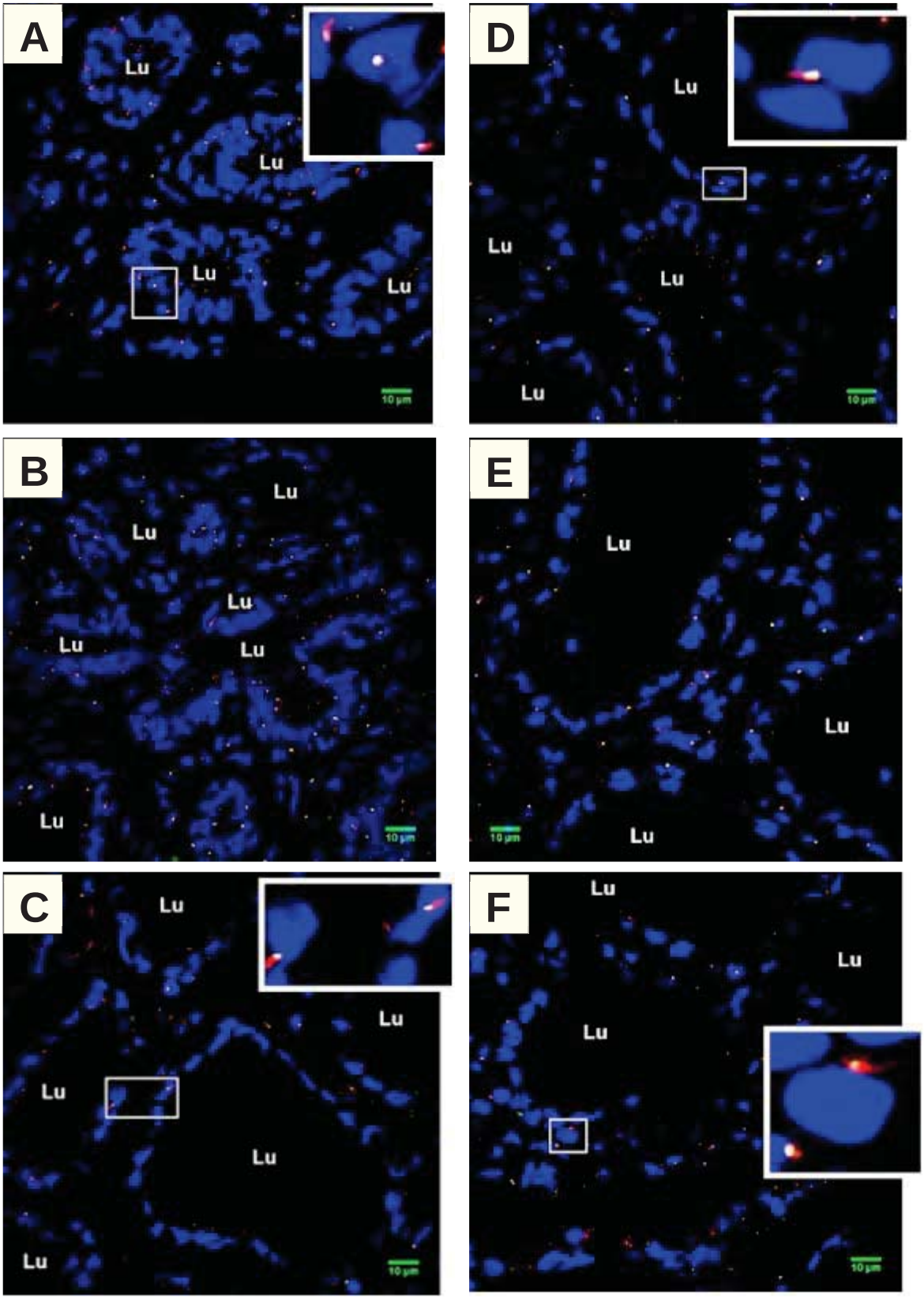

Figure 2.4 Representative composite images of primary cilia in alveolar tissue sections from the 28 d NM (non-milking) group

Figure 2.2 to 2.4 (pages 70 to 72) Representative composite images of primary cilia (PC) in alveolar tissue sections from each group following extended periods of non-milking. The PC were identified by green basal body/centriole staining (will appear yellow when all layers are merged) and co-localisation with red axoneme staining in close proximity to the blue-stained nuclei of the alveoli. Fig. 2.2, A to F: Lactating (control group, 0 d NM). Fig. 2.3, A to F: 7 d NM (non-milking) group. Fig. 2.4, A to F: 28 d NM group. Abbreviations: Lu: luminal space. Scale bars are 10 µm. White lines indicate areas of enlargement

2.3.3 Comparison of manual and automatic nuclei count

Hoechst-stained nuclei were counted manually and automatically to make predictions on the ImageJ 1.45s software to determine accurate automated nuclei counting (Fig. 2.5). During the stages of active lactation and/or early involution (i.e. 0 d NM or 7 d NM) numbers of nuclei counted manually or automatically were very similar. However, as the process of involution and remodelling of the mammary gland proceeds, more connective tissue is present. This in turn leads to more nuclei present and results in overlapping nuclei boundaries within the image which makes it more difficult for the program (ImageJ 1.45s) to discriminate the individual nuclei. Hence, counting nuclei automatically is more accurate when the alveoli are open, relaxed and individual nuclei are easier to distinguish from one another. Nonetheless, overall data obtained on numbers of nuclei present in each image were very comparable, and, thus, it was concluded that nuclei could be counted automatically for future experiments (Pearson correlation coefficient $R=0.97$) ($P<0.001$) (Fig. 2.5).

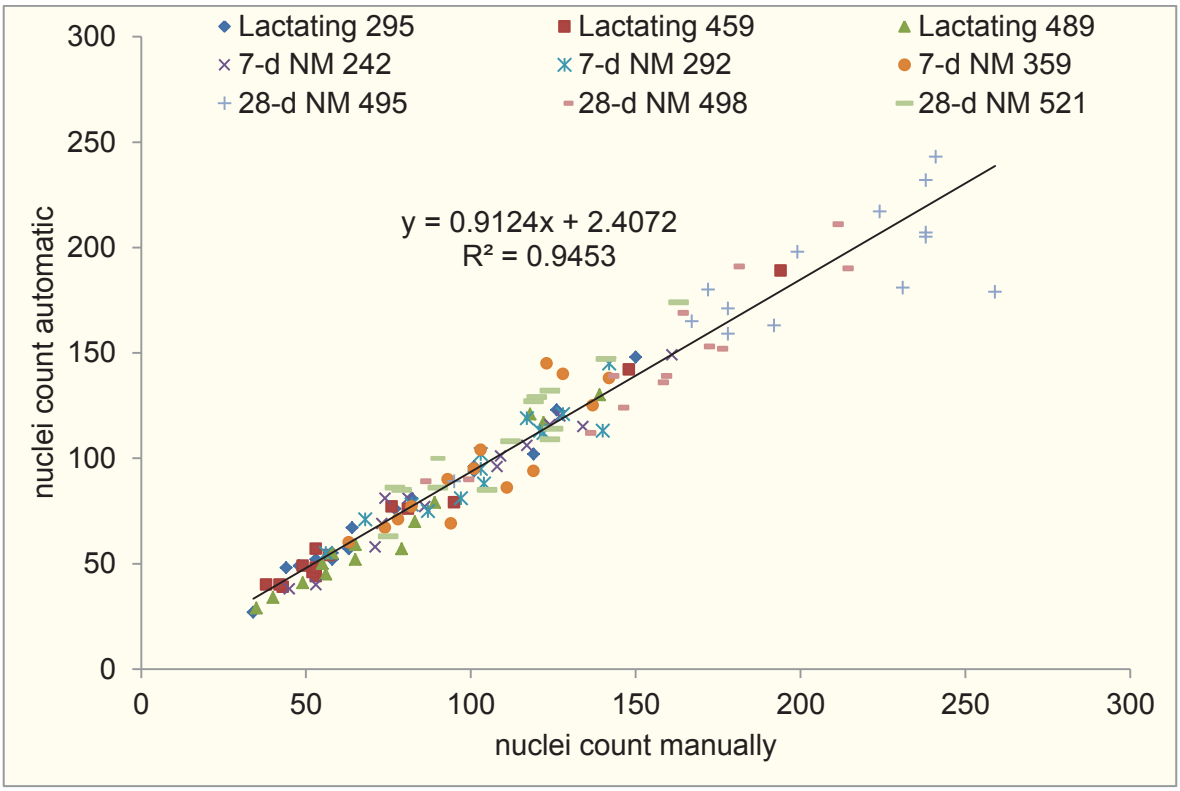

Figure 2.5 Comparison of manual and automatic nuclei count

Note: During the stages of active lactation and/or early involution (i.e. 0 d NM or 7 d NM) numbers of nuclei counted manually or automatically were very similar. However, as the process of involution and remodelling of the mammary gland proceeds, more connective tissue is present. This in turn leads to more nuclei present and results in overlapping nuclei boundaries within the image which makes it more difficult to distinguish the individual nuclei. Overall, however, nuclei numbers obtained were very similar

2.3.4 Primary cilia analysis

Using representative composite micrographs, multiple tissue sections from each animal were analysed to gather data on the total PC incidence and the PC incidence for luminal MECs in order to determine changes in PC distribution following extended periods of non-milking (Fig. 2.6). Overall, the longer the period of non-milking, the more tissue (represented by the nuclei) was present per area analysed as a result of the increase in collapsed alveoli. Consequently, more PC could be detected in the 7 d NM and the 28 d NM groups in the total and the luminal fraction. Furthermore, in the 28 d NM group there was a significant increase in total cilia relative to the luminal cilia present ($P<0.05$) which indicates an increase in connective tissue within the inter-lobular space.

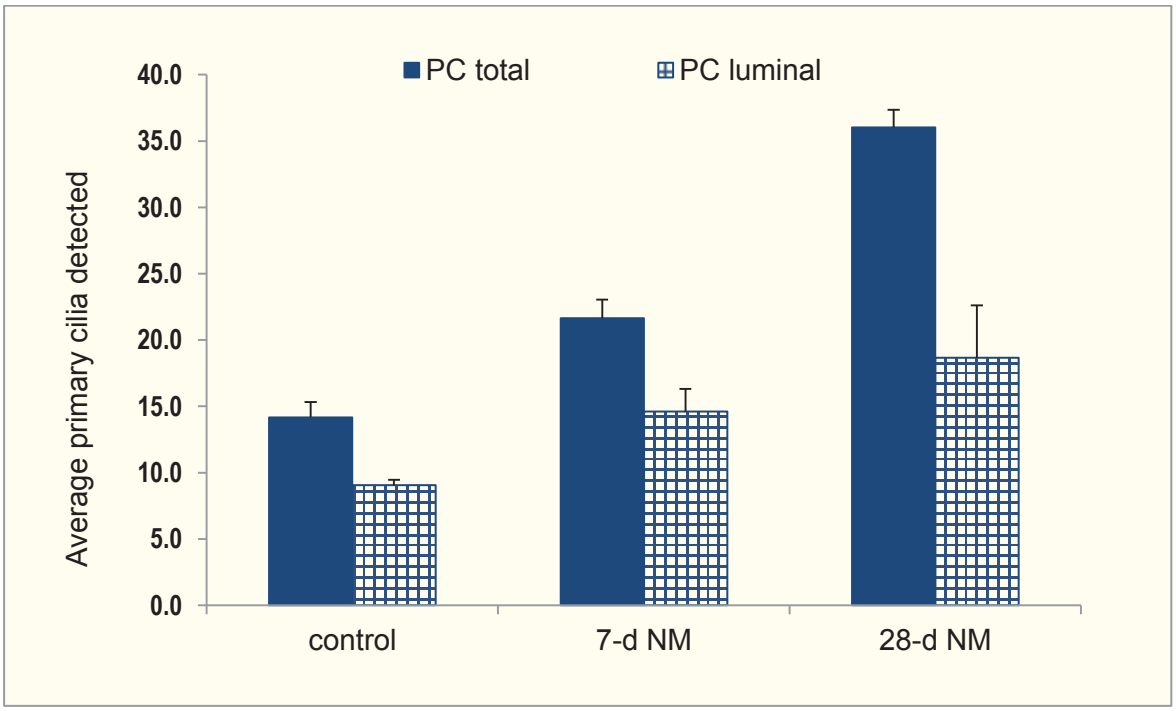

Figure 2.6 Average of total and luminal primary cilia within each experimental group (n=3/group), using representative composite micrographs, multiple tissue sections from each animal were analysed to collect and average the total PC count and the PC count for luminal MEC (±SEM)

2.3.4.1 Primary cilia incidence

Data on cilia incidence was gathered from luminal cells as well as total alveolar cells (epithelial and myoepithelial cells), obtaining the number of Hoechst-stained nuclei and the number of associated PC (Fig. 2.7).

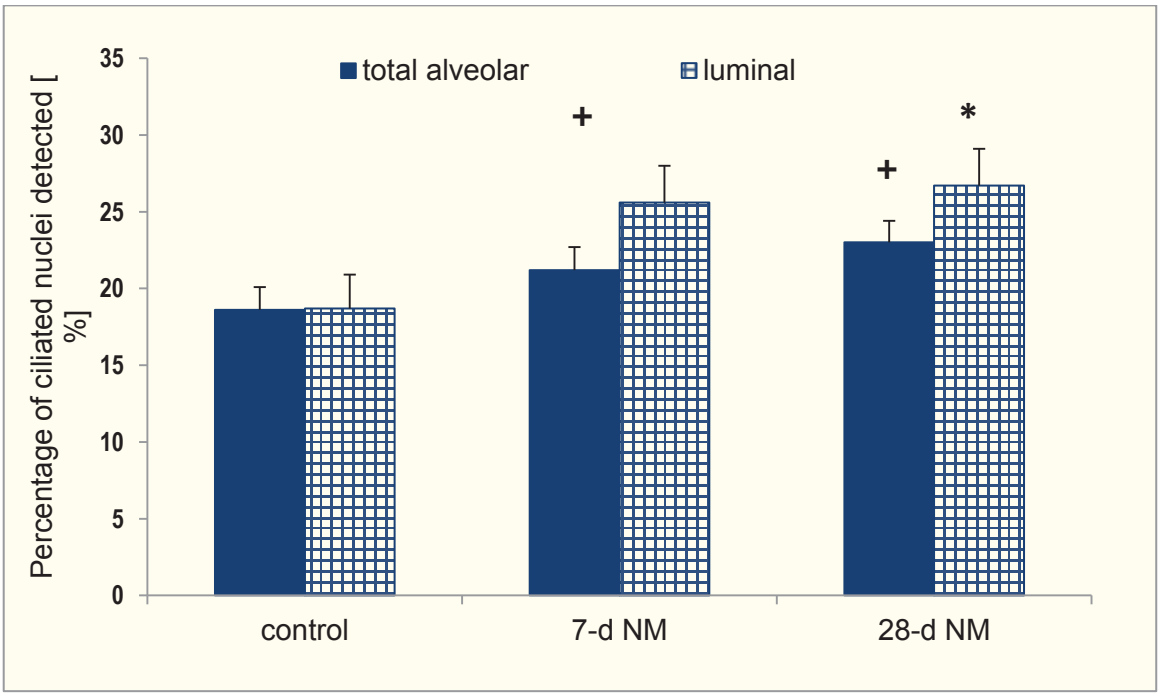

Figure 2.7 Percentage of cilia detected per treatment group (±SEM). Data was gathered from luminal cells as well as alveolar cells (n=3/group), obtaining the number of Hoechst-stained nuclei and the number of associated PC with its centriole. * $P < 0.05$; $^{+}$ $P < 0.1$

Both groups (total alveolar and luminal) showed an increase in cilia incidence present per nuclei over the course of this study. However, there was no significant change in the number of cells (nuclei) ciliated in the total alveolar fraction. In the luminal fraction, cilia present per nuclei significantly increased in the 28 d NM group relative to lactation. Nevertheless, the average depth of Z-stacks was 1.5 µm, while the tissue sections were 7 µm, both considerably less

than the average width of a luminal MEC (Millier, 2013). Therefore, the proportion of cilia detected will most likely be underestimates of the actual biological incidence.

2.3.4.2 Primary cilia morphology analysis

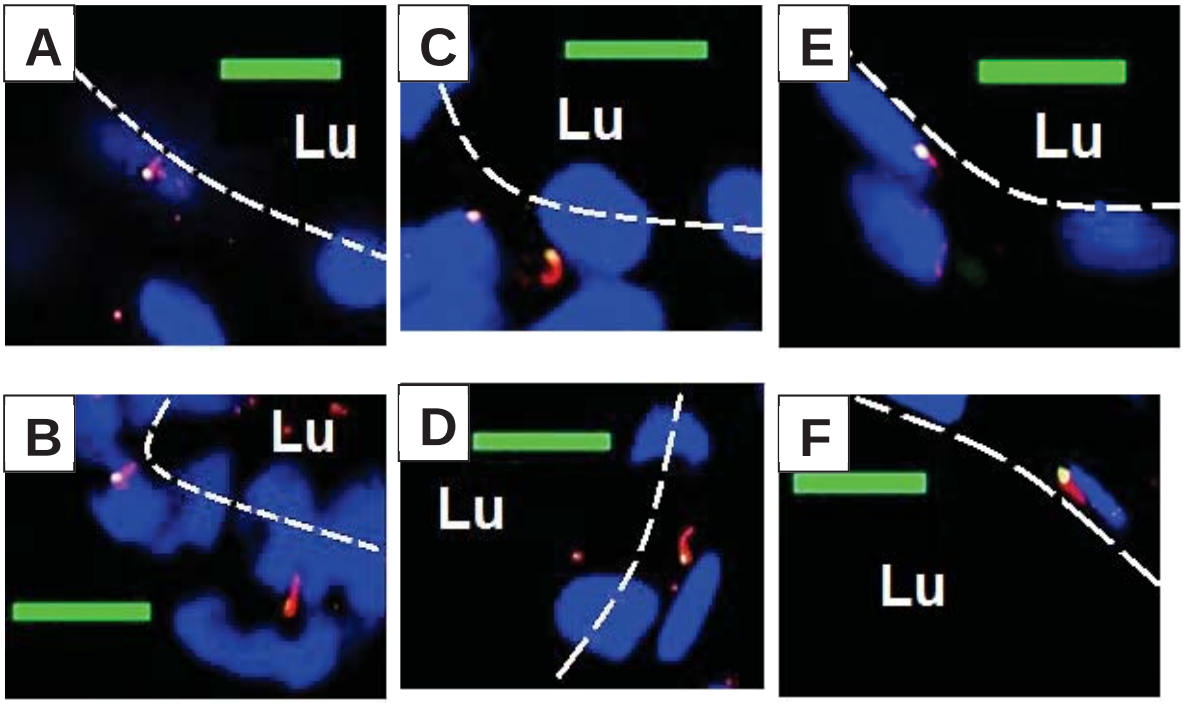

Figure 2.8 Representative composite micrographs of variations in cilium morphogolgy. Confocal composite images showing straight (perpendicular to alveolar wall) (A and B), bent (C and D) and deflected (E and F) primary cilia. Primary cilia were identified by green basal body/centriole staining (will appear yellow when all layers are merged) and co-localisation with red axoneme staining in close proximity to the blue-stained nuclei of the alveoli. Scale bars (green bar) are 10 µm. White lines indicate epithelial cell layer. Abbreviations: Lu: luminal space

Primary cilia could be detected in mammary tissue sections from all three experimental groups and the majority of the PC appeared to be deflected against the luminal cell surface. However, variations in shape and orientation of PC could

commonly be observed throughout all composite images (Fig. 2.8; A to F). Within the same alveolus, different PC morphologies could be detected. Furthermore, some PC appeared to be projected straight towards the luminal space (Fig. 2.8; A and B), while others appeared to be bent (Fig. 2.8; C and D) or deflected flat against the cell surface (Fig. 2.8; E and F) (as described in Materials and Methods 2.2.3.1.1). Only cilia with clear visible axoneme, basal body and associated nuclei in close proximity where used during this analysis

Differences in the PC morphologies were detected and analysed amongst the treatment groups. However, within each treatment a similar distribution pattern of the three different morphologies was displayed. The average number of bent cilia identified was low in all three treatment groups. Furthermore, the average number of deflected cilia was higher than the average number of cilia projecting towards the lumen in all treatment groups (Fig. 2.9).

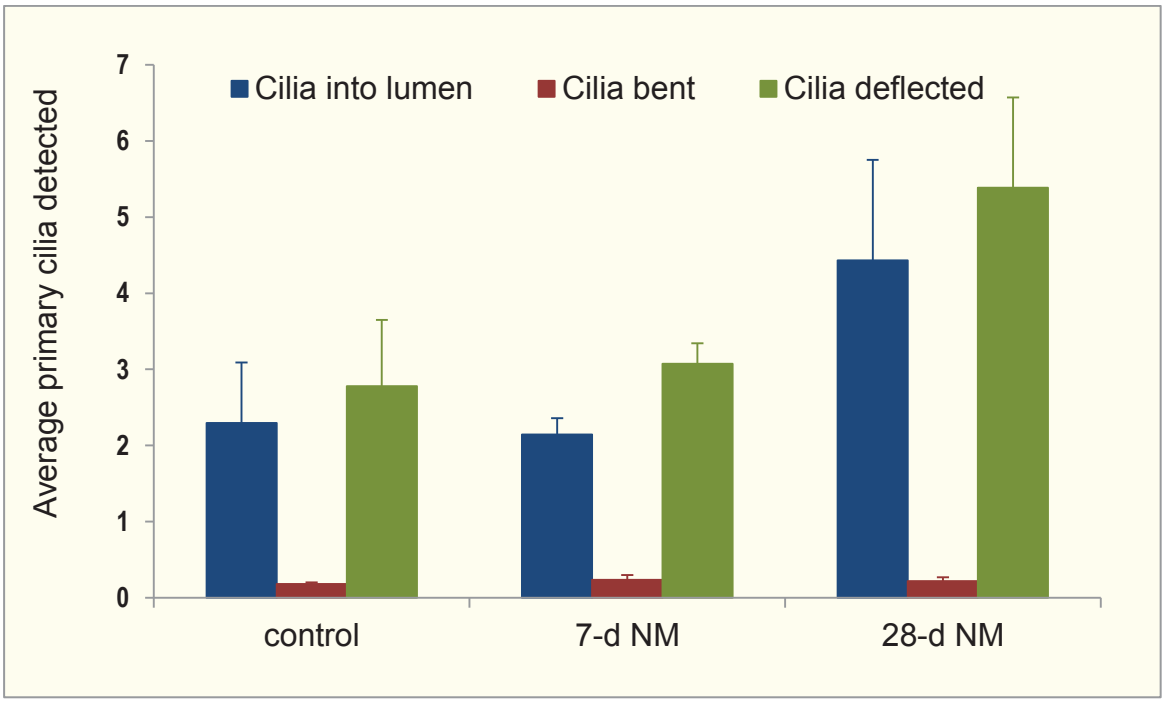

Figure 2.9 Average number of different primary cilia morphologies within each experimental group Note: Cilia morphology was assessed for the three experimental groups (n=3/group). Using composite micrographs, clearly visible cilia were either classed as bent, deflected or projecting towards the lumen in accordance with their appearance/morphology (±SEM)

2.3.5 Analysis of qRT-PCR

Quantitative RT-PCR was performed to investigate changes in mRNA expression levels of genes of interest after extended periods on non-milking (Fig. 2.10 and Fig. 2.11). The mRNA levels of αS1-casein were significantly reduced after 7 d NM and 28 d NM by 42-fold and 16-fold, respectively, relative to control. Similar effects were detected in gene expression levels of α-lactalbumin. Following 7 d NM and 28 d NM, there was a significant decrease in gene expression by 157-fold and 27-fold, respectively. The mRNA levels of κ-casein were also decreased after 7 d NM and 28 d NM by 5-fold and by 8-fold, respectively (Fig. 2.10).

Lactoferrin, in contrast, showed a numerical increase in mRNA levels, after 7 d NM and 28 d NM relative to lactating controls by 5-fold and 7-fold, respectively, but not of statistical significance. Comparing individual expression levels within the lactating/control group, it became clear that the animals express lactoferrin at different levels during active lactation which impacted on the overall results (Fig. 2.11).

Although there was an overall numerical increase in STAT6 mRNA levels following 7 d NM and 28 d NM by 3-fold and 10-fold, respectively, no significant change could be detected. Furthermore, individual expression levels indicated an outlier within the control (0 d NM) group; however, due to the small sample size the results of all animals were included in the analysis (Fig. 2.11).

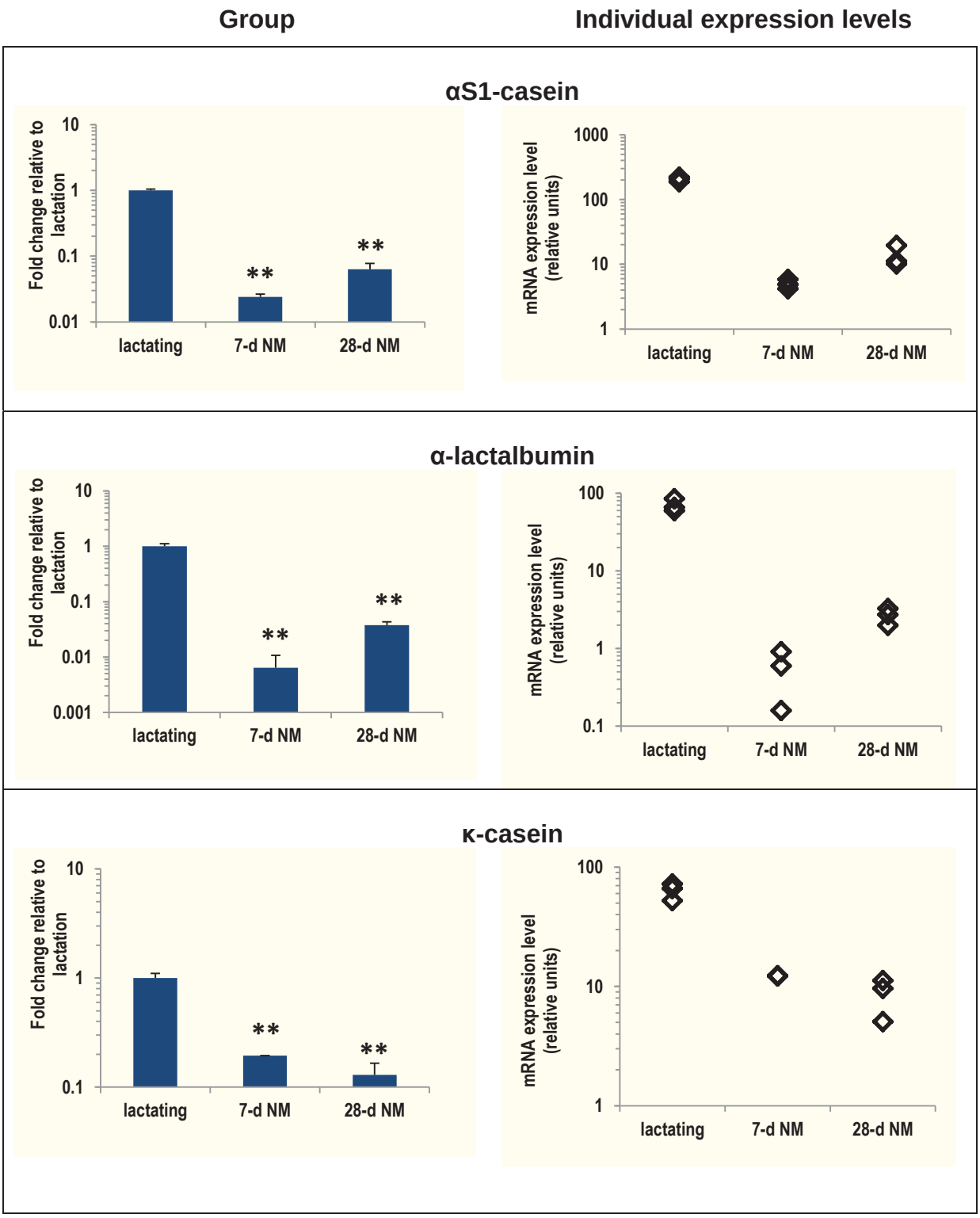

Figure 2.10 Differences in gene expression levels of αS1-casein, α-lactalbumin and κ-casein following extended periods of non-milking. Data from each group are expressed as back-transformed fold-change relative to lactation with the SEM to compare lactating/control and engorged/non-milked glands (n=3/group). Data from individual animals are expressed as normalised, back-transformed mRNA expression levels. ** P <0.01

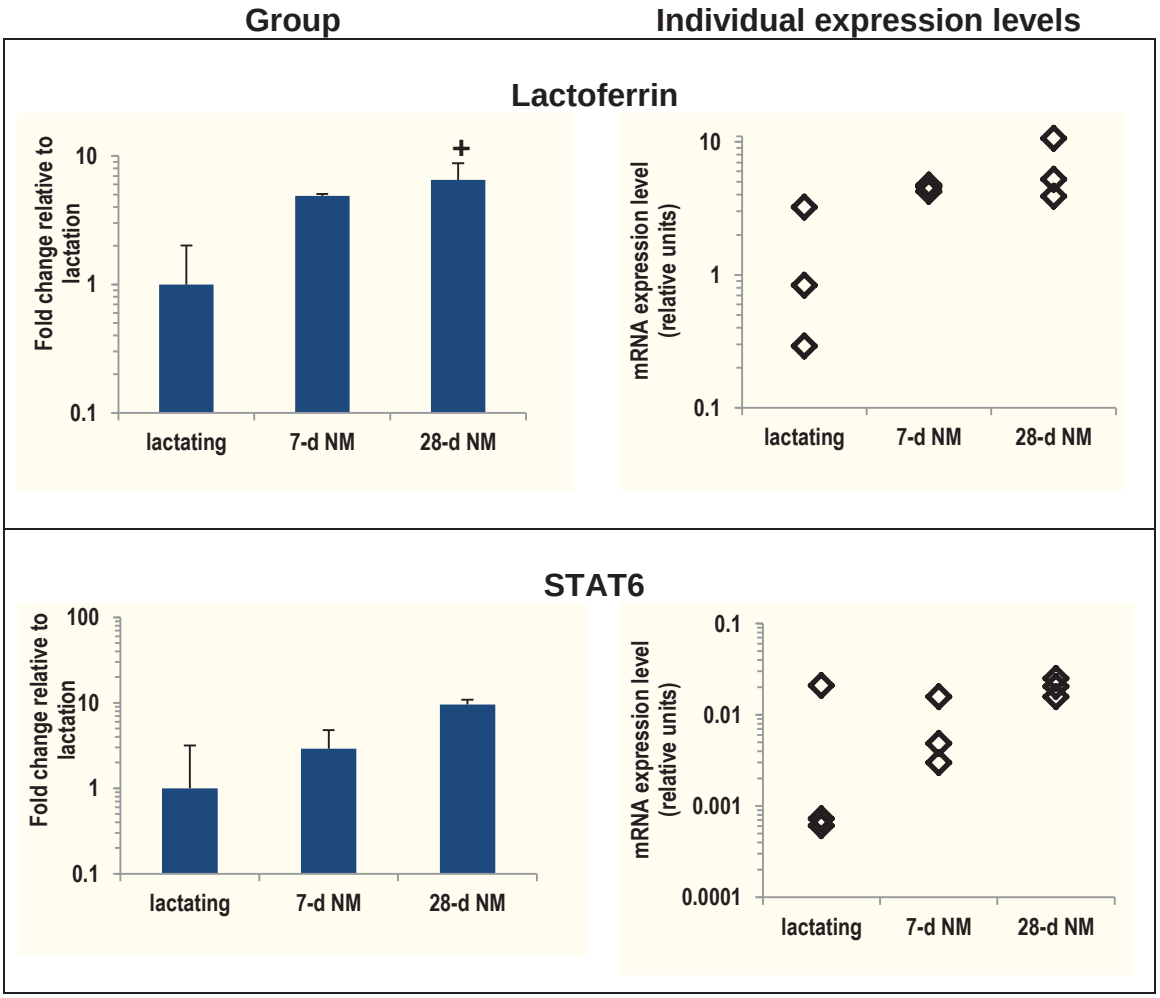

Figure 2.11 Changes in gene expression levels of lactoferrin and STAT6 following extended periods of non-milking. The data from each group are expressed as back-transformed fold-change relative to lactation with the SEM to compare lactating/control and engorged/non-milked glands (n=3/group). Data from individual animals are expressed as normalised, back-transformed epression levels. $^{+}$ P <0.1

2.3.6 Western blot analysis of (p)STAT6 protein expression

Western blot analysis was used to determine the pattern of (p)STAT6 protein expression at different stages of lactation.

2.3.6.1 Protein integrity

Confirmation of equivalent sample loading of SDS-PAGE gels was obtained by Coomassie blue staining of untransferred gels for soluble protein fractions (Fig. 2.12), while the effective transfer of proteins onto a nitrocellulose membrane was confirmed by Ponceau S staining (results not shown).

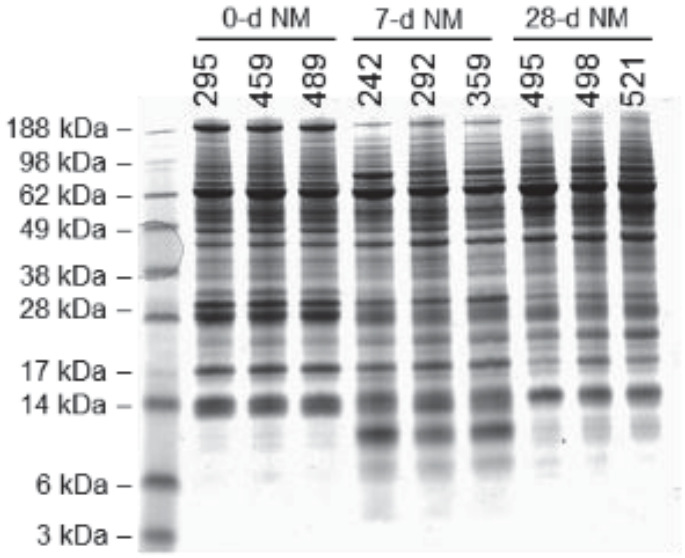

Figure 2.12 Representative image of a Coomassie blue stained gel loaded with protein samples extracted from bovine mammary glands following extended periods of non-milking. Representative Bis-Tris protein gel (10 %) containing protein samples of each animal from the control (0 d NM), the 7 d NM, and the 28 d NM group (n=3/group) used for the protein analyses. Each lane was loaded with 20 µg of total protein from the soluble fraction, except the marker lane which contained 5 µl of the SeeBlue® Plus2 Pre-Stained Standard

.

2.3.6.2 STAT6 antibody testing

Prior to sample analysis by Western blotting, a commercially available STAT6-positive control was used to confirm specific STAT6-protein detection (Fig. 2.13). Three samples (one from each experimental group) were randomly chosen and 20 µg of total protein were loaded onto a gel as well as 2 µl of positive control. In each sample as well as the positive control a single band could be detected, at the expected size, and very little to no background was observed. The predicted size for bovine STAT6 protein is 95 kDa (source: uniprot.org). Therefore, it was concluded that the STAT6 antibody specifically detected bovine STAT6 in these samples.

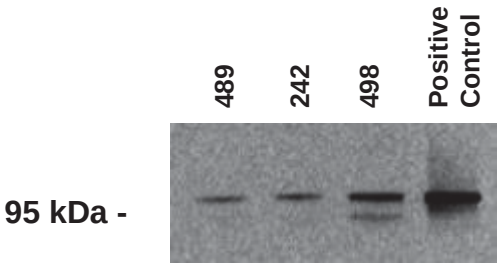

Figure 2.13 Representative image of Western blot after STAT6-antibody testing. Three samples (one from each experimental group) were randomly chosen and 20 µg of total protein was loaded onto a gel as well as 2 µl of positive control. In each sample, a single band could be detected at 95 kDa, including the positive control, and very little to no background was observed

2.3.6.3 pSTAT6 antibody testing

Similar to the STAT6 antibody testing (section 2.3.6.2), three samples (one from each experimental group) were randomly chosen and 20 µg of total protein were loaded onto a gel as well as 2 µl of positive control. Furthermore, different primary antibody titres (1:300; 1:1000 and 1:3000) were tested. Although little to no background could be observed, no specific signal of the pSTAT6 protein could be identified. Therefore, it was concluded that the antibody tested in this experiment may not specifically detect bovine pSTAT6 and would not be used for further analyses.

2.3.6.4 STAT6 protein expression following extended periods of non-milking

To determine changes in the pattern of STAT6 protein expression after extended periods of non-milking, densitometric analysis of western blotting was carried out (Figs. 2.14 and 2.15).

Following a period of non-milking for seven days, STAT6 protein expression numerically increased by 1.7-fold. Furthermore, a significant increase in STAT6 protein expression by 3.8-fold could be determined following 28 days of non-milking relative to control (0 d NM).

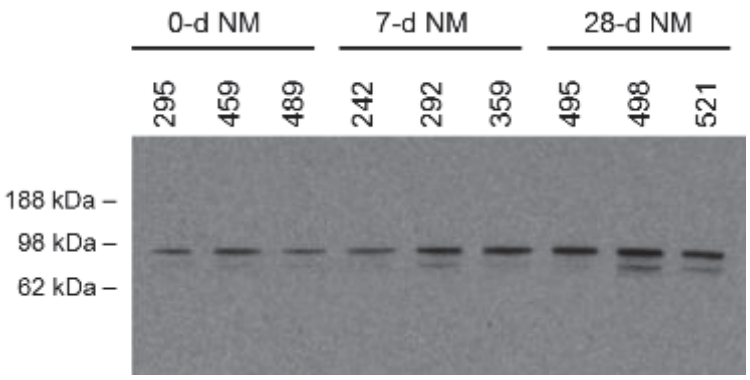

Figure 2.14 Representative image of Western blot to determine patterns of STAT6 protein expression following extended periods of non-milking (n=3/group). Each lane was loaded with 20 µg of total protein. The primary antibody used was rabbit anti-STAT6 (polyclonal, 1:1000 dilution)

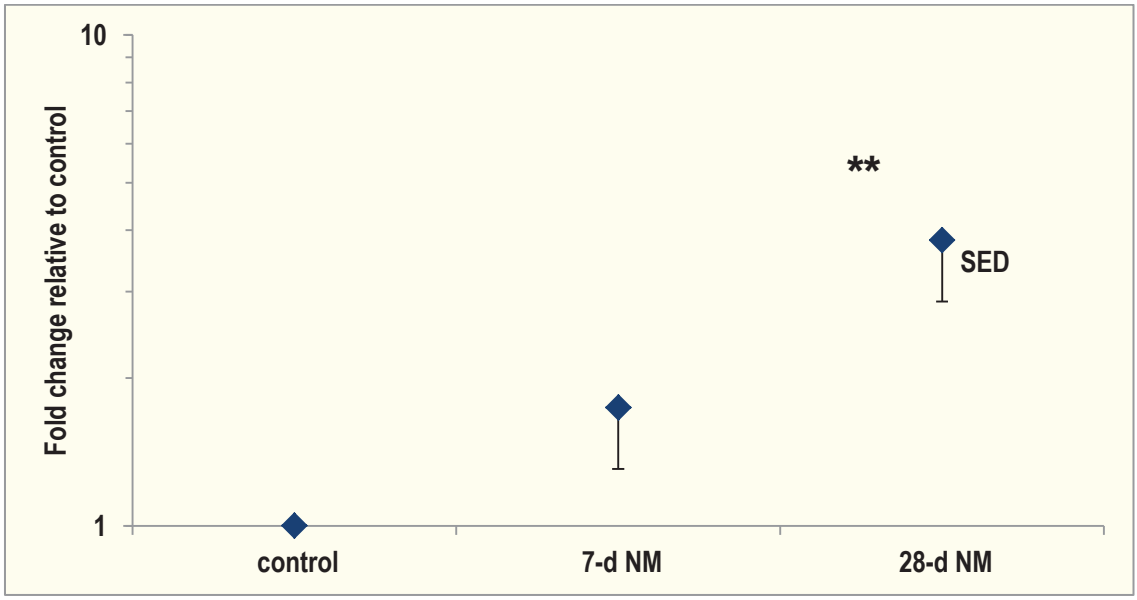

Figure 2.15 Densitometric analysis of Western blots to determine changes in STAT6 protein expression in the mammary gland following extended periods of non-milking (n=3/group). Results are graphed as back-transformed mean fold changes relative to the control (0 d NM) with the SED. ** P <0.01

2.4 Discussion

Mammary tissue is composed of different tissues and cell types, and mammary gland function is tightly coordinated by various factors/stimuli, systemic as well as local. Moreover, the optimal development of the highly organised lobular-alveolar structures is important to ensure sufficient milk production to nurse the offspring (Knight & Peaker, 1982; Plath *et al.*, 1997). After weaning, however, in most mammalian species, extensive tissue remodelling occurs to prepare the mammary gland for a subsequent pregnancy-lactation-involution cycle (Anderson *et al.*, 2007).

In the dairy cow, the majority of the alveolar structure remains intact during involution. However, it is proposed that senescent cells are replaced by mammary progenitor cells to ensure sufficient milk yield in the subsequent lactation period (Capuco & Akers, 1999; Capuco *et al.*, 2003). In our study, the overall structure of the mammary gland remained visible in all three treatment groups. However, heterogeneity in the tissue structures was observed. As previously described, within the same animal, it was found that areas of lobules showing signs of active lactation, while other areas appeared to be involuted (Molenaar *et al.*, 1992). Nonetheless, with longer periods of non-milking, more collapsed alveoli were observed and the overall tissue structure appeared less organised.

In mice, insufficient clearance of cell debris or milk constituents could lead to tissue scarring and reduced milk production in subsequent lactations (Atabai *et*

al., 2005). Furthermore, locally secreted cytokines are important for controlling lineage commitment during pregnancy as well as controlling and coordinating cell death and tissue remodelling during involution (Watson & Kreuzaler, 2011). Although there is a growing body of knowledge in regulatory aspects of milk production and maintenance (Wilde *et al.*, 1995; Accorsi *et al.*, 2002; Singh *et al.*, 2008), the question of how these stimulatory factors mediate a local cellular response remains unanswered.

Recently, the primary cilium has emerged as a mechanosensor in numerous tissues, such as bone (Nguyen & Jacobs, 2013), liver (Masyuk *et al.*, 2008), kidney (Praetorius & Spring, 2001) and lungs (Ellerman & Bisgaard, 1997), sensing not only fluid flow (Schwartz *et al.*, 1997), but also mechanical signals, such as pressure (Poole *et al.*, 1985), touch and vibration (Singla & Reiter, 2006; Hoey *et al.*, 2012). Furthermore, PC and their role as potential mechanosensors have been linked to mammary gland development in mice (McDermott *et al.*, 2010). However, their role in mammary gland involution remains elusive. To our knowledge, only two previous studies investigated and described PC in the bovine mammary gland during and after lactation (Nickerson, 1989; Millier *et al.*, 2013).

In agreement, the present study shows PC are present on luminal epithelial cells as well as myoepithelial cells, in the bovine mammary gland. However, the overall number of ciliated MEC was low. Furthermore, the number of MEC ciliated during active lactation was lower than MEC ciliated following extended periods of non-milking. Similar observations have been reported previously (Nickerson, 1989;

McDermott *et al.*, 2010; Millier *et al.*, 2013). In fact, in the mouse mammary gland, PC numbers decreased once mammary gland tissue was fully developed (McDermott *et al.*, 2010). During active lactation, however, the epithelial cell layer is fully differentiated and highly metabolically active (Larson, 1985a) and it has been postulated that a state of high secretion may not be compatible with maintaining a PC (Millier *et al.*, 2013). Furthermore, during lactation the epithelial cell layer is a tight network with cell-cell junctions, such as TJs, and cell-matrix junctions, including FAs, playing an important role during cell communication (Chen *et al.*, 2004). Thus, there may not be a need for every cell to be ciliated in order to achieve synchronised milk secretion.

In the lactating mammary gland, the majority of the secreted milk is stored in the alveolar compartment which in turn leads to fluid accumulation and intra-mammary pressure increase (Peaker, 1980; Bruckmaier, 2005). Luminal epithelial PC are exposed to the extracellular environment, in this case the fluid-filled alveolar lumen, where they could act as sensor for pressure dynamics in the mammary alveoli or for fluid flow in the mammary ducts during milk removal. Therefore it was not surprising to see more PC deflected flat against the apical cell surface rather than projecting towards the lumen. During milk stasis, however, no milk is removed from the mammary gland which in turn leads to the absence of fluid flow and, thus, no PC bending. In the absence of fluid flow, the proteolytically cleaved carboxy-terminal region of PC-1 translocates to the nucleus, where it associates with the transcription factor STAT6 and the co-activator p100 to stimulate gene expression (Low *et al.*, 2006; Berbari *et al.*, 2009). The STAT6 transcription factor and its upstream cytokines, IL-4 and IL-13,

appear to play a role during the expansion of the luminal lineage as well as post-lactational tissue regression and are linked to PC signalling (Khaled *et al.*, 2007; Zhang *et al.*, 2008; O'Brien *et al.*, 2010; Hughes & Watson, 2012; O'Brien *et al.*, 2012). Furthermore, previously shown to be upregulated during lactation (Broadhurst & Wheeler, 2001), the p100 co-activator has also been identified as a promoter of cell growth (Tong *et al.*, 1995) and forms a stable complex with PC-1 which is sequestered at the PC (Nauli *et al.*, 2003).

In this study, it is reported that extended periods of non-milking resulted in the onset of early involution (as indicated by gene expression and histology described above) in the bovine mammary gland. Moreover, there was a significant increase in STAT6 gene as well as protein expression; however, the STAT6 phosphorylation status was not determined. Therefore, no conclusions on the STAT6 activation status following extended periods of non-milking can be made. While the STAT6 transcription factor is important for commitment of luminal epithelial cells to the alveolar lineage in the mammary gland development (Khaled *et al.*, 2007; McDermott *et al.*, 2010), it has also been linked to the immune system by playing a role in the differentiation of T-helper cells (Hughes & Watson, 2012). Furthermore, while STAT3 and STAT5 transcription factors are activated by various external stimuli including growth factors, hormones, and cytokines, the STAT6 transcription factor is activated by a small group of cytokines, mainly interleukin-4 (IL-4) and interleukin-13 (IL-13) (Bromberg, 2000; Haricharan & Li, 2013). Previously, IL-4 and IL-13 have been shown to act as macrophage chemoattractants (Hiester *et al.*, 1992) and to induce an alternative M2 form of macrophage activation (Gordon, 2003), which has been shown to be

involved in wound healing and tissue remodelling/repair (O'Brien *et al.*, 2010). In the mouse mammary gland, gene expression profiling during post-lactational tissue regression showed an increase in genes previously linked to the immune system (Clarkson *et al.*, 2004) which coincides with increasing levels of IL-4 and IL-13 potentially acting as macrophage chemoattractants (O'Brien *et al.*, 2010).

Taken together, these results indicate a potential role for PC as mechanosensors in the bovine mammary gland. Assessment of histological features as well as decreased milk protein gene expression levels showed an overall increase in the degree of involution and number of features associated with involution in both treatment groups (Holst *et al.*, 1987; Capuco & Akers, 1999; Singh *et al.*, 2008). Furthermore, extended periods of non-milking resulted in an increase in ciliated luminal MECs in both treatment groups which could be an indicator of epithelial cell dedifferentiation, reassembling their PC for correct mammary gland development, and, thus, replacement of senescent cells in preparation of the next lactation period. Finally, extended periods of non-milking resulted in an increase in STAT6 gene and protein expression in both treatment groups. In the absence of fluid flow (i.e. milk stasis), STAT6 transcription factor activation could stimulate IL-4 and IL-13 gene expression. This results in a feedback loop with IL-4 and IL-13, inducing further STAT6 gene expression as well as acting as chemoattractant for macrophages to promote tissue remodelling and to clear the gland from cell-debris and/or milk constituents.

Chapter 3:

Effects of Mechanical Strain on Cellular Adhesion Structures in Bovine MEC *in vitro*

Chapter 3 Introduction

The bovine mammary gland consists of a branching network of ducts and secretory alveoli clustered together creating a tubulo-alveolar structure that can repeatedly undergo the different phases of the lactation cycle: growth, functional differentiation, lactation, and regression (Akers, 2002; McManaman & Neville, 2003). During lactation, secretory MECs are highly metabolically active and columnar in shape with a polarised structure (Linzell & Peaker, 1971; Larson, 1985b; McManaman & Neville, 2003). Individual cells are connected via a series of junctional complexes, including TJs, desmosomes, and adherent junctions. Cell-cell and cell-matrix junctions provide tissue integrity and promote cell polarity. Furthermore, they guarantee sufficient communication between cells to ensure synchronised milk secretion and support cell survival (Mepham, 1987; Mitic & Anderson, 1998; Maeda *et al.*, 2005). Thus, milk components are synthesised by the MECs, secreted into the lumen, and subsequently removed from the gland (McManaman & Neville, 2003).

After weaning however, milk stasis occurs which, through local factors, prompts extensive lobular-alveolar remodelling process, called involution (Marti *et al.*, 1994; Marti *et al.*, 1997). Consequently, the mammary gland loses its ability to produce milk due to morphological changes (Mielke, 1986). Although the actual trigger to initiate the process of involution is still unknown, it has been proposed that gland engorgement due to milk accumulation results in alveolar cells being subjected to mechanical strain (Marti *et al.*, 1997; Quaglino *et al.*, 2009). This mechanical stimulation, *per se*, could play a key role in the initiation of the process of involution (Marti *et al.*, 1999).

3.1 Mechanotransduction

Tissues grow and remodel in response to changes in mechanical forces. These mechanical forces play a fundamental role in regulation of cell function, including gene induction, protein synthesis, cell growth and death, cell morphology and differentiation, which are essential for tissue homeostasis. Conversely, abnormal mechanical loading conditions alter cellular functions and change structure and composition of the extracellular matrix (ECM). Therefore, depending on their respective needs, tissues constantly adapt to the environmental mechanical stress by modulating sensitivity to exogenous stimuli (Alenghat *et al.*, 2004; Chen *et al.*, 2004; Ingber, 2006). As an example, MECs respond to the stiffness of its matrix environment by altering differentiation, development or even induction of a malignant phenotype (Paszek *et al.*, 2005; Nelson & Bissell, 2006).

Moreover, stress-induced signal transduction is at least 40 times faster than growth factor-induced signal transduction (Na *et al.*, 2008), can be highly directional and thereby conveys and transmits complex information directly in three dimensions (Wells, 2013). Furthermore, mechanical signalling pathways are likely to induce cell-type- and stimulus-type-specific cellular responses (Bukoreshtliev *et al.*, 2013).

Mechanobiology/mechanotransduction intends to reveal mechanical properties of a cell as a singular unit (Bukoreshtliev *et al.*, 2013). Therefore, by definition, mechanical signalling requires a component that responds to an applied external force without necessarily being triggered by a specific chemical stimulus (Janmey & McCulloch, 2007). Numerous molecules and subcellular structures could

potentially mediate mechanical stress due to force-induced changes in protein conformation (Ingber, 1993; Ingber, 1997, 2006; Schwartz, 2010). These force-induced effects on conformation change represent a general mechanism which may regulate enzymatic activity, enable new molecular interactions, or liberate soluble bond factors which in turn may activate signalling pathways in an autocrine and paracrine fashion (Nelson & Gleghorn, 2011; Hoey *et al.*, 2012; Jones & Nauli, 2012). Therefore, a complex network of protein-protein interactions providing a direct linkage between cells and the nuclei could play a key part in rapidly transferring mechanical stimuli, such as strain or vibrations, from cell surface receptors to distinct structures in the cell and nucleus (Maniotis *et al.*, 1997; Gonzalez *et al.*, 2011). This in turn could activate and/or alter epigenetic mechanisms that are critical for tissue-specific gene expression, such as milk gene expression in the mammary gland (Gonzalez *et al.*, 2011).

3.1.1 Mechanotransduction in *in vitro* studies

Over the past decades, research in mechanotransduction has expanded from sensory cells, such as hair cells in the inner ear, to diverse cell types, such as smooth muscle cells, MECs, chondrocytes and alveolar type cells, which shows its involvement in a broad range of cellular functions (Jaalouk & Lammerding, 2009).

In vivo, cells are subjected to stresses of 0.01 to 0.1 atm which is equivalent to 1 to 10 nN per cell contact, therefore, even small changes in magnitudes or distribution of forces may lead to compensatory remodelling of cellular adhesion

structures and change gene expression levels in a tissue-specific manner (Close *et al.*, 1997; Chen *et al.*, 2004). For example, changes in MEC shape cause transcriptional and post-transcriptional regulation of lactoferrin mRNA (Close *et al.*, 1997). Furthermore, integrin-mediated response to BM components is critical for regulating oestrogen receptor-α expression and function in MECs (Novaro *et al.*, 2003). Three-dimensional cultures of MECs containing a laminin-rich ECM induced cell rounding and histone deacetylation affecting chromatin condensation which in turn alters gene expression levels (Le Beyec *et al.*, 2007). Cell stretch leads to an initial switch from survival to apoptotic mode by reproducing weaning-like events with cultured MECs which are comparable to *in vivo* actions occurring during the involution process (Quaglino *et al.*, 2009).

Overall, several experiments have shown that stretching different types of epithelial cells attached to a substratum results in elevated levels of proliferation and apoptosis in a stretch-dependent manner. These results indicate that cell stretch may cause a cell turnover in order to replace senescent cells and to keep homeostasis. In cases where homeostasis cannot be maintained, uncontrolled cell growth may cause tumorous growths which can cause cancer (Tschumperlin *et al.*, 2000; Li *et al.*, 2001; Zhang, Li, Sanders*, et al.*, 2003; Ali *et al.*, 2006; Chaturvedi, Marsh, & Basson, 2007; Chaturvedi, Marsh, Shang*, et al.*, 2007; Craig *et al.*, 2007; Hammerschmidt *et al.*, 2007; Mohan *et al.*, 2007; Amura *et al.*, 2008; Gayer, Chaturvedi, Wang, Alston*, et al.*, 2009; Gayer, Chaturvedi, Wang, Craig*, et al.*, 2009; Koshihara *et al.*, 2010).

3.1.2 Objective

Cell-cell and cell-matrix junctions provide tissue integrity, promote cell polarity, guarantee sufficient communication between cells to ensure synchronised milk secretion and support cell survival. Their disruption may be one of the first initiators of the mammary gland remodelling process. Therefore, an *in vitro* approach using a homemade cell stretching device, which clearly separates the effects of physical stretching of MECs from the actions of possible chemical inhibitors in milk, was chosen for this study. The effect of stretching MECs *in vitro* on the expression of TJ proteins and FAs was determined. For that purpose a custom-made cell stretch device was designed to test the hypothesis that the stretching of MECs *in vitro* induces changes in the gene or protein expression of FAs (β1-integrin, (p)AKT) and TJ components (occludin, claudin-1 and ZO-1).

3.2 Materials and Methods

3.2.1 Cell stretch device

A device was specially fabricated, which was designed (co-designed and fabricated by Brian Atkins, Steve Gebbie and Scott Sevier, AgResearch) to apply a controlled, static equibiaxial strain to cells attached to a flexible membrane similar to those previously presented (Hung & Williams, 1994; Lee *et al.*, 1996; Tschumperlin & Margulies, 1998). The device consists of an aluminium alloy metal cassette which holds a six-well BioFlex plate (35 mm diameter, 0.020" thick, Flexcell International, Hillsborough, USA) over six hollow plastic circular indenters (27.8 mm diameter; PETP-TX) that are fixed underneath the centre of each well (Fig. 3.1 and Fig. 3.2). Flexible membranes at the bottom of each well serve as the deformable substratum for cell attachment. All six wells can be stretched simultaneously by moving the indenters upwards until the membranes are displaced to the required depth. The indenters are hollow to minimise the area of contact with the membrane, reduce friction and give a uniform membrane deformation. Furthermore, the hollow design allows the use of an inverted microscope to observe the cells during the experiment to ensure firm attachment. A digital indicator enables accurate measures of the displacement ($1/10^{th}$ of a millimetre) of the indenters to ensure reproducibility for each experiment.

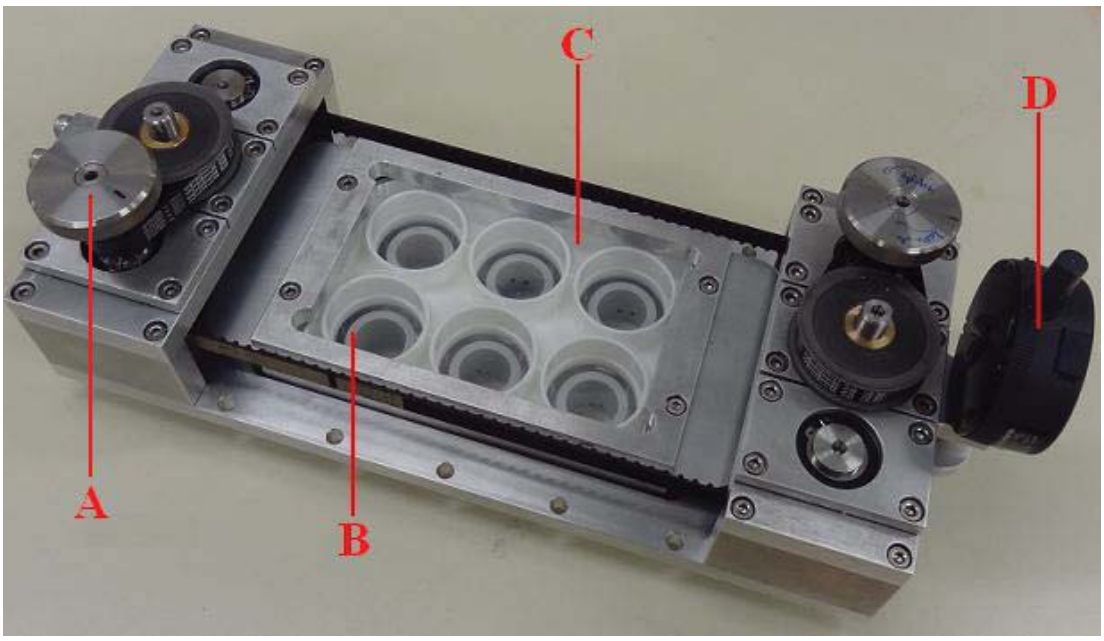

Figure 3.1 A custom-made device to stretch MECs *in vitro*. A: hand wheel to decrease/increase indentation; B: hollow indenters; C: 6-well plate with flexible bottom; D: digital indicator to measure indentation

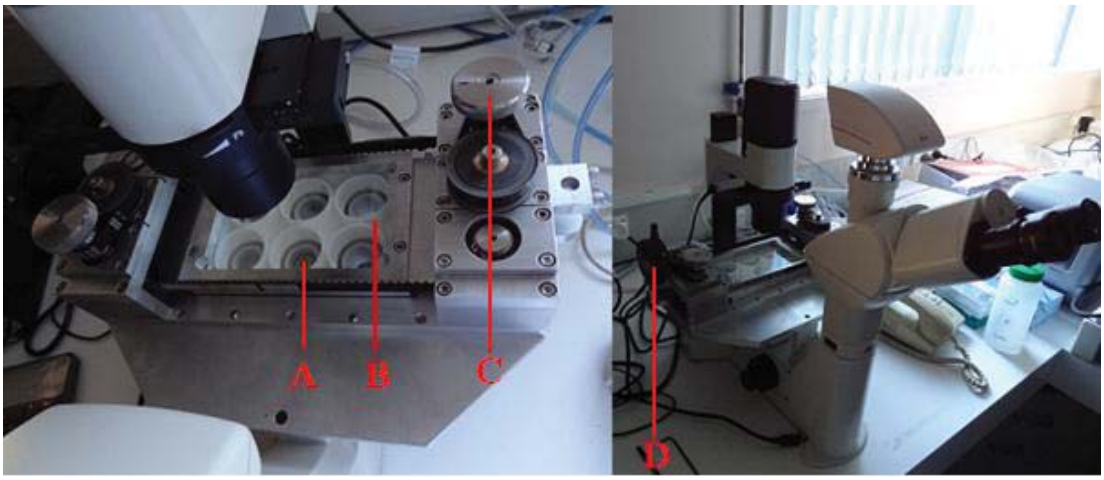

Figure 3.2 Custom-made cell stretch device fully assembled under the microscope. A: objective lens from microscope; B: 6-well plate with flexible bottom coated; C: hand wheel to decrease/increase indentation; D: digital indicator to measure indentation

The depth of the displacement of the membrane by the indenters directly influences the magnitude of stretch applied to the membrane and subsequently the cells attached to the membrane (Fig. 3.3). Uniform equibiaxial stretch of equal magnitude is achieved by using circular indenters of nearly the same diameter as the flexible membrane (Schaffer *et al.*, 1994). For the majority of the membrane this can be assumed to be true, however, the strain at the edges of the membrane will not be uniform (Dr Paul Shorten, AgResearch, personal communication). This is comparable to similar existing devices capable of applying uniform equibiaxial strain, whether using indenter displacement of membranes (Hung & Williams, 1994; Schaffer *et al.*, 1994; Tschumperlin & Margulies, 1998), or vacuum-operated membrane deformation across loading posts such as the Flexcell® FX-5000™ Tension System (Flexcell International).

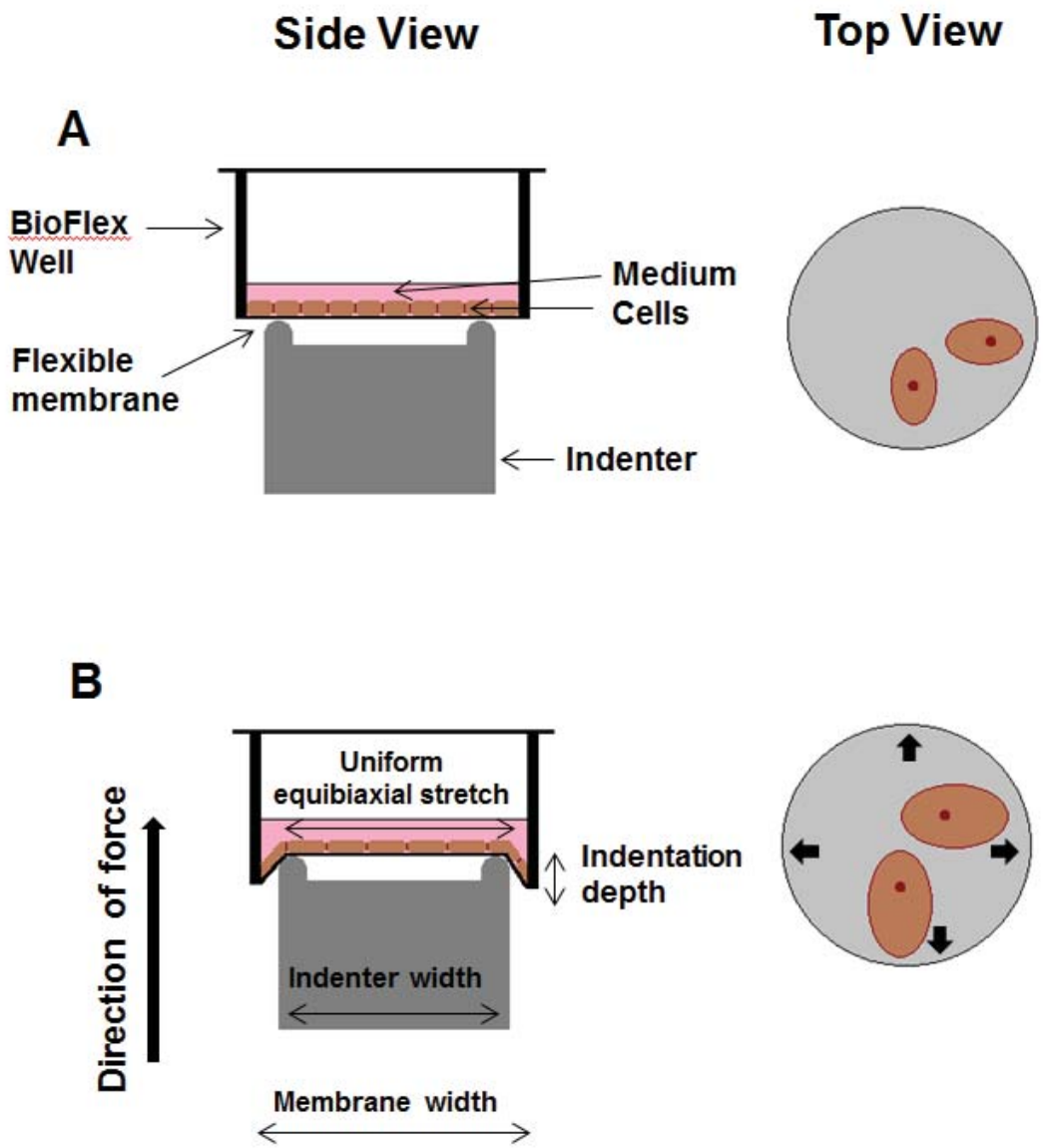

Figure 3.3 Schematic of the principal function of a custom-made device designed to stretch MECs *in vitro*. Depicted are the side view and the top view of the flexible membrane in the (A) rest position and (B) deformed over the indenters during uniform equibiaxial stretching. Note: the strain at the edges of the membrane (where it does not stretch across the indenter) will not be uniform. The diagram is not drawn to scale

Stretching the membranes will result in an increase of membrane surface area (MSA). The %-change in MSA (ΔMSA) for each indentation is represented by the following equation:

$$\%\Delta MSA = \left(\frac{\left[\frac{\pi r_0^2 + S}{\pi r_1^2} \right]}{1} - 1 \right) \times 100$$

Where:

$$S = \pi (r_1 + r_0) \sqrt{d^2 + (r_1 - r_0)^2}$$

r_1 = ½(27.5) mm = radius of the indenters

r_0 = ½(35) mm = radius of the wells

d = number of turns x 1.5 mm = indentation depth

(Equations were kindly derived by Dr Paul Shorten, AgResearch Ruakura)

The relationship between the indentation depth and the % ΔMSA is shown in Fig. 3.4.

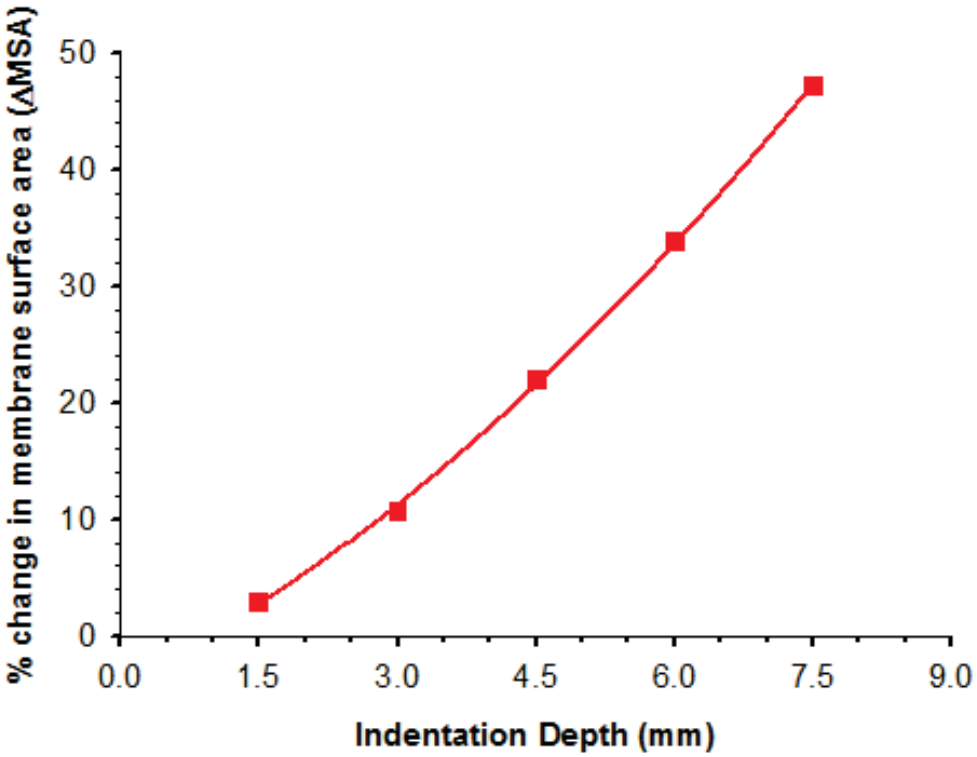

Figure 3.4 The relationship between the indentation depth (mm) of the cell-stretch device and the maximum % change in membrane surface area (ΔMSA). Where one turn of the cell-stretch device is equal to an indentation depth of 1.5 mm and the maximum number of turns that can be done is 5, corresponding to a maximum ΔMSA of 47 %

3.2.2 Primary cell extraction

Primary cells for the *in vitro* stretch experiments were isolated from third-trimester, non-lactating, pregnant cows (45 days prepartum) as described by Swanson *et al.* (2009) (Swanson *et al.*, 2009). Briefly, approximately 100 g of alveolar tissue was removed immediately after slaughter and cut into 1 cm^3 pieces, removing fat and connective tissue. Next, the tissue was placed in 250 ml of digest media [HBSS with 0.4 % BSA (w/v), 2 mM glutamine, MEM AA solution (Invitrogen, Carlsbad, USA), 5.5 mM glucose, 1.2 mg/mL of collagenase IV (Worthington BiochemicalCorp.), 0.02 mg/mL of DNase I, 0.5 mg/mL of

hyaluronidase (Sigma, St. Louis, USA), 1 µg/mL of cortisol, 5 µg/mL of insulin, and antibiotic-antimycotic (Invitrogen)] and incubated for 2 h on an orbital shaker (110 rpm) at 37°C. Following the digest, cellular debris and single cells were removed by centrifugation (80 x g; 5 min). The remaining tissue was minced using opposing scalpel blades, digested for an additional 3 h and filtered through 150 µm mesh and centrifuged (100 x g; 10 min). After a wash in HBSS, cells were fractioned on a Percoll (Sigma) gradient. After centrifugation (800 x g; 20 min), epithelial cells banded at 1.03 to 1.05 g/ml fractions. The resulting cells were washed and cryopreserved at a concentration of 20×10^6 cells/ml in 90 % foetal calf serum/10 % dimethylsulfoxide for future experiments.

3.2.3 Cell culture

The extracted primary bovine mammary cells were used in all stretch experiments. Furthermore, the cells were only used up to passage 3 after initial isolation. Primary cell aliquots were thawed and grown to confluence in 75 cm^2 flasks (Nunc, ThermoFischer, Waltham, USA) in a growth medium which is a composite medium [4.75 g/ml M199 (Gibco; Invitrogen, Carlsbad, USA)/ 5.32 g/l HamF12 (Gibco, Invitrogen)] supplemented with 10 mM HEPES (Gibco; Invitrogen), 10 % foetal calf serum (Sigma, St. Louis, USA), 10 % horse serum (heat-inactivated; Sigma), 200 U/ml penicillin (Gibco; Invitrogen); 200 U/ml streptomycin (Gibco; Invitrogen), 5 µg/ml insulin (Sigma), 1 µg/ml cortisol (Sigma) and 10 ng/ml epidermal growth factor (EGF; Sigma) at 37°C in an atmosphere of 5 % CO_2 and 95 % air at all times. Subsequently, cells were trypsinised using TrypleExpress® (Gibco; Invitrogen), split into two 6-well BioFlex plates (FlexCell

International) and incubated in attachment media (same as growth medium, but with the addition of 3 µg/ml PRL and 0.05 % transferrin and without EGF) for 24 h to ensure cell attachment to the membrane. Next, the medium was changed to growth medium and the cells were cultured to confluence (media changed every second day), serum-starved for 24 h (same as growth medium, but without serum or EGF) and primed for an additional 48 h by adding 3 µg/ml PRL and 0.05 % transferrin (Sigma) to induce MEC differentiation. To perform cell stretch experiments, an additional 2 ml of media was added to each well of both 6-well plates. One plate served as control and remained untreated, while the other was placed in the cell stretch device. During the stretch experiment, membranes were continuously stretched at 25 % ΔMSA for the required length of time. Immediately following stretching, cells were washed, lysed and total RNA/Protein was extracted as described in section 3.2.9.

3.2.4 Immunocytochemistry

Initially, an immunocytochemistry (ICC) method was used to confirm that the majority of cells grown on the 6-well culture plates were of epithelial lineage. Keratin18 (CTK18; Abcam, Cambridge, UK) was used as a marker for epithelial cells, smooth muscle cell actin (SMA; Sigma) was used as a positive control and C2C12 murine myoblast cells as a negative control.

In preparation for the ICC experiments, the cells (primary and C2C12) were grown on coverslips (LabServ; ThermoFisher, Waltham, USA) precoated with 1 % sterile gelatine (Sigma), then fixed with 4 % paraformaldehyde (Acros

Organics, ThermoFisher, Waltham, USA) and permeabilised with 1x PBS (Oxoid Limited, Hampshire, UK) with 0.5 % Tween (Sigma). Nonspecific antigens were blocked at RT using an avidin/biotin block (10 min; Dako, Agilent Technologies, Santa Clara, USA), an endogenous enzyme block (10 min; Dako) and 2.5 % BSA (Gibco) in 1x PBS (30 min; Oxoid). The cells were then incubated with the primary antibody (CTK18 at 1:300; SMA at 1:300) overnight at 4°C, followed by incubation with the secondary antibody (biotiylated anti-rabbit Ig) (1:500; BioGenex, Fremont, USA) at RT for 30 min and a further incubation with a third antibody (peroxidase-conjugated streptavidin) (1:100; BioGenex) also at RT for 30 min. Next, the cells were incubated with 1x DAB substrate (Roche, Basel, Switzerland) for approximately 10 min until a distinct brown staining became visible. The nuclei were counterstained with hematoxylin, and mounted upside down onto microscopy slides using DePex mounting media (Gurr®, VWR, Radnor, USA).

3.2.4.1 Imaging immunocytochemistry staining

Two stained coverslips of the same type cell were mounted onto each microscopy slide, one with primary antibody added overnight and one without to serve as control. Images of each coverslip were produced using an Olympus BH-2 (Olympus, Shinjuku, Japan) with a ProgRes® C14 camera attached and 20x and 40x objectives, respectively. Per coverslip, five or six images were taken to analyse the degree of positively stain cells. ImageJ 1.45s (National Institutes of Health, Bethesda, USA) was used to process all TIF files, enhance contrast and add scale bars.

3.2.5 Testing of different membrane coatings

The cell stretch device was designed to use commercially available 6-well BioFlex plates (Flexcell International) of which a wide variety of membrane coatings are available. Preliminary experiments were conducted to determine the most suitable coating for the stretch experiments with the focus on cell attachment, growth and differentiation. Four different types of coating, which naturally occur in the basement membrane or the connective tissue of the mammary gland, were tested: collagen type I and IV, laminin and ProNectin (RGD-binding site; Flexcell International). Primary cells were cultured as described in section 3.2.3, and monitored daily. Furthermore, a period of stretch at a maximum of 47 % ΔMSA for 3 h was applied to test cell attachment before and after cell stretch.

3.2.5.1 Imaging of membrane testing

Images of the cells grown on differently coated substrata were produced using an Olympus BH-2 (Olympus) with a ProgRes® C14 camera attached and 20x and 40x objectives. Per culture plate, 6 images were taken to analyse cell growth and attachment. ImageJ 1.45s (National Institutes of Health) was used to process all TIF files, enhance contrast and add scale bars.

3.2.6 Cell stretch experiments

Primary cells were grown on collagen type IV flexible membranes in 35 mm BioFlex six-well plates (Flexcell International) as described in section 3.2.3.

Afterwards, cells were subjected to static stretching at 25 % ΔMSA for 1, 3, 5, 15, 24 or 48 h, respectively. Each time point included a non-stretched plate to provide a control and was repeated three times. Immediately following treatments, cells were washed twice with 1x PBS (Oxoid), lysed and total RNA/Protein was extracted as described in section 3.2.9.

3.2.7 Sample extraction

Total RNA and total protein from each well were extracted using the column-based GE Healthcare illustra™ triplePrep Kit (GE Healthcare Life Sciences, Little Chalfont, UK) according to manufacturer's manual.

3.2.7.1 RNA preparation

The amount of extracted RNA and potential solvent and/or protein contamination in each sample was measured using the NanoDrop™spectrophotometer (NanoDrop Products, Wilmington, USA; results not shown) according to manufacturer's manual. The RNA quality was measured by confirming the RIN were above 7 using the Agilent 2100 bioanalyzer system in conjunction with the Agilent RNA 6000 Nano Kit according to manufacturer's instructions (Agilent Technologies, Santa Clara, USA, results not shown).

3.2.7.1.1 cDNA synthesis

One µg of total RNA was used to synthesise first-strand cDNA using the SuperScript™III First-Strand Synthesis System for RT-PCR according to the

manufacturer's manual (Invitrogen). RNA was primed using the oligo(dT)20 system component. The generated cDNA was diluted three-fold (equivalent to approximately 17 ng/µl reverse transcribed total RNA) in nuclease-free water (Ambion®, Life Technologies, Carlsbad, USA) for downstream analysis.

3.2.7.1.2 Quantitative Real-Time PCR

Each RNA sample (1 µl) was assayed in triplicate, by qRT-PCR with SYBR Premix Ex Taq System (Takara, Otsu, Japan) using a Corbett Thermocycler (Corbett Life Science, Qiagen, Venlo, Netherlands). Three different reference genes were used as endogenous control: GAPDH, ubiquitin, and cyclophilin A. Additionally, each assay included RT-negative and 'no-template' control reactions for each primer pair. Real-time PCR experiments were performed under the following conditions: initially 95°C for 3 min; followed by 40 cycles of 95°C for 10 s, 58 or 60°C for 20 s, 72 or 75°C for 20 s (for individual experimental conditions refer to Table 1). Following the final cycle of each RT-PCR experiment a dissociation curve was obtained starting at 72°C, followed by a continuous temperature increase in 1 degree increments every 30 s until 95°C were reached.

Analysis of the melting temperature (Tm) of amplified products allowed for the detection of the target product as well as any non-specific products, including primer dimers which typically had a lower Tm of between 70-75 °C.

One PCR reaction mix (total final reaction volume = 10 µl) contained 5 µl SYBR Premix Ex Taq System (Takara), 3.8 µl of sterile, nuclease-free water (Ambion®, Life Technologies), 1 µl of cDNA and 0.1 µl of each of the forward and reverse

primers. All Primers were used at a final concentration of 100 nM in each 10 µl real-time reaction.

Prior to each experiment, optimal experimental conditions, such as annealing and acquisition temperatures, were determined in separate experiments to maximise the amplification of a single specific product and prevent primer dimer formation during the final PCR reactions for each gene of interest.

The primer sequences and other relevant details about individual experimental conditions are outlined in Table 3.1.

Table 3.1 Sequences of PCR primers (forward and reverse), primer position, PCR product sizes and individual experimental conditions of bovine nucleic acid sequences used for investigating gene expression by real-time RT-PCR

Gene	Nuclei Acid Sequence	Primer sequence (5'→3')	Primer position[1] [bp]	Product size [bp]	Annealing [°C]	Acquisition [°C]
Bax	AC_000175.1	Forward: cga gtg gcg gct gaa atg tt	314	166	60	72
		Reverse: gca gcc gct ctc gaa gga agt	479			
Bcl-2	AC_000181.1	Forward: atg tgt gtg gag agc gtc aa	439	201	60	72
		Reverse: cag act gag cag tgc ctt ca	639			
Claudin	AC_000158.1	Forward: gct agt gac aac atc gtg ac	128	395	58	72
		Reverse: atg aag aga gcc tga cca aa	522			
Cyclophilin A[2]	AC_000167.1	Forward: gca tac agg tcc tgg cat ct	310	279	60	72
		Reverse: tct cct ggg cta cag aag ga	589			
GAPDH[2]	AC_000162.1	Forward: ctc cca acg tgt ctg ttg tg	141	222	60	72
		Reverse: tga gct tga caa agt ggt cg	362			
Occludin	AC_000177.1	Forward: gac ctg atg aat tca aac cta atc	272	183	58	72
		Reverse: cga tac caa gca tag aca gga t	454			
Ubiquitin[3]	AC_000176.1	Forward: ggc aag acc atc acc ctg gaa	731	200	60	72
		Reverse: gcc acc cct cag acg aag ga	931			
ZO-1	AC_000178.1	Forward: cgt ctt cgt ctt cat ctt cc	4364	303	58	72
		Reverse: gat tca cac caa aac cat aca c	4666			
αS1-casein	AC_000163.1	Forward: tac cct gag ctt ttc aga ca	547	201	60	72
		Reverse: cat aac tgt gga gtc cct ca	747			
β1-integrin	AC_000170.1	Forward: cag atg agg tga aca gcg aa	1443	289	60	80
		Reverse: atg cag gaa gtg gta ccc ag	1731			

[1] Refers to the 5' position of the primers in the nucleic acid sequence [2] Primer sequence previously described in Coussens and Nobis, 2002 [3] Primer sequence previously described in Singh et al., 2008

PCR products were then QIAquick column-purified (Qiagen, Venlo, Netherlands) and submitted for DNA sequencing which verified their authenticity (University of Canterbury, New Zealand, DNA Sequencing Facility, results not shown).

3.2.7.1.3 Agarose gel electrophoresis for DNA

Agarose gels (1.5 % (w/v)), containing 1x TAE (40 mM Tris, 0.1 % (v/v) glacial acetic acid, 1 mM EDTA pH 8.0) and 1x SYBR® Safe DNA gel stain (Life Technologies), were used to visualise DNA samples. Wells were loaded with 5 µl of PCR product mixed with DNA loading buffer (0.25 % (w/v) bromophenol blue, 0.25 % (w/v) xylene cyanol FF, 30 % (v/v) glycerol) in 12 µl total volume. The gel was run at a constant 100 V in electrophoresis buffer (1x TAE, 1x SYBR® Safe DNA gel stain) for approximately 1 h. The DNA was then visualised under UV transillumination using a Gel Doc and Quantity One software (Bio-Rad Laboratories, Hercules, USA) to confirm the size and number of bands present.

3.2.7.1.4 Analysis of qRT-PCR data

Following qRT-PCR experiments, average take-off values for reference genes and genes of interest were generated for each sample using the Rotor-Gene Q software (version: 2.1.0). The take-off value represents the cycle number at which the fluorescence of each reaction crossed the threshold, which was placed above background fluorescence and within the log-linear phase of exponential product amplification. Therefore, the lower the take-off value the higher the amplification of PCR products. Relative quantification of gene expression was performed using comparative quantification to analyse changes in gene expression in samples of

stretched cells relative to the non-stretched controls. The amount of gene of interest in each sample was normalised by dividing by the amount of reference gene and the resulting values $\log_{10}$-transformed before statistical analysis.

3.2.8 Protein preparation

Protein samples were mixed with loading buffer (62.5 mM Tris pH 6.8, 2 % (w/v) SDS, 5 % (v/v) BME, 10 % (v/v) glycerol) (Laemmli, 1970), boiled for 5 min, and stored at -20˚C until required for subsequent western analysis. Prior to mixing in loading buffer, the amount of protein present in 1 µl of each sample was determined using Qubit® 2.0 Fluorometer in conjunction with the Qubit® Protein Assay kit as per the manufacturer's instructions (Invitrogen).

3.2.8.1 Protein integrity

Bis-Tris protein gels (10 %, Life Technologies) were loaded with samples from cell culture plates stretched for extended periods of time as well as their corresponding control samples (not stretched). Each lane was loaded with 20 µg of total protein, except the marker lane which contained 5 µl of the SeeBlue® Plus2 Pre-Stained Standard (Life Technologies). After SDS-Page electrophoresis, gels were stained and fixed for 2 h, then de-stained overnight in 20 % methanol.

3.2.8.2 Western blot analysis

Protein samples (20 µg) from the non-stretched control (n=6) and stretched (n=6) cells at each time point were loaded onto a precast NuPAGE® Novex® Bis-Tris Protein Gel (Life Technologies). Electrophoresis was then carried out in the XCell4 SureLock™ Midi-Cell apparatus (Life Technologies) for approximately 1 h at 200 V in 1x NuPAGE® MES SDS running buffer (Life Technologies). Next, separated proteins were transferred onto Hybond-ECL nitrocellulose membranes (Amersham Biosciences, GE Healthcare, Little Chalfont, UK) using the Trans-Blot Cell (Bio-Rad Laboratories) wet blotting system. After transfer, membranes were stained with Ponceau S (0.1 % (v/v) Ponceau S; 1.0 % (v/v) acetic acid) to visualise successful transfer of proteins onto the membranes, scanned using a GS-800 densitometer (Bio-Rad Laboratories) and washed with distilled water to remove the ponceau stain. Blocking of non-specific binding was achieved by immersing the membrane in a solution of 4 % NFMP overnight at 4°C on a rocker. Subsequent, membranes were probed with primary antibodies (for detailed information on antibodies please refer to Table 3.2) overnight at 4°C on a rocker, followed by incubation with horseradish-conjugated secondary antibody (goat-anti-rabbit at 1:10,000 dilution) for 1 h at RT. Slides were washed in multiple changes of wash buffer (1x PBS/0.1 % Tween 20) following each antibody incubation. Immunoreactive protein bands were detected using a chemioluminescence system (Amersham ECL Western Blotting Detection Reagents; GE Healthcare Life Sciences), BioMax XAR film (Kodak, Rochester, USA) and the 100 Plus film processor (AllPro^{TM}Imaging, Melville, USA). The developed films were scanned using the GS-800 densitometer (Bio-Rad Laboratories) and analysed using the Quantity One software (version 4.6.6).

Table 3.2 Information on antibodies used for Western Blot analysis, including species of origin, molecular weight, supplier, dilution and gel percentage for used SDS page gel electrophoresis

Antibody	Species of origin	Molecular Weight [kDa]	Supplier	Dilution	Gel % [1]
ZO-1	rabbit	220	Pierce	1:1000	4 to 12
Occludin	rabbit	60-82	Pierce	1:1000	10
Akt1/2/3 (H-136)	rabbit	1=62; 2=56; 3=62	SantaCruz	1:1000	10
pAkt1/2/3	rabbit	1=62; 2=56; 3=62	SantaCruz	1:5000	10

[1] Precast NuPAGE® Novex® Bis-Tris Protein Gel (Life Technologies) were used for all SDS page gel electrophoresis experiments in combination with the 1x NuPAGE® MES SDS running buffer (Life Technologies)

3.2.9 Statistical analysis

3.2.9.1 Statistical analysis of qRT-PCR results

The levels of mRNA expression from each time point were expressed as back-transformed mean fold-changes relative to the non-stretched controls. Differences in levels of mRNA expression from each group were analysed using the Student's paired t-test with a two-tailed distribution (MS Excel, 2010). Data are presented as the means for each treatment group with the standard error of the mean (SEM) between means with their corresponding P-values. Means were considered different at $P<0.05$ and within the range of a statistical trend at $P<0.1$. ** $P<0.01$, * $P<0.05$, $^{+}$ $P<0.1$.

3.2.9.2 Statistical analysis of Western blot results

Densitometry data from western blotting were $\log_{10}$-transformed and analysed by ANOVA in GenStat (16th edition, version 16.1.0.10916 (64-bit version)) with

blocking on replicate and adjusting for between gel variations to detect differences between control and stretched samples at each time point. In order to minimise between gel variations, each gel was loaded with four randomly chosen samples from each time point (1 h, 3 h, 5 h, 15 h, 24 h, and 48 h of *in vitro* cell stretch). Furthermore, each time point is represented by two 'stretched' (S) and two non-stretched (NS=control) samples per gel. Results are graphed as back-transformed mean fold changes relative to the control (NS) with the SED. Means were considered different at $P<0.05$ and within the range of a statistical trend at $P<0.1$. ** $P<0.01$, * $P<0.05$, $^{+}$ $P<0.1$.

3.3 Results

3.3.1 Histological analysis

The primary cells were isolated directly from the mammary gland; thus, isolates contained epithelial cells along with myoepithelial cells, adipocytes, and fibroblasts. Therefore, confirmation that the majority of cells grown in culture are of epithelial origin was required. For this purpose, primary cells of different passages were stained with CTK18 as a marker for epithelial cells to demonstrate that even in higher passage numbers (>3 passages) the primary cells would not lose their epithelial phenotype.

The CTK18-positively labelled primary cells contained a blue-counterstained nuclei and brown-coloured surrounding cytokeratin filaments (Fig. 3.5; A to D). Fig. 3.5; A and D are representative images of the CTK18-positively stained primary cells using a 20x objective. Fig. 3.5; B and D are representative images of the CTK18-positively labelled primary cells using a 40x objective. Using the ICC method, the majority of primary cells were positively stained using the CKT18 antibody. The negative control using C2C12 myoblasts did not show any CKT18-positive labelled cells (Fig. 3.5; F), while the positive control using a smooth muscle actin antibody showed a positive labelling of all cells present (Fig. 3.5; E). Hence, ICC confirmed that the majority of primary cells present were of epithelial origin. Furthermore, it was concluded that ICC can be used as a method to detect and confirm cells of epithelial origin.

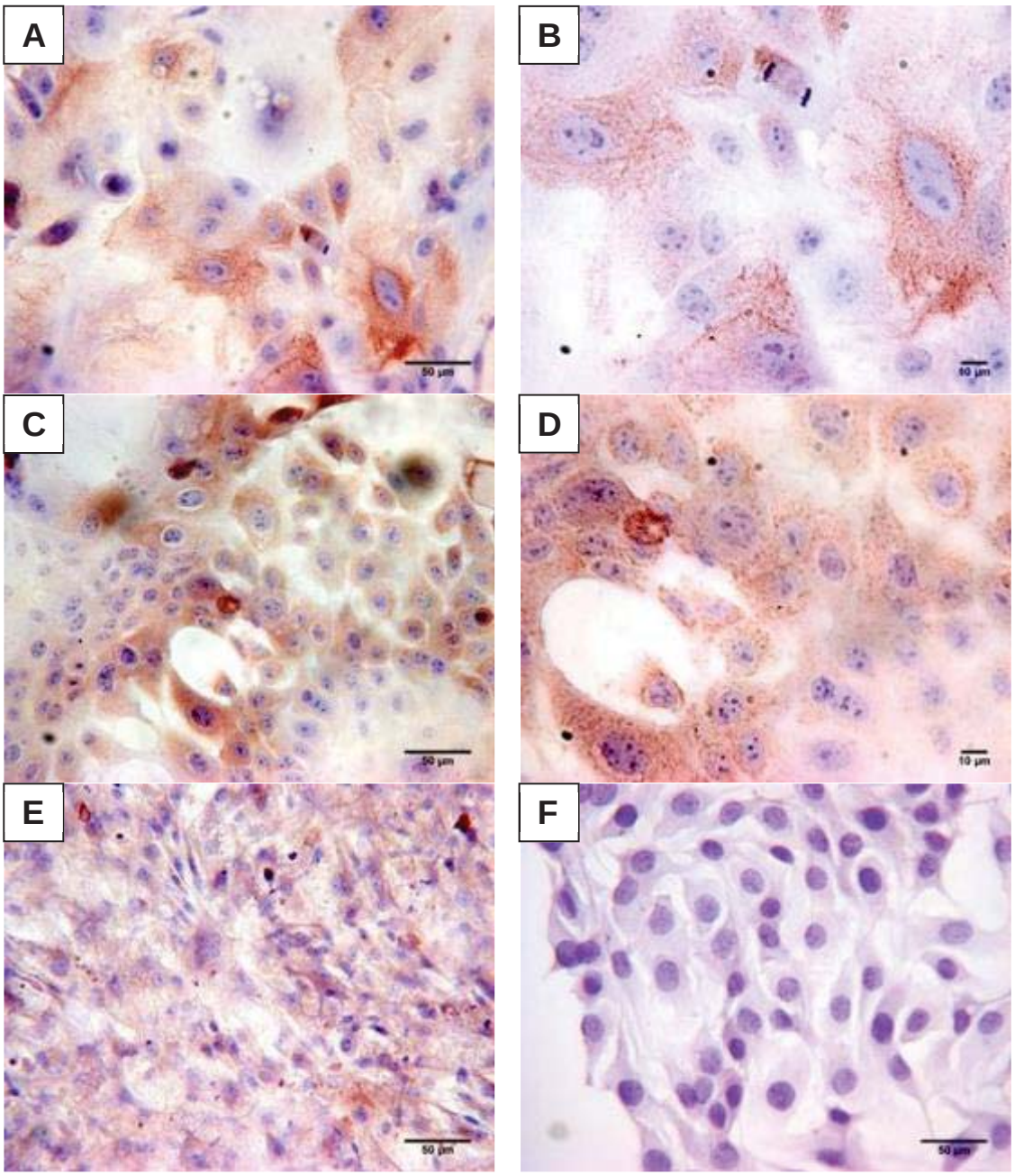

Figure 3.5 Representative images of ICC staining to confirm epithelial phenotype in cell culture, including positive and negative control. A and C: primary cells stained with CTK18 antibody, 20x magnification, nuclei counterstained with hematoxylin; B and D: Primary cells stained with CTK18 antibody, 40x magnification, nuclei counterstained with hematoxylin; E: positive control, primary cells stained with smooth muscle actin antibody, 20x magnification, nuclei counterstained with hematoxylin; F: negative control, C2C12, murine myoblasts, cells stained with CTK18 antibody, 40x magnification, nuclei counterstained with hematoxylin. Images A, C, E and F: Scale bar is 50 µm. Images B and D: Scale bar is 10 µm

3.3.2 Assessment of different membrane coatings

Preliminary experiments were conducted to determine the most suitable coating for the stretch experiments with the focus on cell attachment, growth and differentiation. The primary cells responded differently to each type of coating. Each coating was tested three times by carrying out a 3 h static stretch experiment by causing an increase in surface area of approximately 50 %. While good attachment during and after stretching was observed on all four types of coating, cell growth to a confluent monolayer was not always achieved. In particular, the cells grown on ProNectin (RDG-binding site) coatings had large gaps within the cell monolayer which would not close during a 14 day growth period with regular media change every 2 to 3 days (Fig. 3.6; A). Cells grown on laminin showed good cell growth, but this was not in a single monolayer. Mammosphere-like formations could be observed which would make it difficult to predict how those domes would react during stretch (Fig. 3.6; B). Type I and type IV collagen (Fig. 3.6; C and D, respectively) showed good cell growth in a single monolayer, but small gaps could be detected in the cell layer grown on type I collagen. Based on the overall cell growth, single confluent monolayer formation, and the attachment during stretch experiments type IV collagen was the most suitable for further stretch experiments.

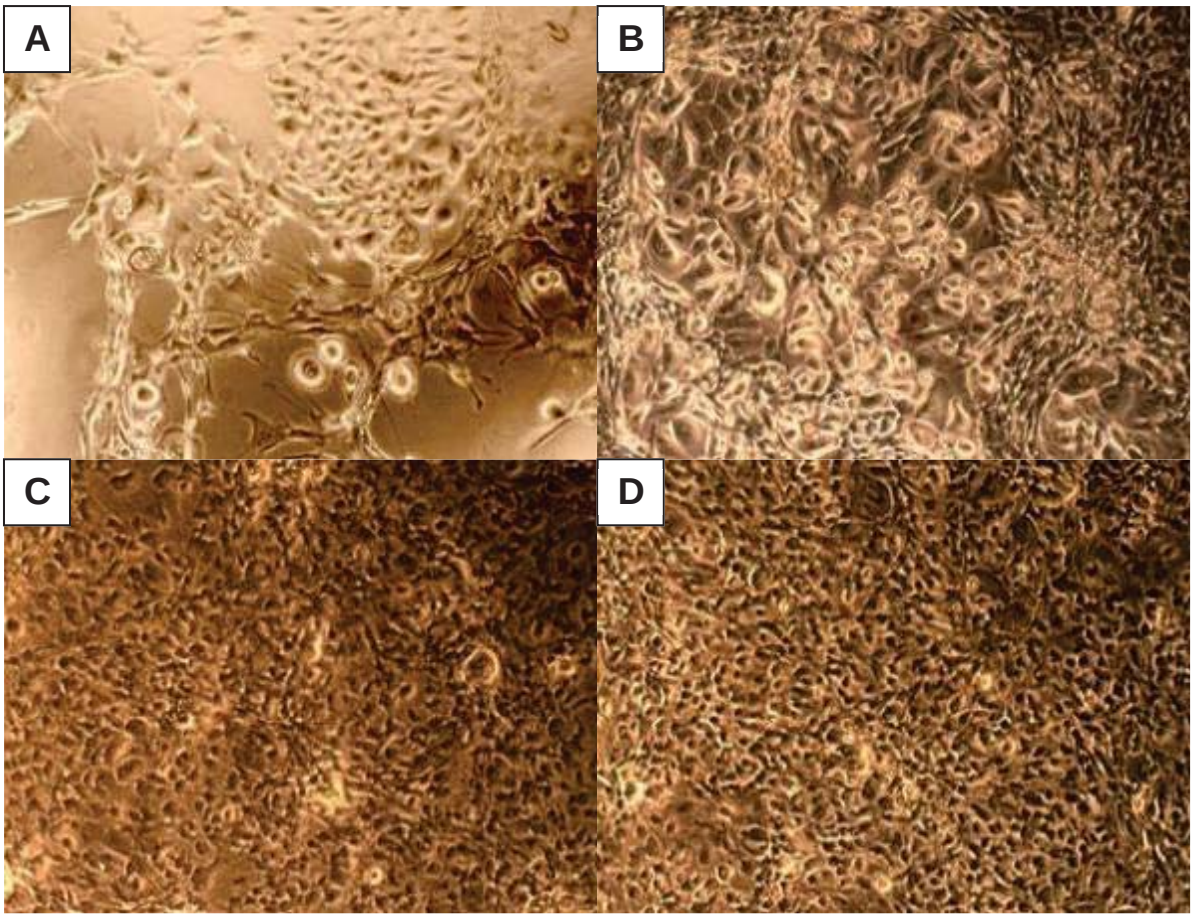

Figure 3.6 Representative images of primary cells grown for 9 days on different types of membrane precoating. A: ProNectin (RGD-binding site); B: laminin; C: type I collagen; D: type IV collagen

3.3.3 qRT-PCR results after *in vitro* stretch experiments

Quantitative RT-PCR was performed to determine the temporal changes in gene expression levels for αS1-casein, β1-integrin, occludin, claudin-1, ZO-1, bcl-2 and bax during *in vitro* cell stretch experiments for different periods of time relative to their respective control samples.

3.3.3.1 Gene expression of αS1-casein

Although there was an initial numerical decrease in αS1-casein mRNA levels following one hour of static cell stretch, there were no significant changes in αS1-casein mRNA expression following different periods of static *in vitro* cell stretch (Fig. 3.7).

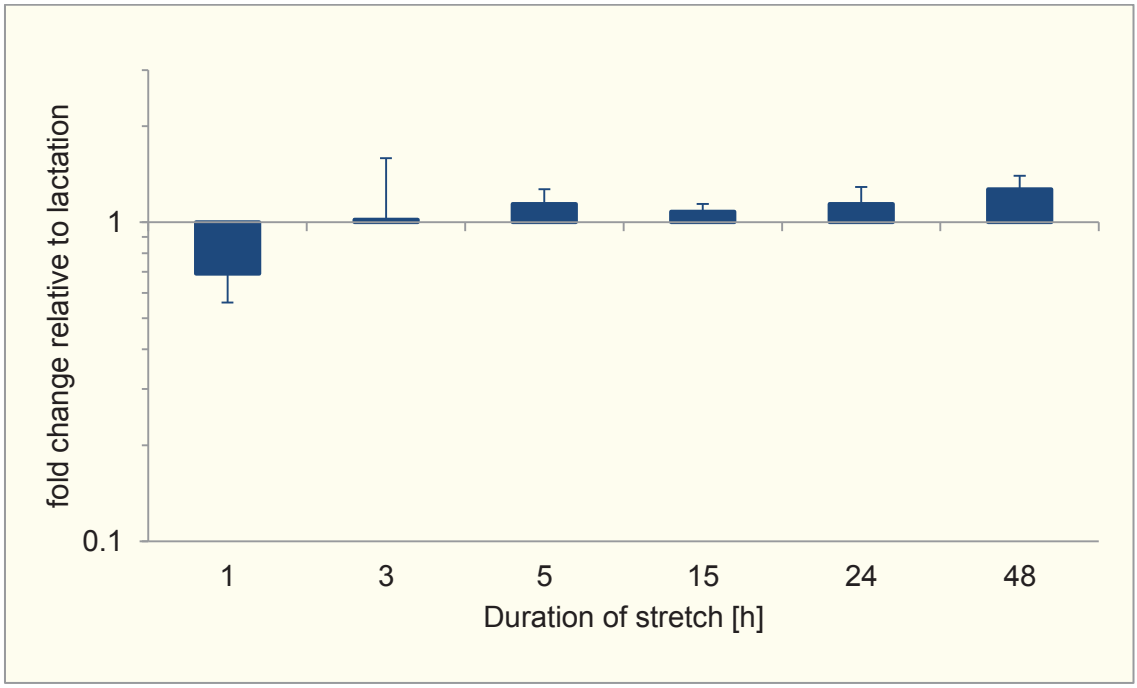

Figure 3.7 Changes in αS1-casein gene expression levels following different periods of static stretch applied *in vitro* (n=18/group). Data are expressed on a log_{10}-scale as normalised, back-transformed mean fold changes relative to control (±SED)

3.3.3.2 Gene expression of tight junction proteins

Although, the pattern of change in mRNA levels was similar among claudin, occludin and ZO-1 (Fig. 3.8), there was no statistically significant change for occludin and ZO-1 mRNA levels following different periods of *in vitro* cell stretch compared with unstretched controls at each time point. Overall, the lowest mRNA levels for all three TJ proteins were detected following 15 h of static *in vitro* cell stretch. After 15 h of stretch mRNA levels were numerically decreased for claudin, ZO-1 and occludin of 1.7-fold, 2.7-fold and 2.6-fold, respectively, compared with unstretched controls. However, following 24 h of static stretch, occludin mRNA levels increased by 1.4-fold, while following 48 h of static stretch, claudin mRNA levels significantly increased by 1.1-fold.

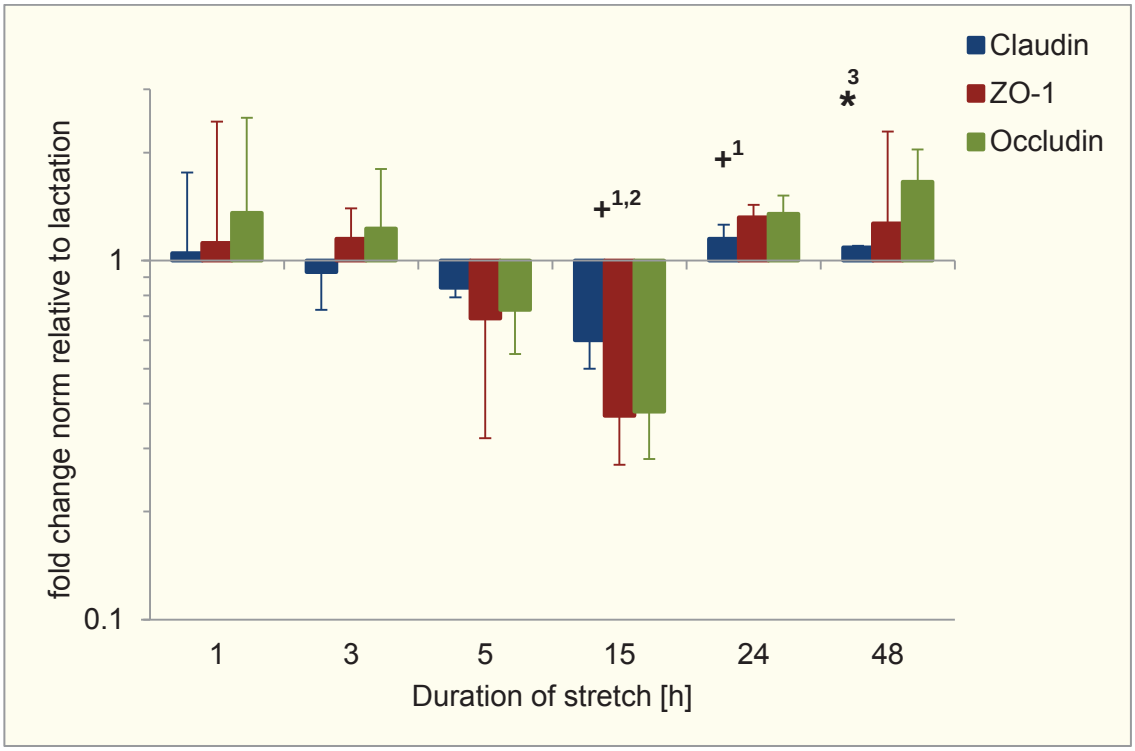

Figure 3.8 Changes in TJ gene expression levels following different periods of static stretch applied *in vitro* (n=18/group). Data are expressed on a log_{10}-scale as normalised, back-transformed mean fold changes relative to control (±SED). [1] occludin, [2] ZO-1, [3] claudin, [+] P<0.1, * P<0.05

3.3.3.3 Gene expression of β1-Integrin

Although, there were no significant changes following static *in vitro* cell stretch experiments, β1-integrin mRNA levels showed a similar pattern of change as observed with TJ protein gene expression. Following 15 h of cell stretch β1-integrin mRNA levels declined by 2.9-fold compared with unstretched controls (Fig. 3.9). Following 24 h of static stretch, β1-integrin mRNA levels numerically increased by 1.3-fold and 48 h of static stretch resulted in a numerical increase by 1.6-fold relative to the control samples. However, overall, no significant changes in β1-integrin mRNA expression could be determined compared with unstretched controls.

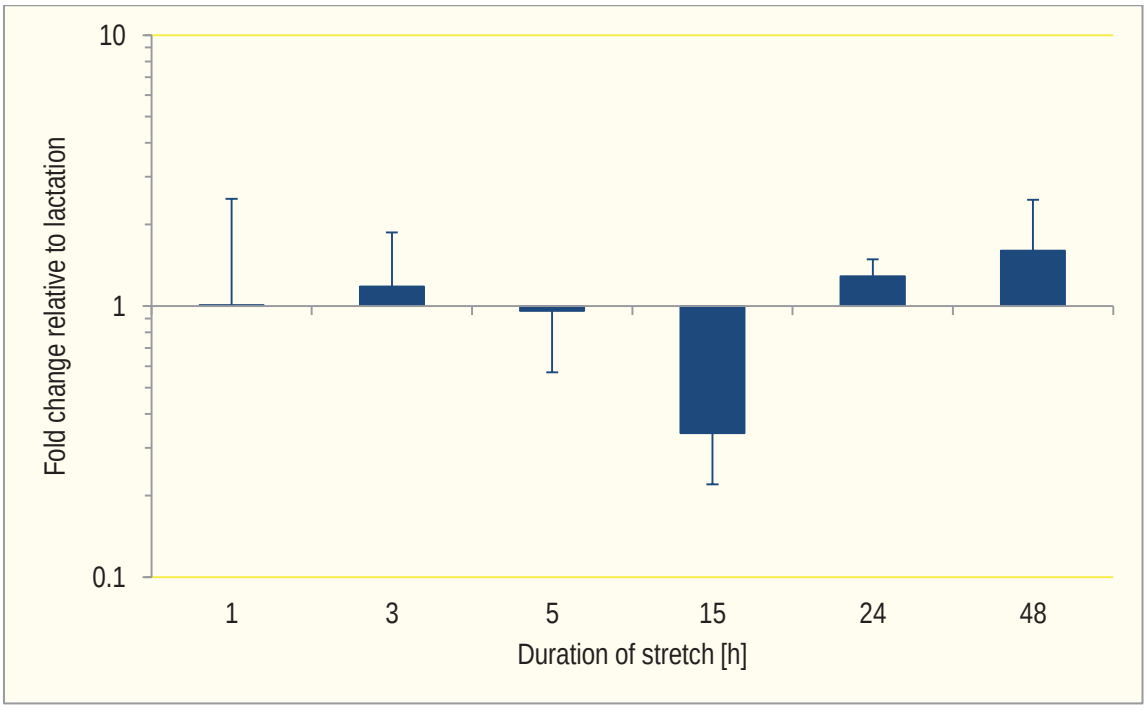

Figure 3.9 Changes in β1-integrin gene expression levels following different periods of static stretch applied *in vitro* (n=18/group). Data are expressed on a log_{10}-scale as normalised, back-transformed mean fold changes relative to control (±SED)

3.3.3.4 Gene expression of bax and bcl-2

Following different periods of static *in vitro* cell stretch, there was no change in bcl-2 mRNA levels. Changes in the bax mRNA levels, however, are similar to those detected in TJ components and β1-integrin (Fig. 3.10). There is a numerical decrease in bax mRNA levels until its lowest expression following 15 h of cell stretch. After 24 h of static stretch, however, expression levels of bax significantly increased by 1.5-fold. There was no further change following 48 h of cell stretch.

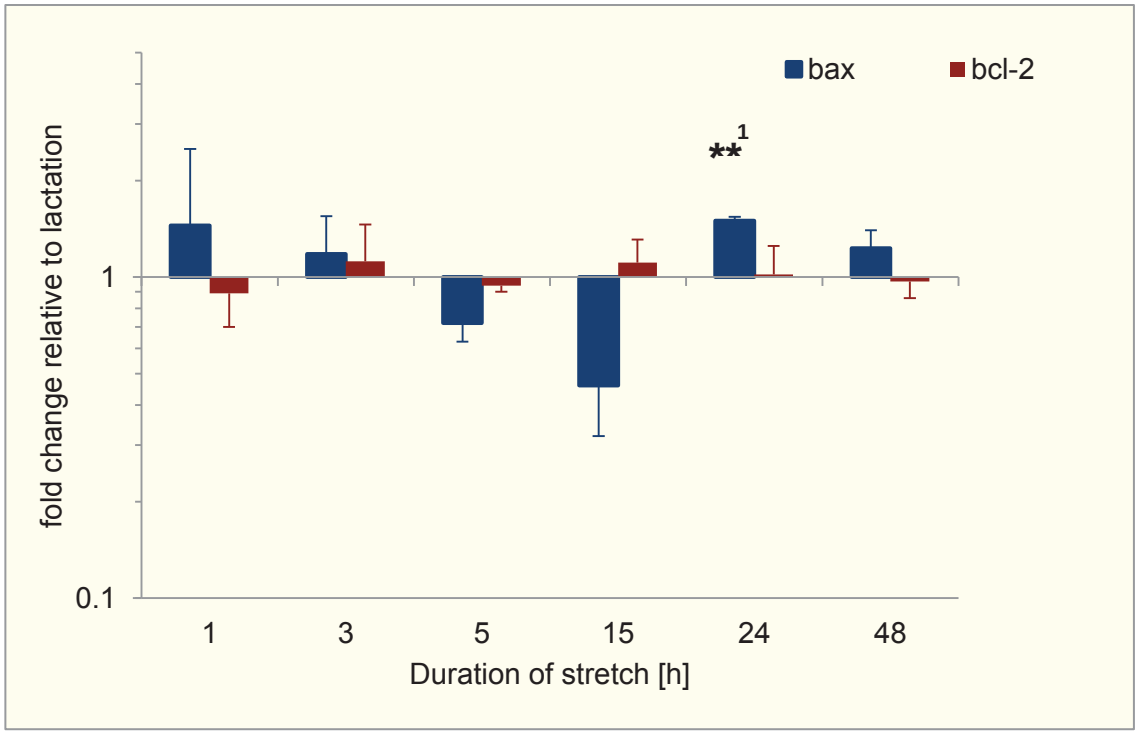

Figure 3.10 Changes in bax and bcl-2 gene expression levels following different periods of static stretch applied *in vitro* (n=18/group). Data are expressed on a log_{10}-scale as normalised, back-transformed mean fold changes relative to control (±SED). [1] bax, ** P<0.01

3.3.4 Analysis of levels of protein expression after *in vitro* stretch experiments

Western Blot analysis was used to determine the pattern of TJ protein expression as well as (p)Akt protein expression after extended periods of *in vitro* stretch experiments.

3.3.4.1 Protein integrity

Confirmation of equivalent sample loading of SDS-PAGE gels was obtained by Coomassie blue staining of untransferred gels (Fig. 3.11), while the effective transfer of proteins onto a nitrocellulose membrane was confirmed by Ponceau S staining (results not shown).

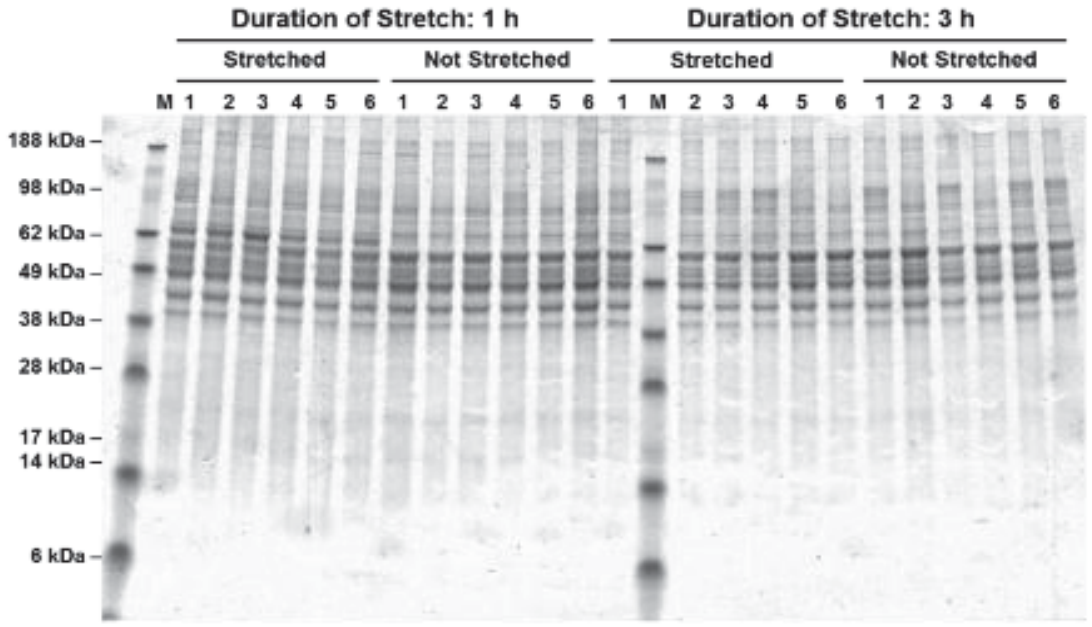

Figure 3.11 Representative image of a Coomassie blue stained gel loaded with protein samples extracted from bovine primary cell culture experiments following extended periods of *in vitro* stretch. The Bis-Tris protein gel (10 %) was loaded with samples from cell culture plates stretched for one and three hours, respectively, including their corresponding control samples (not stretched). Each lane was loaded with 20 µg of total protein, except the marker lane which contained 5 µl of the SeeBlue® Plus2 Pre-Stained Standard

3.3.4.2 Tight junction protein expression

Changes in TJ protein levels (ZO-1 and occludin) were examined following extended periods of *in vitro* cell stretch (Figs. 3.12 and 3.13). Following 1 and 3 h of *in vitro* cell stretch experiments, although not statistically significant, ZO-1 protein expression levels were increased by 1.1- and 1.5-fold, respectively (Fig. 3.13 A). However, after 5 h of *in vitro* stretch experiments, the ZO-1 protein level was significantly decreased by 3.6-fold. Following 15 h of cell stretch, there was a numerical increase in ZO-1 protein by 2.1-fold. Followed by a significant decrease in ZO-1 protein levels by 2.7-fold after 24 hours of *in vitro* stretch compared with non-stretched controls. After 48 h of cell stretch experiments, no differences between the stretched samples and their corresponding control samples could be detected.

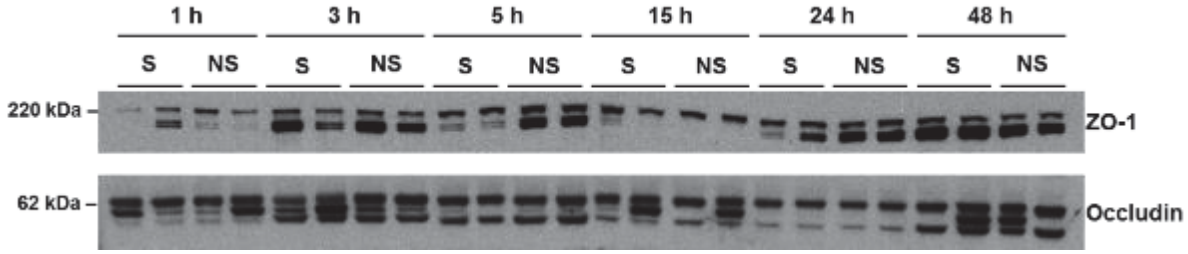

Figure 3.12 Representative image of Western blot to determine patterns of TJ protein expression following extended periods of *in vitro* cell stretch. Each time point is represented by two 'stretched' (S) and two non-stretched (NS=control) samples. Each lane was loaded with 20 µg of total protein. The primary antibodies used were rabbit anti-ZO-1 (1:1000 dilution) and rabbit anti-occludin (1:1000 dilution)

Occludin protein expression increased by 1.4-fold after one hour of *in vitro* stretch. However, following three hours of cell stretch, occludin expression levels numerically decreased by 1.2-fold and no further differences in occludin protein expression levels were found at longer periods of stretch (Fig. 3.13 B).

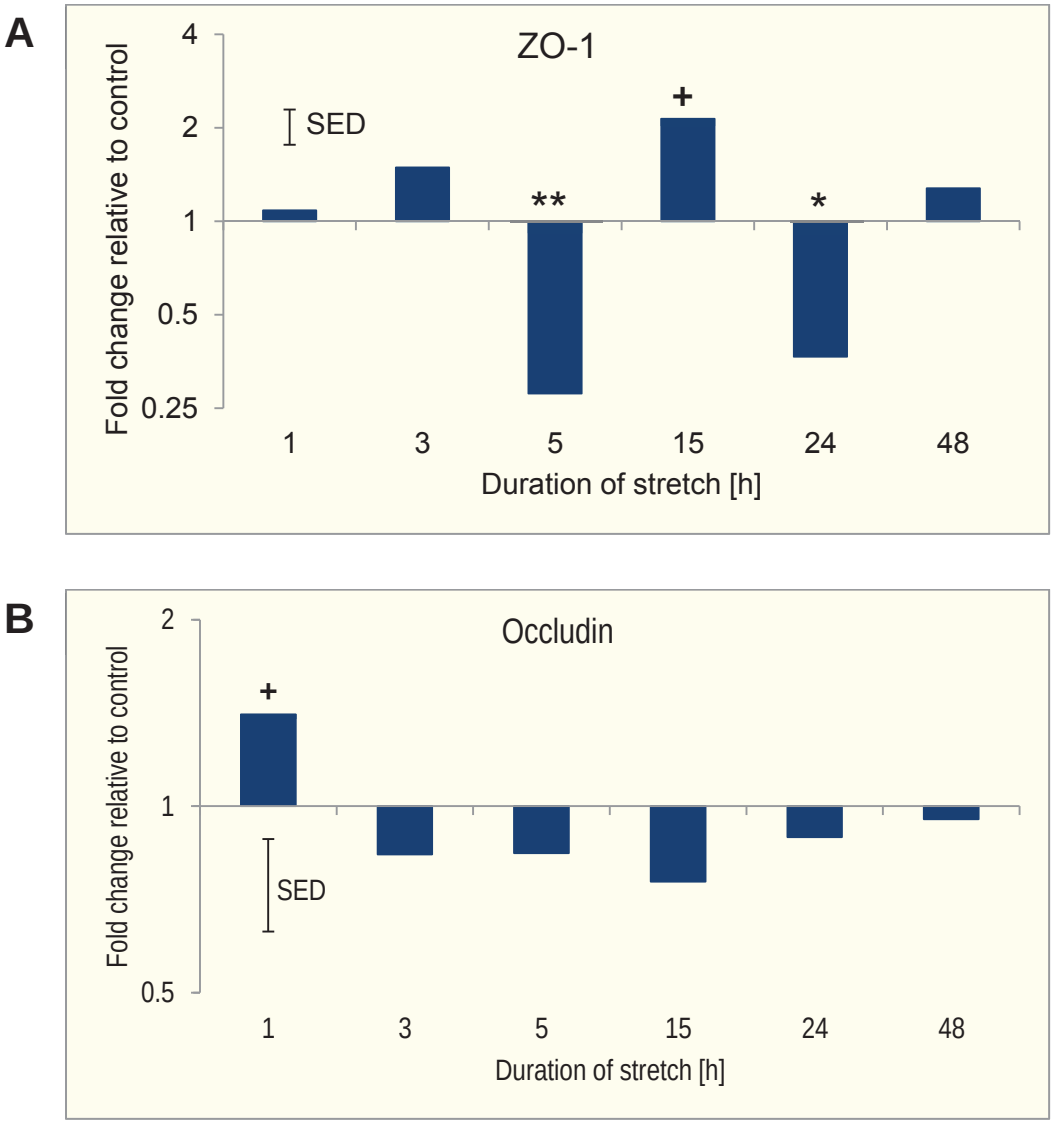

Figure 3.13 Densitometric analyses of Western blots to determine changes in TJ protein expression levels following *in vitro* cell stretch (n=18/group). A: ZO-1 protein levels. B: Occludin protein levels. Results are graphed as back-transformed mean fold changes relative to the control on a $\log_2$-scale with the SED. ** P<0.01; * P<0.05; + P<0.1

3.3.4.3 (p)Akt protein expression

Changes in (p)Akt protein expression were examined as an indicator of ECM-cell communication following extended periods of *in vitro* cell stretch (Figs. 3.14 and 3.15). After three hours of *in vitro* cell stretch, there was a significant decrease in Akt protein levels by 1.3-fold relative to the non-stretched control samples. However, no further differences in Akt protein levels were found at other time points (Fig. 3.15 A). The pAkt protein level was significantly increased by 1.8-fold after one hour of stretch. Following three hours of cell stretch, there was a significant decline in pAkt protein levels by 3.1-fold, compared with non-stretched controls. No further differences in pAkt protein levels could be detected following extended periods of cell stretch experiments (Fig. 3.15 B).

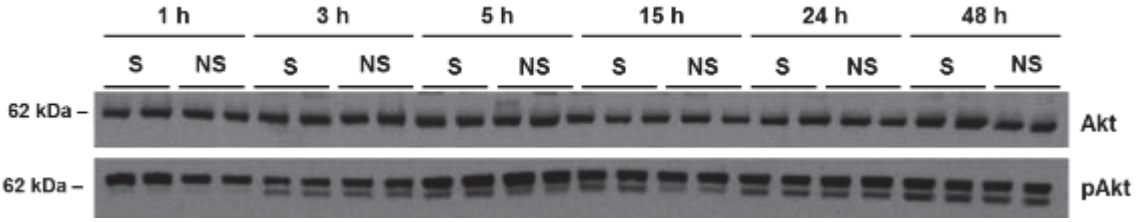

Figure 3.14 Representative image of Western blot to determine patterns of (p)Akt protein expression following extended periods of *in vitro* cell stretch. Each time point is represented by two 'stretched' (S) and two non-stretched (NS=control) samples. Each lane was loaded with 20 µg of total protein. The primary antibodies used were rabbit anti-Akt (1:1000 dilution) and rabbit anti-pAkt (1:5000 dilution)

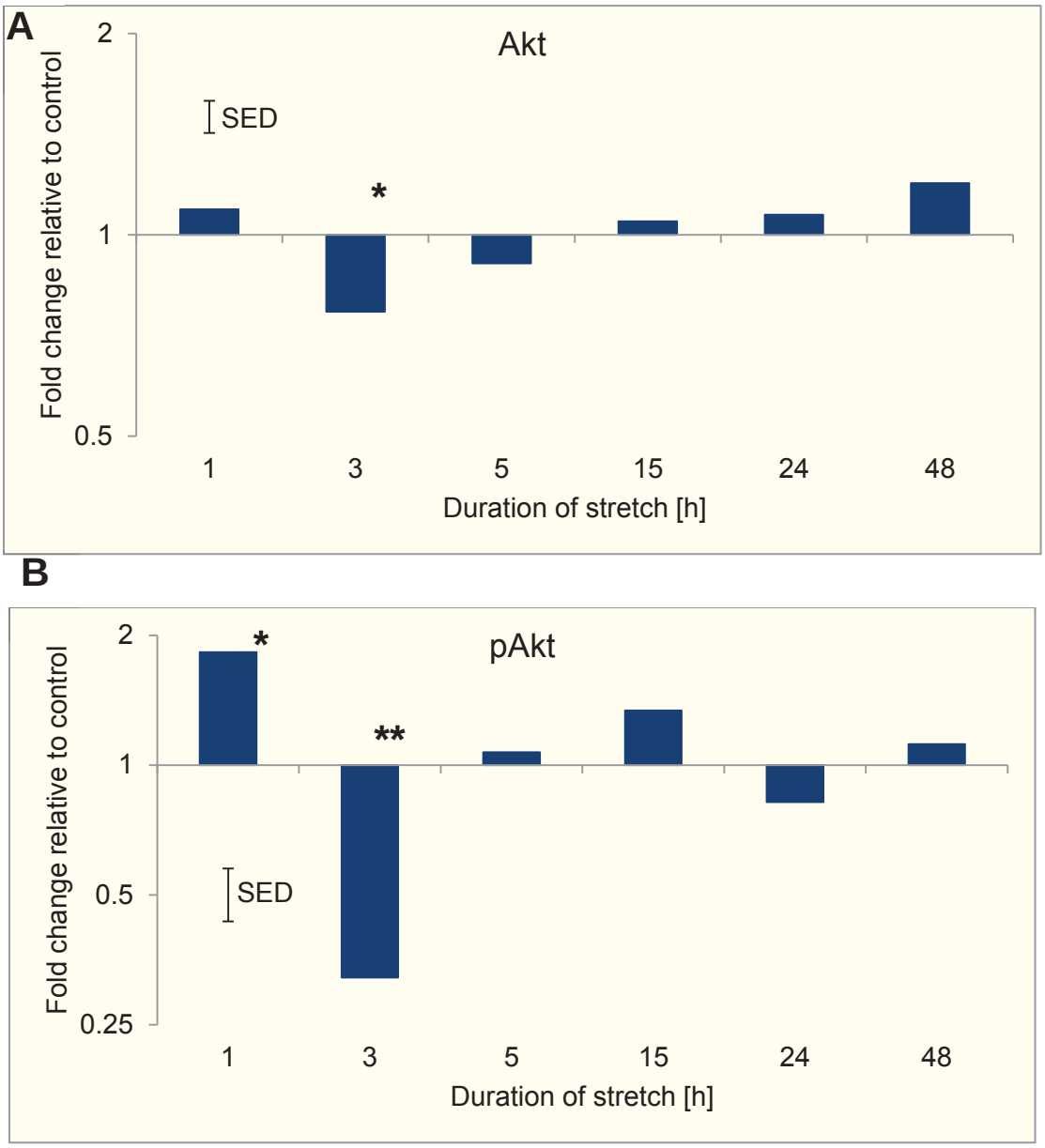

Figure 3.15 Densitometric analyses of Western blots to determine changes in (p)Akt protein expression levels following *in vitro* cell stretch (n=18/group). A: Akt protein levels. B: pAkt protein levels. Results are graphed as back-transformed mean fold changes relative to the control on a $\log_2$-scale with the SED. ** P<0.01; * P<0.05

3.4 Discussion

Mammary gland engorgement as a result of milk accumulation leads to changes in cell morphology, stress on cellular structures, and has been recognised as a potential key initiator of involution and remodelling of the mammary gland (Paszek *et al.*, 2005). In this study, the goal was to investigate the effect of mechanical strain on cellular adhesion structures and their potential role in the initiation of the involution process.

For that purpose, a cell-stretching device for 6-well plates was designed and built in order to separate the effects of mechanical stimulation of bovine MECs from the actions of possible chemical inhibitors in milk. The device is able to accurately apply static equibiaxial strain to MECs grown on a flexible substratum in confluent single layers. Similar experimental approaches have been described where cells grown on flexible substrata are used to explore biological responses to mechanical stress (Rana *et al.*, 2008; Quaglino *et al.*, 2009; Fujita *et al.*, 2010). Our low-cost, specially fabricated cell stretch device can be used with commercially available 6-well culture plates with flexible substratum. Furthermore, the design allows for all six wells to be ‘stretched’ simultaneously and hollow indenters allow the use of an inverted microscope to monitor cultured cells and ensure firm attachment while strain is applied. The compact design allows stretching protocols to be performed inside an incubator. Moreover, with the use of commercially available 6-well plates, there is no need for sterilisation by autoclaving.

Before commencing the stretch experiments, different commercially available membrane coatings were tested to determine the most suitable for our experiments. Close contact to the ECM for cell communication (stroma and/or basement membrane) is crucial for the survival of anchorage-dependent epithelial cells (Wernig *et al.*, 2003; Orr *et al.*, 2006; Reichelt, 2007). Although, type I collagen is widely used for such experiments, it has been shown to not be the most suitable to support MEC survival in culture (Novaro *et al.*, 2003). In fact, close contact to BM, rather than stromal tissue, appears to be more important for MEC survival and differentiation (Pullan *et al.*, 1996). Preliminary tests showed that type IV collagen was the most appropriate for our experiments and it was confirmed that the majority of primary cells grown in culture were of epithelial origin using CTK 18 as a maker for luminal epithelial cells.

Once the device was developed, a suitable membrane coating was determined and the epithelial origin of the cultured cells was confirmed, the effect of physically stretching of bovine MECs in culture was investigated. The focus of this investigation was on two cellular adhesion structures (TJs and FAs) which have previously been shown to play a part in the initiation of involution (Cavanaugh *et al.*, 2001; Lee & Streuli, 2014).

Initially, temporal changes in mRNA expression of ZO-1, claudin and occludin, all part of the TJ complex, were analysed. During lactation, TJs form a tight barrier to prevent paracellular movement of milk components between the blood stream and alveolar lumen where the milk collects (Neville, 2009). The loss of TJ integrity may allow pro-apoptotic factors to relocate from the apical to the basolateral side

of MECs and either induce apoptosis directly or antagonise survival signals (Green & Streuli, 2004). Furthermore, temporal changes in gene expression of β1-integrin as part of the FA complex were investigated. Integrins appear to be the main mechanoreceptors that link the ECM with the cytoskeleton and have been shown to play a major role in transmitting incoming survival signals from the ECM (Prince *et al.*, 2002; Naylor *et al.*, 2005). Based on previous studies, at 18 h post termination of milk removal, communication between the ECM and the MEC becomes compromised (Singh *et al.*, 2005) and the tight-junctional barrier is disrupted and becomes permeable for milk molecules (Stelwagen *et al.*, 1995). In agreement with these earlier studies, the lowest levels of mRNA expression of TJ components as well as β1-integrin were identified following 15 h of *in vitro* cell stretch.

However, at the protein level, occludin expression increased after one hour of static cell stretch, but no further change occurred. In contrast, ZO-1 protein levels decreased after three and 24 hours and increased following 15 hours of *in vitro* cell stretch. I speculate that the increase in occludin and ZO-1 protein expression could be related to the repair of potentially compromised TJs following static stretch. Furthermore, occludin has been shown to undergo Tyr-phosphorylation following the disruption of TJs as a requirement for the hydrogen peroxide-induced disassembly of TJs (Rao, 2009). Western blot analysis showed changing patterns of protein bands detected for occludin after different periods of *in vitro* cell stretch. The different sized occludin protein bands were assumed to be differences in occludin phosphorylation. The highest level of phosphorylation of occludin occurred following three hours of static stretch. Therefore, it was

concluded that static mechanical strain applied *in vitro* is sufficient to cause a disruption of TJ integrity which in turn could lead to exposure of luminal, pro-apoptotic factors onto the basolateral side of the MECs.

As part of the signalling pathway downstream of β1-integrin, the changes in protein expression of (p)Akt were analysed following *in vitro* cell-stretch experiments. Several studies described the impact of mechanical stimulation on Akt expression/activation in epithelial cells in the intestine (Zhang, Li, Sanders*, et al.*, 2003; Gayer, Chaturvedi, Wang, Craig*, et al.*, 2009), in the lung (Tschumperlin & Margulies, 1998; Tschumperlin *et al.*, 2000; Hammerschmidt *et al.*, 2007; Crosby *et al.*, 2011), and in murine MECs (Provenzano *et al.*, 2009; Quaglino *et al.*, 2009). Furthermore, Akt has been shown to play an essential role during MEC differentiation and maintaining lactation/delaying involution (Chen *et al.*, 2010; Creamer *et al.*, 2010). In our study, Akt and its activated form pAkt were significantly decreased after three hours of static stretch. This suggests that mechanical strain applied *in vitro* induces a decline in Akt/pAkt expression which in turn could initiate a switch from MEC survival to apoptosis.

Finally, it was determined that the ratio of bcl-2 (apoptosis suppressor) and bax (apoptosis inducer) gene expression as a marker for MEC commitment to undergo apoptosis and the overall initiation of involution following the infusion experiment (Jurgensmeier *et al.*, 1998; Colitti, 2012). Following 24 hours of static cell stretch, bax gene expression is significantly increased. However, there is no change in bcl-2 gene expression following *in vitro* cell stretch experiments. This suggests that mechanical strain applied to MECs *in vitro* induces molecular

events associated with the initiation of the involution process. However, mechanical stimulation alone may not be sufficient to trigger the entire program of post-lactational tissue remodelling.

In conclusion, following different periods of static, biaxial *in vitro* cell stretch using a homemade cell stretch device: 1) mechanical strain applied to bovine MECs induces molecular events previously linked to the initiation of post-lactational tissue regression and 2) significant changes in protein expression occur before changes in gene expression.

Chapter 4:

Acute physical distension and its potential role in bovine mammary involution

Chapter 4 Introduction

In dairy cattle, milk production is determined by the number and the secretory activity of MECs (Capuco *et al.*, 2001). Following peak lactation, the progressive decline in milk production is associated with a loss of MEC through apoptosis (Capuco *et al.*, 2003). Hormonal regulation of MEC apoptosis in rodents (Sheffield & Kotolski, 1992; Feng *et al.*, 1995; Travers *et al.*, 1996; Flint *et al.*, 2005) and more recently in bovine (Accorsi *et al.*, 2002; Boutinaud *et al.*, 2012) has been described. In addition, local intra-mammary signals in response to the absence of milk removal also play a role in initiating MEC apoptosis and involution of the mammary gland in rodents (Quarrie *et al.*, 1996; Travers *et al.*, 1996; Li *et al.*, 1997) and in ruminants (Quarrie *et al.*, 1994; Wilde *et al.*, 1997). The molecular and genetic mechanisms regulating mammary function have primarily been investigated in rodents, (Kritikou *et al.*, 2003; Schere-Levy *et al.*, 2003; McGee *et al.*, 2006; Quaglino *et al.*, 2007; Strange *et al.*, 2007; Gjorevski & Nelson, 2011; Watson & Kreuzaler, 2011). However, studies using cattle as a model found that the process of involution in the bovine mammary gland follows a different pattern and the overall remodelling process is not as extensive in the bovine mammary gland as it is in the rodent mammary gland (Capuco *et al.*, 2001; Capuco *et al.*, 2002; Capuco *et al.*, 2003). Transcription profiling of rodent (Clarkson *et al.*, 2004; Stein *et al.*, 2004; Stein *et al.*, 2007) and bovine (Singh *et al.*, 2008) mammary gland involution models have shown many genes are differentially expressed in response to milk stasis. However, the mechanisms initiating these changes and the involution process are unclear and may be due to biochemical factors and/or physical distension of the epithelium.

Nonetheless, research suggests that much of the information that specifies patterning within the mammary gland is produced locally by the epithelium itself (Li *et al.*, 1997; Davis *et al.*, 1999; Stelwagen, 2001; Nelson & Gleghorn, 2011).

4.1 Local control of milk production

Half-udder milking frequency experiments where treatment (e.g., once or thrice daily milking) was applied to one udder half, while the control half was milked twice a day, indicated that milk yield may be influenced by local rather than systemic factors (Stelwagen, 2001; Wall & McFadden, 2012). Research showed that local, intra-mammary effects of milking frequency on milk yield can range from -38 % with once daily (1X) milking to +32 % with more frequent milking (Stelwagen, 2001). Furthermore, total milk yield is a function of the number of secretory epithelial cells and their metabolic activity (Carruthers *et al.*, 1993; Capuco *et al.*, 2002; Bruckmaier, 2005). An increase in mammary cell activity as well as an increase in key mammary enzyme activity, such as fatty acid synthetase and galactosyltransferase, was measured after increasing milking frequency from twice daily (2X) to thrice daily (3X) in both, goats and cows (Wilde *et al.*, 1987; Hillerton *et al.*, 1990). Moreover, a long-term increase in milking frequency to 3X (i.e. 9 months) resulted in an increase in parenchyma in goats, indicating an increase in mammary cell number (Henderson *et al.*, 1985). However, the process of milk secretion is also regulated by completeness of milk removal (Wilde *et al.*, 1995). Therefore, the amount of residual milk in the udder after each milking is important for persistency. During a normal lactation the volume of residual milk remains constant, around 5 to 15 % (Schmidt, 1971; Negrão & Marnet, 2006). High levels of residual milk may reduce secretory activity by increasing the number of distended non-secretory alveoli within the mammary gland and, thus, causing a decline in milk secretion (Carruthers *et al.*, 1993).

4.1.1 Alveolar distension

When milk accumulates within the bovine mammary gland, the majority of the milk (i.e. approx. 80 %) is stored in the alveolar compartment (Bruckmaier, 2005). Capillary forces and valve-like structures of secretory epithelia, at the point of attachment of the alveolus to the ducts, provide resistance to free alveolar drainage causing milk accumulation in the alveolar compartment (Caruolo, 1980). As a result, gland engorgement due to accumulating milk leads to an increase in intra-mammary pressure and causes secretory epithelial cells to exhibit a flattened morphology which in turn puts strain on the cell's adhesion and/or cell's surface molecules and may result in the loss of cell-survival signal (Richardson, 1947; Davis *et al.*, 1999; Green & Streuli, 2004). This may in turn initiate a cascade of cellular and molecular events that eventually initiate the process of involution. For example, at about 17 to 20 h post-milking, TJs become leaky due to an increase in intra-mammary pressure which results in an accelerated efflux of lactose from milk to plasma that represents approximately 20 % of milk loss observed during 1X milking (Stelwagen, Davis, Farr, Prosser*, et al.*, 1994; Stelwagen & Knight, 1997). When infused with an intra-mammary isosmotic solution of sucrose and lactose equivalent in volume to 5 h worth of milk secretion (based on individual milk yield prior to start of the experiment), TJs became leaky much earlier (at 7 h instead of 17 h) and milk secretion was inhibited more than in 1X control cows (Stelwagen *et al.*, 1998). The loss of TJ integrity may allow pro-apoptotic factors to relocate from the apical to the basolateral side of MECs and either induce apoptosis directly or antagonise survival signals (Green & Streuli, 2004). Hence, alveolar distention with potential disruption of the cell contacts to the surrounding tissue for survival signalling will occur before udder capacity is

reached and, in mice, alveolar distension has been shown to be correlated with a wide array of changes in expression of genes involved in involution (Li *et al.*, 1997). In cows, unilateral 1X milking induced cell remodelling processes which correspond to the early stages of mammary gland involution (Boutinaud *et al.*, 2013).

Even though evidence suggests that milk yield is influenced by local, intra-mammary factors, the local mechanisms regulating milk production are not well understood. It is postulated that mammary gland engorgement may cause changes in the mechanical micro-environment resulting in changes in cell shape which in turn may initiate a decline in milk production in the mammary gland (Davis *et al.*, 1999). Recent studies suggest that mechanotransduction is an important trigger of signalling events in tissues, such as lung, bladder and uterus, which cause changes in gene expression and modification of cellular function (Alenghat *et al.*, 2004; Michaelson & Huang, 2012; Bukoreshtliev *et al.*, 2013; Ricca *et al.*, 2013).

4.1.2 Mechanotransduction

Changes in MEC shape due to milk accumulation could ultimately be the first trigger of the involution process in the mammary gland. The MECs exist and interact with their surrounding environment via numerous structures and signalling molecules. A plethora of chemical, mechanical and electrical signals contained within the environment guide cellular phenotype. Conversely, MECs

play an important role in dynamically modifying and remodelling the extracellular matrix and/or their interaction with their neighbouring cells.

Therefore, depending on their respective needs, tissues constantly adapt to the environmental mechanical stress by modulating sensitivity to exogenous stimuli (Nelson & Bissell, 2006; Schwartz, 2010; DuFort *et al.*, 2011). Several subcellular structures have been linked to transduce extracellular forces into intracellular biochemical and mechanical signals, such as PC (Berbari *et al.*, 2009; Jones & Nauli, 2012), TJs (Schedin & Keely, 2011; Michaelson & Huang, 2012) or FAs (Ingber, 1997; Schwartz, 2010; Schwarz & Gardel, 2012). The transduction of physical forces appears to occur through changes in protein conformation. These force-induced effects on conformation change represent a general mechanism which may regulate enzymatic activity, enable new molecular interactions, or liberate soluble bond factors which in turn may activate signalling pathways in an autocrine and paracrine fashion. This ability to react to environmental signals may be a fundamental mechanism whereby cells sense, integrate and coordinate responses to combined physical and chemical signals (Huang & Ingber, 1999; Orr *et al.*, 2006; Wang & Thampatty, 2006; Reichelt, 2007; Schwartz & DeSimone, 2008; Jones & Nauli, 2012). For example, lengthening of the ECM protein fibronectin, due to tension, exposes cryptic binding sites, and mechanical stretching of immobilised fibronectin induces matrix assembly by exposing self-assembly sites (Hocking *et al.*, 1994).

4.2 Objective

This study aimed to investigate the effect of acute physical distension of the bovine mammary gland on changes in MEC sensing and signalling, and the initiation of the involution process.

The role of physical distension of the mammary epithelium in triggering the disruption of TJ and FA function and the initiation of mammary gland remodelling was examined using an *in vivo* experimental approach. Bovine mammary glands were artificially distended, using a sterile, isosmotic saline solution, in order to investigate changes in cellular signalling pathways associated with cell survival, such as TJ integrity or β1-integrin disruption. The effect of acute physical distension *in vivo* on the gene and protein expression of TJ proteins and FAs was determined.

4.3 Materials and Methods

4.3.1 Animal experiment

Eight multiparous, non-pregnant Friesian cows at peak lactation (78±20 DIM) were used during the experiment. Prior to the start of the experiment, all cows were fed pasture, milked twice a day (6 am and 2 pm) and monitored for signs of clinical mastitis. Before the infusion experiment commenced, cows were milked with the aid of oxytocin (20 IU per cow; intramuscular, SVS Veterinary Supplies Ltd., Hamilton, New Zealand) to ensure complete milk removal. Subsequently, one rear quarter was infused with a sterile saline solution (300 mOsm; Baxter, Auckland, New Zealand) equivalent in volume to 5 h worth of milk secretion (calculated based on the normal milk volume in the infused gland). Fifteen hours later, all animals were sedated (0.5 ml Dormosedan, intravenous, SVS Veterinary Supplies Ltd.) and a local anaesthetic (Lopain, 2 x 5 ml, SVS Veterinary Supplies) was administered into each hind quarter directly. Once the animals were sedated and the glands anaesthetised, mammary gland biopsies were collected from both hind quarters. The infused and the non-infused quarters served as the treatment and control samples, respectively. The tissue collected was stored in RNA*later*® (LifeTechnologies, Carlsbad, USA) solution overnight at 4°C to avoid RNA degradation. To prevent infections following the biopsies, a systemic antibiotic (Excede®, 20 ml per animal, subcutaneous, SVS Veterinary Supplies Ltd.) was administered as well as an anti-inflammatory drug (Metacam®, 12 ml per animal, subcutaneous, SVS Veterinary Supplies). For seven days following the biopsy, glands were hand-stripped to remove any blood clots that may inhibit milk

removal. Milk samples were collected before and after the infusion for fat, protein, lactose and somatic cell count (SCC) analysis (Fossomatic equipment, LIC Herd Testing Station, Hamilton, New Zealand). All animal experimental procedures were conducted in compliance with the Ruakura Animal Ethics Committee.

4.3.1.1 Tissue processing

All biopsy samples were placed in Tissue-Tek III cassettes (Sakura-Finetekq Europe BV, Alphen aan den Rijn, Netherlands) and fixed in RNA*later*® (LifeTechnologies) solution overnight at 4°C. Half of the tissue samples were routinely processed using the Leica TP 1050 tissue processor (Leica, Solms, Germany) and paraffin embedded using a tissue embedding machine (Thermolyne Sybron, Milwaukee, USA). Seven-µm thick serial sections of approximately 10 x 10 mm^2 cross-sectional area were cut onto polysine-coated glass slides for histological analysis. The remainder of the tissue was snap frozen in liquid nitrogen, pulverised and stored at -80°C for downstream analysis.

4.3.2 Histological analysis

Seven- µm thick paraffin-embedded sections were dewaxed, rehydrated and stained with hematoxylin and eosin as per standard staining protocol (Fischer *et al.*, 2008). To assess histological features of lactation and involution, a grading criteria was adopted to categorise the lactation state for each tissue section with a score of between 0 and 4 as previously described by Mallah(2013) (Mallah, 2013).

Briefly, the entire tissue section was divided into ten sub-sections and scored according to the following scale: 4 ≥ 95 % lactating alveoli; 3 > 50 %. 2 ≤ 50 %; 1 ≤ 5 %; 0 = 0 %. Features considered to be of a non-lactating appearance included lipid-engorged MECs, darkly-stained luminal contents, condensed alveoli, increased inter-alveolar stromal area, shed MECs, and frequent leukocytes. Three tissue sections from each animal were analysed and the average of the ten scores for each section (± SEM) was recorded as the overall lactation grade for each animal. The SEM reflects both the inter-lobular as well as the inter-animal variation observed within the tissue.

4.3.2.1 Imaging of hematoxylin- and eosin-stained-tissue

Three sections from each animal were randomly chosen from the top, mid and bottom section of each biopsy to counteract heterogeneity within the mammary gland. Images were produced using an Olympus BH-2 (Olympus) with a ProgRes® C14 camera attached and 10x, 20x and 40x objectives, respectively. Ten images per section were captured to analyse the degree of milk stasis and signs of involution. ImageJ 1.45s (National Institutes of Health, Bethesda, USA) was used to process all TIF files, enhance contrast and add scale bars.

4.3.3 RNA preparation

Total RNA was extracted from 100 mg of ground tissue resuspended in 1 ml of TRIzol® solution (Invitrogen, Carlsbad, USA) and homogenised for 10 s using a mechanical homogeniser (Omni PCR Tissue Homogenizing Kit, Omni International Inc., Kennesaw, USA) according to the manufacturer's instructions.

After extraction, the RNA was purified and digested with DNaseI to remove potential DNA contaminations by using the RNeasy® Kit according to the manufacturer's manual (Qiagen, Venlo, Netherlands). The amount of extracted RNA and potential solvent and/or protein contamination in each sample was measured using the NanoDrop™spectrophotometer (NanoDrop Products, Wilmington, USA; results not shown). The RNA quality was measured by confirming RIN were above 7 using the Agilent 2100 bioanalyzer system in conjunction with the Agilent RNA 6000 Nano Kit according to manufacturer's instructions (Agilent Technologies, Santa Clara, USA, results not shown).

4.3.3.1 cDNA synthesis

One µg of total RNA was used to synthesise first-strand cDNA using the SuperScript™III First-Strand Synthesis System for RT-PCR according to the manufacturer's manual (Invitrogen). RNA was primed using the oligo(dT)20 system component. The generated cDNA was diluted 3-fold (equivalent to approximately 17 ng/µl reverse transcribed total RNA) in nuclease-free water (Ambion®, Life Technologies, Carlsbad, USA) for subsequent analysis.

4.3.3.2 Quantitative Real-Time PCR

Each RNA sample (1 µl) was assayed in triplicate, by qRT-PCR with SYBR Premix Ex Taq System (Takara, Otsu, Japan) using a Corbett Thermocycler (Corbett Life Science, Qiagen, Venlo, Netherlands). Three different reference genes were used as endogenous control: GAPDH; ubiquitin; and cyclophilin A. Additionally, each assay included RT-negative and 'no-template' control

reactions. Quantitative RT-PCR experiments were performed under the following conditions: initially 95°C for 3 min; followed by 40 cycles of 95°C for 10 s, 58 or 60°C for 20 s, 72 or 75°C for 20 s (for individual experimental conditions see Table 4.1). After the last cycle of each RT-PCR assay, a dissociation curve was obtained starting at 72°C, followed by a continuous temperature increase by 1 degree increments every 30 s until 95°C were reached. Analysis of the melting temperature (Tm) of amplified products allowed for detection of the target product as well as any non-specific products, including primer dimers which typically have a lower Tm of between 70-75 °C. One PCR reaction mix (total final reaction volume = 10 µl) contained 5 µl SYBR Premix Ex Taq System (Takara), 3.8 µl of sterile, nuclease-free water (Ambion®, Life Technologies), 1 µl of cDNA and 0.1 µl of each of the forward and reverse primers. All primers were used at a final concentration of 100 nM in each 10 µl real-time reaction.

Prior to amplification of each gene of interest, optimal experimental conditions, such as annealing and acquisition temperatures, were determined in separate experiments to maximise the amplification of a single specific product and to prevent primer dimer formation.

Table 4.1 Sequences of PCR primers (forward & reverse), primer position, PCR product sizes & individual experimental conditions of bovine nucleic acid sequences used for investigating gene expression by quantitative Real-Time PCR

Gene	Nuclei Acid Sequence	Primer sequence (5'→3')	Primer position[1] [bp]	Product size [bp]	Annealing [°C]	Acquisition [°C]
Bax	AC_000175.1	Forward: cga gtg gcg gct gaa atg tt	314	166	60	72
		Reverse: gca gcc gct ctc gaa gga agt	479			
Bcl-2	AC_000181.1	Forward: atg tgt gtg gag agc gtc aa	439	201	60	72
		Reverse: cag act gag cag tgc ctt ca	639			
Claudin	AC_000158.1	Forward: gct agt gac aac atc gtg ac	128	395	58	72
		Reverse: atg aag aga gcc tga cca aa	522			
Cyclophilin A[2]	AC_000167.1	Forward: gca tac agg tcc tgg cat ct	310	279	60	72
		Reverse: tct cct ggg cta cag aag ga	589			
GAPDH[2]	AC_000162.1	Forward: ctc cca acg tgt ctg ttg tg	141	222	60	72
		Reverse: tga gct tga caa agt ggt cg	362			
Lactoferrin[3]	AC_000179.1	Forward: ggc ctt tgc ctt gga atg tat c	484	338	60	72
		Reverse: att tag cca cag ctc cct gga g	821			
Occludin	AC_000177.1	Forward: gac ctg atg aat tca aac cta atc	272	183	58	72
		Reverse: cga tac caa gca tag aca gga t	454			
Ubiquitin[3]	AC_000176.1	Forward: ggc aag acc atc acc ctg gaa	731	201	60	72
		Reverse: gcc acc cct cag acg aag ga	931			
ZO-1	AC_000178.1	Forward: cgt ctt cgt ctt cat ctt cc	4364	303	58	72
		Reverse: gat tca cac caa aac cat aca c	4666			
α-Lactalbumin	AC_000162.1	Forward: tgg gtc tgt acc acg ttt ca	133	251	60	72
		Reverse: gct tta tgg gcc aac cag ta	383			
αS1-casein	AC_000163.1	Forward: tac cct gag ctt ttc aga ca	547	201	60	72
		Reverse: cat aac tgt gga gtc cct ca	747			

Table 4.2 Cont. Sequences of PCR primers (forward & reverse), primer position, PCR product sizes & individual experimental conditions of bovine nucleic acid sequences used for investigating gene expression by quantitative Real-Time PCR

Gene	Nuclei Acid Sequence	Primer sequence (5'→3')	Primer position[1] [bp]	Product size [bp]	Annealing [°C]	Acquisition [°C]
β1-integrin	AC_000170.1	Forward: cag atg agg tga aca gcg aa	1443	289	60	80
		Reverse: atg cag gaa gtg gta ccc ag	1731			
K-casein[3]	AC_000163.1	Forward: ata ctg tgc ctg cca agt cc	371	238	60	75
		Reverse: ttg atc tca ggt ggg ctc tc	608			

[1] Refers to the 5' position of the primers in the nucleic acid sequence

[2] Primer sequence previously described in Coussens and Nobis, 2002

[3] Primer sequence previously described in Singh et al., 2008

Two milk protein genes (αS1-casein and α-lactalbumin) and one component of the body's immune response (lactoferrin), which is generally up-regulated during mammary gland involution, were tested as indicators for overall milk production and progression of involution. To determine changes in the gene expression levels of junctional proteins due to mechanical stimulation by the infusion, the mRNA levels of ZO-1, occludin, and claudin-1 (TJ components) were determined as well as the levels of β1-integrin (FA component). The levels of mRNA expression of bcl-2 and bax during the infusion experiment relative to their respective control samples were determined as an indicator of the onset of involution. The primer sequences and other relevant details for individual experimental conditions are outlined in Table 4.1.

PCR products were then QIAquick column-purified (Qiagen) and submitted for DNA sequencing which verified their authenticity (University of Canterbury, New Zealand, DNA Sequencing Facility, results not shown).

4.3.3.3 Agarose gel electrophoresis for DNA

Agarose gels (1.5 % (w/v)), containing 1x TAE (40 mM Tris, 0.1 % (v/v) glacial acetic acid, 1 mM EDTA pH 8.0) and 1x SYBR® Safe DNA gel stain (Life Technologies, Carlsbad, USA), were used to visualise DNA samples. Wells were loaded with 5 µl of PCR product mixed with DNA loading buffer [0.25 % (w/v) bromophenol blue, 0.25 % (w/v) xylene cyanol FF, and 30 % (v/v) glycerol)] in 12 µl total volume. The gel was run at a constant 100 V in electrophoresis buffer (1x TAE, 1x SYBR® Safe DNA gel stain) for approximately 1 h. The DNA was then visualised under UV transillumination using a Gel Doc and Quantity One

software (Bio-Rad Laboratories, Hercules, USA) to confirm the size and number of bands present.

4.3.3.4 Analysis of qRT-PCR data

Following qRT-PCR experiments, average take-off values for reference genes and genes of interest were generated for each sample using the Rotor-Gene Q software (version: 2.1.0). The take-off value represents the cycle number at which the fluorescence of each reaction crossed the threshold, which was placed above background fluorescence and within the log-linear phase of exponential product amplification. Therefore, the lower the take-off value the higher the amplification of PCR products. Relative quantification of gene expression was performed using comparative quantification to analyse changes in gene expression in a given sample relative to the non-infused control sample. The amount of gene of interest in each sample was normalised by dividing by the amount of reference genes and the resulting values $\log_{10}$-transformed before statistical analysis. Averages for each treatment group were back-transformed and results expressed as the fold change relative to respective control samples.

4.3.4 Protein preparation

One hundred mg of ground tissue was resuspended in 1 ml low salt buffer (10 mM 4-[2-hydroxyethyl]-1-piperazineethanesulphonic acid (HEPES), pH 7.9, 1.5 mM magnesium chloride, 10 mM potassium chloride) containing 1 % (v/v) NP-40 detergent and protease inhibitors (1 mM sodium orthovanadate (Sigma, St. Louis, USA), 1 tablet protease inhibitor cocktail per 10 ml buffer (Roche, Basel,

Switzerland)), homogenised using an Omni Tissue Homogeniser (Omni PCR Tissue Homogenizing Kit, Omni International Inc., Kennesaw, USA) and rotated for 30 min at 4 °C. A 500 µl aliquot was saved for analysis of the total homogenate fraction. The remaining homogenate was centrifuged at 10,000 x g for 30 min at 4 °C and the supernatant collected as the NP-40-soluble protein fraction. To collect the NP-40-insoluble protein fraction, the remaining pellet was resuspended by sonication in 250 µl low salt buffer (containing 1 % (v/v) NP-40 detergent, 1 % (w/v) SDS and protease inhibitors) and rotated for 30 min at 4 °C. Samples were mixed with loading buffer (62.5 mM Tris pH 6.8, 2 % (w/v) SDS, 5 % (v/v) BME, 10 % (v/v) glycerol) (Laemmli, 1970), boiled for 5 min, and stored at -20 ˚C until required for subsequent western analysis. Prior to mixing with loading buffer, the amount of protein present in 1 µl of each sample was determined using Qubit® 2.0 Fluorometer in conjunction with the Qubit® Protein Assay kit as per the manufacturer's instructions (Invitrogen, Carlsbad, USA).

4.3.4.1 Western blot analysis

Protein samples (20 µg) from the control (n=8) and infused (n=8) glands and 5 µl of SeeBlue® Plus2 Pre-stained Protein Standard (LifeTechnologies) were loaded onto a precast NuPAGE® Novex® Bis-Tris protein gel (LifeTechnologies). Electrophoresis was then carried out in the XCell4 SureLock™ Midi-Cell apparatus (LifeTechnologies) for approximately 1 h at 200 V in 1x NuPAGE® MES SDS running buffer (LifeTechnologies). Separated proteins were transferred onto Hybond-ECL nitrocellulose membranes (Amersham Biosciences) using the Trans-Blot Cell (Bio-Rad Laboratories) wet blotting system. After transfer, membranes were stained with Ponceau S (0.1 % (v/v) Ponceau S; 1.0 % (v/v)

acetic acid) to visualise successful transfer of proteins onto the membranes, scanned using a GS-800 densitometer (Bio-Rad Laboratories) and washed with distilled water to remove the ponceau stain. Blocking of non-specific binding was achieved by immersing the membrane in a solution of 4 % NFMP overnight at 4°C on a rocker. Subsequent, membranes were probed with primary antibodies (for detailed information on antibodies refer to Table 4.2) overnight at 4°C on an orbital rocker, followed by incubation with horseradish-conjugated secondary antibody for 1 h at RT (goat-anti rabbit secondary antibody, 1:10,000 dilution). Slides were washed in multiple changes of wash buffer (1x PBS/0.1 % Tween 20) following each antibody incubation. Immunoreactive protein bands were detected using a chemioluminescence system (Amersham ECL Western Blotting Detection Reagents; GE Healthcare Life Sciences, Little Chalfont, UK), BioMax XAR film (Kodak, Rochester, USA) and the 100 Plus film processor (AllPro^{TM}Imaging, Melville, USA). The developed films were scanned using the GS-800 densitometer (Bio-Rad Laboratories) and analysed using the Quantity One software (version 4.6.6).

Western blot analysis was used to determine the pattern of TJ proteins ZO-1 and occludin as well as (p)Akt protein expression following the infusion experiment (Table 4.2).

4.3.5 Statistical analysis

4.3.5.1 Statistical analysis of histological differences

To eliminate potential bias, sections were selected randomly and the histological assessment and grading was conducted blind. For each animal, three tissue sections from each hind quarter were assessed and the assigned grades per section analysed by ANOVA in GenStat (16th edition, version 16.1.0.10916 (64-bit version)) taking cow effects into account. Data are presented as averaged means for each treatment group with the standard error of the mean (SEM) with the corresponding P-value. Means were considered different at $P<0.05$. * $P<0.05$, ** $P<0.01$, *** $P<0.001$.

4.3.5.2 Statistical analysis of milk composition

Differences in milk composition were analysed by ANOVA in GenStat (16th edition, version 16.1.0.10916 (64-bit version)) taking cow effects into account. Furthermore, to compensate for the dilution of milk components due to the infusion of sterile saline solution into one hind quarter, a 20 % correction factor was applied after the experiment for the infused quarter. Data are presented as means with the SED with the corresponding P-value. Means were considered different at $P<0.05$ and within the range of a statistical trend at $P<0.1$. * $P<0.05$, ** $P<0.01$, *** $P<0.001$.

4.3.5.3 Statistical analysis of qRT-PCR results

The levels of mRNA expression from each treatment group (control and infused) were expressed as back-transformed mean fold changes relative to the lactating group. Differences in levels of mRNA expression from each group were analysed using the Student's paired t-test with a two-tailed distribution (MS Excel, 2010). Data are presented as the means for each treatment group with the SEM between means with their corresponding P-values. Data from individual animals are expressed as back-transformed mRNA expression levels (relative units). Means were considered different at $P<0.05$ and within the range of a statistical trend at $P<0.1$. * $P<0.05$, ** $P<0.01$, *** $P<0.001$.

4.3.5.4 Statistical analysis of Western Blot results

Densitometry data were $\log_{10}$-transformed and analysed by ANOVA in GenStat (16th edition, version 16.1.0.10916 (64-bit version)) with blocking on replicate and adjusting for between gel variations to detect differences between control and infused samples. Results are graphed as mean fold change relative to lactation on a $\log_2$-scale with their corresponding SED. Means were considered different at $P<0.05$ and within the range of a statistical trend at $P<0.1$. * $P<0.05$, ** $P<0.01$, *** $P<0.001$.

4.4 Results

4.4.1 Histological analysis

Representative alveolar tissue sections from the control glands and their respective treatment glands were used for histology analysis (Figure 4.1). Mammary biopsies were collected after 15 h of natural milk accumulation. Therefore, treatment glands would contain approximately 20 h worth of fluid, due to the extra volume infused which was equivalent in volume to '5 h worth' of individual milk production.

Overall, the control samples showed signs of active milk secretion. Milk accumulated within the alveolar lumen, which resulted in larger, engorged alveoli lined with a single layer of stretched, flattened MECs. At a lower magnification, the majority of the alveoli appeared to be of similar size, open and relaxed (Figure 4.1; A and C). Minimal variation in size of alveoli and thickness of alveolar walls was observed across all alveoli. Although, it is worth noting that heterogeneity was present within animals, which could be observed at low magnification in both groups. For example, in the control samples, although most alveoli were still large with a stretched morphology, a few localised collapsed areas were apparent. These were characterised by smaller alveoli with a "ruffled" appearance (Figure 4.1; C and G).

However, the treatment glands had a non-lactating, or early involution appearance. This was characterised by collapsed alveoli, abundance of large

vesicles within MECs and alveolar lumens, thickened areas of stromal tissue between alveoli and broad bands of supportive connective tissue containing adipocytes (Figure 4.1; B and D). The majority of tissue was dominated by a non-lactating appearance (Figure 4.1; B, D, F and H). At higher magnification, large vacuoles containing fat droplets and material from secretory vesicles were present within MEC and high numbers of vesicles containing coalescing fat droplets and proteins were associated with the apical side of cells (Figure 1; F and H). Moreover, the majority of alveoli were collapsed with ruffled edges, had cells protruding into the lumen and with discernible gaps between adjacent cells (Figure 4.1; B, D, F and H).

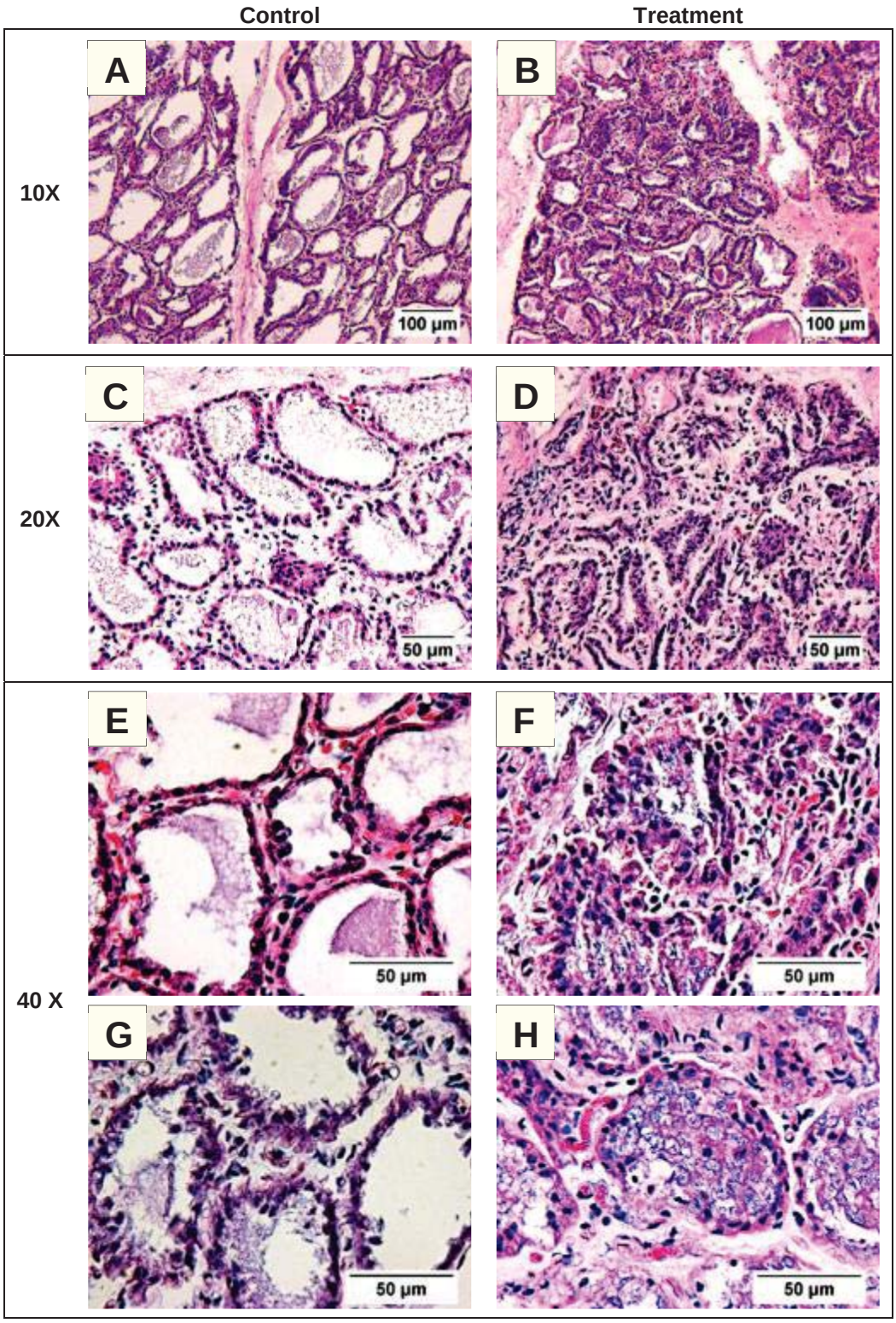

Figure 4.1 Morphological differences between the control and infused treatment group. Note: Representative haematoxylin and eosin stained sections of mammary tissue from the control glands and their respective treatment glands. Please refer to the text for detailed description of histological features. Images A and B: Scale bar is 100 µm. Images C to F: Scale bar is 50 µm. Images A and B: 10x objective used. Images C and D: 20x objective used. Images E to H: 40x objective used

4.4.1.1 Assessment of histological features

A grading criterion was adopted to categorise the lactation state for each tissue section with a score of between 0 and 4 to assess and compare histological features of lactation and involution between the control and the treatment group (Fig. 4.2). The average lactation grade was significantly lower in the infused samples compared with the control samples.

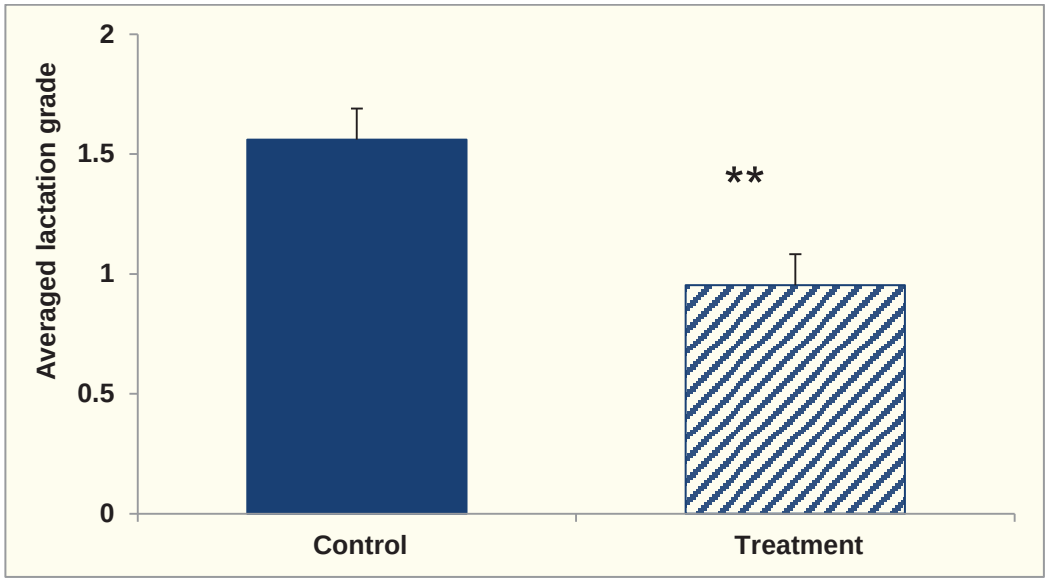

Figure 4.2 Lactation grades after assessment of histological features to compare morphological differences between the control and treatment group (n=8/group)
For each animal, three sections from each hind quarter were assessed and the averaged lactation grades (±SEM) for both experimental groups are presented. The SEM reflects both the inter-lobular as well as the inter-animal variation observed within the tissue and ** - P<0.01

4.4.2 Milk composition data

Milk samples taken from each hind quarter (control and treatment), before and after the infusion experiment, were used to determine differences in milk composition from each cow.

4.4.2.1 Milk fat

No significant differences in fat content between the quarters could be detected (Fig. 4.3). However, both samples (treatment and control) showed a decline in milk fat content of approximately 3.5 % following infusion compared with the start of the treatment period.

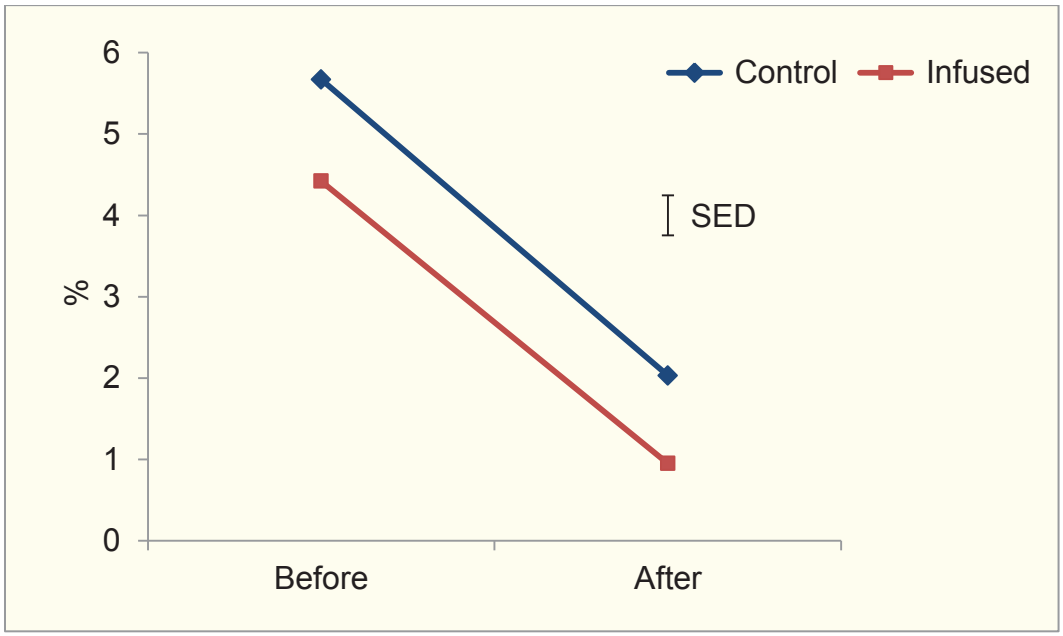

Figure 4.3 Milk fat content determined in milk samples collected from each hind quarter (control and treatment) before and after the infusion experiment (n=8/group) (Results are graphed as means with the SED)

4.4.2.2 Milk protein

After infusion, the total milk protein content of infused glands was significantly decreased, while the protein content of the control samples remained the same prior to and after the treatment period (Fig. 4.4).

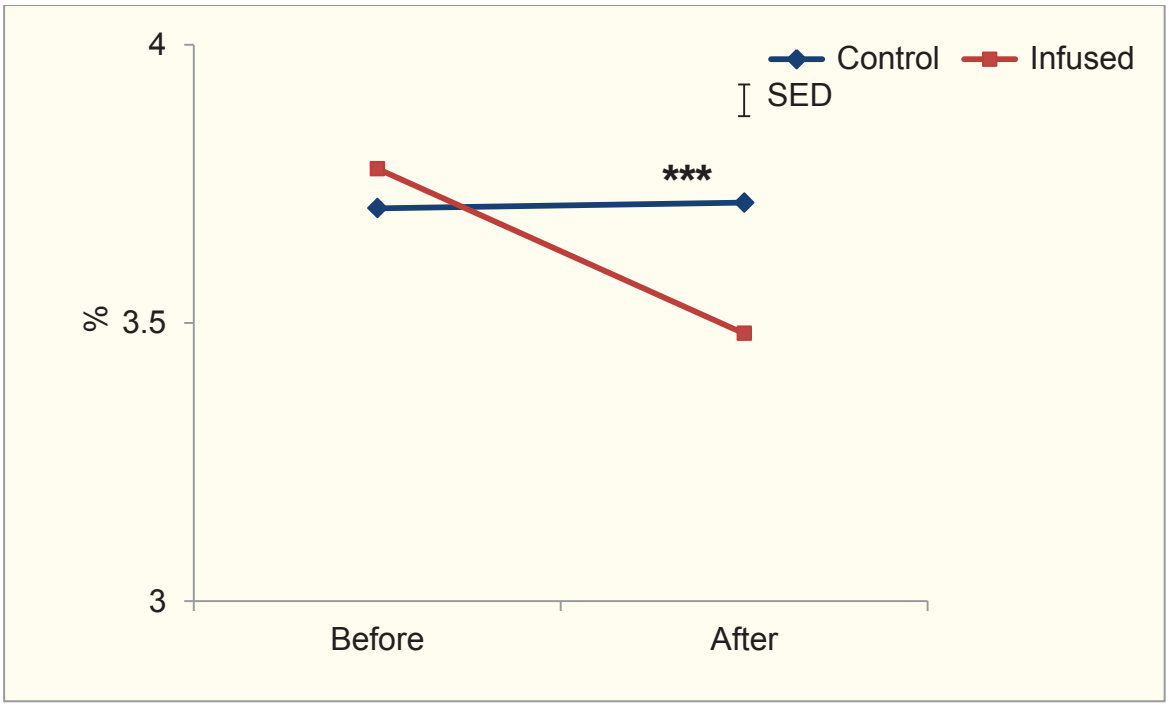

Figure 4.4 Total milk protein content determined in milk samples collected from each hind quarter (control and treatment) before and after the infusion experiment (n=8/group) (Results are graphed as means with the SED and *** = P<0.001)

4.4.2.3 Somatic cell count

Following the infusion, the SCC significantly increased in the infused samples, while the control samples were the same before and after the infusion (Fig. 4.5).

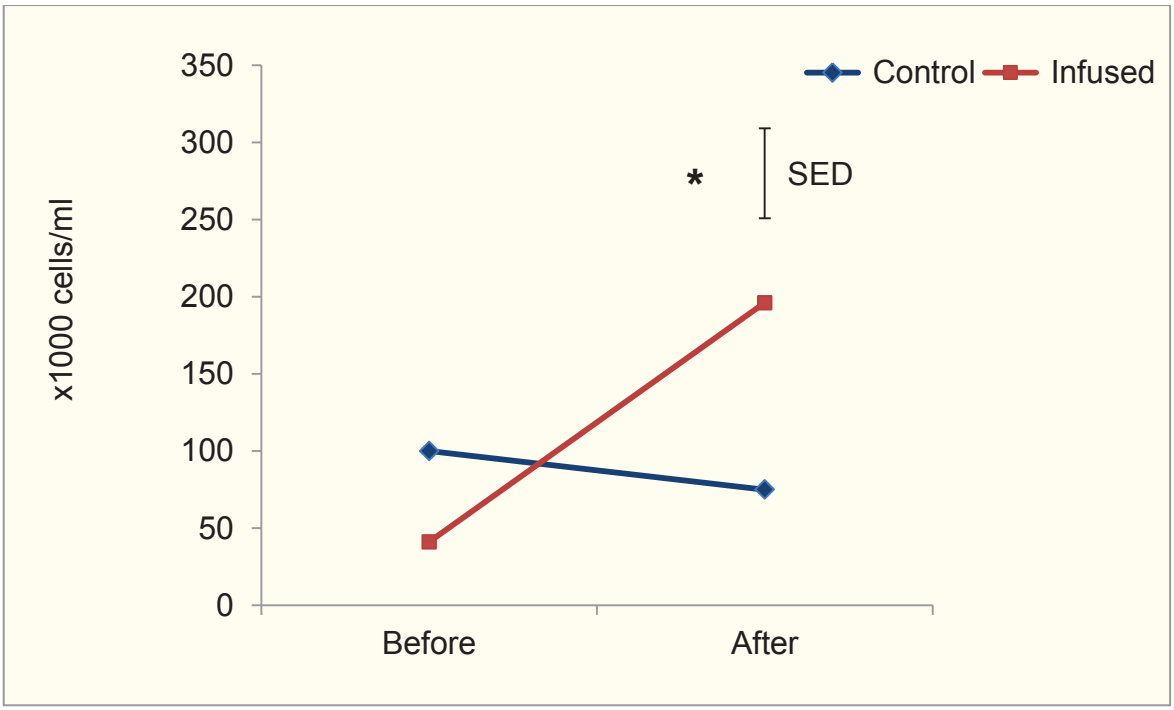

Figure 4.5 Somatic cell count determined in milk samples collected from each hind quarter (control and treatment) before and after the infusion experiment (n=8/group) (Results are graphed as means with the SED and * = P <0.05)

4.4.2.4 Lactose

Lactose content significantly declined in the treatment group following the infusion experiment (Fig. 4.6). In the control samples, however, the lactose content increased following 15 h of natural milk accumulation.

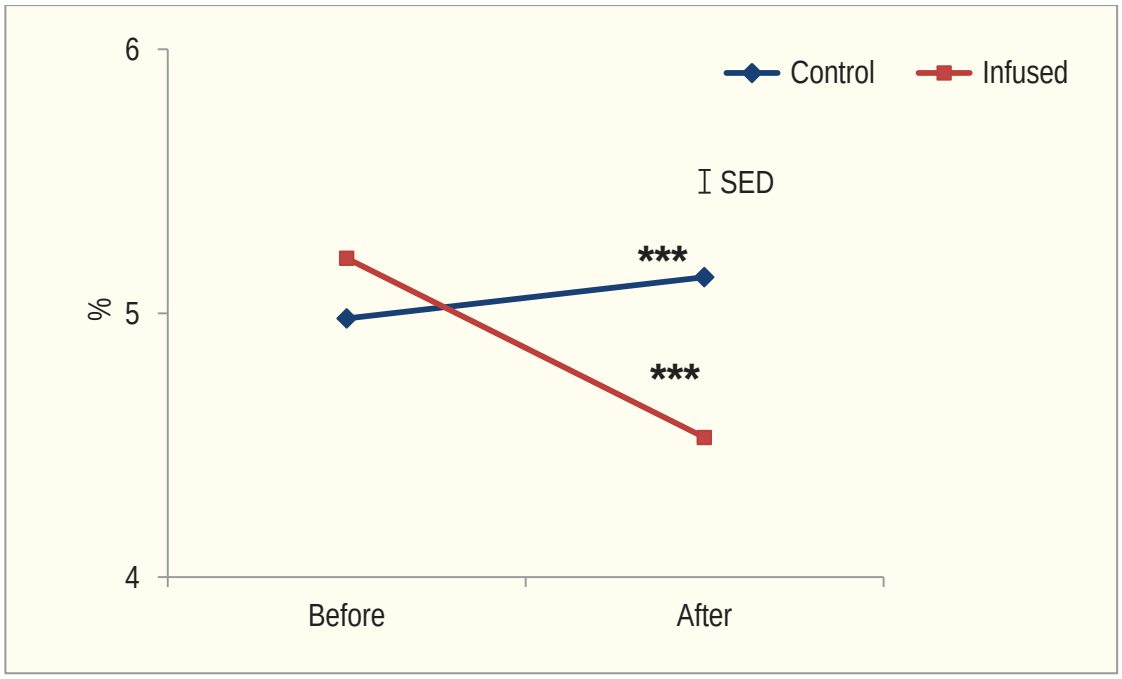

Figure 4.6 Lactose content determined in milk samples collected from each hind quarter (control and treatment) before and after the infusion experiment (n=8/group) (Results are graphed as means with the SED and *** = P<0.001)

4.4.2.5 Total milk solids

Although the overall amount of total milk solids (fat, lactose, protein, and trace minerals) declined in the treatment samples as well as in the control samples compared with before treatment controls, no significant differences in the total milk solids content between the groups could be detected (Fig. 4.7).

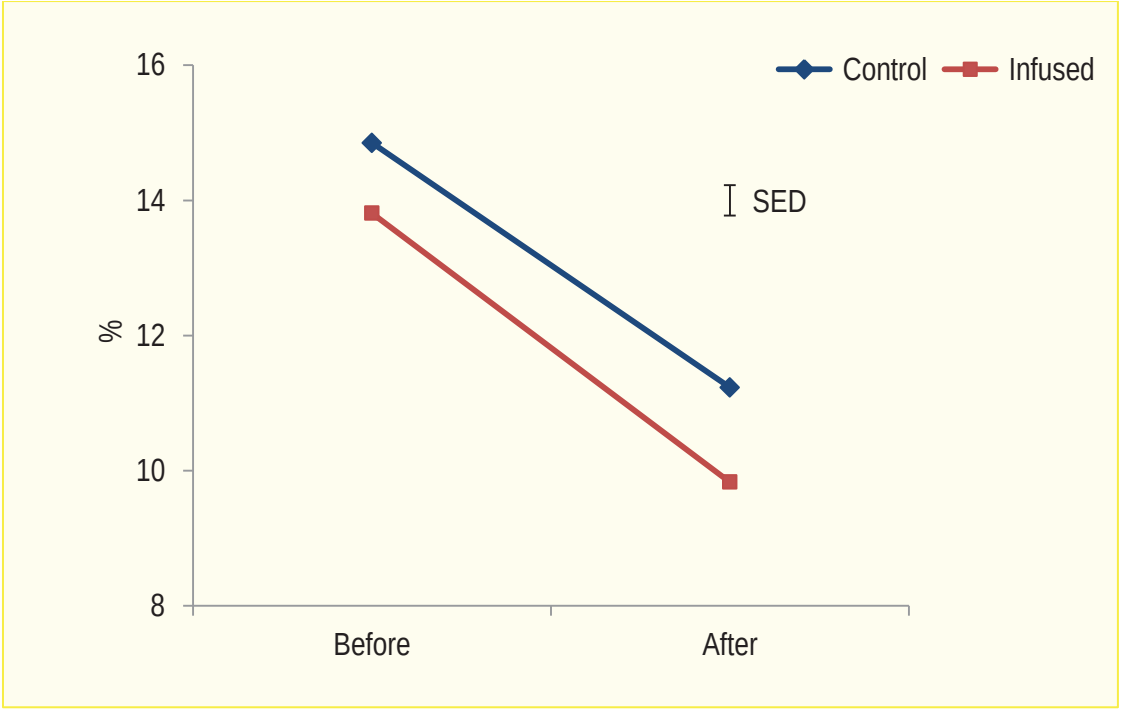

Figure 4.7 Total milk solids content determined in milk samples collected from each hind quarter (control and treatment) before and after the infusion experiment (n=8/group) (Results are graphed as means with the SED)

4.4.3 qRT-PCR results after infusion experiment

Following the infusion experiment, α-lactalbumin gene expression was reduced by 1.4-fold, compared with non-infused controls. However, there was no difference in αS1-casein gene expression following the experiment (Fig. 4.8). Furthermore, there were no differences in mRNA expression for lactoferrin, ZO-1, claudin, occludin, β1-integrin, bax, or bcl-2 following the infusion, compared with non-infused controls (Fig. 4.9 and 4.10).

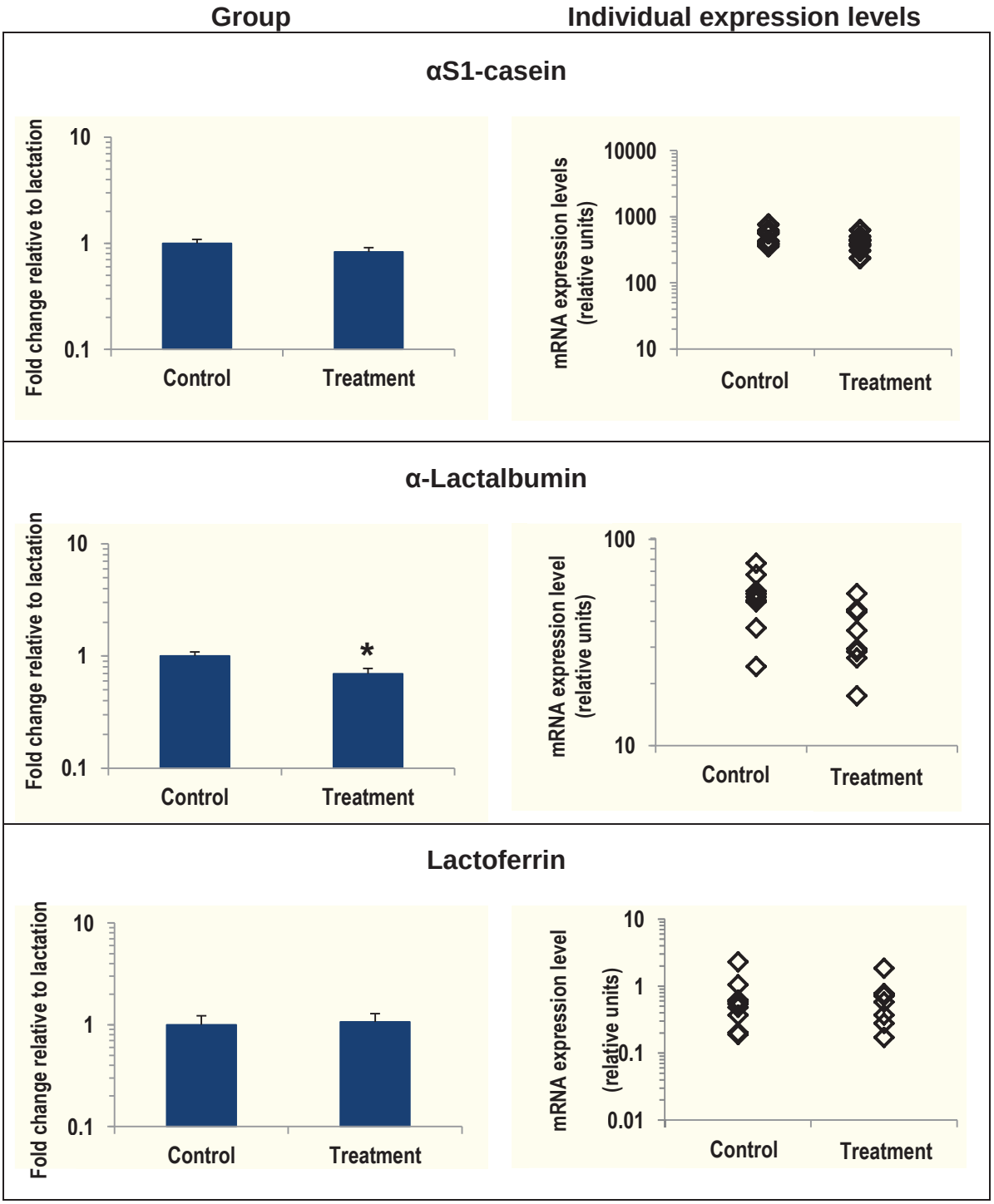

Figure 4.8 Changes in gene expression levels of αS1-casein, α-lactalbumin and lactoferrin following the infusion of one hind quarter compared with non-infused controls (n=8/group).

Data from each group are expressed as back-transformed fold-change relative to lactation with the SEM to compare control and infused glands.

Data from individual animals are expressed as back-transformed mRNA expression levels and * = P<0.05

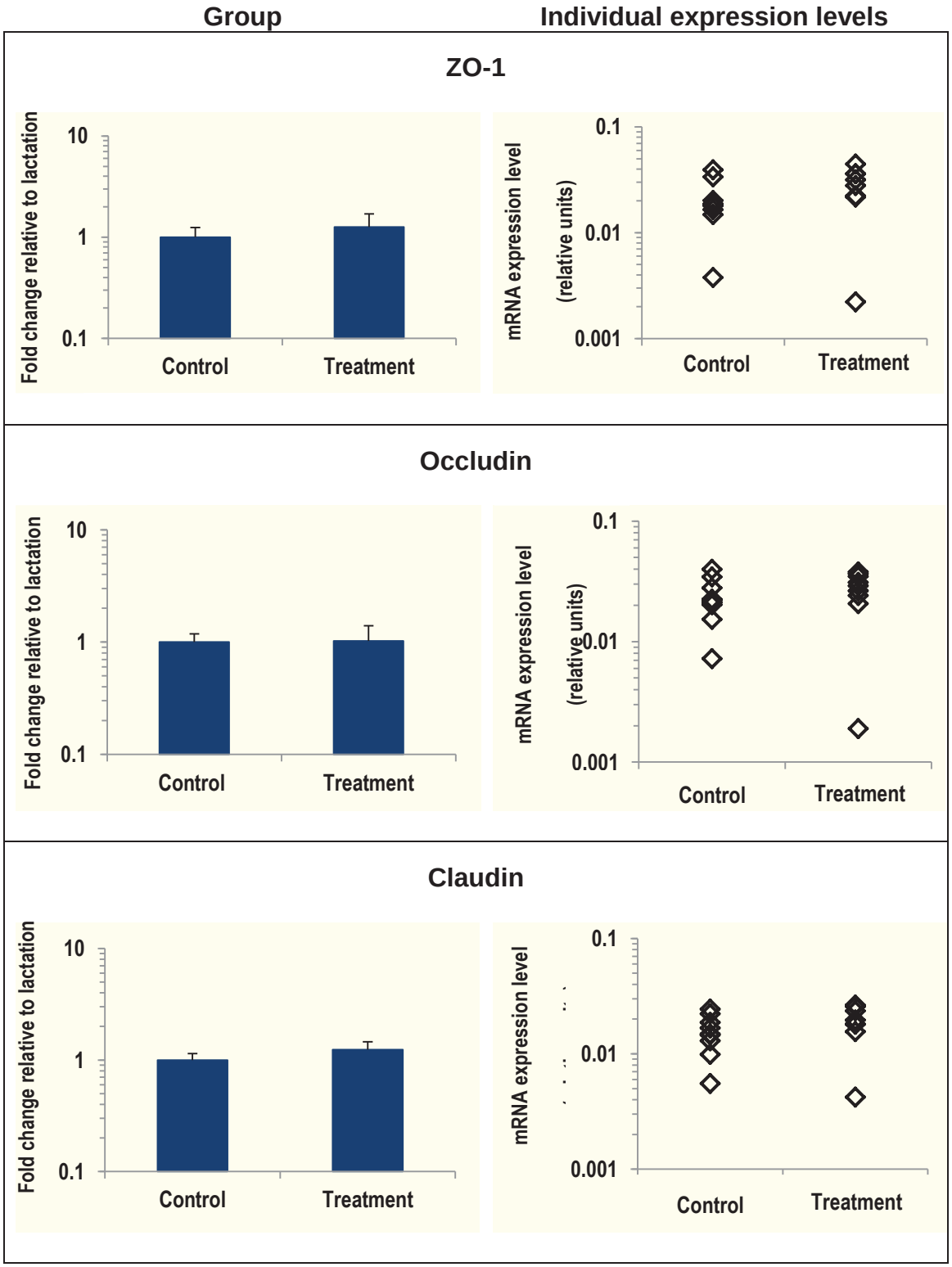

Figure 4.9 Changes in gene expression levels of TJ proteins, ZO-1, occludin, and claudin, following the infusion of one hind quarter compared with non-infused controls (n=8/group).

Data from each group are expressed as back-transformed fold-change relative to lactation with the SEM to compare control and infused glands.

Data from individual animals are expressed as back-transformed mRNA expression levels

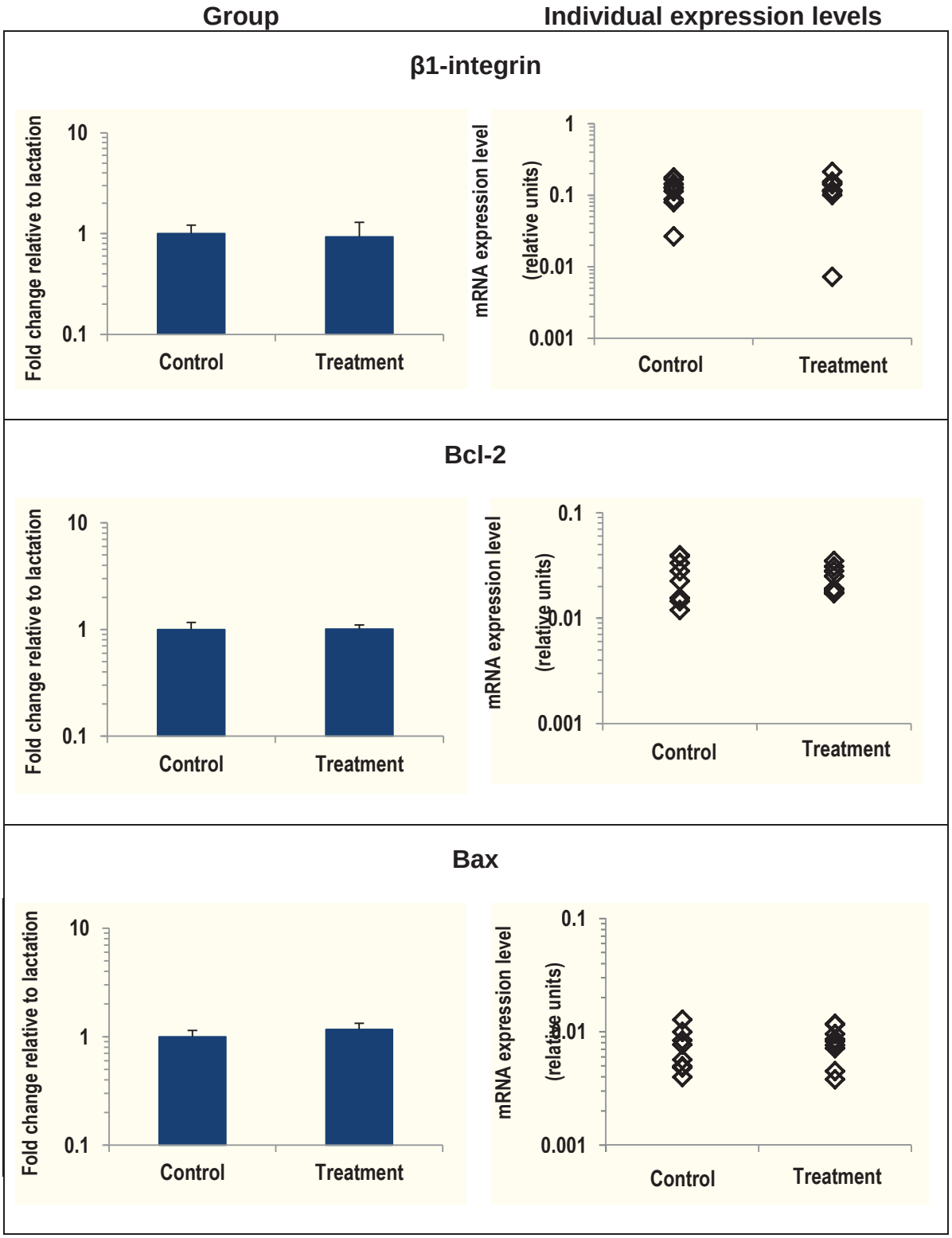

Figure 4.10 Changes in gene expression levels of β1-integrin, bcl-2 and bax, following the infusion of one hind quarter compared with non-infused controls (n=8/group).

Data from each group are expressed as back-transformed fold-change relative to lactation with the SEM to compare control and infused glands and data from individual animals are expressed as back-transformed mRNA expression levels

4.4.4 Analysis of levels of protein expression after infusion experiment

Western blot analysis was used to determine the pattern of TJ and (p)Akt protein expression following the infusion experiment.

4.4.4.1 Protein integrity

Confirmation of equivalent sample loading of SDS-PAGE gels was obtained by Coomassie blue staining of untransferred gels for soluble and insoluble protein fractions (results not shown), while the effective transfer of proteins onto a nitrocellulose membrane was confirmed by Ponceau S staining (Fig. 4.11, soluble protein fraction).

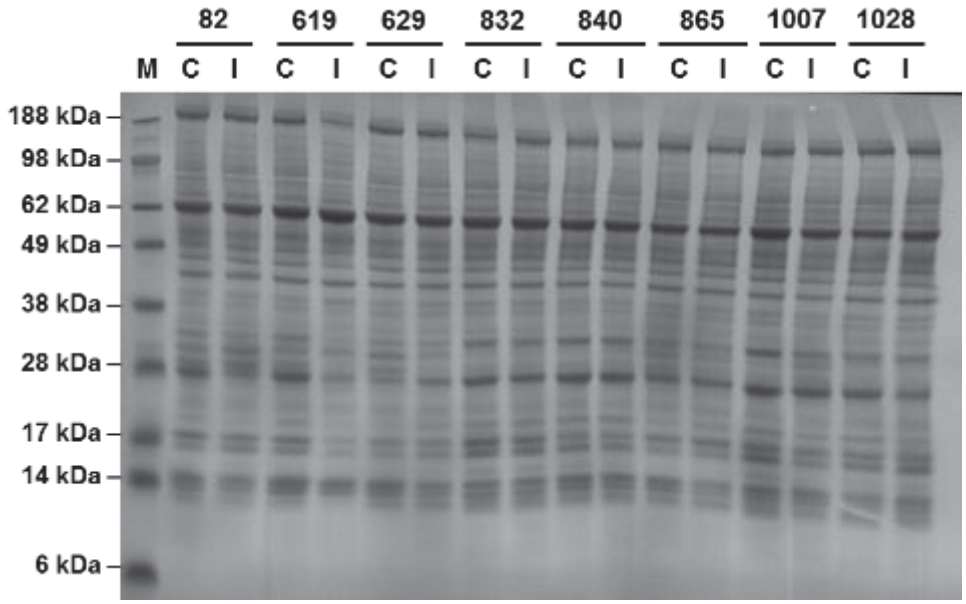

Figure 4.11 Representative image of Ponceau S-stained nitrocellulose membrane after protein transfer.

Bis-Tris protein gels (10 %) were loaded with samples extracted from the infused glands (I) and their corresponding control samples (C) from each animal.

Each lane was loaded with 20 µg of total protein (soluble fraction), except the marker lane which contained 5 µl of the SeeBlue® Plus2 Pre-Stained Standard

4.4.4.2 Tight junction protein expression

Changes in TJ protein expression (ZO-1 and occludin) were examined to determine TJ protein expression patterns following the infusion experiment (Fig. 4.12).

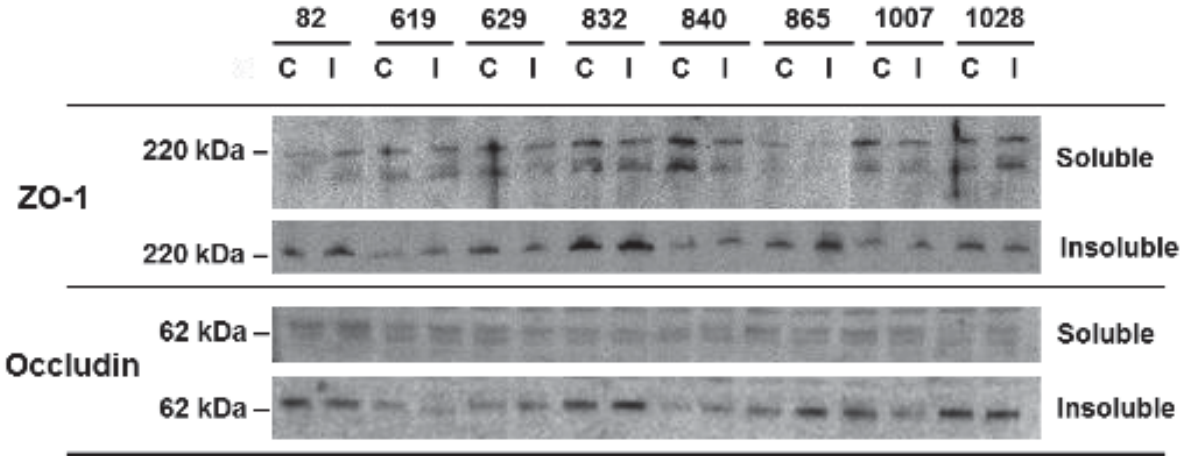

Figure 4.12 Representative images of Western blots to determine changes in TJ protein expression following the infusion experiment (n=8/group).
The experiment was set-up as a within cow experiment to compensate for inter-animal differences (C = control, I = infused). Furthermore, the soluble and insoluble protein fractions from each quarter were used to determine TJ protein expression levels.
Each lane was loaded with 20 µg of total protein.
The primary antibodies used were rabbit anti-ZO-1 (1:1000 dilution) and rabbit anti-occludin (1:1000 dilution)

Both, soluble and insoluble, protein fractions were used to determine changes in TJ protein expressions. Following the infusion, ZO-1 protein levels in the soluble fraction decreased by 1.6-fold relative to control (Fig. 4.13 A). However, no difference in ZO-1 protein levels could be detected for the insoluble fraction. There were no significant differences in occludin protein levels in either the soluble or insoluble protein fractions following the infusion, compared with non-infused controls (Fig. 4.13, B).

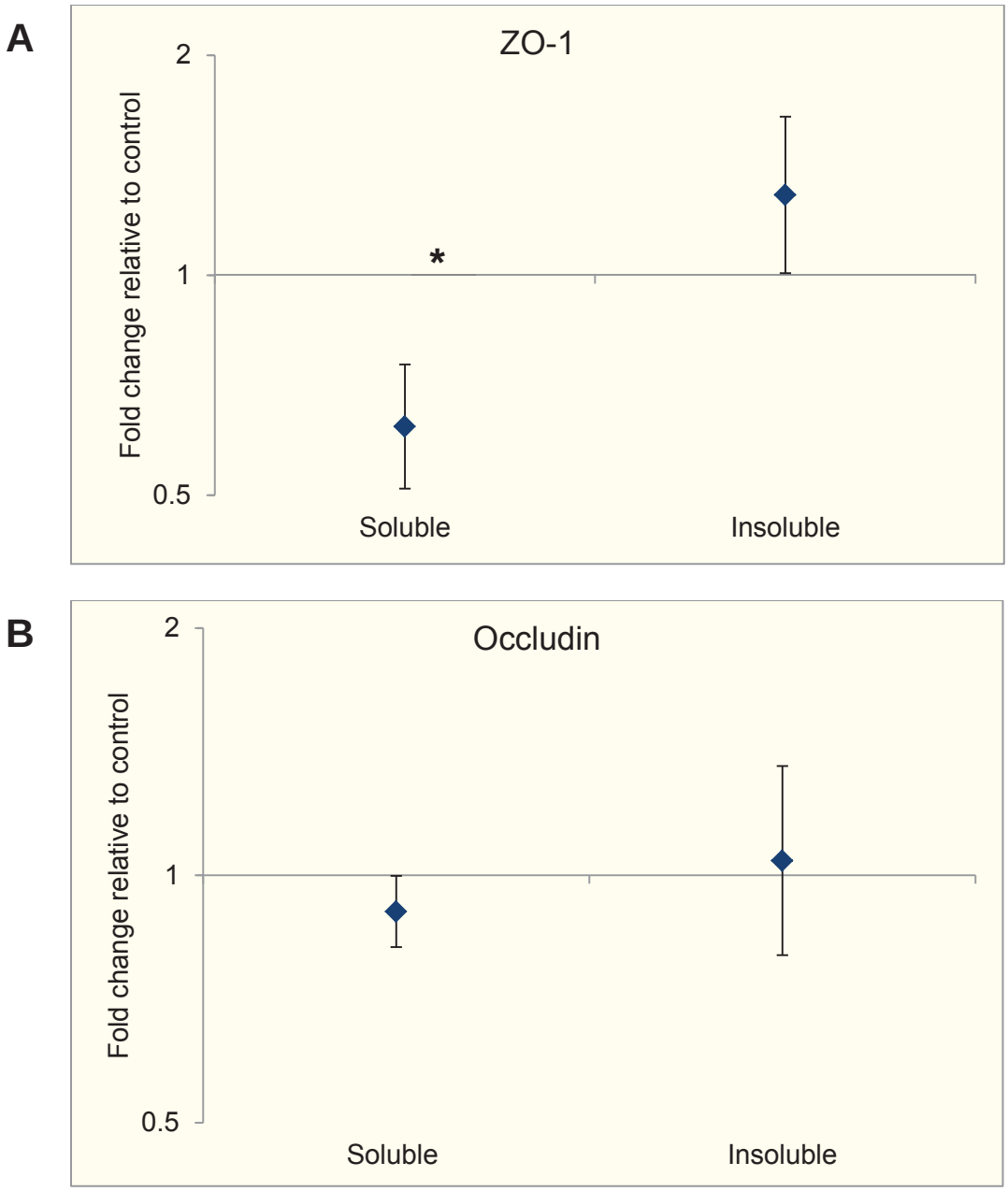

Figure 4.13 Densitometric analysis of Western blots to determine changes in TJ proteins expressions following the infusion experiment (n=8/group).

A: Analysis of ZO-1 protein expression levels following the infusion experiment, compared with non-infused controls.

B: Analysis of occludin protein expression levels following the infusion experiment, compared with non-infused controls.

Results are graphed as fold change relative to lactation on a $\log_2$-scale with their corresponding SED and * = P <0.05

4.4.4.3 (p)Akt protein expression

Changes in (p)Akt protein expression were examined as an indicator of ECM-cell communication for survival signalling following the infusion experiment (Fig. 4.14). Both, soluble and insoluble, protein fractions were used to determine changes in (p)Akt protein levels. No significant differences in Akt protein levels could be identified in either protein fraction, soluble or insoluble, following infusion compared with non-infused controls (Fig. 4.15 A). However, pAkt protein levels decreased by 2.5-fold in the soluble protein fraction of the infused samples relative to their controls (Fig. 4.15 B). No difference in pAkt protein levels could be detected for the insoluble fraction.

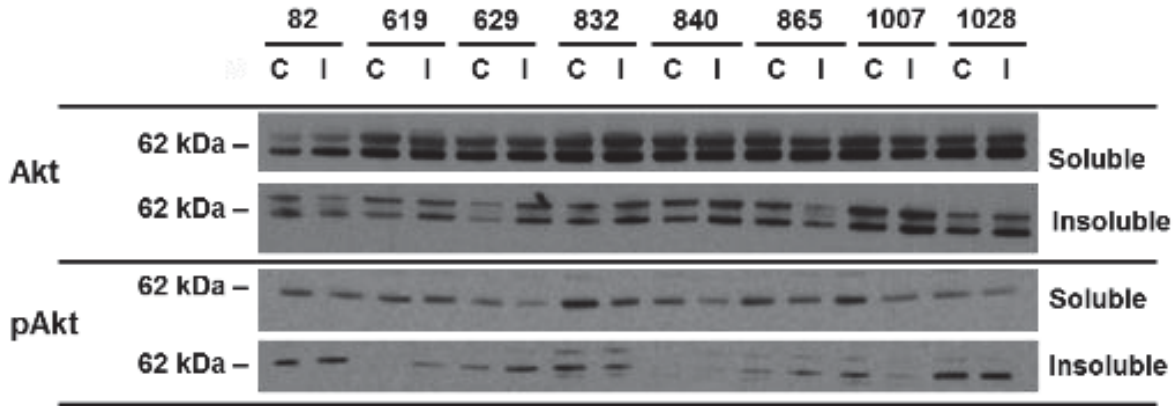

Figure 4.14 Representative images of Western blots to determine patterns of (p)Akt protein expression following the infusion experiment (n=8/group).

The experiment was set-up as a within cow experiment to compensate for inter-animal differences (C = control, I = infused).

Furthermore, the soluble and insoluble protein fractions from each quarter were used to determine (p)Akt protein expression levels.

Each lane was loaded with 20 µg of total protein.

The primary antibodies used were rabbit anti-Akt (1:1000 dilution) and rabbit anti-pAkt (1:5000 dilution)

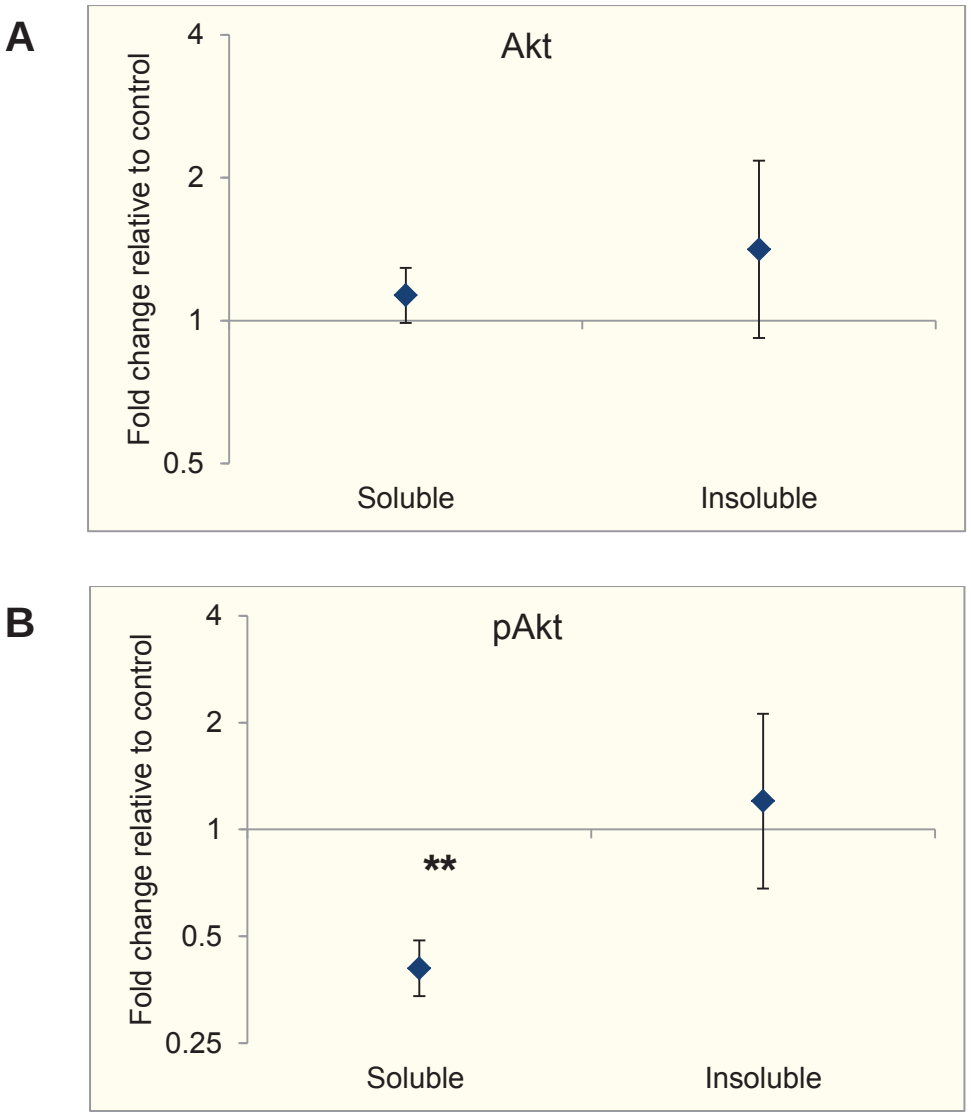

Figure 4.15 Densitometric analysis of Western blots to determine changes in (p)Akt protein expressions following the infusion experiment (n=8/group).

A: Analysis of Akt protein expression levels following the infusion experiment, compared with non-infused controls.

B: Analysis of pAkt protein expression levels following the infusion experiment, compared with non-infused controls.

Results are graphed as fold change relative to lactation on a $\log_2$-scale with their corresponding SED amd ** = P <0.01

4.5 Discussion

Milk production is determined by the number and activity of secretory cells present, which can differ depending on the species. Until peak lactation, the udder continues to grow, due to an increase in the number of secretory cells. Once peak yield is reached, a shift occurs and the rate of apoptosis increases in contrast to rate of proliferation (Capuco *et al.*, 2001; Capuco *et al.*, 2003; Boutinaud *et al.*, 2004). In recent years, research indicated a potential role of mechanotransduction in the initiation of the mammary involution process *in vitro* in rodents (Quaglino *et al.*, 2009) and *in vivo* (Phyn *et al.*, 2007). In this study, artificial distension of bovine mammary glands by infusion of a sterile saline solution near peak lactation induced molecular events that occur in the mammary gland during early involution (Hurley, 1989; Li *et al.*, 1997).

Histological assessment of tissues collected from infused glands showed an overall increase in the degree of involution and number of features associated with involution compared to their respective control gland (non-infused). The treatment glands (infused) displayed general histological characteristics, such as collapsed alveoli or gaps in epithelial cell layer, that have previously been described in involuting mammary tissue (Holst *et al.*, 1987; Capuco & Akers, 1999). Furthermore, a grading criteria was applied in order to quantify differences in features associated with active lactation, such as open, relaxed alveoli lined by single MEC layer, to those associated with involution. This showed a significant difference between the two glands. However, the heterogeneity observed within and between lobules, and between different animals in the actively lactating mammary gland in the present study is in agreement with previous observations

(Molenaar *et al.*, 1992). Consequently, collecting samples by biopsy could result in sampling an area of tissue that, although actively lactating, may contain large areas of non-secretory active alveoli/lobules.

Milk composition analysis showed a significant reduction in protein and lactose content, as well as an increase in SCC in milk samples collected from infused glands. Taken together these events indicate that in the infused glands only, milk production decreased and more cells were being shed into the alveolar lumen which is an early sign of the onset of involution (Stefanon *et al.*, 2002).

In the present study, the milk fat content decreased following the infusion treatment. However, although each cow was milked twice a day, the time period between the afternoon milking and the next morning milking is much longer (16 h) than the morning and afternoon interval (8 h). As a result, milk fat content varies considerably between morning and afternoon milking (AJ Molenaar, unpublished data). Furthermore, oxytocin administration prior to milking results in an elevated transfer of milk fat globules, normally sequestered in the alveolar compartment, into the cisternal compartment. Due to anatomical restrictions keeping milk fat globules in the alveolar compartment, alveolar milk is 2.5 to 5 times higher in fat content than cisternal milk (Lollivier *et al.*, 2002; Ayadi *et al.*, 2004). Thus, the effect of oxytocin in conjunction with differences between morning and afternoon milking intervals, may partly explain the lack of significant differences in milk fat content between treatment and control samples. Following the infusion, α-lactalbumin gene expression decreased significantly in the treatment samples. As one of the major whey proteins, α-lactalbumin acts as a cofactor for

galactosyltransferase regulating its activity and specificity. Together they form lactose synthase which in turn catalyses lactose synthesis from glucose and galactose in the lactating mammary gland (Permyakov & Berliner, 2000). Additionally, due to its osmoregulatory properties, lactose plays an important role in the overall milk yield (Liu *et al.*, 2013). Therefore, it was concluded that milk secretion decreased in the treatment gland only following the infusion experiment which in turn conforms with the early signs of involution (Li *et al.*, 1997). In this study, the impact of artificial distension on two cellular adhesion structures (TJs and FAs) were analysed, because they have previously been shown to play a part in the initiation of mammary gland involution (Cavanaugh *et al.*, 2001; Lee & Streuli, 2014).

First, temporal changes in mRNA and protein expression of ZO-1, claudin, and occludin, all part of the tight junctional complex, were analysed. During lactation, TJs form a tight barrier to prevent paracellular movement of milk components between the blood stream and milk compartments (Neville, 2009). Thus, the loss of TJ integrity may allow pro-apoptotic factors to relocate from the apical to the basolateral side of MECs and either induce apoptosis directly or antagonise survival signals (Green & Streuli, 2004). Furthermore, temporal changes in gene expression of β1-integrin as part of the FA complex were investigated. Integrins appear to be the main mechanoreceptors that link the ECM with the cytoskeleton and have been shown to play a major role in transmitting incoming survival signals from the ECM (Prince *et al.*, 2002; Naylor *et al.*, 2005). Additionally, changes in protein expression of (p)Akt following the infusion experiment were analysed as part of the signalling pathway downstream of β1-integrin. Several

studies have described the impact of mechanical stimulation on Akt expression/activation in epithelial cells in the intestine (Zhang, Li, Sanders*, et al.*, 2003; Gayer, Chaturvedi, Wang, Craig*, et al.*, 2009), in the lung (Tschumperlin & Margulies, 1998; Tschumperlin *et al.*, 2000; Hammerschmidt *et al.*, 2007; Crosby *et al.*, 2011), and in murine MECs (Provenzano *et al.*, 2009; Quaglino *et al.*, 2009). Moreover, Akt has been shown to play an essential role during MEC differentiation and maintaining lactation/delaying involution (Chen *et al.*, 2010; Creamer *et al.*, 2010). Based on previous studies, at 18 h post termination of milk removal, communication between the ECM and the MECs becomes compromised (Singh *et al.*, 2005) and the tight-junctional barrier is disrupted and becomes permeable for milk molecules (Stelwagen *et al.*, 1995). Although no significant changes were detected at the gene level, ZO-1 and pAkt protein expression levels decreased significantly following the infusion. Since ZO-1 forms a link between the actin cytoskeleton and other TJ components (Fanning *et al.*, 1998), a decrease in ZO-1 protein expression indicates a potential disruption of communication between the two. Furthermore, decreased pAkt protein expression levels may demonstrate a loss of communication between the MEC and its ECM which are important for systemic survival signalling (Schwertfeger *et al.*, 2001).

Finally, it was determined that the levels of Bcl-2 (apoptosis suppressor) and bax (apoptosis inducer) gene expression as a marker for MEC commitment to undergo apoptosis and the overall initiation of involution following the infusion experiment (Jurgensmeier *et al.*, 1998; Colitti, 2012). However, there were no

differences in bcl-2 or bax gene expression following the acute physical distension of the mammary gland.

It was concluded that acute physical distension (i.e. mechanical strain applied to MECs) induces molecular events associated with the initiation of the involution process. However, mechanical stimulation alone may not be sufficient to trigger the entire program of post-lactational tissue remodelling.

Chapter 5:

General Discussion and Conclusions

Chapter 5 General Discussion and Conclusions

During active lactation, highly organised lobular-alveolar structures are important to ensure sufficient milk secretion to nurse the offspring (Knight & Peaker, 1982; Plath *et al.*, 1997). After weaning/drying off, however, large populations of terminally differentiated and highly secretory active MEC are no longer necessary and lobular-alveolar tissue remodelling occurs. In dairy cows, however, the overall alveolar structure is maintained throughout the dry period (Capuco & Akers, 1999). Nonetheless, cessation of milk removal leads to milk accumulation within the mammary gland which in turn results in increased intra-mammary pressure (Peaker, 1980; Bruckmaier, 2005). Thus, it has been postulated that mammary gland engorgement may cause changes in the mechanical micro-environment resulting in changes in cell shape which in turn may initiate a decline in milk production (Davis *et al.*, 1999; Stelwagen, 2001).

The primary goal of this research was to determine the potential effects of MEC stretch and change in cell shape on lactation and involution in dairy cattle. Previous studies show that tissues grow and remodel in response to changes in mechanical forces. These mechanical forces play a fundamental role in regulation of cell function, including gene induction, protein synthesis, cell growth and death, cell morphology and differentiation, which are essential for tissue homeostasis (Huang & Ingber, 1999; Chen *et al.*, 2004; Huang *et al.*, 2004; Jaalouk & Lammerding, 2009; Mammoto *et al.*, 2012). In general, transduction of physical forces appear to occur through force-induced changes in protein confirmation which may regulate enzymatic activity, enable new molecular interactions, or

liberate soluble bond factors which in turn may activate signalling pathways in an autocrine and paracrine fashion (Huang & Ingber, 1999; Orr *et al.*, 2006; Reichelt, 2007; Jones & Nauli, 2012). During this investigation, particular emphasis was put on three potential mechanosensors, TJ, FA, and PC, and their regulation in during different stages of involution using *in vivo* and *in vitro* approaches.

In the mammary gland, β1-integrin-mediated ECM adhesion plays a fundamental role in cell survival signalling (Li *et al.*, 2005; Naylor *et al.*, 2005) and its disruption following cessation of milk removal has been linked to the onset of mammary involution in rats (McMahon *et al.*, 2004) and cows (Singh *et al.*, 2005). TJs, on the other hand, form a barrier that helps to distinguish the apical from the basolateral domain of the cell and thus, inhibits paracellular exchange of substances between vascular and milk compartments. Hence, their disruption may allow pro-apoptotic factors to relocate from the apical to the basolateral side of MECs and either induce apoptosis directly or antagonise survival signals (Green & Streuli, 2004). Based on previous studies, at 18 h post termination of milk removal communication between the ECM and the MEC becomes compromised (Singh *et al.*, 2005) and the tight-junctional barrier is disrupted and becomes permeable for milk molecules (Stelwagen *et al.*, 1995).

In the present study, mechanical strain applied to bovine mammary primary cells *in vitro* for different periods of time using a specially fabricated cell stretch device resulted in changes in mRNA levels for ZO-1, occludin and claudin (TJ proteins) following 15, 24, and 48 h of applied stretch. At the protein level, mechanical strain applied *in vitro* resulted in changes in occludin and ZO-1 protein levels

following 1, 5, 15, and 24 h of cell stretch. Furthermore, mechanical strain induced changes in protein levels for Akt and pAkt (part of FA signalling pathway) following 1 and 3 h of *in vitro* cell stretch. Following acute, artificial physical distension of the bovine mammary gland *in vivo*, ZO-1 and pAkt protein expression levels decreased significantly. Since ZO-1 forms a link between the actin cytoskeleton and other TJ components (Fanning *et al.*, 1998), a decrease in ZO-1 protein expression indicates a potential disruption of communication between the two. Furthermore, decreased pAkt protein expression levels may demonstrate a loss of communication between the MEC and its ECM which are important for systemic survival signalling (Schwertfeger *et al.*, 2001).

The disruption of cell-ECM or cell-cell interactions occurs very early during the weaning/drying off process (Prince *et al.*, 2002; Strange *et al.*, 2007; Beeman *et al.*, 2009). Beta1-integrin, in particular, appears to be functionally important during the onset of mammary involution (Prince *et al.*, 2002). The integrins' ability to initiate a range of signalling pathways regulate various cellular behaviours (Streuli & Akhtar, 2009). As an example, genetic analyses indicate their role in establishing luminal cell polarity by orienting the microtubule network into an apical-basal direction which is important during milk secretion (Akhtar & Streuli, 2013; Lee & Streuli, 2014). TJs ensure close contact and communication between luminal epithelial cells and their disruption is one of the early signs of MEC apoptosis during involution (Hernandez *et al.*, 2011). Taken together, these results imply that mechanical stimulation induced molecular changes in FA and TJ structures previously associated with the onset of mammary involution *in vivo* as well as *in vitro*.

However, the results also show that changes in TJ protein expression following mechanical stimulation in the bovine mammary gland appear to occur asynchronously. Following different periods of static, biaxial cell stretch *in vitro*, changes in ZO-1 and occludin mRNA levels occur after 15 h of stretch, while changes in ZO-1 and occludin protein levels occurred following 1 and 5 h of *in vitro* cell stretch. Changes in claudin mRNA levels did not occur until 48 h of static *in vitro* cell stretch. I speculate that the increase in occludin and ZO-1 protein expression could be related to the repair of potentially compromised TJ following static stretch. Furthermore, occludin has been shown to undergo Tyr-phosphorylation following the disruption of TJ as a requirement for the hydrogen peroxide-induced disassembly of TJs (Rao, 2009). Moreover, experimentally-induced truncation of occludin results in MEC apoptosis both *in vivo* and *in vitro* (Beeman *et al.*, 2009), indicating a potential role as MEC survival 'signal'. Western blot analysis showed changing patterns of protein bands detected for occludin after different periods of *in vitro* cell stretch. The different sized occludin protein bands were assumed to be differences in occludin phosphorylation. The highest level of phosphorylation of occludin occurred following three hours of static stretch. Therefore, I conclude that static mechanical strain applied *in vitro* is sufficient to cause a disruption of TJ integrity which in turn could lead to exposure of luminal, pro-apoptotic factors onto the basolateral side of the MECs. Additionally, ZO-1 and occludin appear to be more responsive to mechanical strain than claudin 1. However, other members of the claudin family (Kobayashi & Kumura, 2011) or other scaffolding and signalling proteins linked to the TJ (Aijaz *et al.*, 2006) may be down-regulated earlier than the proteins studied here and could be subject of future studies. Furthermore, milk stasis induced local

synthesis of serotonin has been shown to play an important role in the disruption of TJ permeability and to act as a feedback inhibitor of lactation in the bovine mammary gland (Matsuda *et al.*, 2004; Hernandez *et al.*, 2011). Thus, future experiments could be conducted in order to establish a more precise timeline between the mechanically- and the serotonin-induced disruption of TJs. Recently, PC have emerged as a mechanosensor in numerous tissues (Praetorius & Spring, 2001; Masyuk *et al.*, 2008; Nguyen & Jacobs, 2013) and, in mice, they have been linked to play a role mammary in gland development (McDermott *et al.*, 2010). However, their role in mammary involution remains elusive and, to our knowledge, only two previous studies investigated and described PC in the bovine mammary gland during and after lactation (Nickerson, 1989; Millier *et al.*, 2013).

This PC experiment was designed to investigate whether any changes in PC distribution and morphology can be detected during the involution process and if PC could play a role in the overall remodelling process by investigating STAT6 expression levels. Therefore, the experimental groups chosen (lactating, 7-d NM and 28-d NM), were spread further apart to ensure detectable differences in involution progression between the three groups. The present study shows PC are present on luminal epithelial and myoepithelial cells in the bovine mammary gland. However, the overall number of ciliated MEC was low. Furthermore, the number of MEC ciliated during active lactation was lower than MEC ciliated following extended periods of non-milking. Similar observations have been reported previously (Nickerson, 1989; McDermott *et al.*, 2010; Millier *et al.*, 2013). In fact, in the mouse mammary gland, PC numbers decreased once mammary

gland tissue was fully developed (McDermott *et al.*, 2010). During active lactation, the epithelial cell layer is fully differentiated and highly metabolically active (Larson, 1985a) and it has been postulated that such a state of high secretion may not be compatible with maintaining a PC (Millier *et al.*, 2013). Moreover, during lactation the epithelial cell layer contains a tight network with cell-cell junctions, such as TJs, and cell-matrix junctions, including FAs, playing an important role during cell communication (Chen *et al.*, 2004). Thus, there may not be a need for every cell to be ciliated in order to achieve synchronised milk secretion. Extended periods of non-milking also resulted in an increase in STAT6 gene and protein expression (signalling pathway linked to PC). The STAT6 transcription factor has been shown to act as a regulator of murine mammary gland differentiation (Khaled *et al.*, 2007). Furthermore, in the absence of fluid flow (i.e. milk stasis), the proteolytically cleaved carboxy-terminal region of PC-1 translocates to the nucleus, where it associates with the transcription factor STAT6 and the co-activator p100 to stimulate gene expression (Low *et al.*, 2006; Berbari *et al.*, 2009). The STAT6 transcription factor activation stimulates IL-4 and IL-13 gene expression (Bromberg, 2000). Previously, IL-4 and IL-13 have been shown to act as macrophage chemoattractants (Hiester *et al.*, 1992) and to induce an alternative M2 form of macrophage activation (Gordon, 2003), which has been shown to be involved in wound healing and tissue remodelling/repair (O'Brien *et al.*, 2010). Up-regulation of IL-4 and IL-13 results in a feedback loop inducing further STAT6 gene expression as well as acting as chemoattractant for macrophages to promote tissue remodelling and to clear the gland from cell-debris and/or milk constituents (Hiester *et al.*, 1992; Gordon, 2003; O'Brien *et al.*, 2012). However, the STAT6 phosphorylation status was not determined.

Therefore, changes in the STAT6 activation status following extended periods of non-milking should be subject of future investigations.

Overall, it is tempting to say that following mechanical stimulation applied to bovine MEC, FA and TJ structures may be disrupted before changes related to PC signalling occur. However, the cell's adhesion structures are linked to each other via the cytoskeleton and additional proteins that possibly provide a direct link to the nucleus (Reichelt, 2007; Jones & Nauli, 2012). Therefore, these cellular structures are not stand-alone individual focal points for transmission of mechanical strain. It is more likely that they act in concert, stimulating a time- and tissue-specific cellular response. Furthermore, every point of contact between the MEC and its surrounding environment could act as a mechanosensor initiating various cellular responses following mechanical stimulation (Ingber, 2006). For example, cadherins have been shown to act as mechanosensors modifying cell functions in response to mechanical force (Leckband *et al.*, 2011) and could, thus, be subject of future research. Additionally, data on PC signalling was gathered following 7 and 28 days of non-milking. At that time a lot of events related to the bovine involution process will already have been initiated. Therefore, future experiments should investigate PC related changes immediately following weaning/drying off in order to directly compare changes related to mechanical force.

In summary, this study supports the hypothesis that local factors play an important role during mammary gland involution and that mechanical stimulation may play a part in the initiation of this process. Static, biaxial *in vitro* cell stretch

and acute physical distension *in vivo* resulted in changes in TJ proteins implying a potential disruption of cell-cell communication as well as communication with the cell's cytoskeleton. Furthermore, down-regulation of Akt and pAkt following 3 h of mechanical strain applied *in vitro* and decreased levels of pAkt following acute physical distension *in vivo* indicate disruption of β1-integrin-FAK survival signalling through the downstream PI3K-Akt pathway. Increased numbers of ciliated MEC following 28 days of non-milking indicate a dedifferentiation of MEC, while increased levels of STAT6 imply elevated IL-4 and IL-13 expression which in turn leads to macrophage accumulation and promotion of tissue remodelling of the mammary gland. The results presented in this thesis provide a foundation from which to examine the role of mechanotransduction in the bovine mammary gland in more detail.

Although previous research indicated that milk yield and persistency may be influenced by local rather than systemic factors (Stelwagen, 2001; Wall & McFadden, 2012), the actual triggers are not known. This study provides evidence that mechanotransduction may play a role in bovine mammary gland through co-ordination of PC, cell-cell and cell-ECM communication for regulation of cell signalling events that occur during early involution. Understanding how the MECs respond to changes in their micro-environment, such as physical stimuli, during the early stages of involution in the bovine mammary gland may be central for understanding the regulation of mammary gland remodelling, which is crucial for subsequent lactations and also for improving milk production traits such as persistency.

References

Chapter 6 References

Abou Alaiwi, Lo, & Nauli. (2009). Primary Cilia: Highly Sophisticated Biological Sensors. *Sensors, 9*(9), 7003-7020.

Accorsi, Pacioni, Pezzi, Forni, Flint, & Seren. (2002). Role of Prolactin, Growth Hormone and Insulin-Like Growth Factor 1 in Mammary Gland Involution in the Dairy Cow. *Journal of Dairy Science, 85*(3), 507-513. doi: 10.3168/jds.S0022-0302(02)74102-7.

Aijaz, Balda, & Matter. (2006). Tight junctions: molecular architecture and function. *Int Rev Cytol, 248*, 261-298. doi: 10.1016/S0074-7696(06)48005-0.

Akers. (2002). *Lactation and the Mammary Gland*: Wiley.

Akhtar, & Streuli. (2013). An integrin–ILK–microtubule network orients cell polarity and lumen formation in glandular epithelium. *Nat Cell Biol, 15*(1), 17-27. doi: 10.1038/ncb2646.

Alberts, Johnson, Lewis, Raff, Roberts, & Walter. (2002). *Molecular Biology of the Cell* (4th ed.): New York: Garland Science.

Alenghat, Nauli, Kolb, Zhou, & Ingber. (2004). Global cytoskeletal control of mechanotransduction in kidney epithelial cells. *Exp Cell Res, 301*(1), 23-30. doi: 10.1016/j.yexcr.2004.08.003.

Ali, Mungai, & Schumacker. (2006). Stretch-induced phosphorylation of focal adhesion kinase in endothelial cells: role of mitochondrial oxidants. *American Journal of Physiology - Lung Cellular and Molecular Physiology, 291*(1), L38-L45. doi: 10.1152/ajplung.00287.2004.

Amura, Brodsky, Gitomer, McFann, Lazennec, Nichols, . . . Brian Doctor. (2008). CXCR2 agonists in ADPKD liver cyst fluids promote cell proliferation. *American Journal of Physiology - Cell Physiology, 294*(3), C786-C796. doi: 10.1152/ajpcell.00457.2007.

Anderson. (1985). Mammary Gland. *Iowa State University Press, Ames (USA), Lactation*, p. 3-38.

Anderson, Rudolph, McManaman, & Neville. (2007). Key stages in mammary gland development. Secretory activation in the mammary gland: it's not just about milk protein synthesis! *Breast Cancer Res, 9*(1), 204. doi: 10.1186/bcr1653.

Anderson, & Van Itallie. (2009). Physiology and function of the tight junction. *Cold Spring Harb Perspect Biol, 1*(2), a002584. doi: 10.1101/cshperspect.a002584.

Atabai, Fernandez, Huang, Ueki, Kline, Li, . . . Sheppard. (2005). Mfge8 is critical for mammary gland remodeling during involution. *Mol Biol Cell, 16*(12), 5528-5537. doi: 10.1091/mbc.E05-02-0128.

Aumailley, & Gayraud. (1998). Structure and biological activity of the extracellular matrix. *Journal of Molecular Medicine, 76*(3), 253-265. doi: 10.1007/s001090050215.

Ayadi, Caja, Such, Rovai, & Albanell. (2004). Effect of different milking intervals on the composition of cisternal and alveolar milk in dairy cows. *J Dairy Res, 71*(3), 304-310. doi: 10.1017/S0022029904000329.

Badano, Mitsuma, Beales, & Katsanis. (2006). The ciliopathies: an emerging class of human genetic disorders. *Annu Rev Genomics Hum Genet, 7*, 125-148. doi: 10.1146/annurev.genom.7.080505.115610.

Badylak, Freytes, & Gilbert. (2009). Extracellular matrix as a biological scaffold material: Structure and function. *Acta Biomaterialia, 5*(1), 1-13. doi: 10.1016/j.actbio.2008.09.013.

Barnes. (1961). Ciliated secretory cells in the pars distalis of the mouse hypophysis. *Journal of Ultrastructure Research, 5*(5), 453-467. doi: 10.1016/S0022-5320(61)80019-1.

Baxter, Neoh, & Tevendale. (2007). The Beginning of the End: Death Signaling in Early Involution. *Journal of Mammary Gland Biology and Neoplasia, 12*(1), 3-13. doi: 10.1007/s10911-007-9033-9.

Beeman, Baumgartner, Webb, Schaack, & Neville. (2009). Disruption of occludin function in polarized epithelial cells activates the extrinsic pathway of apoptosis leading to cell extrusion without loss of transepithelial resistance. *BMC Cell Biology, 10*(1), 85. doi: 10.1186/1471-2121-10-85.

Berbari, O'Connor, Haycraft, & Yoder. (2009). The primary cilium as a complex signaling center. *Curr Biol, 19*(13), R526-535. doi: 10.1016/j.cub.2009.05.025.

Boutinaud, Galio, Lollivier, Finot, Wiart, Esquerré, & Devinoy. (2013). Unilateral once daily milking locally induces differential gene expression in both mammary tissue and milk epithelial cells revealing mammary remodeling. *Physiological Genomics, 45*(20), 973-985. doi: 10.1152/physiolgenomics.00059.2013.

Boutinaud, Guinard-Flamenta, & Jammes. (2004). The number and activity of mammary epithelial cells, determining factors for milk production. *Reprod Nutr Dev, 44*(5), 499-508.

Boutinaud, Lollivier, Finot, Bruckmaier, & Lacasse. (2012). Mammary cell activity and turnover in dairy cows treated with the prolactin-release inhibitor quinagolide and milked once daily. *J Dairy Sci, 95*(1), 177-187. doi: 10.3168/jds.2011-4461.

Broadhurst, & Wheeler. (2001). The p100 coactivator is present in the nuclei of mammary epithelial cells and its abudance is increased in response to prolactin in culture and in mammary tissue during lactation. *Journal of Endocrinology, 171*(2), 329-337. doi: 10.1677/joe.0.1710329.

Bromberg. (2000). Signal transducers and activators of transcription as regulators of growth, apoptosis and breast development. *Breast Cancer Res, 2*(2), 86-90.

Bruckmaier. (2005). Normal and disturbed milk ejection in dairy cows. *Domest Anim Endocrinol, 29*(2), 268-273. doi: 10.1016/j.domaniend.2005.02.023.

Bruckmaier, & Blum. (1998). Oxytocin Release and Milk Removal in Ruminants. *Journal of Dairy Science, 81*(4), 939-949. doi: 10.3168/jds.S0022-0302(98)75654-1.

Bukoreshtliev, Haase, & Pelling. (2013). Mechanical cues in cellular signalling and communication. *Cell Tissue Res, 352*(1), 77-94. doi: 10.1007/s00441-012-1531-4.

Capuco, & Akers. (1999). Mammary involution in dairy animals. *J Mammary Gland Biol Neoplasia, 4*(2), 137-144.

Capuco, Ellis, Hale, Long, Erdman, Zhao, & Paape. (2003). Lactation persistency: Insights from mammary cell proliferation studies. *Journal of Animal Science, 81*(suppl 3), 18-31.

Capuco, Li, Long, Ren, Hruska, Schorr, & Furth. (2002). Concurrent pregnancy retards mammary involution: effects on apoptosis and proliferation of the mammary epithelium after forced weaning of mice. *Biol Reprod, 66*(5), 1471-1476.

Capuco, Wood, Baldwin, McLeod, & Paape. (2001). Mammary Cell Number, Proliferation, and Apoptosis During a Bovine Lactation: Relation to Milk Production and Effect of bST. *J Dairy Sci, 84*(10), 2177-2187. doi: 10.3168/jds.S0022-0302(01)74664-4.

Carruthers, Davis, Bryant, Henderson, Morris, & Copeman. (1993). Response of Jersey and Friesian cows to once a day milking and prediction of response based on udder characteristics and milk composition. *Journal of Dairy Research, 60*(01), 1-11. doi: doi:10.1017/S0022029900027291.

Caruolo. (1980). Scanning electron microscope visualization of the mammary gland secretory unit and of myoepithelial cells. *J Dairy Sci, 63*(12), 1987-1998. doi: 10.3168/jds.S0022-0302(80)83174-2.

Cattaruzza, Dimigen, Ehrenreich, & Hecker. (2000). Stretch-induced endothelin B receptor-mediated apoptosis in vascular smooth muscle cells. *The FASEB Journal, 14*(7), 991-998.

Cavanaugh, Oswari, & Margulies. (2001). Role of stretch on tight junction structure in alveolar epithelial cells. *Am J Respir Cell Mol Biol, 25*(5), 584-591. doi: 10.1165/ajrcmb.25.5.4486.

Chaturvedi, Marsh, & Basson. (2007). Src and focal adhesion kinase mediate mechanical strain-induced proliferation and ERK1/2 phosphorylation in human H441 pulmonary epithelial cells. *Am J Physiol Cell Physiol, 292*(5), C1701-1713. doi: 10.1152/ajpcell.00529.2006.

Chaturvedi, Marsh, Shang, Zheng, & Basson. (2007). Repetitive Deformation Activates Focal Adhesion Kinase and ERK Mitogenic Signals in Human Caco-2 Intestinal Epithelial Cells through Src and Rac1. *Journal of Biological Chemistry, 282*(1), 14-28. doi: 10.1074/jbc.M605817200.

Chen, Boxer, Stairs, Portocarrero, Horton, Alvarez, . . . Chodosh. (2010). Akt is required for Stat5 activation and mammary differentiation. *Breast Cancer Research, 12*(5). doi: 10.1186/bcr2640.

Chen, Tan, & Tien. (2004). Mechanostransduction at Cell-matrix and Cell-cell Contacts. *Annual Review of Biomedical Engineering, 6*(1), 275-302. doi: doi:10.1146/annurev.bioeng.6.040803.140040.

Christensen, Clement, Satir, & Pedersen. (2012). Primary cilia and coordination of receptor tyrosine kinase (RTK) signalling. *Journal of Pathology, 226*(2), 172-184. doi: 10.1002/path.3004.

Clarkson, Wayland, Lee, Freeman, & Watson. (2004). Gene expression profiling of mammary gland development reveals putative roles for death receptors and immune mediators in post-lactational regression. *Breast Cancer Res, 6*(2), R92-109. doi: 10.1186/bcr754.

Close, Howlett, Roskelley, Desprez, Bailey, Rowning, . . . Yaswen. (1997). Lactoferrin expression in mammary epithelial cells is mediated by changes in cell shape and actin cytoskeleton. *Journal of Cell Science, 110*(22), 2861-2871.

Colitti. (2012). BCL-2 Family of Proteins and Mammary Cellular Fate. *Journal of Veterinary Medicine Series C: Anatomia Histologia Embryologia*. doi: 10.1111/j.1439-0264.2012.01134.x.

Costa. (2003). *The need for stimulation in various bovine breeds and other species*. Paper presented at the 100th Centenary International Dairy Federation, Bruges, Belgium.

Craig, Zhang, & Basson. (2007). Cytoskeletal signaling by way of [alpha]-actinin-1 mediates ERK1/2 activation by repetitive deformation in human Caco2 intestinal epithelial cells. *The American Journal of Surgery, 194*(5), 618-622. doi: 10.1016/j.amjsurg.2007.08.001.

Creamer, Sakamoto, Schmidt, Triplett, Moriggl, & Wagner. (2010). Stat5 promotes survival of mammary epithelial cells through transcriptional activation of a distinct promoter in Akt1. *Mol Cell Biol, 30*(12), 2957-2970. doi: 10.1128/MCB.00851-09.

Crosby, Luellen, Zhang, Tague, Sinclair, & Waters. (2011). Balance of life and death in alveolar epithelial type II cells: Proliferation, apoptosis, and the effects of cyclic stretch on wound healing. *American Journal of Physiology - Lung Cellular and Molecular Physiology, 301*(4), L536-L546. doi: 10.1152/ajplung.00371.2010.

Davis, Farr, & Stelwagen. (1999). Regulation of yield loss and milk composition during once-daily milking: a review. *Livestock Production Science, 59*(1), 77-94. doi: 10.1016/S0301-6226(98)00204-8.

DeMaio, Chang, Gardner, Tarbell, & Antonetti. (2001). Shear stress regulates occludin content and phosphorylation. *Am J Physiol Heart Circ Physiol, 281*(1), H105-113.

DiPaolo, Lenormand, Fredberg, & Margulies. (2010). Stretch magnitude and frequency-dependent actin cytoskeleton remodeling in alveolar epithelia. *Am J Physiol Cell Physiol, 299*(2), C345-353. doi: 10.1152/ajpcell.00379.2009.

DuFort, Paszek, & Weaver. (2011). Balancing forces: architectural control of mechanotransduction. *Nat Rev Mol Cell Biol, 12*(5), 308-319. doi: 10.1038/nrm3112.

Ellerman, & Bisgaard. (1997). Longitudinal study of lung function in a cohort of primary ciliary dyskinesia. *European Respiratory Journal, 10*(10), 2376-2379.

Eyckmans, Boudou, Yu, & Chen. (2011). A hitchhiker's guide to mechanobiology. *Dev Cell, 21*(1), 35-47. doi: 10.1016/j.devcel.2011.06.015.

Fanning, Jameson, Jesaitis, & Anderson. (1998). The Tight Junction Protein ZO-1 Establishes a Link between the Transmembrane Protein Occludin and the Actin Cytoskeleton. *J Biol Chem, 273*(45), 29745-29753. doi: 10.1074/jbc.273.45.29745.

Feng, Marti, Jehn, Altermatt, Chicaiza, & Jaggi. (1995). Glucocorticoid and progesterone inhibit involution and programmed cell death in the mouse mammary gland. *J Cell Biol, 131*(4), 1095-1103.

Fischer, Jacobson, Rose, & Zeller. (2008). Hematoxylin and eosin staining of tissue and cell sections. *CSH Protoc, 2008*, pdb prot4986. doi: 10.1101/pdb.prot4986.

Flint, Boutinaud, Tonner, Wilde, Hurley, Accorsi, . . . Allan. (2005). Insulin-like growth factor binding proteins initiate cell death and extracellular matrix

remodeling in the mammary gland. *Domest Anim Endocrinol, 29*(2), 274-282. doi: 10.1016/j.domaniend.2005.02.021.

Frandson. (1992). *Anatomy and Physiology of Farm Animals* (Vol. 5 th edition).

Fujita, Hida, Kanemoto, Fukuda, Nagata, & Awazu. (2010). Cyclic stretch induces proliferation and TGF-β1-mediated apoptosis via p38 and ERK in ureteric bud cells. *American Journal of Physiology - Renal Physiology, 299*(3), F648-F655. doi: 10.1152/ajprenal.00402.2009.

Furuse. (2010). Molecular basis of the core structure of tight junctions. *Cold Spring Harb Perspect Biol, 2*(1), a002907. doi: 10.1101/cshperspect.a002907.

Garcia, Prota, Morales, Romero, Zin, & Rocco. (2006). Understanding the mechanisms of lung mechanical stress. *Brazilian Journal of Medical and Biological Research, 39*, 697-706.

Gayer, Chaturvedi, Wang, Alston, Flanigan, & Basson. (2009). Delineating the signals by which repetitive deformation stimulates intestinal epithelial migration across fibronectin. *American Journal of Physiology - Gastrointestinal and Liver Physiology, 296*(4), G876-G885. doi: 10.1152/ajpgi.90648.2008.

Gayer, Chaturvedi, Wang, Craig, Flanigan, & Basson. (2009). Strain-induced Proliferation Requires the Phosphatidylinositol 3-Kinase/AKT/Glycogen Synthase Kinase Pathway. *Journal of Biological Chemistry, 284*(4), 2001-2011. doi: 10.1074/jbc.M804576200.

Gilula, & Satir. (1972). The ciliary necklace. A ciliary membrane specialization. *J Cell Biol, 53*(2), 494-509.

Gjorevski, & Nelson. (2011). Integrated morphodynamic signalling of the mammary gland. *Nat Rev Mol Cell Biol, 12*(9), 581-593.

Glukhova, & Streuli. (2013). How integrins control breast biology. *Current Opinion in Cell Biology*(0). doi: 10.1016/j.ceb.2013.06.010.

Gonzalez, Aguilera, Urzua, Quest, Molina, Alliende, . . . Gonzalez. (2011). Mechanotransduction and epigenetic control in autoimmune diseases. *Autoimmun Rev, 10*(3), 175-179. doi: 10.1016/j.autrev.2010.09.022.

Gordon. (2003). Alternative activation of macrophages. *Nat Rev Immunol, 3*(1), 23-35. doi: 10.1038/nri978.

Grant, Heathcote, & Orkin. (1981). Current concepts of basement-membrane structure and function. Review. *Bioscience Reports, 1*(11), 819-842.

Green, & Streuli. (2004). Apoptosis regulation in the mammary gland. *Cellular and Molecular Life Sciences, 61*(15), 1867-1883. doi: 10.1007/s00018-004-3366-y.

Hammerschmidt, Kuhn, Gessner, Seyfarth, & Wirtz. (2007). Stretch-Induced Alveolar Type II Cell Apoptosis: Role of Endogenous Bradykinin and PI3K-Akt Signaling. *Am. J. Respir. Cell Mol. Biol., 37*(6), 699-705. doi: 10.1165/rcmb.2006-0429OC.

Hammerschmidt, Kuhn, Sack, Schlenska, Gessner, Gillissen, & Wirtz. (2005). Mechanical stretch alters alveolar type II cell mediator release toward a proinflammatory pattern. *Am J Respir Cell Mol Biol, 33*(2), 203 - 210.

Han, Li, Sumpio, & Basson. (1998). Strain induces Caco-2 intestinal epithelial proliferation and differentiation via PKC and tyrosine kinase signals. *American Journal of Physiology - Gastrointestinal and Liver Physiology, 275*(3), G534-G541.

Han, Sumpio, & Basson. (1998). Mechanical Strain Rapidly Redistributes Tyrosine Phosphorylated Proteins in Human Intestinal Caco-2 Cells. *Biochemical and Biophysical Research Communications, 250*(3), 668-673. doi: 10.1006/bbrc.1998.9372.

Haricharan, & Li. (2013). STAT signaling in mammary gland differentiation, cell survival and tumorigenesis. *Mol Cell Endocrinol*. doi: 10.1016/j.mce.2013.03.014.

Henderson, Blatchford, & Peaker. (1985). The effects of long-term thrice-daily milking on milk secretion in the goat: Evidence for mammary growth. *Quarterly Journal of Experimental Physiology, 70*(4), 557-565.

Hennighausen, & Robinson. (2001). Signaling Pathways in Mammary Gland Development. *Developmental cell, 1*(4), 467-475.

Hennighausen, & Robinson. (2005). Information networks in the mammary gland. *Nat Rev Mol Cell Biol, 6*(9), 715-725.

Hernandez, Collier, Vomachka, Collier, & Horseman. (2011). Suppression of lactation and acceleration of involution in the bovine mammary gland by a selective serotonin reuptake inhibitor. *J Endocrinol, 209*(1), 45-54. doi: 10.1530/joe-10-0452.

Hernandez, Limesand, Collier, Horseman, & Collier. (2009). The bovine mammary gland expresses multiple functional isoforms of serotonin receptors. *J Endocrinol, 203*(1), 123-131. doi: 10.1677/JOE-09-0187

Hickson, Lopez-Villalobos, Dalley, Clark, & Holmes. (2006). Yields and Persistency of Lactation in Friesian and Jersey Cows Milked Once Daily. *Journal of Dairy Science, 89*(6), 2017-2024. doi: 10.3168/jds.S0022-0302(06)72269-X.

Hiester, Metcalf, & Campbell. (1992). Interleukin-4 is chemotactic for mouse macrophages. *Cellular Immunology, 139*(1), 72-80. doi: 10.1016/0008-8749(92)90100-4.

Hillerton, Knight, Turvey, Wheatley, & Wilde. (1990). Milk yield and mammary function in dairy cows milked four times daily. *J Dairy Res, 57*(3), 285-294.

Hocking, Sottile, & McKeown-Longo. (1994). Fibronectin's III-1 module contains a conformation-dependent binding site for the amino-terminal region of fibronectin. *J Biol Chem, 269*(29), 19183-19187.

Hoey, Downs, & Jacobs. (2012). The mechanics of the primary cilium: An intricate structure with complex function. *Journal of Biomechanics, 45*(1), 17-26. doi: 10.1016/j.jbiomech.2011.08.008.

Holst, Hurley, & Nelson. (1987). Involution of the Bovine Mammary Gland: Histological and Ultrastructural Changes. *J Dairy Sci, 70*(5), 935-944. doi: 10.3168/jds.S0022-0302(87)80097-8.

Huang, & Ingber. (1999). The structural and mechanical complexity of cell-growth control. *Nat Cell Biol, 1*(5), E131-E138.

Huang, & Ingber. (2000). Shape-dependent control of cell growth, differentiation, and apoptosis: switching between attractors in cell regulatory networks. *Exp Cell Res, 261*(1), 91-103. doi: 10.1006/excr.2000.5044.

Huang, Kamm, & Lee. (2004). Cell mechanics and mechanotransduction: pathways, probes, and physiology. *American Journal of Physiology - Cell Physiology, 287*(1), C1-C11. doi: 10.1152/ajpcell.00559.2003.

Hughes, & Watson. (2012). The spectrum of STAT functions in mammary gland development. *JAK-STAT, 1*(3), 151-158.

Hung, & Williams. (1994). A method for inducing equi-biaxial and uniform strains in elastomeric membranes used as cell substrates. *J Biomech, 27*(2), 227 - 232.

Hurley. (1989). Mammary Gland Function During Involution. *Journal of Dairy Science, 72*(6), 1637-1646. doi: DOI: 10.3168/jds.S0022-0302(89)79276-6.

Hurley, & Loor. (2011). MAMMARY GLAND | Growth, Development and Involution. In W. F. John (Ed.), *Encyclopedia of Dairy Sciences* (pp. 338-345). San Diego: Academic Press.

Ingber. (1993). Cellular tensegrity: defining new rules of biological design that govern the cytoskeleton. *Journal of Cell Science, 104*(3), 613-627.

Ingber. (1997). Tensegrity: the architectural basis of cellular mechanotransduction. *Annu Rev Physiol, 59*, 575-599. doi: 10.1146/annurev.physiol.59.1.575.

Ingber. (2006). Cellular mechanotransduction: putting all the pieces together again. *Faseb J, 20*(7), 811-827. doi: 10.1096/fj.05-5424rev.

Itoh, & Bissell. (2003). The organization of tight junctions in epithelia: implications for mammary gland biology and breast tumorigenesis. *J Mammary Gland Biol Neoplasia, 8*(4), 449-462. doi: 10.1023/B:JOMG.0000017431.45314.07.

Jaalouk, & Lammerding. (2009). Mechanotransduction gone awry. *Nat Rev Mol Cell Biol, 10*(1), 63-73.

Janmey, & McCulloch. (2007). Cell mechanics: integrating cell responses to mechanical stimuli. *Annu Rev Biomed Eng, 9*, 1-34. doi: 10.1146/annurev.bioeng.9.060906.151927.

Jones, & Nauli. (2012). Mechanosensory calcium signaling. *Adv Exp Med Biol, 740*, 1001-1015. doi: 10.1007/978-94-007-2888-2_46.

Jurgensmeier, Xie, Deveraux, Ellerby, Bredesen, & Reed. (1998). Bax directly induces release of cytochrome c from isolated mitochondria. *Proc Natl Acad Sci U S A, 95*(9), 4997-5002.

Kass, Erler, Dembo, & Weaver. (2007). Mammary epithelial cell: Influence of extracellular matrix composition and organization during development and tumorigenesis. *The International Journal of Biochemistry & Cell Biology, 39*(11), 1987-1994. doi: 10.1016/j.biocel.2007.06.025.

Khaled, Read, Nicholson, Baxter, Brennan, Came, . . . Watson. (2007). The IL-4/IL-13/Stat6 signalling pathway promotes luminal mammary epithelial cell development. *Development, 134*(15), 2739-2750. doi: 10.1242/dev.003194.

Knight, & Peaker. (1982). Development of the mammary gland. *Journal of Reproduction and Fertility, 65*(2), 521-536. doi: 10.1530/jrf.0.0650521.

Kobayashi, & Kumura. (2011). Distinct behavior of claudin-3 and -4 around lactation period in mammary alveolus in mice. *Histochemistry and Cell Biology, 136*(5), 587-594. doi: 10.1007/s00418-011-0863-6.

Koshihara, Matsuzaka, Sato, & Inoue. (2010). Effect of Stretching Force on the Cells of Epithelial Rests of Malassez In Vitro. *International Journal of Dentistry, 2010*. doi: 10.1155/2010/458408.

Kritikou, Sharkey, Abell, Came, Anderson, Clarkson, & Watson. (2003). A dual, non-redundant, role for LIF as a regulator of development and STAT3-mediated cell death in mammary gland. *Development, 130*(15), 3459 - 3468.

Kumar, Vadlamudi, & Adam. (2000). Apoptosis in mammary gland and cancer. *Endocrine-Related Cancer, 7*(4), 257-269. doi: 10.1677/erc.0.0070257.

Laemmli. (1970). Cleavage of Structural Proteins during the Assembly of the Head of Bacteriophage T4. *Nature, 227*(5259), 680-685.

Larson. (1985a). Biosynthesis and cellular secretion of milk. *Iowa State University Press, Lactation*, 129–163.

Larson. (1985b). *Lactation*: Iowa State University Press, Ames (USA).

Le Beyec, Xu, Lee, Nelson, Rizki, Alcaraz, & Bissell. (2007). Cell shape regulates global histone acetylation in human mammary epithelial cells. *Experimental Cell Research, 313*(14), 3066-3075. doi: 10.1016/j.yexcr.2007.04.022.

LeBleu, MacDonald, & Kalluri. (2007). Structure and Function of Basement Membranes. *Experimental Biology and Medicine, 232*(9), 1121-1129. doi: 10.3181/0703-mr-72.

Leckband, le Duc, Wang, & de Rooij. (2011). Mechanotransduction at cadherin-mediated adhesions. *Curr Opin Cell Biol, 23*(5), 523-530. doi: 10.1016/j.ceb.2011.08.003.

Lee, Delhaas, Waldman, MacKenna, Villarreal, & McCulloch. (1996). An equibiaxial strain system for cultured cells. *Am J Physiol, 271*(4 Pt 1), C1400 - 1408.

Lee, & Streuli. (2014). Integrins and epithelial cell polarity. *J Cell Sci*. doi: 10.1242/jcs.146142.

Li, Duzgun, Sumpio, & Basson. (2001). Integrin and FAK-mediated MAPK activation is required for cyclic strain mitogenic effects in Caco-2 cells. *American Journal of Physiology - Gastrointestinal and Liver Physiology, 280*(1), G75-G87.

Li, Liu, Robinson, Bar-Peled, Wagner, Young, . . . Furth. (1997). Mammary-derived signals activate programmed cell death during the first stage of mammary gland involution. *Proc Natl Acad Sci USA, 94*(7), 3425 - 3430.

Li, Zhang, Naylor, Schatzmann, Maurer, Wintermantel, . . . Hynes. (2005). β1 integrins regulate mammary gland proliferation and maintain the integrity of mammary alveoli. *24*(11), 1942-1953. doi: 10.1038/sj.emboj.7600674.

Linzell, & Peaker. (1971). Mechanism of milk secretion. *Physiol Rev, 51*(3), 564-597.

Liu, Zhao, & Liu. (2013). Effects of Glucose Availability on Expression of the Key Genes Involved in Synthesis of Milk Fat, Lactose and Glucose Metabolism in Bovine Mammary Epithelial Cells. *PLoS ONE, 8*(6), e66092. doi: 10.1371/journal.pone.0066092.

Lollivier, Guinard-Flament, Ollivier-Bousquet, & Marnet. (2002). Oxytocin and milk removal: two important sources of variation in milk production and milk quality during and between milkings. *Reprod Nutr Dev, 42*(2), 173-186.

Low, Vasanth, Larson, Mukherjee, Sharma, Kinter, . . . Weimbs. (2006). Polycystin-1, STAT6, and P100 function in a pathway that transduces ciliary mechanosensation and is activated in polycystic kidney disease. *Dev Cell, 10*(1), 57-69. doi: 10.1016/j.devcel.2005.12.005.

Lund, Romer, Thomasset, Solberg, Pyke, Bissell, . . . Werb. (1996). Two distinct phases of apoptosis in mammary gland involution: proteinase-independent and -dependent pathways. *Development, 122*(1), 181-193.

Maeda, Johnson, & Wheelock. (2005). Cadherin switching: essential for behavioral but not morphological changes during an epithelium-to-

mesenchyme transition. *Journal of Cell Science, 118*(5), 873-887. doi: 10.1242/jcs.01634.

Mallah. (2013). *Potential role for cyclo-glycyl-proline during mammary involution through insulin-like growth factor-I regulation.* (Thesis in fulfilment of the requirements for enrolment in Doctor of Philosophy), University of Auckland.

Mammoto, Mammoto, & Ingber. (2012). Mechanosensitive mechanisms in transcriptional regulation. *J Cell Sci, 125*(Pt 13), 3061-3073. doi: 10.1242/jcs.093005.

Maniotis, Chen, & Ingber. (1997). Demonstration of mechanical connections between integrins, cytoskeletal filaments, and nucleoplasm that stabilize nuclear structure. *Proc Natl Acad Sci U S A, 94*(3), 849-854.

Marti, Feng, Altermatt, & Jaggi. (1997). Milk accumulation triggers apoptosis of mammary epithelial cells. *Eur J Cell Biol, 73*(2), 158 - 165.

Marti, Jehn, Costello, Keon, Ke, Martin, & Jaggi. (1994). Protein kinase A and AP-1 (c-Fos/JunD) are induced during apoptosis of mouse mammary epithelial cells. *Oncogene, 9*(4), 1213-1223.

Marti, Lazar, Ritter, & Jaggi. (1999). Transcription factor activities and gene expression during mouse mammary gland involution. *J Mammary Gland Biol Neoplasia, 4*(2), 145-152.

Marti, Ritter, Jager, Lazar, Baltzer, Schenkel, . . . Jaggi. (2001). Mouse mammary gland involution is associated with cytochrome c release and caspase activation. *Mech Dev, 104*(1-2), 89-98. doi: S0925477301003811 [pii].

Masyuk, Masyuk, & LaRusso. (2008). Cholangiocyte primary cilia in liver health and disease. *Developmental Dynamics, 237*(8), 2007-2012. doi: 10.1002/dvdy.21530.

Matsuda, Imaoka, Vomachka, Gudelsky, Hou, Mistry, . . . Horseman. (2004). Serotonin regulates mammary gland development via an autocrine-paracrine loop. *Dev Cell, 6*(2), 193-203.

McDermott, Liu, Tlsty, & Pazour. (2010). Primary Cilia Regulate Branching Morphogenesis during Mammary Gland Development. *Current Biology, 20*(8), 731-737. doi: 10.1016/j.cub.2010.02.048.

McGee, Lanigan, Gilligan, & Groner. (2006). Mammary gland biology and breast cancer. Conference on Common Molecular Mechanisms of Mammary Gland Development and Breast Cancer Progression. *EMBO Rep, 7*(11), 1084-1088. doi: 10.1038/sj.embor.7400839.

McGlashan, Jensen, & Poole. (2006). Localization of extracellular matrix receptors on the chondrocyte primary cilium. *J Histochem Cytochem, 54*(9), 1005-1014. doi: 10.1369/jhc.5A6866.2006.

McMahon, Farr, Singh, Wheeler, & Davis. (2004). Decreased expression of β1-integrin and focal adhesion kinase in epithelial cells may initiate involution of mammary glands. *Journal of Cellular Physiology, 200*(2), 318-325. doi: 10.1002/jcp.20011.

McManaman, & Neville. (2003). Mammary physiology and milk secretion. *Advanced Drug Delivery Reviews, 55*(5), 629-641. doi: 10.1016/s0169-409x(03)00033-4.

Mepham. (1987). *Physiology of Lactation*.

Michaelson, & Huang. (2012). Cell-cell junctional proteins in cardiovascular mechanotransduction. *Ann Biomed Eng, 40*(3), 568-577. doi: 10.1007/s10439-011-0439-6.

Mielke. (1986). *Physiology of lactation*. Stuttgart: Gustav-Fischer-Verlag.

Millier. (2013). *Primary Cilia in the Bovine Mammary Gland: Characterising Ciliary Distribution and Morphology During Lactation and Involution* (Master of Science Master of Science), University of Otago, Dunedin.

Millier, Singh, & Poole. (2013). Characterization of primary cilia distribution and morphology during lactation, stasis, and involution in the bovine mammary gland. *Anat Rec (Hoboken), 296*(12), 1943-1953. doi: 10.1002/ar.22819.

Mitic, & Anderson. (1998). Molecular architecture of tight junctions. *Annu Rev Physiol, 60*, 121-142. doi: 10.1146/annurev.physiol.60.1.121.

Mohan, Sooranna, Lindstrom, Johnson, & Bennett. (2007). The Effect of Mechanical Stretch on Cyclooxygenase Type 2 Expression and Activator Protein-1 and Nuclear Factor-κB Activity in Human Amnion Cells. *Endocrinology, 148*(4), 1850-1857. doi: 10.1210/en.2006-1289.

Molenaar, Davis, & Wilkins. (1992). Expression of alpha-lactalbumin, alpha-S1-casein, and lactoferrin genes is heterogeneous in sheep and cattle mammary tissue. *Journal of Histochemistry & Cytochemistry, 40*(5), 611-618. doi: 10.1177/40.5.1374090.

Mott, & Werb. (2004). Regulation of matrix biology by matrix metalloproteinases. *Current Opinion in Cell Biology, 16*(5), 558-564. doi: 10.1016/j.ceb.2004.07.010.

Na, Collin, Chowdhury, Tay, Ouyang, Wang, & Wang. (2008). Rapid signal transduction in living cells is a unique feature of mechanotransduction. *Proc Natl Acad Sci U S A, 105*(18), 6626-6631. doi: 10.1073/pnas.0711704105.

Nauli, Alenghat, Luo, Williams, Vassilev, Li, Zhou. (2003). Polycystins 1 and 2 mediate mechanosensation in the primary cilium of kidney cells. *Nat Genet, 33*(2), 129-137. doi: 10.1038/ng1076.

Naylor, Li, Cheung, Lowe, Lambert, Marlow, Streuli. (2005). Ablation of β1 integrin in mammary epithelium reveals a key role for integrin in glandular morphogenesis and differentiation. *J Cell Biol, 171*(4), 717-728. doi: 10.1083/jcb.200503144

Negrão, & Marnet. (2006). Milk yield, residual milk, oxytocin and cortisol release during machine milking in Gir, Gir × Holstein and Holstein cows. *Reprod. Nutr. Dev., 46*(1), 77-85.

Nelson, & Bissell. (2006). Of Extracellular Matrix, Scaffolds, and Signaling: Tissue Architecture Regulates Development, Homeostasis, and Cancer. *Annual Review of Cell and Developmental Biology, 22*(1), 287-309. doi: doi:10.1146/annurev.cellbio.22.010305.104315.

Nelson, & Gleghorn. (2011). Sculpting Organs: Mechanical Regulation of Tissue Development. *Annu Rev Biomed Eng*. doi: 10.1146/annurev-bioeng-071811-150043.

Neville. (2009). Introduction: tight junctions and secretory activation in the mammary gland. *J Mammary Gland Biol Neoplasia, 14*(3), 269-270. doi: 10.1007/s10911-009-9150-8.

Neville, & Daniel. (1987). *The Mammary gland: development, regulation, and function*: Plenum Press.

Newby, Streets, Zhao, Harris, Ward, & Ong. (2002). Identification, characterization, and localization of a novel kidney polycystin-1-polycystin-2 complex. *J Biol Chem, 277*(23), 20763-20773. doi: 10.1074/jbc.M107788200.

Nguyen, & Jacobs. (2013). Emerging role of primary cilia as mechanosensors in osteocytes. *Bone, 54*(2), 196-204. doi: 10.1016/j.bone.2012.11.016

Nickerson. (1989). Cilia on bovine mammary epithelium: ultrastructural observations. *Cell Tissue Res, 255*(3), 675-677.

Niessen. (2007). Tight junctions/adherens junctions: basic structure and function. *J Invest Dermatol, 127*(11), 2525-2532. doi: 10.1038/sj.jid.5700865.

Novaro, Roskelley, & Bissell. (2003). Collagen-IV and laminin-1 regulate estrogen receptor α expression and function in mouse mammary epithelial cells. *Journal of Cell Science, 116*(14), 2975-2986. doi: 10.1242/jcs.00523.

O'Brien, Lyons, Monks, Lucia, Wilson, Hines, . . . Schedin. (2010). Alternatively activated macrophages and collagen remodeling characterize the postpartum involuting mammary gland across species. *Am J Pathol, 176*(3), 1241-1255. doi: 10.2353/ajpath.2010.090735.

O'Brien, Martinson, Durand-Rougely, & Schedin. (2012). Macrophages are crucial for epithelial cell death and adipocyte repopulation during mammary gland involution. *Development, 139*(2), 269-275. doi: 10.1242/dev.071696.

Olsan, Mukherjee, Wulkersdorfer, Shillingford, Giovannone, Todorov, . . . Weimbs. (2011). Signal transducer and activator of transcription-6 (STAT6) inhibition suppresses renal cyst growth in polycystic kidney disease. *Proceedings of the National Academy of Sciences, 108*(44), 18067-18072. doi: 10.1073/pnas.1111966108.

Orr, Helmke, Blackman, & Schwartz. (2006). Mechanisms of Mechanotransduction. *Developmental cell, 10*(1), 11-20. doi: 10.1016/j.devcel.2005.12.006.

Osada, Iijima, Tanaka, Hirose, Yamamoto, & Watanabe. (1999). Effect of temperature and mechanical strain on gastric epithelial cell line GSM06 wound restoration in vitro. *Journal of Gastroenterology and Hepatology, 14*(5), 489-494. doi: 10.1046/j.1440-1746.1999.01890.x.

Paszek, Zahir, Johnson, Lakins, Rozenberg, Gefen, . . . Boettiger. (2005). Tensional homeostasis and the malignant phenotype. *Cancer Cell, 8*(3), 241 - 254.

Peaker. (1980). The effect of raised intramammary pressure on mammary function in the goat in relation to the cessation of lactation. *J Physiol, 301*, 415-428.

Permyakov, & Berliner. (2000). alpha-Lactalbumin: structure and function. *FEBS Lett, 473*(3), 269-274. doi: S0014-5793(00)01546-5 [pii].

Phyn, Dobson, Davis, Stelwagen, & Singh. (2007). *Induced physical distension of rat mammary glands accelerates the onset of apoptosis and involution compared with milk accumulation alone : Brief Communication* (Vol. 67): New Zealand Society of Animal Production.

Plath, Einspanier, Peters, Sinowatz, & Schams. (1997). Expression of transforming growth factors alpha and beta-1 messenger RNA in the bovine mammary gland during different stages of development and lactation. *J Endocrinol, 155*(3), 501-511.

Poelmann, Van der Heiden, Gittenberger-de Groot, & Hierck. (2008). Deciphering the Endothelial Shear Stress Sensor. *Circulation, 117*(9), 1124-1126. doi: 10.1161/circulationaha.107.753889.

Poole, Flint, & Beaumont. (1985). Analysis of the morphology and function of primary cilia in connective tissues: a cellular cybernetic probe? *Cell Motil, 5*(3), 175-193.

Poole, Jensen, Snyder, Gray, Hermanutz, & Wheatley. (1997). Confocal analysis of primary cilia structure and colocalization with the Golgi apparatus in chondrocytes and aortic smooth muscle cells. *Cell Biol Int, 21*(8), 483-494. doi: 10.1006/cbir.1997.0177.

Poole, Zhang, & Ross. (2001). The differential distribution of acetylated and detyrosinated alpha-tubulin in the microtubular cytoskeleton and primary cilia of hyaline cartilage chondrocytes. *J Anat, 199*(Pt 4), 393-405.

Praetorius, & Spring. (2001). Bending the MDCK cell primary cilium increases intracellular calcium. *J Membr Biol, 184*(1), 71-79.

Prince, Klinowska, Marshman, Lowe, Mayer, Miner, . . . Streuli. (2002). Cell-matrix interactions during development and apoptosis of the mouse mammary gland in vivo. *Dev Dyn, 223*(4), 497-516. doi: 10.1002/dvdy.10070.

Provenzano, Inman, Eliceiri, & Keely. (2009). Matrix density-induced mechanoregulation of breast cell phenotype, signaling and gene expression through a FAK-ERK linkage. *Oncogene, 28*(49), 4326-4343. doi: 10.1038/onc.2009.299.

Pullan, Wilson, Metcalfe, Edwards, Goberdhan, Tilly, . . . Streuli. (1996). Requirement of basement membrane for the suppression of programmed cell death in mammary epithelium. *J Cell Sci, 109 (Pt 3)*, 631-642.

Quaglino, Salierno, Pellegrotti, Rubinstein, & Kordon. (2009). Mechanical strain induces involution-associated events in mammary epithelial cells. *BMC Cell Biology, 10*(1), 55.

Quaglino, Schere-Levy, Romorini, Meiss, & Kordon. (2007). Mouse mammary tumors display Stat3 activation dependent on leukemia inhibitory factor signaling. *Breast Cancer Res, 9*(5), R69.

Quarrie, Addey, & Wilde. (1994). Local regulation of mammary apoptosis in the lactating goat. *Biochem Soc Trans, 22*(2), 178S.

Quarrie, Addey, & Wilde. (1996). Programmed cell death during mammary tissue involution induced by weaning, litter removal, and milk stasis. *J Cell Physiol, 168*(3), 559-569. doi: 10.1002/(SICI)1097-4652(199609)168:3<559::AID-JCP8>3.0.CO;2-O.

Rana, Zobel, Saygili, Brixius, Gramley, Schimpf, . . . Schwinger. (2008). A simple device to apply equibiaxial strain to cells cultured on flexible membranes. *Am J Physiol Heart Circ Physiol, 294*(1), H532 - 540.

Rao. (2009). Occludin Phosphorylation in Regulation of Epithelial Tight Junctions. *Annals of the New York Academy of Sciences, 1165*(1), 62-68. doi: 10.1111/j.1749-6632.2009.04054.x.

Reichelt. (2007). Mechanotransduction of keratinocytes in culture and in the epidermis. *European Journal of Cell Biology, 86*(11-12), 807-816. doi: 10.1016/j.ejcb.2007.06.004.

Ricca, Venugopalan, & Fletcher. (2013). To pull or be pulled: parsing the multiple modes of mechanotransduction. *Current Opinion in Cell Biology*(0). doi: 10.1016/j.ceb.2013.06.002.

Richardson. (1947). Contractile Tissues in the Mammary Gland, with Special Reference to Myoepithelium in the Goat. *Proceedings of the Royal Society of London. Series B - Biological Sciences, 136*(882), 30-45. doi: 10.1098/rspb.1949.0004.

Rosenbaum, & Witman. (2002). Intraflagellar transport. *Nat Rev Mol Cell Biol, 3*(11), 813-825. doi: 10.1038/nrm952.

Rosfjord, & Dickson. (1999). Growth factors, apoptosis, and survival of mammary epithelial cells. *J Mammary Gland Biol Neoplasia, 4*(2), 229-237.

Roth, Rieder, & Bowser. (1988). Flexible-substratum technique for viewing cells from the side: some in vivo properties of primary (9+0) cilia in cultured kidney epithelia. *Journal of Cell Science, 89*(4), 457-466.

Satir, & Christensen. (2007). Overview of structure and function of mammalian cilia. *Annu Rev Physiol, 69*, 377-400. doi: 10.1146/annurev.physiol.69.040705.141236.

Satir, Pedersen, & Christensen. (2010). The primary cilium at a glance. *J Cell Sci, 123*(Pt 4), 499-503. doi: 10.1242/jcs.050377.

Schaffer, Rizen, L'Italien, Benbrahim, Megerman, Gerstenfeld, & Gray. (1994). Device for the application of a dynamic biaxially uniform and isotropic strain to a flexible cell culture membrane. *J Orthop Res, 12*(5), 709-719. doi: 10.1002/jor.1100120514.

Schedin, & Keely. (2011). Mammary gland ECM remodeling, stiffness, and mechanosignaling in normal development and tumor progression. *Cold Spring Harb Perspect Biol, 3*(1), a003228. doi: 10.1101/cshperspect.a003228.

Schere-Levy, Buggiano, Quaglino, Gattelli, Cirio, Piazzon, . . . Kordon. (2003). Leukemia inhibitory factor induces apoptosis of the mammary epithelial cells and participates in mouse mammary gland involution. *Exp Cell Res, 282*(1), 35 - 47.

Schmidt. (1971). *Biology of lactation*: San Francisco, USA: W. H. Freeman ft Co.

Schneeberger, & Lynch. (1992). Structure, function, and regulation of cellular tight junctions. *Am J Physiol, 262*(6 Pt 1), L647-661.

Schwartz. (2010). Integrins and Extracellular Matrix in Mechanotransduction. *Cold Spring Harbor Perspectives in Biology, 2*(12). doi: 10.1101/cshperspect.a005066.

Schwartz, & DeSimone. (2008). Cell adhesion receptors in mechanotransduction. *Current Opinion in Cell Biology, 20*(5), 551-556. doi: 10.1016/j.ceb.2008.05.005.

Schwartz, Leonard, Bizios, & Bowser. (1997). Analysis and modeling of the primary cilium bending response to fluid shear. *Am J Physiol, 272*(1 Pt 2), F132-138.

Schwarz, & Gardel. (2012). United we stand - Integrating the actin cytoskeleton and cell-matrix adhesions in cellular mechanotransduction. *Journal of Cell Science, 125*(13), 3051-3060.

Schwertfeger, Richert, & Anderson. (2001). Mammary gland involution is delayed by activated Akt in transgenic mice. *Mol Endocrinol, 15*(6), 867 - 881.

Sheffield, & Kotolski. (1992). Prolactin inhibits programmed cell death during mammary gland involution. *Faseb J*(6:A1184).

Singh, Davis, Dobson, Molenaar, Wheeler, Prosser, . . . Stelwagen. (2008). cDNA microarray analysis reveals that antioxidant and immune genes are upregulated during involution of the bovine mammary gland. *J Dairy Sci, 91*(6), 2236-2246. doi: 10.3168/jds.2007-0900.

Singh, Dobson, Phyn, Davis, Farr, Molenaar, & Stelwagen. (2005). Milk accumulation decreases expression of genes involved in cell–extracellular matrix communication and is associated with induction of apoptosis in the bovine mammary gland. *Livestock Production Science, 98*(1–2), 67-78. doi: 10.1016/j.livprodsci.2005.10.016.

Singh, Swanson, Henderson, & Stelwagen. (2012). *The effect of re-milking following extended non-milking periods on lactation in dairy cows* (Vol. 72): New Zealand Society of Animal Production.

Singla, & Reiter. (2006). The Primary Cilium as the Cell's Antenna: Signaling at a Sensory Organelle. *Science, 313*(5787), 629-633. doi: 10.1126/science.1124534.

Smith, Gourdon, Little, Kubow, Eguiluz, Luna-Morris, & Vogel. (2007). Force-induced unfolding of fibronectin in the extracellular matrix of living cells. *PLoS Biol, 5*(10), e268. doi: 10.1371/journal.pbio.0050268.

Stanley, Woodley, Katz, & Martin. (1982). Structure and function of basement membrane. *J Invest Dermatol, 79 Suppl 1*, 69s-72s.

Stefanon, Colitti, Gabai, Knight, & Wilde. (2002). Mammary apoptosis and lactation persistency in dairy animals. *J Dairy Res, 69*(1), 37-52.

Stein, Morris, Davies, Weber-Hall, Duffy, Heath, . . . Gusterson. (2004). Involution of the mouse mammary gland is associated with an immune cascade and an acute-phase response, involving LBP, CD14 and STAT3. *Breast Cancer Res, 6*(2), R75-91. doi: 10.1186/bcr753.

Stein, Salomonis, & Gusterson. (2007). Mammary gland involution as a multi-step process. *Journal of Mammary Gland Biology and Neoplasia, 12*(1), 25-35. doi: 10.1007/s10911-007-9035-7.

Stelwagen. (2001). Effect of Milking Frequency on Mammary Functioning and Shape of the Lactation Curve. *Journal of Dairy Science, 84*, E204-E211. doi: 10.3168/jds.S0022-0302(01)70219-6.

Stelwagen, Davis, Farr, Eichler, & Politis. (1994). Effect of once daily milking and concurrent somatotropin on mammary tight junction permeability and yield of cows. *J Dairy Sci, 77*(10), 2994-3001. doi: 10.3168/jds.S0022-0302(94)77240-4.

Stelwagen, Davis, Farr, Prosser, & Sherlock. (1994). Mammary epithelial cell tight junction integrity and mammary blood flow during an extended milking interval in goats. *J Dairy Sci, 77*(2), 426-432. doi: 10.3168/jds.S0022-0302(94)76969-1.

Stelwagen, Farr, Davis, & McFadden. (1995). *Inhibition of Milk Secretion and the Extent of Filling of the Bovine Mammary*. Poster at Conference. AgResearch.

Stelwagen, Farr, Davis, & McFadden. (1998). Inhibition of milk secretion and the extent of filling of the bovine mammary gland. *J Dairy Sci, 81 (Supplement 1)*, 376.

Stelwagen, Farr, McFadden, Prosser, & Davis. (1997). Time course of milk accumulation-induced opening of mammary tight junctions, and blood clearance of milk components. *Am J Physiol, 273*(1 Pt 2), R379-386.

Stelwagen, & Knight. (1997). Effect of unilateral once or twice daily milking of cows on milk yield and udder characteristics in early and late lactation. *J Dairy Res, 64*(4), 487-494.

Stelwagen, & Singh. (2013). The Role of Tight Junctions in Mammary Gland Function. *J Mammary Gland Biol Neoplasia*. doi: 10.1007/s10911-013-9309-1.

Strange, Westerlind, Ziemiecki, & Andres. (2007). Proliferation and apoptosis in mammary epithelium during the rat oestrous cycle. *Acta Physiologica, 190*(2), 137-149. doi: 10.1111/j.1748-1716.2007.01704.x.

Streuli, & Akhtar. (2009). Signal co-operation between integrins and other receptor systems. *Biochem J, 418*(3), 491-506. doi: 10.1042/bj20081948.

Swanson, Stelwagen, Dobson, Henderson, Davis, Farr, & Singh. (2009). Transcriptome profiling of Streptococcus uberis-induced mastitis reveals fundamental differences between immune gene expression in the mammary gland and in a primary cell culture model. *J Dairy Sci, 92*(1), 117-129. doi: 10.3168/jds.2008-1382.

Talhouk, Bissell, & Werb. (1992). Coordinated expression of extracellular matrix-degrading proteinases and their inhibitors regulates mammary epithelial function during involution. *The Journal of Cell Biology, 118*(5), 1271-1282. doi: 10.1083/jcb.118.5.1271.

Tarbell. (2010). Shear stress and the endothelial transport barrier. *Cardiovasc Res, 87*(2), 320-330. doi: 10.1093/cvr/cvq146.

Tong, Drapkin, Yalamanchili, Mosialos, & Kieff. (1995). The Epstein-Barr virus nuclear protein 2 acidic domain forms a complex with a novel cellular coactivator that can interact with TFIIE. *Molecular and Cellular Biology, 15*(9), 4735-4744.

Travers, Barber, Tonner, Quarrie, Wilde, & Flint. (1996). The role of prolactin and growth hormone in the regulation of casein gene expression and mammary cell survival: relationships to milk synthesis and secretion. *Endocrinology, 137*(5), 1530-1539. doi: 10.1210/endo.137.5.8612482.

Tschumperlin, & Margulies. (1998). Equibiaxial deformation-induced injury of alveolar epithelial cells in vitro. *American Journal of Physiology - Lung Cellular and Molecular Physiology, 275*(6), L1173-L1183.

Tschumperlin, Oswari, Margulies, & S.S. (2000). Deformation-Induced Injury of Alveolar Epithelial Cells . Effect of Frequency, Duration, and Amplitude. *Am. J. Respir. Crit. Care Med., 162*(2), 357-362.

Van Itallie, & Anderson. (2004). The Molecular Physiology of Tight Junction Pores. *Physiology, 19*(6), 331-338. doi: 10.1152/physiol.00027.2004.

Veland, Awan, Pedersen, Yoder, & Christensen. (2009). Primary cilia and signaling pathways in mammalian development, health and disease. *Nephron Physiol, 111*(3), p39-53. doi: 10.1159/000208212.

Villard, Kalyuzhniy, Riccio, Potekhin, Melnik, Kajava, . . . Corradin. (2006). Synthetic RGD-containing α-helical coiled coil peptides promote integrin-dependent cell adhesion. *Journal of Peptide Science, 12*(3), 206-212. doi: 10.1002/psc.707.

Vogel, & Sheetz. (2006). Local force and geometry sensing regulate cell functions. *Nat Rev Mol Cell Biol, 7*(4), 265-275.

Wall, & McFadden. (2012). *Milk Removal: The Key to Maintaining Milk Production and a Tool to Enhance Efficiency*.

Wang, & Thampatty. (2006). An Introductory Review of Cell Mechanobiology. *Biomechanics and Modeling in Mechanobiology, 5*(1), 1-16. doi: 10.1007/s10237-005-0012-z.

Wann, Zuo, Haycraft, Jensen, Poole, McGlashan, & Knight. (2012a). Primary cilia mediate mechanotransduction through control of ATP-induced Ca2+ signaling in compressed chondrocytes. *The FASEB Journal, 26*(4), 1663-1671. doi: 10.1096/fj.11-193649.

Wann, Zuo, Haycraft, Jensen, Poole, McGlashan, & Knight. (2012b). The primary cilium conducts chondrocyte mechanotransduction. *Cilia, 1* (Suppl. 1), 59. doi: 10.1186/2046-2530-1-S1-P59.

Watson, & Kreuzaler. (2011). Remodeling mechanisms of the mammary gland during involution. *International Journal of Developmental Biology, 55*(7-9), 757-762. doi: 10.1387/ijdb.113414cw.

Watson, Oliver, & Khaled. (2011). Cytokine signalling in mammary gland development. *Journal of Reproductive Immunology, 88*(2), 124-129. doi: 10.1016/j.jri.2010.11.006.

Wattiaux. (2013). *Milk Secretion in the Udder of a Dairy Cow Dairy Essentials* Retrieved from http://babcock.wisc.edu/node/120.

Wells. (2013). Tissue mechanics and fibrosis. *Biochim Biophys Acta, 1832*(7), 884-890. doi: 10.1016/j.bbadis.2013.02.007.

Wernig, Mayr, & Xu. (2003). Mechanical Stretch-Induced Apoptosis in Smooth Muscle Cells Is Mediated by β1-Integrin Signaling Pathways. *Hypertension, 41*(4), 903-911. doi: 10.1161/01.hyp.0000062882.42265.88.

Wilde, Addey, Boddy, & Peaker. (1995). Autocrine regulation of milk secretion by a protein in milk. *Biochem J, 305 (Pt 1)*, 51-58.

Wilde, Henderson, Knight, Blatchford, Faulkner, & Vernon. (1987). Effects of long-term thrice-daily milking on mammary enzyme activity, cell population and milk yield in the goat. *J Anim Sci, 64*(2), 533-539.

Wilde, Quarrie, Tonner, Flint, & Peaker. (1997). Mammary apoptosis. *Livestock Production Science, 50*(1-2), 29-37. doi: Doi: 10.1016/s0301-6226(97)00070-5.

Woods, Sherwin, Sasse, MacRae, Baines, & Gull. (1989). Definition of individual components within the cytoskeleton of Trypanosoma brucei by a library of monoclonal antibodies. *J Cell Sci, 93 (Pt 3)*, 491-500.

Yuan, Frolova, Xie, Wang, Cook, Kwon, . . . Frost. (2010). Primary cilia are decreased in breast cancer: analysis of a collection of human breast cancer cell lines and tissues. *J Histochem Cytochem, 58*(10), 857-870. doi: 10.1369/jhc.2010.955856.

Yurchenco, & Schittny. (1990). Molecular architecture of basement membranes. *The FASEB Journal, 4*(6), 1577-1590.

Zamir, & Geiger. (2001). Molecular complexity and dynamics of cell-matrix adhesions. *Journal of Cell Science, 114*(20), 3583-3590.

Zhang, Li, Sanders, Sumpio, Panja, & Basson. (2003). Regulation of the intestinal epithelial response to cyclic strain by extracellular matrix proteins. *The FASEB Journal*. doi: 10.1096/fj.02-0663fje.

Zhang, Li, Sumpio, & Basson. (2003). Fibronectin blocks p38 and jnk activation by cyclic strain in Caco-2 cells. *Biochemical and Biophysical Research Communications, 306*(3), 746-749. doi: 10.1016/s0006-291x(03)01044-1.

Zhang, Li, Yang, Li, Yuan, Liu, . . . Chorney. (2008). IL-4-induced Stat6 activities affect apoptosis and gene expression in breast cancer cells. *Cytokine, 42*(1), 39-47. doi: 10.1016/j.cyto.2008.01.016.

Zhou. (2009). Polycystins and primary cilia: primers for cell cycle progression. *Annu Rev Physiol, 71*, 83-113. doi: 10.1146/annurev.physiol.70.113006.100621.

Appendix

Appendix I: List of publications arising from this project

7.1 Conference abstracts

Biet, J., Stelwagen, K., Margerison, J., Poole, C. A., Cullum, A., Singh, K. (2013): Changes in the mechanical microenvironment of the bovine mammary gland and their effect on mammary function. *Journal of Dairy Science (E-Suppl. 1) 95: 570.*

Biet, J., Stelwagen, K., Margerison, J., Poole, C. A., Singh, K. (2012): The effect of saline infusion of the bovine mammary gland on mammary epithelial cell shape. *Queenstown Molecular Biology Conference, Queenstown, New Zealand.*

7.1.1 Poster presentations

Biet, J., Stelwagen, K., Margerison, J., Poole, C. A., Cullum, A., Singh, K. (2013): Changes in the mechanical microenvironment of the bovine mammary gland and their effect on mammary function. *Journal of Dairy Science (E-Suppl. 1) 95: 570.*

Biet, J., Stelwagen, K., Margerison, J., Poole, C. A., Singh, K. (2012): The effect of saline infusion of the bovine mammary gland on mammary epithelial cell shape. *Queenstown Molecular Biology Conference, Queenstown, New Zealand.*

7.2 Oral presentations

Biet, J., Stelwagen, K., Margerison, J., Poole, C. A., Singh, K. (2011): The role of mammary epithelial cell stretch in regulating milk production in dairy cows. *Invited seminar at Otago University, Dunedin, New Zealand.*

Biet, J., Stelwagen, K., Margerison, J., Poole, C. A., Singh, K. (2012): Potential role of mammary epithelial cell stretch in regulating milk production in dairy cattle. *PhD confirmation seminar, Massey University, Palmerston North, New Zealand.*

Biet, J., Stelwagen, K., Margerison, J., Poole, C. A., Singh, K. (2013): The role of cell stretch of mammary epithelial cells in involution and regulation of milk production in dairy cattle. *Invited seminar at Ohio State University, Wooster, USA.*

Biet, J., Stelwagen, K., Margerison, J., Poole, C. A., Singh, K. (2013): Can stretched cells cause milk loss?. *Three-Minute-Thesis competition, Massey University, Palmerston North, New Zealand.*